Enhanced PV module efficiency to boost hybrid microgrid power and microgrid ancillary services market creation

A thesis presented in fulfilment of the requirements for the degree of

Doctor of Philosophy

at the University of Strathclyde

by

Linus Orokpo Idoko

B.Eng (Hons.), MSc. (Electrical & Electrical Engineering)

Institute for Energy & Environment
Department of Electronic and Electrical Engineering
University of Strathclyde
Glasgow G1 1XW

October 2018

Declaration

This thesis is the result of the author's original research. It has been composed by the author and has not been previously submitted for examination, which has led to the award of a degree.

Signed: ----------

Date: ----------

Acknowledgement

First and foremost, I would like to thank my principal supervisor, Professor Olimpo Anaya-Lara for providing me with advice, guidance and useful comments throughout my Ph.D. study. Without Professor Olimpo, my goal of submitting my thesis would not have been accomplished.

Thanks to my second supervisor, Dr. Alasdair McDonald, your advice, encouragement and valuable links contributed greatly to my current achievements. Many thanks to Drew Smith for your massive support, thanks to Sheila Campbell, Michelle Morrison for your support.

Many thanks to Dr. Ayman Attya and Dr. David Campos-Gaona for the time and effort made to assist me in my academic pursuit.

My gratitude also goes to Dr. Derick Holliday, Mr. George Cochcrane and members of the Electrical workshop for the support given to me during the design of the Aluminium heat sink used in this research work.

My gratitude also goes to Professor Bill Leithhead and Dr. Julian Feuchtwang for your constructive criticism and advice during my review period.

I would like to acknowledge the Petroleum Technology development fund (PTDF) Nigeria, for offering me a scholarship for my Ph.D. studies.

Last but not the least, my heartfelt gratitude goes to my late father, my mum, and Mrs. Rose Okewu for their prayers, support, and encouragement. I deeply appreciate all the sacrifices and endless support of Mrs. Grace Njoku, Mr. Godwin Idoko and my late elder brother, Mr. James Idoko towards my academic pursuit. I also wish to extend my thanks to Senator Abba Moro, Mrs H. J. Nasidi, my brothers, sisters, friends, and well-wishers for their support and encouragement during this research work.

TO GOD BE THE GLORY

Abstract

Gusau, a city in Zamfara state, Nigeria, chosen as the research location is faced with a shortage of power supply as electricity supply from the national grid is unstable and inadequate, besides the majority of those in the remote area are isolated from the grid. The location has the potential for renewable resources. To end this challenge of power supply shortage, a hybrid electric power system, which employs the use of battery storage, solar and wind energy system with a diesel generator as a reserve to provide adequate power to 120 residential apartments in a settlement isolated from the grid is being designed. The result shows the total yearly electricity production is 168,545kWh/yr, the yearly AC primary load consumption is 67160 kWh/yr, and the excess electricity is 88581kWh/yr and the AC primary load was met.

Solar energy is the most promising renewable energy in the location but the PV module, which converts solar energy into electricity is not efficient as the PV module power output reduces at the peak of sunlight. An experiment was conducted to improve the efficiency of the PV module using a multi-concept cooling technique at a derating factor of 80% and 95%. At a derating factor of 80%, an appreciable increase in the module output power was achieved with module + Al hint sink & water-cooling of the module surface temperature to 20°C. An output power increase of 20.96 W at 12:45 pm and an efficiency of over 3% were achieved. This increase in power output exceeds 250watts with 0% losses. At a derating factor of 95%, an increase in power output from 250w to 262.4w was achieved.

The MATLAB modelling of the hybrid PV/wind/diesel generator system shows the PV module contributes more power to the energy system at a temperature of 20°C than at 45°C. Hence, there is an increase in the PV power output to the hybrid energy system with increased module efficiency.
My sponsors motivated this research, as they wanted me to work in this area.

This thesis also contributes to the creation of microgrid ancillary services market, and the provision of voltage control ancillary services to low voltage distributed generation since it is currently applicable to large power networks.

Table of contents

Abbreviations

HOMER	Hybrid optimization model for Electric renewables
CF	Curve factor
PCM	Phase change material
PV	Photovoltaic
DG	Distributed generation
CSP	Concentrated solar power
WECS	Wind energy conversion system
VAWT	Vertical axis wind turbine
HAWT	Horizontal axis wind turbine
FSWT	Fixed speed wind turbine
VSWT	Variable speed wind turbine
PSFC	Partial scale frequency converter
FSFC	Full-scale frequency converter
BDFRG	Brushless Doubly fed induction generator
BDFRG	Brushless Doubly fed reluctance generator
VSC	Voltage source converter
Voc	Open circuit voltage
Isc	Short circuit current
WRIG	Wound rotor induction generator

List of figures

List of tables

Chapter 1:
Introduction

This thesis attempts to develop a new strategy to eradicate inadequate power supply in areas faced with such challenges and to make the PV module more efficient in terms of energy yield. A multi-concept cooling technique to improve the efficiency of the PV module as past research effort done by researchers adopts the single concept of cooling. PV module achieved the reduction of its surface temperature through water spraying while cooling of the rear of the module done through the process of heat extraction with the help of an attached aluminium heat sink. This was done to help tackling the challenge of loss of power output from the PV module during the peak of sunlight. The PV module expected to provide maximum power at the peak of sunlight produces less power instead due to loss of useful power as heat energy. In order to maximize the use of the available sunlight to generate useful power for electricity purpose from the PV module, cooling is a necessity and this is one of the achievements of this research work. With increased power output from the PV module, the energy contribution to the hybrid PV/Wind/ diesel generator system from the PV increases and in the process lead to the increase in power supplied to the micro-grid.

The sizing of the different energy sources in the hybrid micro-grid was done with the help of HOMER simulator software, this helps the project achieved the desired energy mix for the micro-grid. With the appropriate energy mix in place, renewable sources provide power supply to the micro-grid while the diesel generator is only used during a power failure or during inadequate electricity generation from the renewable sources to meet the load demand. This concept facilitates electricity supply to the micro-grid with deep penetration of renewable energy as the appropriate size of the different equipment such as PV array, wind turbine, battery storage, converters and the diesel generator is being implemented in the process. The HOMER software simulator also helped in the design of the system load requirement of the 120 residential apartment used as a case study on this project. The simulation done with the appropriate derating factor for the PV array selected. Furthermore, this research work attempts to provide voltage control as an ancillary service to low voltage distributed generation.

This research work also sheds light on the need for every community to provide its energy needs, from the use of the available renewable resources within the location. As this stands to proffer solution if properly harnessed, to the problem of inadequate power supply to some communities due to factors such as lack of access to the grid, huge capital requirement for adequate energy generation from fossil fuel etc. Wind and sunlight among other resources are renewable resources available in most communities, some locations experience high wind speed than others and some experience long period of sunlight than others.

Locations with sufficient solar and wind energy resources are more favoured in terms of energy generation from renewable resources. A hybrid energy system became a necessity in this project due to the unsteady nature of renewable resources, among the numerous reasons for designing a hybrid energy system. This is to help one of the resources cover up the deficiency of the other source due to changes in weather conditions, which results in low power output.

1.1 Motivation and Background

What motivated and inspired me to carry out this research is the desire to bring to an end the inadequate power supply challenge in Nigeria and other nations with similar challenges. This is because, Nigeria is a country that is rich in several energy resources such as fossil fuel, renewable and nuclear energy resources, but yet to attain economic and social development due to certain hindrances. The challenges involved with Electricity production and distribution remain as one of the major hindrances to development. [1]. The main source of revenue and energy in the country is crude oil; the crude oil reserve is reducing besides at the international market its price is unstable. Its exploration gives room for environmental degradation and the emission of CO_2. Furthermore, there is crisis in the Niger Delta, the major location for oil exploration in the country. These challenges facing the oil sector make renewable energy as an alternative source of energy a necessity [2]. There is an increasing perception that energy resources from the sun and the wind has the potential as in [3] to proffer solution to the challenge of inadequate power in Nigeria as it can also serve as a source of power to settlements that are not connected to the grid.

The price of acquiring renewable system devices is reducing and there is a high probability that it will reduce more as its market expands [4], hence for several developing nations, the use of the renewable energy for rural electrification is a major target. One of the reasons is that adequate electricity is not accessible and affordable to all besides the supply of electricity is unstable for those who can access or afford it as in [5]. Nigeria experiences a lot of solar radiation, hence the target is to strategize on how to achieve an efficient solar powered rural

electrification, as it is environmentally friendly, it does not produce noise, maintenance required is low etc. The amount of sunlight experienced in Nigeria shows that solar energy has the potential to boost electricity supply in the country as the present statistics of electricity production in the country and its distribution is below the energy potential of Nigeria.

The distribution of renewable energy differs from one location to another location as in [6], as their availability is affected by climatic conditions as well as geographical location. Because of the unsteady nature of renewable energy, combining a number of renewable energy sources as a single hybrid energy system becomes inevitable. This enables one energy to make up for the other energy source in times of deficiency. Electricity generation from hybrid energy system is a known technology nationwide, but it has not been used in Gusau, Sokoto state as well as several parts of Nigeria. The benefits attainable from the use of photovoltaic cells to generate electricity from solar energy has increased the interest of both developing and developed countries to create funds and plans to increase the efficiency of the photovoltaic system [7].

1.2 Solar energy potential in Nigeria.

Nigeria, a country in Africa consist of six geopolitical zones, namely NW (North-West), NE (North-East), NC (North-Central), SW (South-West), SE (South-East) and SS (South-south). The geographical locations on the map of Nigeria as well as the solar energy potential of the various geographical locations as in [8] are as shown in figure 1-1 and 1-2 respectively. Figure 1-2 shows the hours of peak sun experienced across the state in the various geopolitical zones in the country.

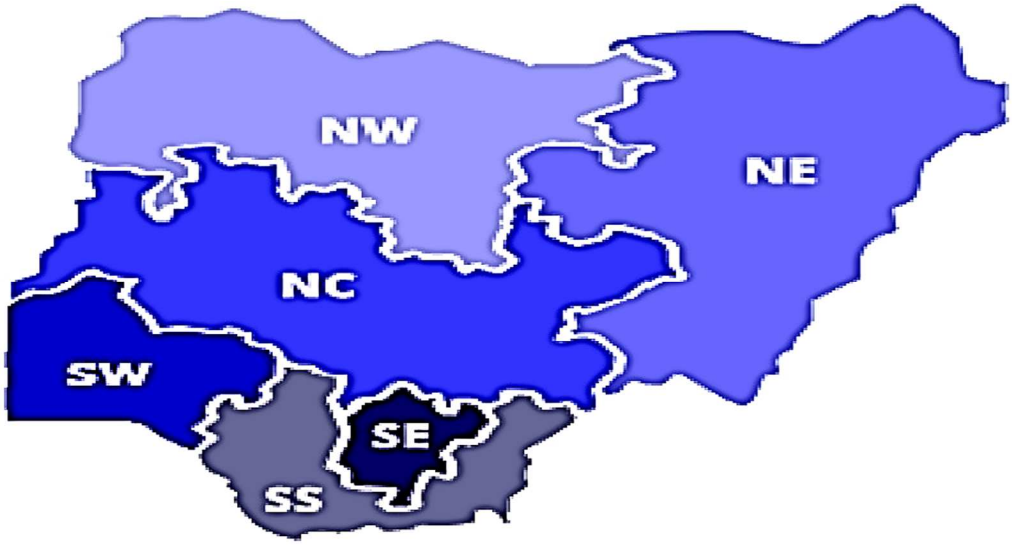

Figure 1-1. Locations of the six geographical zones on Nigerian map

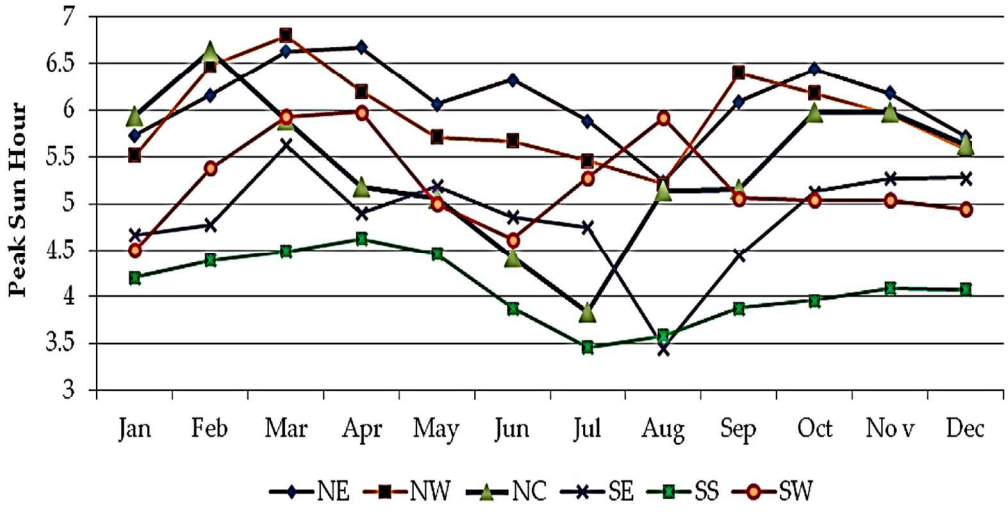

Figure 1-2. The solar energy potential of the six geopolitical zones in Nigeria.

Electricity generation solely from solar energy with photovoltaic modules has been on a steady increase for the past few years; hence, it is gradually becoming a potential contributor to the energy mix globally. The use of the photovoltaic module for electricity generation is very common in countries such as Japan, Germany, USA and other countries, which experiences high solar radiation [9]. The amount of energy from the sun, which strikes the earth hourly, is greater than the amount of energy utilized by humans in one year as in [10] hence there is a need to take advantage of the available solar resources to boost electricity generation globally. Gusau like several other cities in Nigeria, which experiences a long period of sunshine has experienced many failed solar projects because of several factors. This has become a source of worry to several individuals and the government, as the energy yield from the project does not correspond with the huge capital investment involved. Temperature appears to be the most noticeable factor, which affects electricity generation from the PV module in this part of the world [11].

Gusau a city in Northwestern Nigeria experiences a long period of sunshine hours with approximately 7 hours of peak sun and has the potential to provide the community with electricity supply. This research location and several rural communities in Nigeria experience inadequate power supply, several companies and individuals have made attempts to generate electricity with the use of Photovoltaic modules, but got disappointed with the photovoltaic modules as during the peak of sunlight when more power is expected, less power is obtained instead. This reduction in the generated electricity is because of loss of solar energy from the photovoltaic module as heat energy. In order for the PV module to serve us better by generating more electricity during the peak of sunshine, cooling of the PV module is mandatory. As the solar radiation increases, the solar cells produce more power and as the temperature of the

solar cells continues to increase; there is a reduction in the efficiency of the module due to increased PV module surface temperature. This increased module temperature can be minimized by either reducing the module surface temperature through cooling or by heat extraction from the rear of the module [12]

Whenever the PV module is exposed to sunlight, it experiences energy loss as heat energy by conduction, convection, and radiation as shown in figure 1-3.

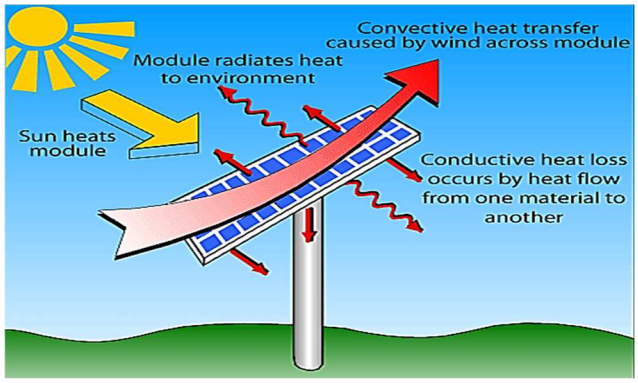

Figure 1-3 forms of heat loss from the surface of the PV module [13]

1.2.1 Usefulness of photovoltaic module as a means of generating electricity from the sun.

In order to achieve maximum power from the photovoltaic module during hot weather conditions or during overheating of the PV module, cooling of the PV module is inevitable. Electricity generation from solar energy via photovoltaic module as an alternative source of electricity is of high interest globally for the following reasons as in [11] [14].

- It does not pollute the environment.
- It does not produce noise.
- It gives an avenue for expansion, as it is modular in nature.
- It is durable and has a long lifespan
- It serves as a means for generating a free source of energy.
- Its installation and operation are achievable anywhere.
- It requires minimum maintenance since no moving part is involved.
- Excess electricity sale is possible with the grid-tie mode.
- It can serve as a source of electricity in times of power blackouts.
- It can serve as a source of electricity for remote locations where the installation of electricity lines is impossible or expensive.
- The extra power generated is stored in the battery for use at night.

- It is a safer source of electricity when compared to the traditional electric current
- It assists the economy as it serves as a source of employment to solar panel installers, manufacturers etc.
- It reduces overdependence on electricity supply from fossil fuel.
- It provides an opportunity for electricity users to be free from using energy from the grid if the electricity generated is adequate for the premises.
- It can be used to power cars, homes etc.

1.2.2 Overview of PV module cooling techniques

The relationship between the solar cell and its efficiency is such that as the temperature increases, the efficiency decreases and the power output drops, the reduction in efficiency becomes evident with the drop in the PV cell open circuit voltage as well as its power output. Increase or decrease in the power output is affected by the temperature of the PV module and can also be determined with the help of the temperature coefficient of power of the selected PV module on the manufacturer's datasheet. The selected model of PV module for this research has a temperature coefficient of power of -0.44%/°C [15]. This means that the PV module maximum power reduces by 0.44%/°C, for every increase in temperature above 25°C. For example, an increase in temperature of a 250W PV module by 10°C, means the operating temperature of 35°C. This implies a reduction in its power by $(35-25)x(0.44\%) \Rightarrow 10x(0.44\%) \Rightarrow 4.4\%$. Therefore, 4.4% reduction in the power generated by a 250W PV gives $4.4\% x 250W = 11W$, hence the power output generated by the PV at 35°C is $239W$. Conversely a reduction of the module temperature by 10°C means an operating temperature of 15°C meaning $(15-25)x(0.44\%) \Rightarrow -10x(0.44\%) \Rightarrow 4.4\%$ gain in power, hence at 15°C, the power output generated will be 261W.

The PV module experiences high temperatures when exposed to high level of irradiation, the module temperature can increase as high as 60-80°C, at this point it requires cooling to be able to function effectively. Parameters of the solar cell such as efficiency, open circuit voltage, curve factor and short circuit current depend on temperature, hence affected in the process. When the temperature of the PV module increase, the short circuit current, Isc increases a little bit, the curve factor, CF reduces and the open circuit voltage, Voc reduces by ~2.3 mV/K [16]. Several cooling techniques adopted in the past to help improve the efficiency of the PV module through cooling as in [17] is classified on the basis of cooling medium into four different categories namely.

- Air based-cooling
- Liquid-based cooling
- Heat-pipe based cooling
- PCM- based cooling

Based on energy usage and technology involved, module cooling is classified as in [18] into several categories as shown in figure 1-4.

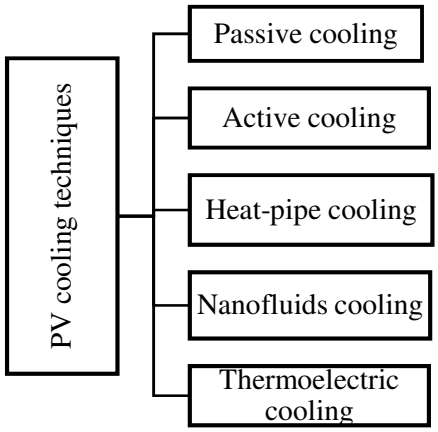

Figure 1-4 Types of PV cooling techniques

The passive cooling method performs the task of heat extraction through the process of natural conduction/convection, there are three major types of passive method, namely conductive cooling, air passive cooling, and water passive cooling. There is another form of passive cooling called phase change material (PCM) cooling. The PCM cooling is also grouped under passive cooling and this is because heat extraction is achieved without any form of extra work. A PCM is a substance that absorbs and releases thermal energy in order to maintain a regulated temperature, the phase of a PCM changes within a certain temperature range. When in the solid state, the PCM absorbs heat as the temperature of its environment increases, the moment the temperature of its environment reaches its melting point, it begins to melt. The PCM absorbs heat at almost no change in temperature during phase change and in the process, provides a cooling effect. PCM cooling is a method of cooling, which uses PCM for cooling.

Furthermore, active cooling, on the other hand, requires energy consumption for heat extraction or cooling. The heat-pipe cooling embraces the use of PCM cooling techniques and the convection of the cooling medium. The thermoelectric cooling technique employs the

application of Peltier effect to module cooling. According to a recent research [19], Peltier effect is an effect, which arises when an electric current passes through an isothermal junction consisting of two different materials resulting in the heating/cooling at the point of contact. On the other hand, a combination of solid nanoparticles and cooling fluids are used in the nanofluids cooling. This research work is basically concerned with heat extraction from the module using the passive cooling technique.

Cooling as a means of heat extraction from the surface of the PV module was implemented in this research work to enhance the efficiency of the PV module and increase the power output obtained from it. It is expected that with the long period of sunshine hours experienced in the selected location and other locations with similar weather conditions, power output contributed to the hybrid micro-grid by the PV module will increase tremendously with the help of enhanced efficiency. The efficiency of the PV module is expressed as shown in equation 1.

$$Efficiency(\eta) = \frac{Power \text{ output (as electricity)}}{Power \text{ available (as solar radiation)}} \quad (1)$$

1.3 Research questions

- Gusau faces inadequate power supply; what is required to end this challenge?
- Electricity supply to Gusau from a single renewable energy source is unsteady, how do we solve this challenge?
- Power output from a PV module at the peak of solar radiation reduces, is it possible to have increased power at the peak of solar radiation?
- PV module efficiency/Power output reduces as the surface temperature of the PV module increases due to overheating; how do we extract this excess heat?
- Voltage control ancillary services are applicable to large power networks presently, how do we apply it to low voltage distributed generation?

1.4 Research aim and objectives

The aim of this thesis is to develop a new strategy to eradicate inadequate power supply in areas faced with such challenges and to make the PV module more efficient in terms of energy yield. The key objectives are to:

- Solve the challenge of inadequate power in a locality with the renewable energy resources in the location.
- Reduce energy wasted as heat at the peak of sunlight considerably and increase PV module efficiency/power output.

- Reduce the PV module surface temperature to 20°C using the multi-concept cooling technique.
- Generate more power from the PV module when the intensity of the sun is very high instead of generating less power at the peak of sunlight
- Reduce instability with a single renewable energy source.
- Employ the use of HOMER software simulator for micro-grid system sizing and adopts its equation for power output as regards the temperature effect.
- Make recommendations to support the creation of microgrid ancillary services market.
- Provide Voltage control ancillary services to a small power system network.

1.5 Methodology

The research methodology used to provide adequate power to the location faced with the inadequate power supply are as follows:

- A hybrid energy system designed for the affected area instead of using a single renewable energy source.
- Procedure to design the load requirement of the affected area
- Procedure to identify the wind and solar energy resources of the research location
- Application of HOMER software simulator for sizing the hybrid PV/Wind/ Diesel generator energy system.
- Design and fabrication of Aluminium heat sink for heat extraction from the rear of the PV module.
- PV module efficiency/power output experiment to demonstrate the impact of the application of water-cooling on the module surface and Aluminium heat sink at the rear of the module.
- Modelling of the hybrid PV/Wind/ Diesel generator energy system using MATLAB.
- Review of existing voltage control ancillary services and Provision of market recommendation for microgrid ancillary services.

1.6 Contributions of the thesis

The major contributions of this thesis are:

- Development of a new concept for cooling the PV module as the multi-concept cooling technique ensures that the module experiences cooling at all times. This is so because in the absence of water-cooling, a certain amount of cooling can be achieved.
- The system allows the module to continue to provide increased power output even at the peak of sunlight

- Creation of the awareness that electricity can be generated from the renewable resources in every location to cater for its power needs.
- Market recommendations for micro-grid ancillary services
- Application of Voltage control ancillary services to low voltage distributed generation.

1.7 Structure of thesis

This thesis comprises seven (7) chapters and is structured as follows:

Chapter one gives the problem of inadequate power in a location and how the inadequate power challenge can be solved using Hybrid PV/wind/ diesel energy system with improved PV module efficiency. It highlights the challenges, which limits the efficiency of the PV module from providing peak power at the peak of sunlight, the objectives, and contributions.

Chapter two reviews solar energy systems including the various types of photovoltaic energy generation technologies. Hybrid energy systems formed with the PV system, the different types as well as the various forms of energy storage were considered. Since, this project focuses on the efficiency of the PV module, the numerous factors, which affect the efficiency of the PV module were reviewed. Wind energy system, which also forms part of the hybrid energy system was also considered, the review also covers the elements of wind energy conversion system, the selected wind turbine and its characteristics. Finally, the PMSG driven wind turbine used for this project was reviewed and the types of power electronics that support the PMSG wind turbine were also considered.

Chapter three embraces the benefits of the hybrid energy system, the different types of the standalone energy system, sizing of the hybrid energy units, and the methods of unit sizing. The different types of simulation software used for sizing hybrid energy system treated. The design of the load profile for the research location, the available wind and solar energy resources in the location were considered. Finally, this chapter also covers the use of the HOMER software simulator for system sizing and the results the simulation done with the use of the HOMER software simulator.

Chapter four contains the survey of past efforts made by researchers to tackle the effect of temperature on the efficiency of the PV module. Other areas covered in this chapter include the temperature effect on the PV module, the PV module temperature coefficient of power, the effect of heat on the PV module, cooling of the PV module. The concept, features and

advantages of the proposed method of cooling, experiments to demonstrate the increase in energy and efficiency with cooling of the PV module to 20°C using the multi-concept cooling technique at a derating factor of 80% and 95% were also analysed.

Chapter five consists of the model composition of the hybrid PV/wind/diesel energy system and the modelling of the individual units that make up the model, such as the modelling of the solar energy system, battery storage, wind energy system, diesel generator energy system, etc. The control of the hybrid energy system, I-V and P-V curve of 60kW PV array, as well as the results obtained from the simulation of the hybrid energy system carried out using MATLAB Simulink, were also treated.

Chapter six covers the different types of ancillary services in power system, including their basis of classification, provision of ancillary services to the microgrid, distributed generation (DG) and the different types of DG classifications. Others areas covered are microgrid ancillary services, market prospects for microgrid voltage control ancillary services, types and techniques of voltage control, reactive power, and power factor.

Chapter seven presents the general conclusions, the key contributions and future works.

1.8 List of publications

The following publication efforts were made as a direct result of research relating to this thesis with contributions from the following individuals: Olimpo Anaya-Lara, Alasdair McDonald, Ayman Attya and David Campos-Gaona.

1.8.1 International Journal Publications

Linus Idoko, Olimpo Anaya-Lara, Alasdair McDonald, "Enhancing PV modules efficiency and power output using multi-concept cooling technique" Energy reports, Elsevier, Vol 4, pp.357-369, DOI:10.1016/j.egyr.2018.05.004, May 2018.

Linus Idoko, Olimpo Anaya-Lara, David Campos-Gaona, "Voltage control ancillary services for low voltage distributed generation" International Journal of Smart Grid and Clean Energy, Vol. 7, Issue 2, pp. 98-108, DOI: 10. 12720/sgce.7.2.98-108, April 2018.

Linus Idoko, Olimpo Anaya-Lara, "Design of a Hybrid PV/Wind/Diesel Generator Energy System for 120 Residential Apartments in Gusau" International Journal of Engineering

Research and Technology, Vol. 6, Issue 05, pp. 758-763, DOI: 10.17577/IJERTV6IS050596, May 2017.

Linus Idoko, Olimpo Anaya-Lara, Ayman Attya, David Campos-Gaona, "Factors affecting the efficiency of PV module: an overview" International Journal of environment and sustainable development, Inderscience Publishers. Submitted August 2018.

1.8.2 International Conference publication

Linus Idoko, Olimpo Anaya-Lara, Ayman Attya, "Increasing hybrid PV/wind/diesel generator power output with increased PV module efficiency" the 8th International Conference on Environmental Science and Engineering (ICESE 2018), Barcelona, Spain. 11-13th March 2018.

1.8.3 Posters

Linus Idoko, Olimpo Anaya-Lara, Alasdair McDonald "Solar and Wind energy potential in Gusau, Nigeria" Faculty Research Presentation Day 2016, University of Strathclyde.

Linus Idoko, Olimpo Anaya-Lara, Alasdair McDonald "Optimization of hybrid PV-wind power for micro-grid support by improving the efficiency of photovoltaic module" Faculty Research Presentation Day 2015, University of Strathclyde.

1.9 References

[1] G. M. Argungu, E. J. Bala, M. Momoh, M. Musa, and K. A. Dabai, "Analysis Of Wind Energy Resource Potentials And Cost Of Wind Power Generation In Sokoto, Northern Nigeria," vol. 2, no. 5, pp. 713–722, 2013.

[2] O. Awogbemi and C. a Komolafe, "Potential for Sustainable Renewable Energy Development in Nigeria .," *Pacific J. Sci. Technol.*, vol. 12, no. 1, pp. 161–169, 2011.

[3] I. A. Adejumobi, S. G. Oyagbinrin, F. G. Akinboro, M. B. Olajide, and O. State, "Hybrid Solar and Wind Power: an Essential for Information Communication Technology Infrastructure and People in Rural Communities," *Int. J. Res. Rev. Appl. Sci.*, vol. 9, no. October, pp. 130–138, 2011.

[4] C. V. Nayar, S. M. Islam, H. Dehbonei, K. Tan, and H. Sharma, *Power electronics for renewable energy sources*, Third Edit. Elsevier Inc., 2011.

[5] M. Usman, "Rural solar electrification in Nigeria: renewable energy potentials distribution for rural development," *Available from http//ases.conference-*

services.net/…/Solar2012_Full%20paper.pdf, pp. 1–8, 2012.

[6] A. V. Anayochukwu, "Energy Optimization Map for Off-Grid Health Clinics in Nigeria," vol. 4, no. 1, 2014.

[7] S. Mekhilef, R. Saidur, and M. Kamalisarvestani, "Effect of dust, humidity and air velocity on efficiency of photovoltaic cells," *Renew. Sustain. Energy Rev.*, vol. 16, no. 5, pp. 2920–2925, 2012.

[8] D. O. Akinyele, R. K. Rayudu, and N. K. C. Nair, "Life cycle impact assessment of photovoltaic power generation from crystalline silicon-based solar modules in Nigeria," *Renew. Energy*, vol. 101, pp. 537–549, 2017.

[9] G. Makrides, B. Zinsser, M. Norton, G. E. Georghiou, M. Schubert, and J. H. Werner, "Potential of photovoltaic systems in countries with high solar irradiation," *Renew. Sustain. Energy Rev.*, vol. 14, no. 2, pp. 754–762, 2010.

[10] G. M. Whitesides and G. W. Crabtree, "Don't forget long-term fundamental research in energy," *Science (80-.).*, vol. 315, no. 5813, pp. 796–798, 2007.

[11] A. S. Sambo, I. H. Zarma, P. E. Ugwuoke, I. J. Dioha, and Y. M. Ganda, "Implementation of Standard Solar PV Projects in Nigeria," *ISSN*, vol. 4, no. 9, pp. 2224–3232, 2014.

[12] J. A. Gotmare, D. S. Borkar, and P. R. Hatwar, "Experimental Investigation of Pv Panel With Fin Cooling Under Natural Convection," *Int. J. Adv. Technol. Eng. Sci.*, vol. 03, no. 02, pp. 447–454, 2015.

[13] "Heat Loss in PV Modules | PVEducation." [Online]. Available: http://www.pveducation.org/pvcdrom/modules/heat-loss-in-pv-modules. [Accessed: 23-Apr-2018].

[14] "Solar Power Advantages and Disadvantages." [Online]. Available: https://www.sepco-solarlighting.com/blog/bid/115086/Solar-Power-Advantages-and-Disadvantages. [Accessed: 24-Apr-2018].

[15] "250 Watts Monocrystalline Solar Module Features." [Online]. Available: https://es-media-prod.s3.amazonaws.com/media/u/bad/9e9/d9b/4a377fac554a5266604e7b20285d4e78/SuntechWd mono(MC4_250_255_260_265)_EN_web.pdf. [Accessed: 16-Sep-2017].

[16] Y. M. Irwan, I. Daut, I. Safwati, M. Irwanto, N. Gomesh, and M. Fitra, "A new technique of photovoltaic/wind hybrid system in Perlis," *Energy Procedia*, vol. 36, pp. 492–501, 2013.

[17] Y. S. Bijjargi, K. SS, and S. K A, "Cooling Techniques for Photovoltaic Module for

Improving Its Conversion Efficiency: a Review," *Int. J. Mech. Eng. Technol.*, vol. 7, no. 4, pp. 22–28, 2016.

[18] T. G. Grubisić-Čabo, F., Nizetić, S., & Marco, "Photovoltaic Panels: A Review of the Cooling Techniques," *Trans. FAMENA*, vol. 40, no. 1, p. p63–74. 12p., 2016.

[19] W. Jin, L. Liu, T. Yang, H. Shen, J. Zhu, W. Xu, S. Li, Q. Li, L. Chi, C. an Di, and D. Zhu, "Exploring Peltier effect in organic thermoelectric films," *Nat. Commun.*, vol. 9, no. 1, pp. 1–6, 2018.

Chapter 2:

Overview of increasing PV module efficiency/power to the hybrid micro-grid

Increasing the efficiency of the PV module is all that is required for the PV module to make a constant and meaningful contribution to power system as a single source of power and also when used as part of a hybrid energy system.

This chapter reviews solar energy systems, including the various types of photovoltaic energy generation technologies. Hybrid energy systems formed with the PV system, the different types as well as the various forms of energy storage were considered. Since, this project focuses on the efficiency of the PV module, the numerous factors, which affect the efficiency of the PV module were reviewed. Wind energy system, which also forms part of the hybrid energy system was also considered, the review also covers the elements of wind energy conversion system, the selected wind turbine and its characteristics. Finally, the PMSG driven wind turbine used for this project was reviewed and the types of power electronics that support the PMSG wind turbine were also considered.

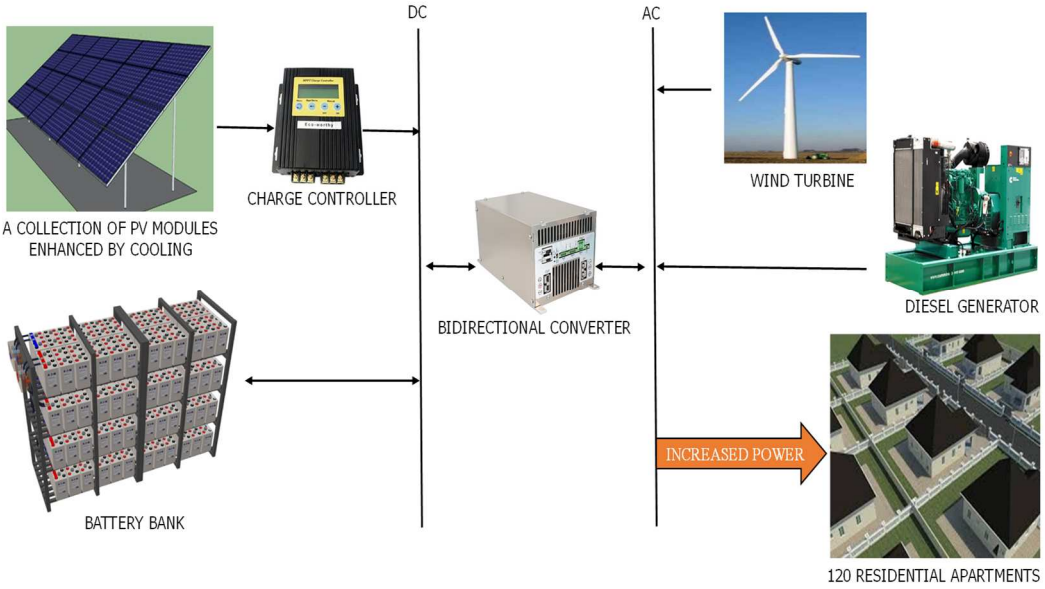

Figure 2-1 Image of research project

This research work attempts to increase the amount of power supply to the hybrid micro-grid by increasing the power generated from the photovoltaic modules. This is achieved by

improving the efficiency of the PV module using three methods of passive cooling. The target is to make use of the available solar energy resources and wind energy resources found in the location. Gusau, Zamfara State in Nigeria was used as a case study. The renewable energy resources are expected to provide adequate power to meet the load demand of the location while a diesel generator is incorporated into the hybrid system to supply electricity to the hybrid micro-grid during periods of inadequate power supply from the renewable energy sources or in the event of power failure. A battery storage system will be connected to the PV system in a manner that it can be charged by all the sources. The general idea of the research project is as shown in figure 2-1. Several technologies, devices, and ideas were considered in this research, these ideas are gathered from the subsequent paragraphs and pages.

2.1 Solar power generation technologies

Electricity can be generated from solar energy in two major ways, namely concentrated solar power (CSP) and solar photovoltaic technologies. In the CSP technology, electricity is generated from solar energy with the help of lenses or mirrors, which helps to reflect and focus sunlight onto receivers, which collects the solar energy and transform it to heat. The acquired thermal energy is converted to electricity via a turbine or a heat engine driving a generator [1] high temperature is required for this technology, as a result, solar radiation requires concentration. For the solar photovoltaic system, the energy obtained from sunlight is directly converted to electricity with the help of photovoltaic effect of semiconductor materials. A photovoltaic module is a device used to collect energy from the sun to generate electricity and the photovoltaic energy system as in [2] is made up of the following devices as the PV modules, charge controller, batteries, and inverter.

A PV module popularly known as the solar panel is a collection of several solar cells that are electrically connected and packed in a single frame, several of such modules can be combined to form a solar array. Most electrical devices such as motors, lighting appliances are designed to utilize AC power, the PV module produces DC power and its usually stored in the batteries, in order for this DC power to be used, an inverter is required to convert the power from DC to AC, the inverter converts DC power stored in the batteries to AC power. In order to protect the system batteries by monitoring the state of charge of the batteries, the charge controller becomes a necessity as it ensures that the batteries are not overcharged, damaged and also that the batteries are charged when charging is required. The energy trapped from sunlight is stored in the batteries to supply electricity during the night or cloudy days [3]

Research on the use of photovoltaic energy to generate electricity from the sun is speedily progressing in numerous fronts, several of these discoveries are in their infant phase and yet to be implemented but may become prevailing in the near future. Energy from the sun is one of the globally accepted sources of energy used in several systems and devices such as the production of electricity via solar cells referred to PV cells, the use of thermal collectors for thermal management [4]. Countries which experience ample exposure to sunlight are at an advantage of generating electricity from solar, several countries currently are shifting their attention from fossil fuel to solar energy as a result of the advantages derived from using solar energy as a source of electricity. In [5], China appears to be the leader in the installation of PV for electricity as an alternative source of power, countries which also employ the installation of photovoltaic energy systems as an alternative source of power include Japan, USA etc as shown in figure 2-2.

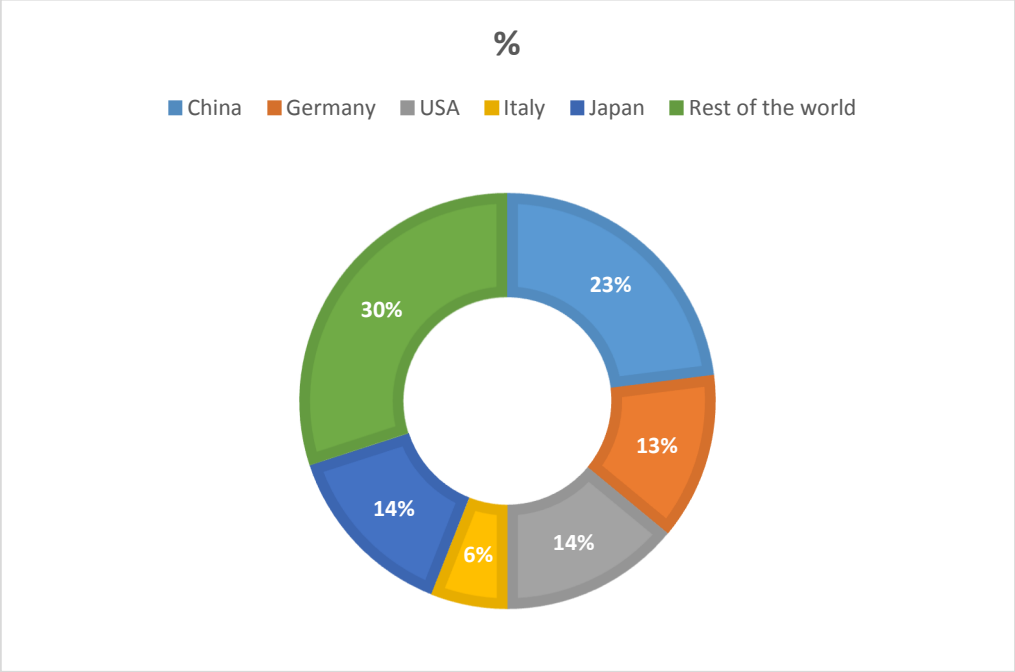

Figure 2-2 2016 cumulative global photovoltaic systems installation

2.1.1 Type of solar Photovoltaic system

The solar PV systems are usually categorized based on the configuration of their components, the operational and functional requirements, mode of connection to electrical loads and other sources of power. The two major types of Photovoltaic systems are the standalone system and the grid-connected system. It can operate independently on its own as in the case of the standalone system, and it can operate with a connection to the grid, it can also operate in connection with energy storage devices or with other sources of energy to form a hybrid

system. Each of the different classes of PV system has advantages and disadvantages, and it can supply AC or /and DC power depending on the requirement of the load it is intended to power [6].

2.1.1.1 PV Direct energy system.

This is the simplest type of photovoltaic power system as it uses the smallest amount of components, it does not require battery storage, hence it comprises basically of the PV modules and the load it is intended to supply with power, for example, ventilation fan, etc. They are usually designed to supply power to the intended load during the daytime since they are not linked to the utility grid. The number and size of the photovoltaic modules used in a PV direct energy system depend on the amount of load to be powered as in [7]. This type of solar energy system load operates using DC electricity since the PV generates DC electricity. The PV direct energy system can be represented as figure 2-3.

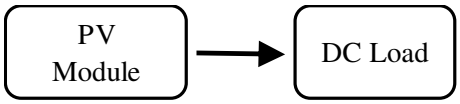

Figure 2-3. PV direct system

2.1.1.2 The off-grid or standalone photovoltaic system

Unlike the PV direct solar energy system, the off-grid system can be used at night as it makes use of batteries to store energy and supply electricity at periods when the photovoltaic module is not active for example during the nights. Its employed in remote buildings and locations where there is no available access to the electricity grid or where the grid is not required. A standalone alone system in which the PV module or a collection of PV modules is connected directly the to the load without a battery system is often referred to as a PV direct system [8]. Because battery storage is involved in this system there is every need to prevent overcharging by monitoring the amount of current flowing into the battery and this is achieved with the help of the charge controller. A good example of a standalone system which supplies electricity to a DC load and an AC load is as shown in figure 2-4.

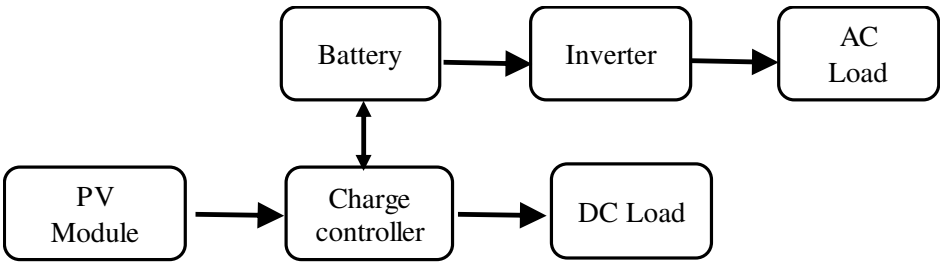

Figure 2-4 Standalone photovoltaic system

Features of the standalone photovoltaic energy system as in are as follows:

- The battery has a short life and it requires maintenance.
- Its installation requires more components and hence more money than the PV direct system.
- It operates independently without connection to the grid
- It is not affected by the utility company's terms/policies
- It is cheaper to manage in a remote location than grid extension to the location
- An alternative source of power as a backup is required to supply power to the load in the event of failure of the PV system.
- Majority of standalone systems utilized generators as a backup source of power in the event of power failure, for example, during days of no sun and these generators are expensive in terms of the cost of purchase, regular fuelling besides they produce noise.
- Power output from the PV module is not used with the batteries fully charged
- System efficiency is affected by batteries and several other factors.

2.1.1.3 The grid-connected photovoltaic system

This is a system which allows you to make use of the electricity you were able to generate from the solar photovoltaic energy system and also make use of electricity supply from the grid. A major component of this system is the inverter also referred to as the power conditioning unit (PDU). It converts the DC produced power from the PV modules to AC power which matches the requirements of the voltage and power of the grid. There is flexibility with this type of PV system as you stand to access continuous electricity supply whether the sun shines or not. During the sunlight hours of the day, the electricity generated from the PV system at home goes to the utility grid while the utility grid supplies electricity to the house during the night. This system makes it possible for the PV system owner to save some money, this is achievable by generating and supplying extra electricity to the grid than the amount of

electricity consumed by the owner at times that the PV does not supply power for example during the night or days that are cloudy [6]. The grid-connected PV is as shown in figure 2-5.

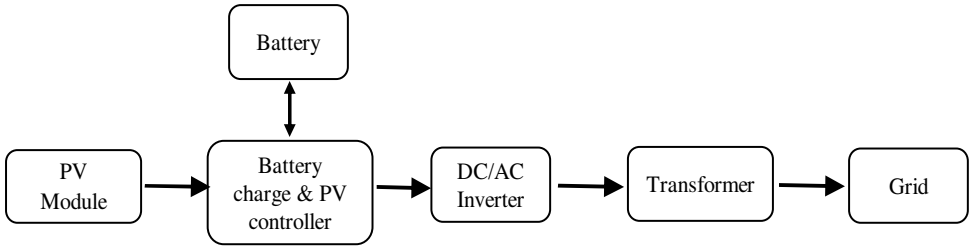

Figure 2-5 Grid-connected photovoltaic system with battery storage.

The grid-connected system can also be achieved without any form of battery storage, usually referred to as a grid-connected solar system without battery backup.

Features of the grid-connected photovoltaic system with battery backup as in [9] are as follows:

- Maintenance of the batteries is required
- Cost of installation is higher than that of grid-direct system
- It's more complex as it required more devices.
- Unlike the standalone alone system where any extra energy is lost when the battery becomes full when the intensity of the sun is high, energy in excess of the home demand is sold to the grid.
- Paperwork is necessary for rebates, incentives, and interconnectivity

2.1.1.4 Hybrid Photovoltaic system

The standalone PV system can also be designed with support from another source of power, this type of PV systems in which energy generation from the PV system is supported with an alternative source of power for example wind, biomass is referred to as a standalone hybrid energy system. It is believed by several experts that we need to combine a number of renewable energy sources to be able to take the place of fossil fuel as an alternative source of energy and it is not a task that can be achieved using a single renewable source of energy as in [10]. A system which embraces the use of more than one source of energy is referred to as Hybrid energy system. The hybrid photovoltaic system can exist in two different forms, namely: the grid mode where it is connected to the grid and the island mode where it is not connected to the grid. More than one type of renewable energy may be used, a typical example of a solar photovoltaic hybrid energy system is as shown below.

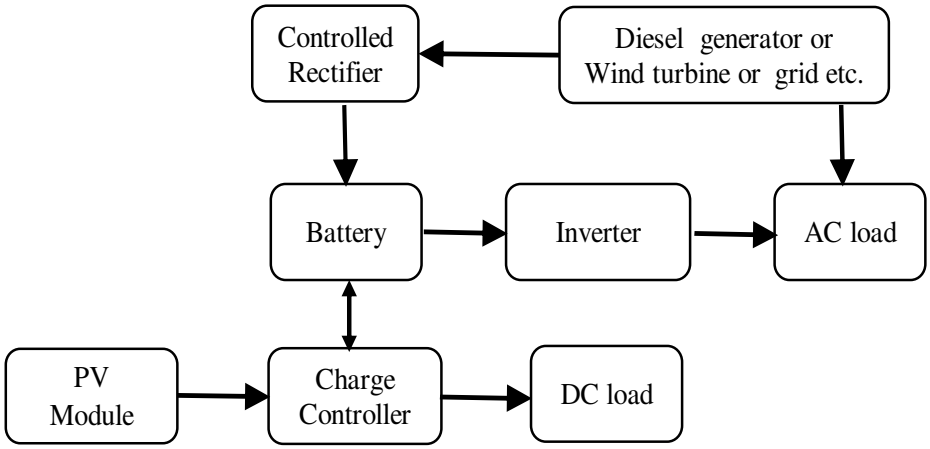

Figure 2-6 Solar photovoltaic hybrid system.

Features of the solar photovoltaic hybrid energy system as in [11] is as follow:

- It involves two or more sources of energy to generate electricity and its electricity production capacity relies on the number of available energy resources
- Regular maintenance is usually required for some of its devices such as generators and wind turbines.
- One of the energy sources usually complements another of the sources in the event of failure as, during a sunny day, the PV charges the battery and when the weather becomes windy and cloudy, the batteries are charged with the wind turbine.
- Its design and installation is more complex
- The capacity of the battery and array size can be reduced
- Power output tends to be more stable
- It encourages better use of energy from renewable sources.
- The wind turbine generates noise
- The presence of a diesel generator as backup produces pollution and noise
- It requires high initial capital

2.2 Mounting of Solar photovoltaic PV system.

In order for the photovoltaic module to generate electricity from sunlight, the PV modules have to be mounted in a manner that it can access the sun without any form of obstruction, this implies that the PV module or array has to be mounted at the proper tilt angle to the module orientation due south (180°) as in [12]. The techniques for mounting the photovoltaic energy systems are as shown in figure 2-7.

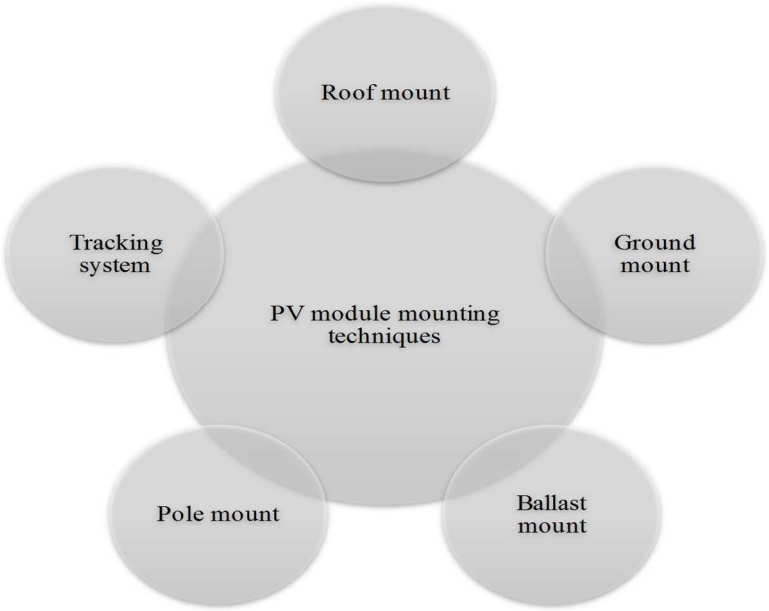

Figure 2-7 PV module-mounting techniques

Each of the techniques in figure 2-7 has its usefulness, for the purpose of this project the ground mount technique is being considered, this project is designed to provide electricity to several residential apartments and as a result, ground mount system appears to be the preferred choice. Other advantages of the ground mount as in [12] are as follows:

- It is very easy and safer to mount as it can be positioned in an open piece of land and does not require any form of roof drilling
- It is more efficient and productive as they are positioned at the proper tilt angle to generate electricity since they are independent of the roof.
- It is safer and more accessible for example, during winter when there are drops of snow, it becomes risky to sweep off the snow from the surface of the panel if roof mounted.
- It facilitates air-cooling of the rear of the PV module and hence the entire module.

2.3 Hybrid system classification

A hybrid energy system is made up of a combination of two or more energy sources. Sources of renewable energy can be integrated to form a hybrid energy system that is stable and friendly to the environment. These renewable energy sources are also referred to as distributed energy resources and the process of producing electricity from these sources is referred to as distributed generation, based on sources of energy generation, distributed generation can be grouped into several categories as shown in figure 2-8.

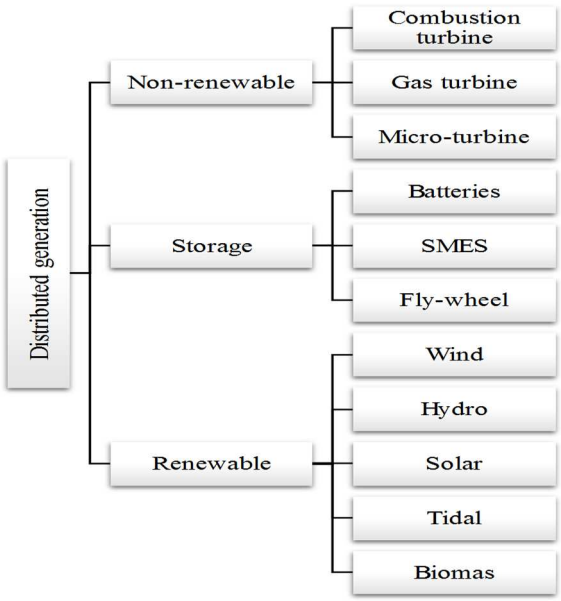

Figure 2-8 Categories of distributed generation

Hybrid energy system refers to an energy system developed through the integration of two or more non-renewable/renewable sources of energy [13]. The hybrid energy systems are classified in several ways as shown in figure 2-9

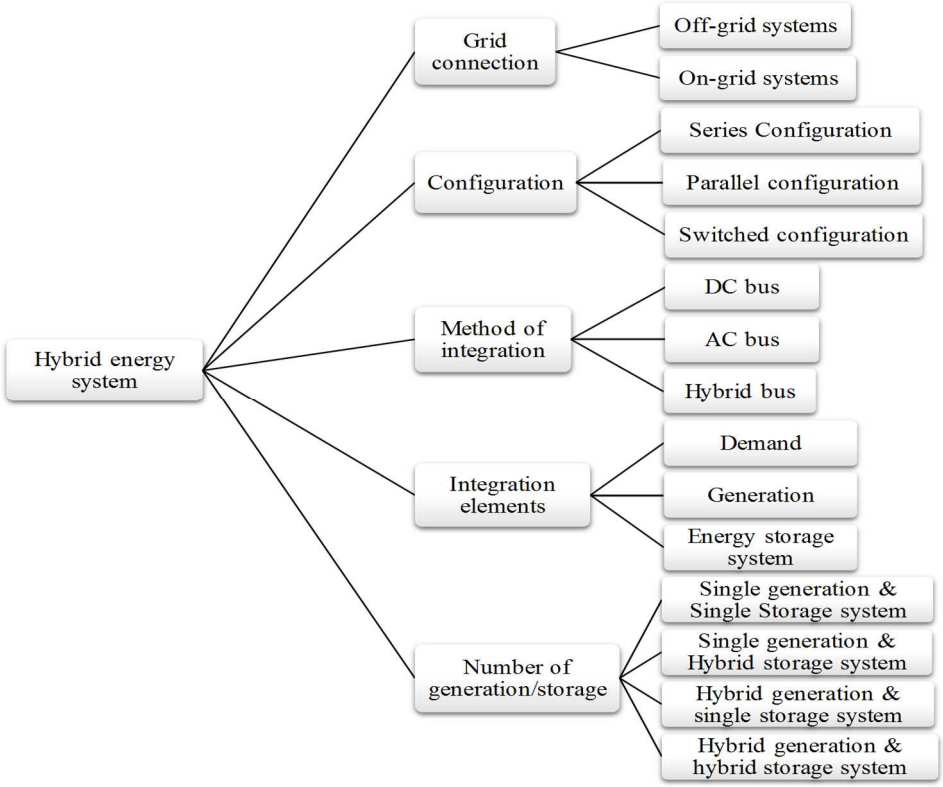

Figure 2-9 classification of hybrid energy systems.

2.3.1 Classification based on Grid integration

Based on the grid connection, a hybrid energy system is grouped into two major categories, namely off-grid or standalone system, and grid-connected system.

2.3.1.1 Off-grid system

As the name implies, it is not connected to the grid and does not benefit from the grid in any way. It is made up of at least a primary source of renewable energy and a non-renewable source of energy and battery storage unit. This type of system is implemented in a location where access to electricity is practically not possible due to geographic reasons, cost, etc. depending on the sources of energy, it can be classified as [14] into

Single source hybrid systems, which is made of two types below

- Single renewable hybrid energy system for example wind, PV, Biomass and hydro
- Single non-renewable hybrid energy system for example Kerosene, Gasoline, diesel etc.

The multi-source hybrid system, which is divided into three different categories as follows

- Off-grid hybrid system
- Grid-connected hybrid system and
- Integrated renewable energy system.

In this example, the PV and the Wind energy system serve as the sources of renewable energy while the diesel generator serves as the backup power source in the event of system failure or inadequate generation from the renewable sources.

An example of an off-grid hybrid energy system is as shown in figure 2-10

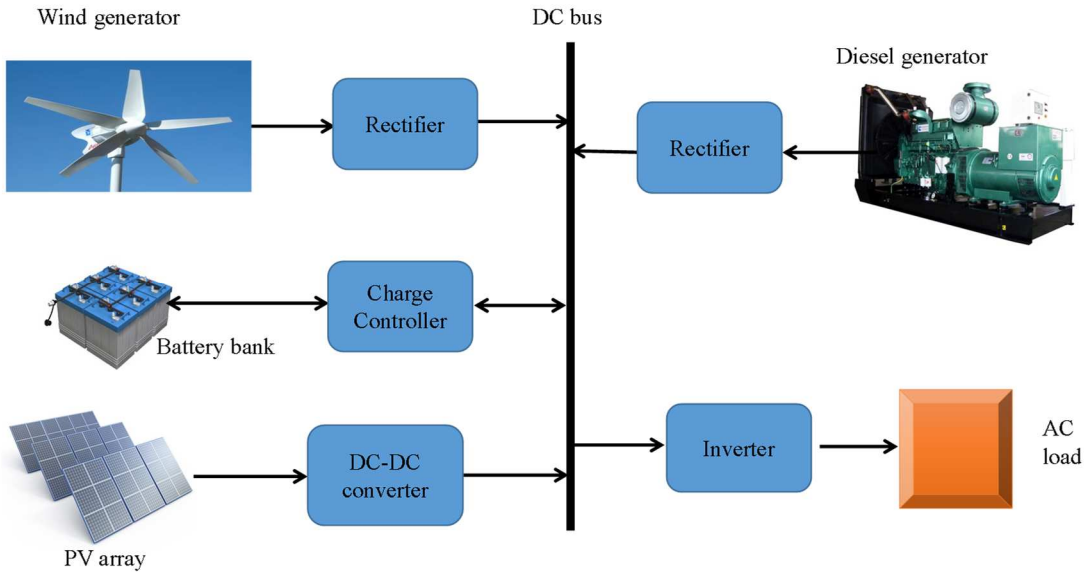

Figure 2-10 Off-grid hybrid energy system

2.3.1.2 On-grid hybrid energy system

This type of hybrid energy system is connected to the grid, as a result, the problem of the unsteady nature of the renewable sources is tackled. With this type of hybrid energy system as in [15], there is an increase in the performance of the system as situations of energy shortage is provided for and when excess energy is generated, it is sold and distributed in the electricity market. Integrating a combination of wind and solar energy system as renewable energy sources to the grid helps to make the supply of electricity from the renewable sources more reliable and it also helps to reduce the total cost of generation [16]. It can be of AC coupling or DC coupling. An example of an on-grid system with DC coupling is as shown in figure 2-11

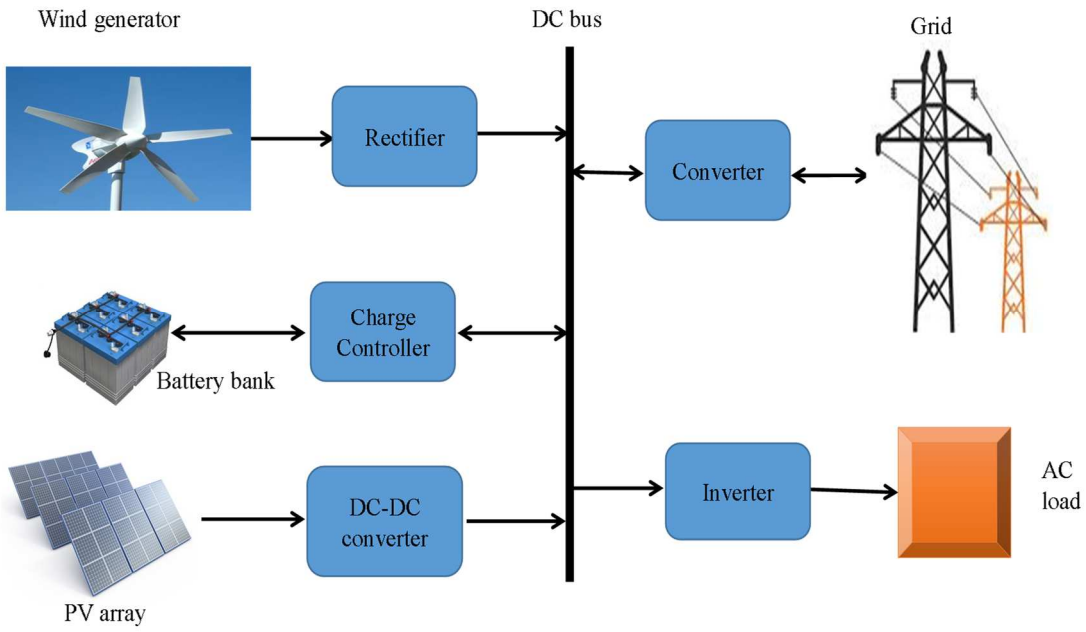

Figure 2-11 On-grid hybrid energy system with DC coupling

Conversely, examples of the on-grid hybrid energy system with AC coupling and that without battery backup, are as shown in figure 2-12 and 2-13 respectively.

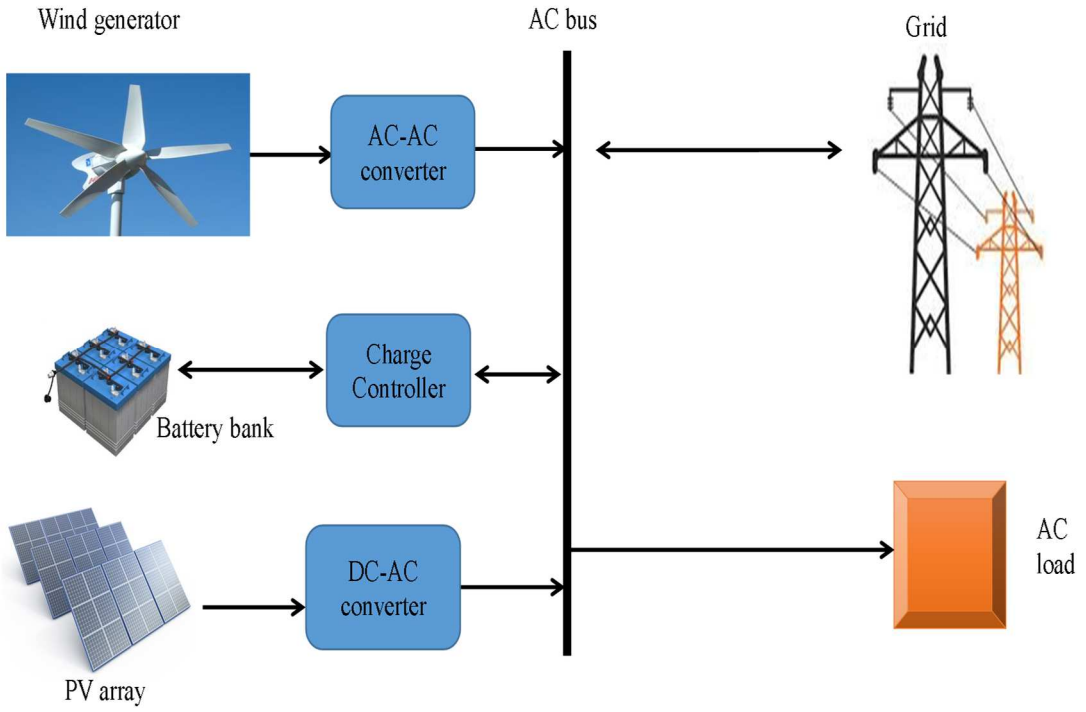

Figure 2-12 On-grid hybrid energy system with AC coupling

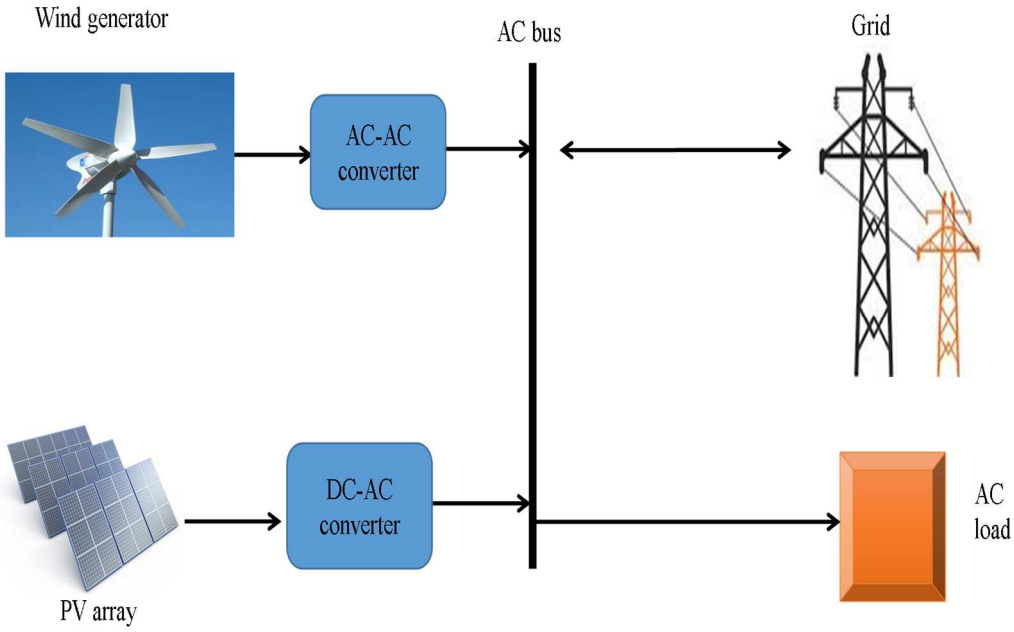

Figure 2-13 On-grid hybrid energy system without battery

2.3.2 Classification based on configuration

Based on configuration, we have three major types of hybrid energy system, namely series, parallel and switched configuration.

2.3.2.1 Series configuration.

This configuration can be implemented using two different bus mode, namely the AC bus mode and the DC bus mode as in [17]. Using the DC mode for illustration, the battery gets DC power from all the different sources of power in the network and each of the devices is connected with a separate power electronics device as shown in figure 2-10

In this configuration all the energy generated from AC sources are converted to DC with the help of the rectifier, to enable the system to achieve peak load, proper sizing of the inverter and diesel generator has to be achieved. In this mode, a great proportion of the generated power passes through the battery storage and as such, the efficiency of the system diminishes due to the elevated battery bank cycling. Furthermore, electricity is provided to the AC load with the help of the inverter. Losses due to conversion are prominent, as power from the diesel generator is converted to DC with the help of the rectifier, after which, it is converted to AC with the help of the inverter. Charge controllers are incorporated into each of the sources to ensure the battery banks are not overcharged [18]. This type of hybrid system is also referred to as centralized DC-bus

Merits of series configuration with DC mode

- Generator start-up does not affect the power delivered to the load.
- The electrical output interface is simple as there is the absence of AC power switching among the different sources of energy
- Square wave, modified square wave, and sine wave can be obtained from the inverter as it now depends on the application

Demerits of series configuration with DC mode.

- The diesel generator cannot provide electricity to the load directly hence, there is a reduction in efficiency.
- Since the generator cannot provide electricity directly to the load, hence inverter failure results in power loss.
- Battery lifetime reduces due to frequent battery bank recycling.

Conversely, for the series configuration with AC coupling as in [19], the point of connection is on the AC side. The diesel generator, the battery, and the PV array are connected to the AC bus with the help of appropriate converters. The bidirectional converter connects the battery storage to the AC bus. The bidirectional converter makes charging of the battery from all the sources possible. Efficiency reduction due to elevated battery bank cycling as in the case with the DC mode is less.

Advantages of AC mode

- The diesel generator can provide electricity to the load directly.
- It is technically simple
- There is a reduced number of converters and hence losses due to conversion are reduced

Disadvantages of AC mode

- Since the Generator cannot provide electricity directly to a DC load connected to the network, the rectifier failure leads to loss of power supply.
- Energy needs to be stored in the battery during the nights, hence its efficiency is less compared to the DC mode.

An example of a series configuration with AC coupling is as shown in figure 2-14

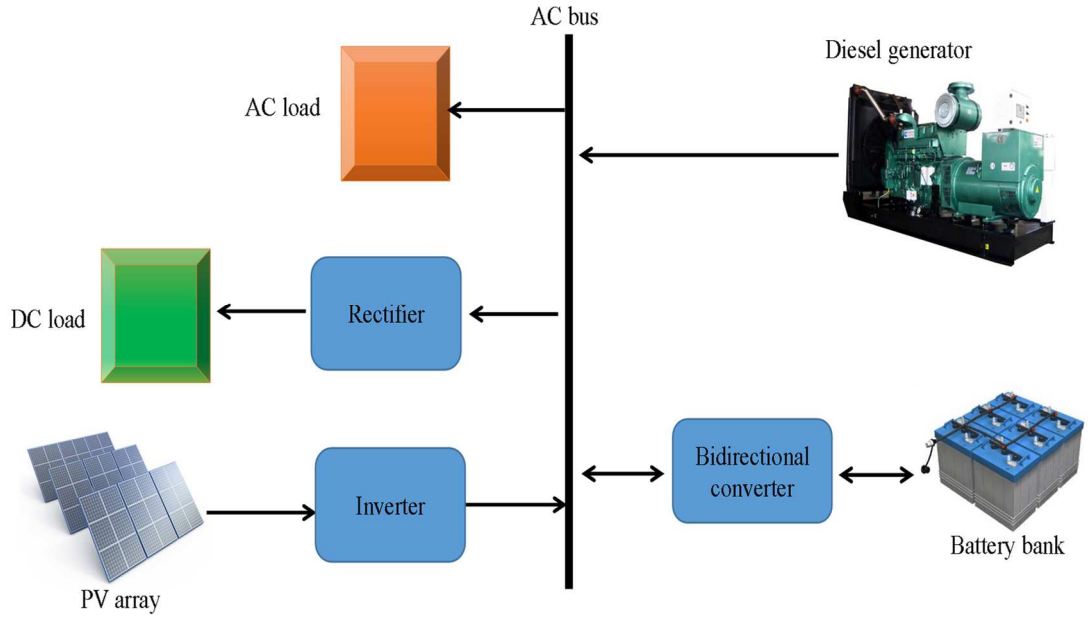

Figure 2-14 Series configuration with AC coupling

2.3.2.2 Switched configuration

It appears to be the commonest hybrid system configuration in countries that are still developing, like the series configuration, there is the absence of parallel operation among the source of electricity generation, but it gives room for the generator or the inverter to operate since each of them produces AC. Unlike the series configuration, the engine-driven generator can provide electricity directly to the load and as such, its total conversion efficiency is higher than the series configuration. The system battery bank is charged with the help of the renewable energy sources and diesel generator. The excess energy obtained from the diesel generator is normally utilized in re-charging the system batteries, in a situation when the demand for electricity is low, the engine-driven generator is put off and, electricity is provided to the load from the photovoltaic panel and the energy stored in the batteries. An example of the switched configuration is as shown in figure 2-15.

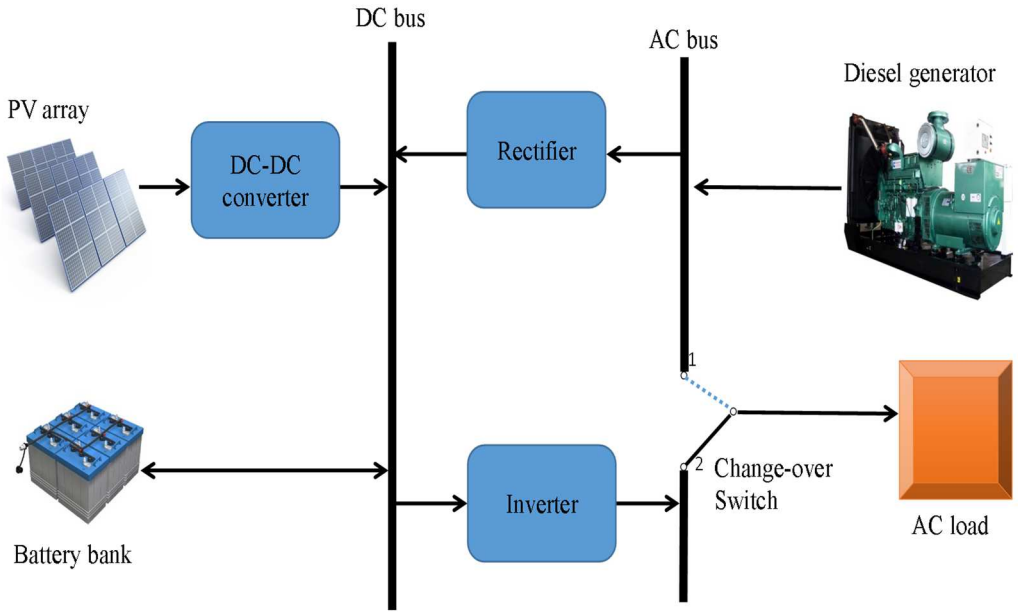

Figure 2-15 switched configuration

Merits of switched configuration

- Like the series configuration, the different inverter waveforms can be generated and that depends on the type of application.
- The load can receive electricity from the diesel generator directly and as such, there is a reduction in fuel consumption and the efficiency is enhanced.

Demerits of switched configuration

- During the transfer of AC sources of power, there is a temporary disturbance in the electricity supply to the load
- Because both the inverter and the engine-driven generator are fashioned to give out peak load, their individual strength to deliver power when each operates partly is reduced.

2.3.2.3 Parallel configuration

This configuration is grouped into two categories; that which requires the coupling with AC and another which requires coupling with DC but in each case, a bi-directional inverter is required to join the battery with an AC source in the system. The AC source, in this case, is usually the diesel generator, this bi-directional inverter can function both as an inverter and as a rectifier, in a situation where the generator is faced with an overload, it can also perform the function of peak shaving. Under normal condition, the bi-directional inverter does convert DC

to AC but performs the function of a rectifier, in the process of charging the batteries when the energy from the generator or the other renewable is in excess. In this type of configuration, energy from renewable sources, e.g. wind, solar, etc are coupled on the DC side.

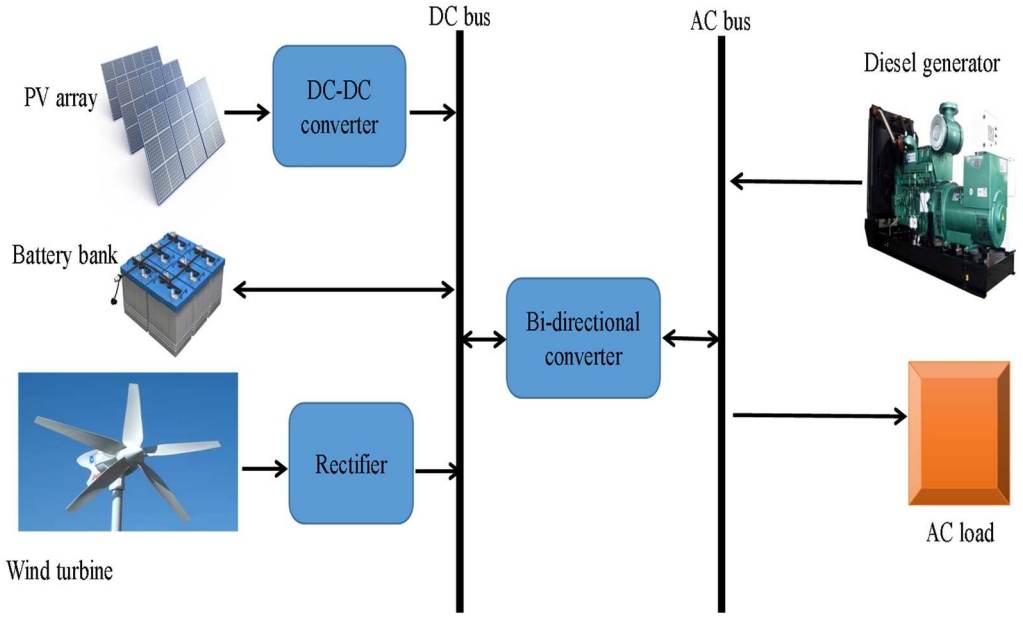

Figure 2-16 Parallel hybrid PV/Wind/Diesel Generator system with DC coupling

The parallel hybrid PV/Wind/Diesel Generator system with AC coupling is as shown in figure 2-17

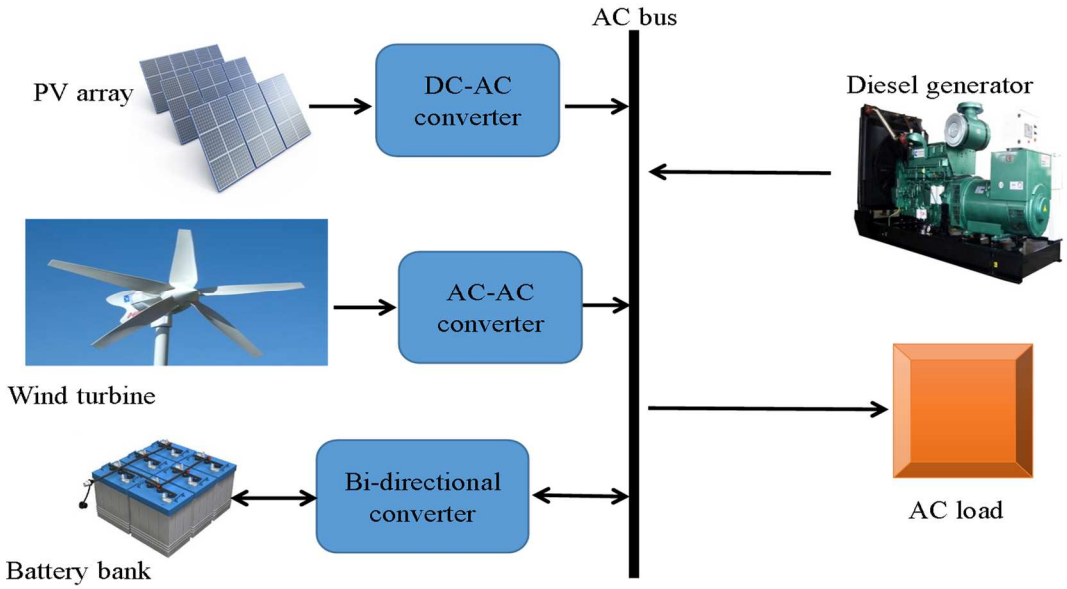

Figure 2-17 Parallel hybrid PV/Wind/Diesel Generator System with AC coupling

2.3.3 Classification based on the method of integration

Hybrid energy is grouped into three different modes based on the bus used for connecting the different component of the hybrid energy system, electricity production and usage depends on the connection requirements of the bus. The three different modes of hybrid energy systems are the DC bus mode, AC bus mode and Hybrid bus mode [20] [15]

2.3.3.1 AC bus hybrid system.

In this type of hybrid energy system, energy from several sources are joined to the AC bus through the help of appropriate power electronic devices. The bus supply electricity to DC loads with the help of the AC/DC converter while the AC loads are supplied with electricity directly from the AC bus. The battery bank used for energy storage is linked to the system with the help of a bi-directional converter [20].

They can be used for higher voltages compared to the DC-coupled hybrid energy system and are technically simple. This configuration is grouped into two modes, namely high-frequency AC mode and power frequency AC mode, an example of an AC coupled hybrid energy system is as shown in figure 2-18.

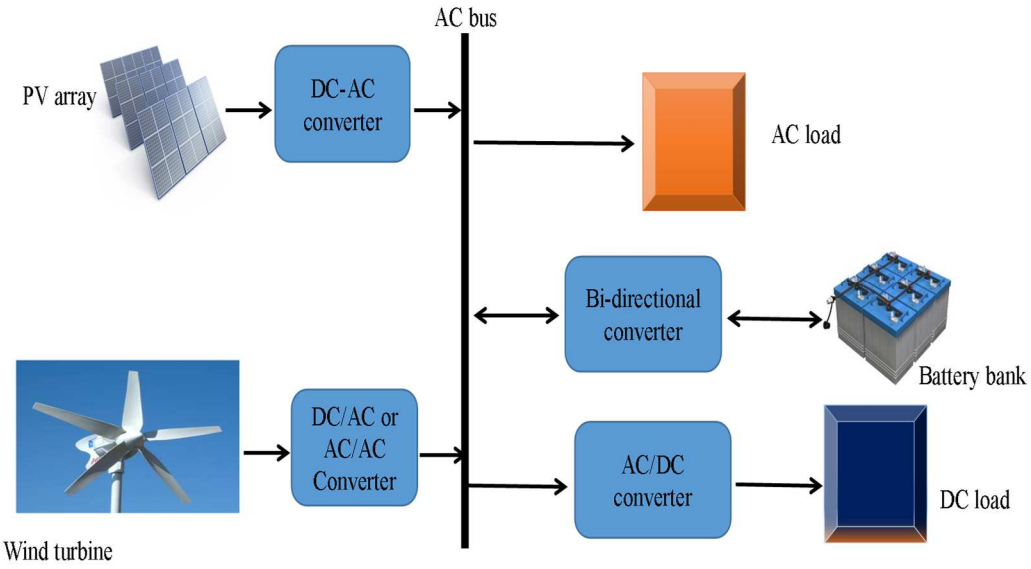

Figure 2-18 AC bus hybrid system

2.3.3.2 DC bus hybrid system.

This type of hybrid system is generally utilized for small size hybrid systems, sources of AC in the network, for example, diesel generator and the Wind turbine are connected to the bus with the help of AC/DC converter [21]. It is usually simple to use and their losses are reduced, the DC loads get electricity supply from the DC side while the AC loads get their electricity

via the converter. The system is a flexible system as in [22] and as such can also be joined to an alternating current load of frequency 50/60hetz. The DC hybrid energy system also has some demerits for example, if the hybrid system is connected to the grid, and the converter, which connects the DC bus, and the grid is faulty, AC power cannot be provided. The DC bus hybrid system is as shown in figure 2-19.

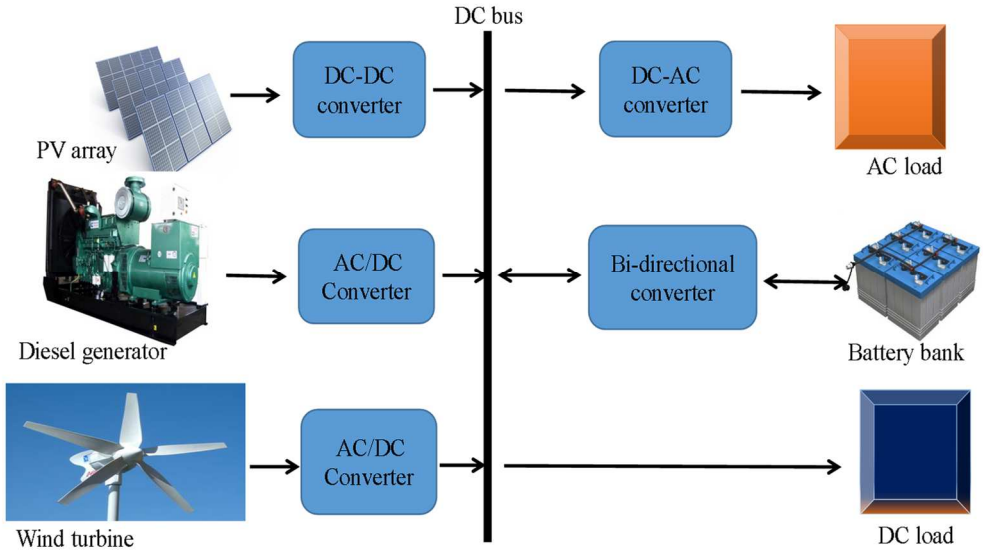

Figure 2-19 DC bus hybrid System

2.3.3.4 Hybrid bus system.

This type of configuration utilizes both AC and DC bus for the connection of the network devices. Solar energy and other sources of DC power are connected to the DC bus. The supply of electricity to the DC load is done directly from the DC bus with or without a DC/DC converter. AC loads can be served from the AC bus. Since the AC loads are supplied with power from the AC bus and the DC loads are supplied with power from the DC bus, the number of converters used in the configuration is reduced. Hence the reduction in the number of converters helps to minimize losses in the system. One of the demerits of this configuration is that its control is more demanding as power balance is required every time with the two different physical links involved [22]. An example of a hybrid bus hybrid system is shown in figure 2-20.

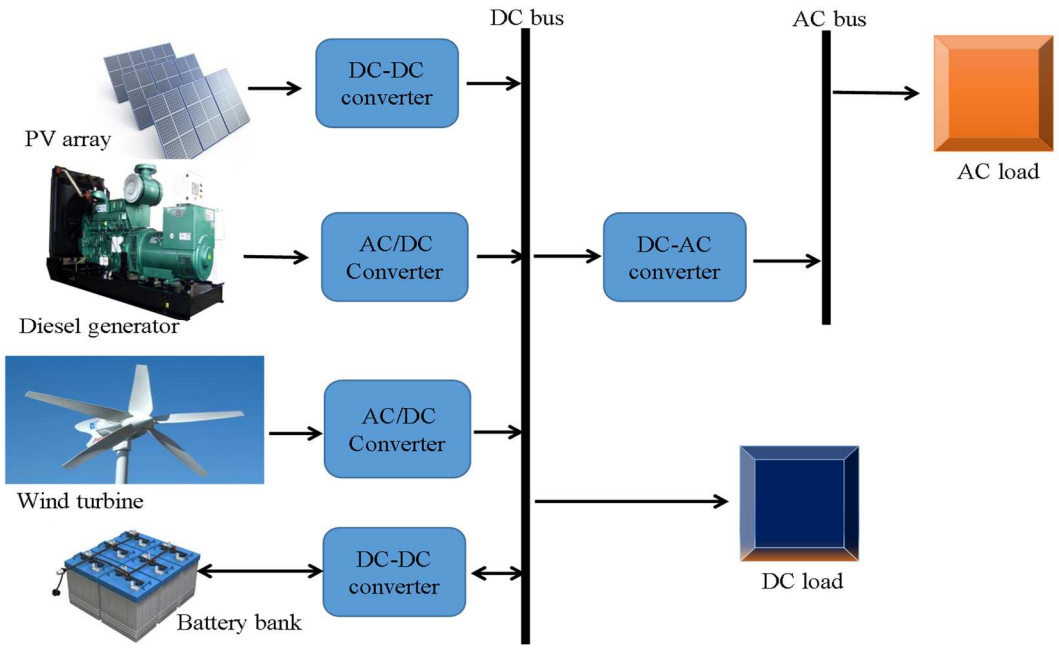

Figure 2-20 Hybrid bus System.

2.3.4 Classification of hybrid systems based on integration elements

The hybrid system comprises several devices integrated together to provide electricity, these different devices used for the integration of the hybrid system determine the battery storage, the generation as well as the demand. On this basis, the hybrid system is defined in terms of demand, generation, and Energy Storage.

2.3.4.1 Demand

The hybrid energy system is considered based on the intended applications to be supplied with electricity, examples of these applications are residential uses, telecommunication stations in isolation, desalinization processes, etc. For grid-connected hybrid energy system, the grid also serves a demand in the times of excess energy or when power is expected to be supplied to the grid or local utility system where power balance is required as reported in previous research [15]. Demand can also be achieved through the combination of one or more sources of renewable energy and a conventional source of energy as in [23]

2.3.4.2 Generation

Hybrid energy system, in this case, is based on the sources integrated for the hybrid power generation, this could be a combination of solar panels and wind turbine, solar panels and hydro turbine, solar panel, hydro turbine, and wind turbine. In most cases, especially in a

standalone system, the diesel generator is often used as the backup source of power in the event of power failure. A hybrid system consisting of wind and solar energy is generally deemed as a justifiable means of producing electricity using renewable energy resources. For grid-connected hybrid energy systems, in a situation of inadequate battery storage and power generation from the renewable energy sources, the grid serves as a generator [15].

2.3.4.3 The energy storage system

The energy storage of small devices is achieved with the aid of Supercapacitors and/or batteries, this ensures the transients which occur during changes in load or generation are absorbed and the internal DC bus voltage is stabilized. The battery or the supercapacitors serve as the available means of storage and hence helps plays an important role in the system operation [15]. For every installation that involves battery installation, the required battery current, as well as its voltage level, is usually achieved by joining the battery cells in parallel and series electrically. Batteries which are usually rated based on their power and energy capacities has some other key properties e.g., lifespan, depth of discharge, operating temperature, energy density and self-discharge as reported in previous work [24]. It is reported in a recent research [20], that energy storage systems can be grouped based on two categories viz:

(a) Timeframe as shown in figure 2-21

(b) The form of energy storage as shown in figure 2-22

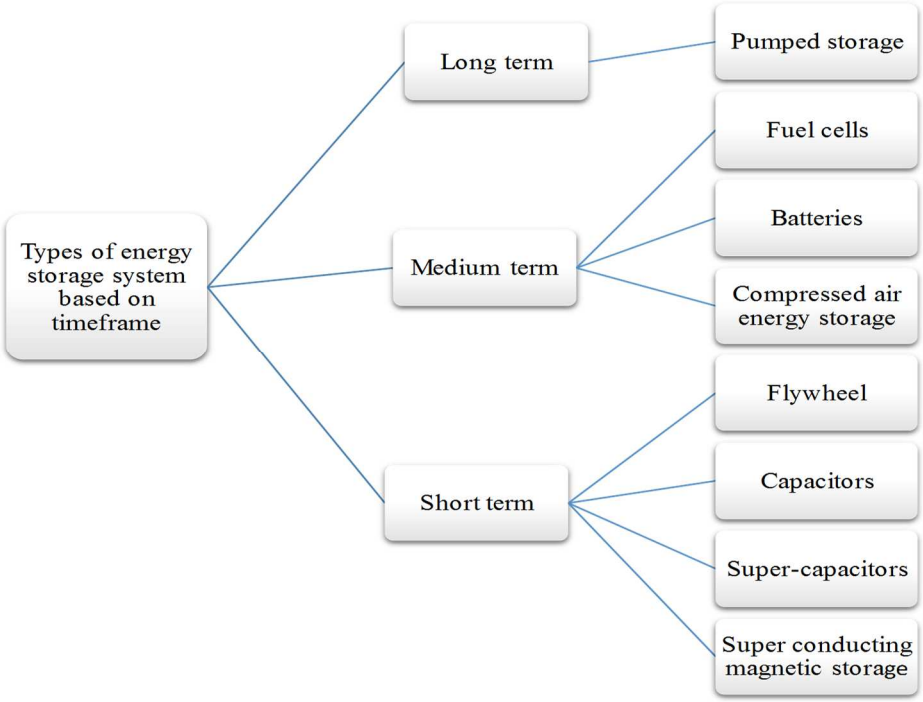

Figure 2-21 Classification of energy storage system based on time frame.

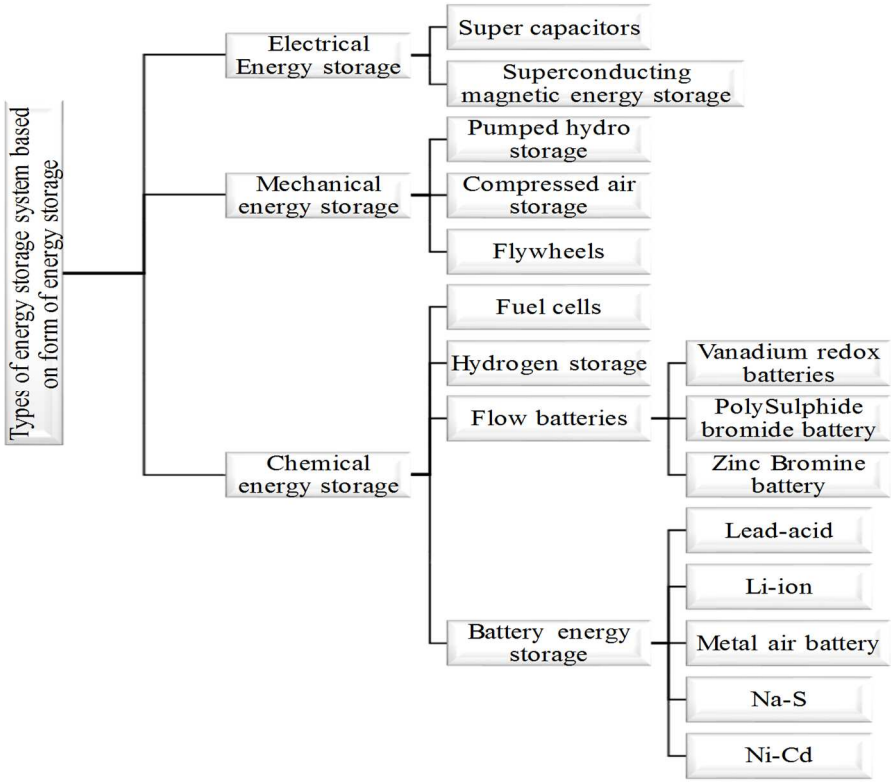

Figure 2-22 Classification of energy storage based on the form of energy storage.

The energy storage system operates in three different modes, namely, storage mode, discharging mode and charging mode.

Storage mode: under this mode, the energy demand is almost equal to the energy generated and energy is stored by the storage system.

Discharging mode: in this mode, the energy demanded by the load is more than the amount of energy generated and the storage system supplies the deficit energy required.

Charging mode: in this case, the energy demanded by the load is less than the amount of energy generated at that time and the excess energy is stored by the storage system.

2.3.5 Classification of hybrid systems based on system configuration

The classification of the hybrid energy system is based on the number of renewable energy sources and battery storage involved. The different types of hybrid energy system under this classification are as given below

- Single generation & single storage system
- Single generation and hybrid storage system
- Hybrid generation and single storage system
- Hybrid generation and hybrid storage system

2.3.5.1 Single generation & single storage system

This refers to a hybrid energy system, which comprises a single source of generation and a single battery storage system. A typical example of this type of hybrid energy system is the hybrid solar energy system in [25] which comprises an off-grid solar energy system with a utility backup power as shown in figure 2-23.

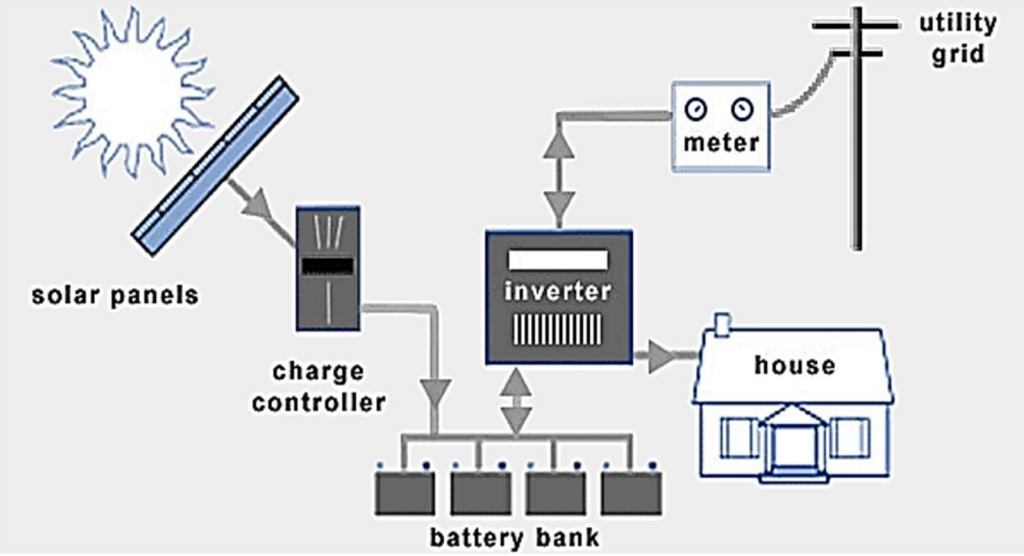

Figure 2-23 Off-grid solar energy system with a utility backup power

The system comprises of solar panels, utility grid, power meter, Battery-based Grid-Tied inverter, Battery bank, DC disconnect, and charge controller.

2.3.5.2 Single generation & hybrid storage system

This is a hybrid energy system which, which is made up of a single source of generation and more than one form of storage. An example of this type of hybrid system as shown in a past research [26] is given in figure 2-24. The energy supply represents, for example, electricity supply from wind turbine generator and the system is supported by two separate means of energy storage.

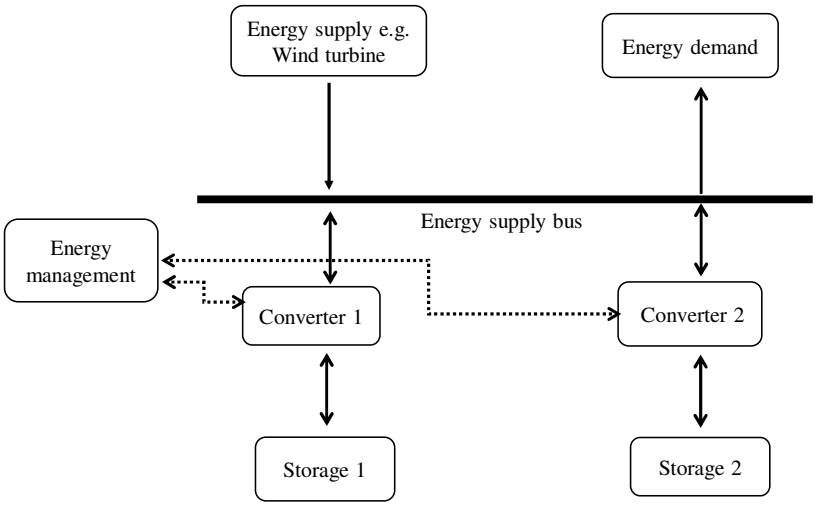

Figure 2-24 Single energy source with hybrid means of storage

2.3.5.3 Hybrid generation and single storage system

This is the commonest type of hybrid energy system, it incorporates more than one source of energy and a single storage system. An example of the grid-connected hybrid energy system with a single source of battery storage is as shown in figure 2-25.

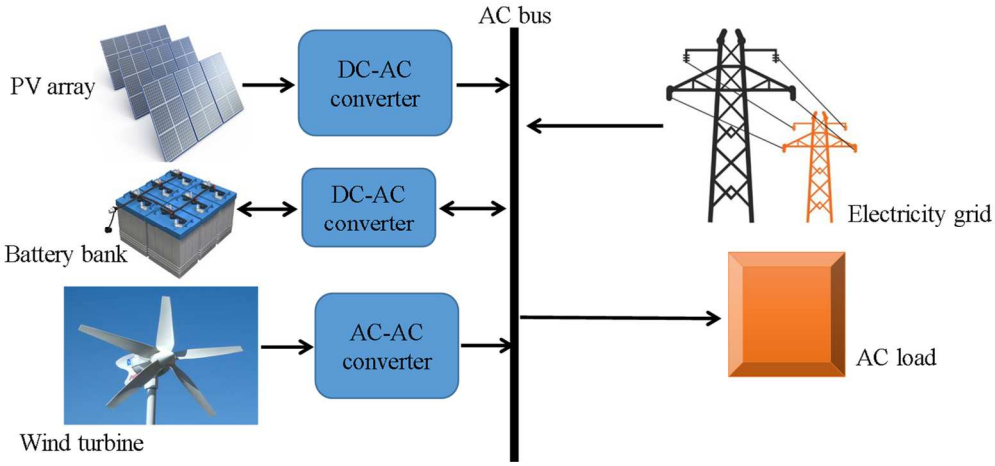

Figure 2-25 hybrid energy sources with a single means of storage

2.3.5.4 Hybrid generation & hybrid storage system.

This type of hybrid system comprises more than one source of energy generation and battery storage, an example of this type of hybrid energy system is studied in [26], where PV array and Wind turbine serve as the sources of renewable energy while the energy storage system is made up of a hybrid of battery and supercapacitor. The hybrid system is as shown in figure 2-26.

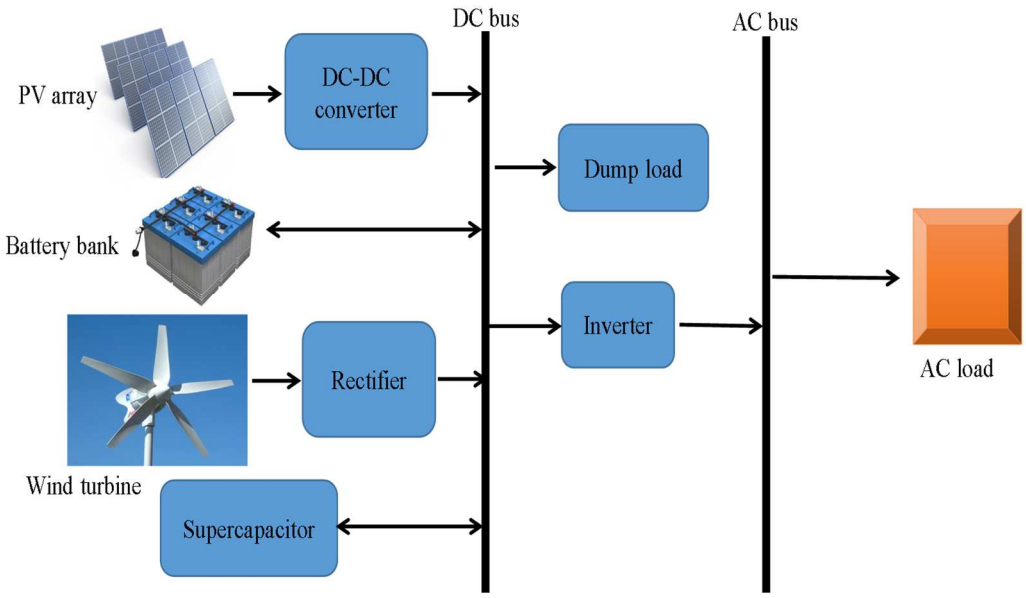

Figure 2-26 PV/Wind energy system with hybrid battery super-capacitor storage system.

For the Photovoltaic module to make a meaning contribution to the hybrid system, power output, efficiency of the PV module is a necessity.

2.4 PV module efficiency.

The research location for this project experiences a long period of sunlight and that offers it a good potential for electricity generation from solar energy. Solar energy at peak of solar radiation produces less energy most importantly when it has been exposed to intense sunlight for a long period of time. The efficiency of the PV module is affected by a number of factors, as mentioned below.

2.5 Factors, which affects the efficiency of the PV module: an overview.

There is a growing interest in the use of the photovoltaic module as a major source of future power generation. Several countries, which experience a long period of sunshine daily, see the PV module as a device that can be used to generate free power if properly utilized. According to a past research [27], energy from the sun is inexhaustible, free and clean and is the focal point of several researchers in power. For efficient utilization of the PV module for electricity generation, there is a need to improve the efficiency of the PV module. The efficiency of the PV module is that section of the energy from the sun falling on the PV module that is transformed into electricity [28].

A recent research [29], reports that Solar cell performance depends on three major factors and these are:

- The kind of semiconductor materials used to absorb photons and change it to electron-hole pairs
- The kind of semiconductor formed that separates the holes and electrons
- The contacts at the rear and front of the solar cell, the channels through which current passes to the external circuit.

For the PV module to serve its desired purpose there is a need for quality. Some of the requirements for a quality photovoltaic energy system according to [30] are as follows:

- The sizing and orientation should be done properly, to supply electrical power and energy
- It must include an efficient control circuit to minimize overcurrent protection, electrical losses etc.
- It must contain an efficient charge controller and a battery storage system should batteries are involved.

The PV module efficiency is affected by several factors as shown in figure 2-27 and these factors are grouped into three categories namely, cell materials, PV system devices, and Environmental factors.

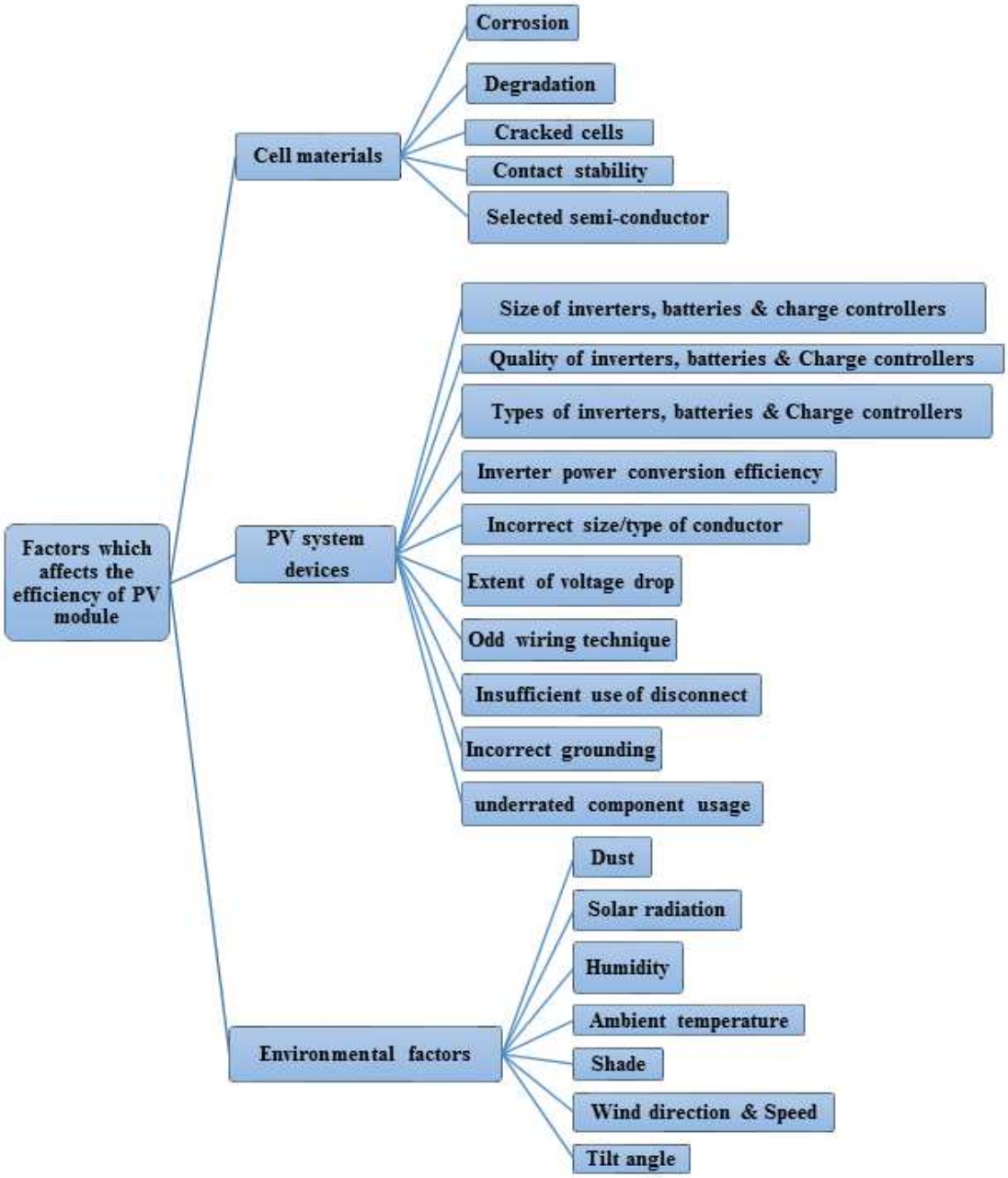

Figure 2-27. Factors, which affects the efficiency of photovoltaic module performance [30]

2.5.1 Cell materials

The solar cell is made of semiconductor materials, the commonest of these materials are the monocrystalline silicon, amorphous silicon, polycrystalline silicon and copper-indium selenide (CIS). These materials, which are used for the fabrication of the photovoltaic modules are affected by a number of factors, which retards their ability to generate electricity. These factors are:

2.5.1.1 Effect of corrosion on PV module efficiency

Corrosion is said to have taken place when a material begins to decay due to the chemical reaction between the material and its surrounding environment. A metallic surface is affected by corrosion when liquid or gas makes contact with any of its exposed parts, the process of corrosion usually is triggered by the presence of salts, acids, and warm temperature. Corrosion affects the majority of metals [32]. A recent research [33], reports that the corrosion of the PV module conductive layer occurs when moisture penetrates the edges of the module. Thin film modules mostly are affected by moisture, which enters via the edges of the module because they are frameless. Another research [34], reports that the series resistance of the module is usually increased by corrosion, and that corrosion results in the significant loss in the module performance and hence the module efficiency reduces

2.5.1.2 Effect of degradation on PV efficiency

Degradation appears as a major factor, which decreases the PV module lifetime; the process of degradation depends on climatic and physical factors. Degradation results in the decrease in the quantity of electricity generated from the module and this reduction in the capacity of the module to generate power becomes evident in the module characteristics such as the short-circuit current, open-circuit voltage, fill factor (FF), maximum power output (Pmax), maximum output voltage (Voc), P-V and I-V curves [35]. The efficiency of the PV module reduces with increase in the module degradation and the different types of module degradation as reported in a past research [36] is as shown in figure 2-28

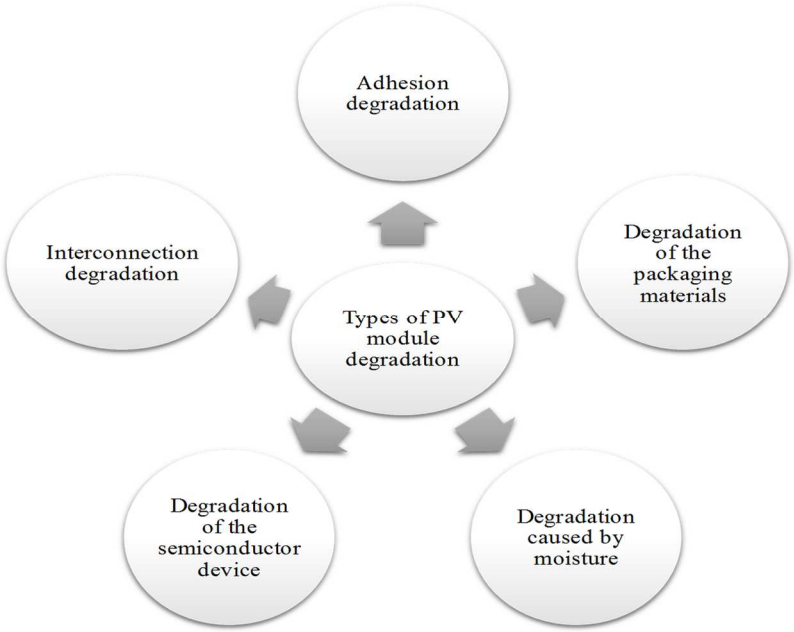

Figure 2-28 Types of PV module degradation

2.5.1.3 The effect of cracked cells on PV module efficiency.

Cracking of PV module cells is an inevitable problem that is common with the PV technology, the presence of cracks on a PV module affects the module's lifespan as well as its efficiency. Cracks in a solar cell present a different effect on the module's power output. If a particular single crack creates a disconnection of a vital cell element, it could lead to a significant loss in the module output power. Conversely, if the crack does not result in the disconnection of a vital element of the cell, the module performance is affected lightly [37]. A recent research work [38] reports that factors like hailstorms, heavy wind, as well as snow loads, have the ability to cause cracks on the surface of the modules. Essential parts of the cell may be disconnected due to these cracks and result in a reduction in the ability of the module to generate maximum power and hence the efficiency is reduced. According to the same research work, there different kinds of cracks that affect the PV module and these are as shown in figure 2-29.

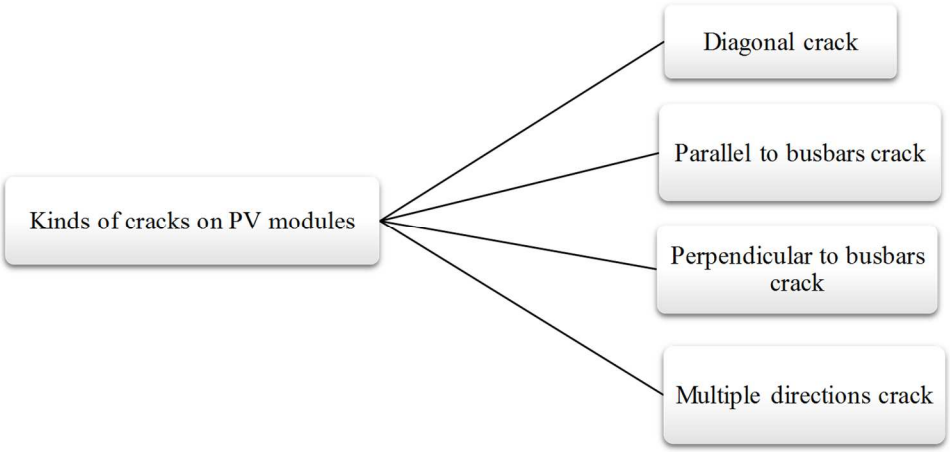

Figure 2-29 Kinds of cracks on PV modules

2.5.1.4 The effect of contact stability on PV module efficiency

The contact at the rear and front of the solar cell, the channels through which current move to the external circuit also has a role to play in the performance of the solar cell. The moment the holes and electrons are separated in the module semiconductor, they need to be collected in order for them to flow through an electrical circuit, hence there is a need for an electrical contact. The contact on the surface of the panel where light passes should be in a manner that it can gather as much carrier as possible and it must not shade more than 10% of the surface of the cell. Conversely, the surface contact of the rear of the panel has to be a metal sheet. There is a need for the creation of a good ohmic contact between the semiconductor and the metal interface to minimize losses as the module performance increases as the losses decrease

[29]. Recent research work [39], reports that the mechanical stability of photovoltaic cells affects both the reliability of the module and potential power degradation. Conversely, the research stated that the mechanical stability of the cells in a PV module reduces as the cell thickness reduces.

2.5.1.5 Effect of the selected semiconductor on solar panel performance

Asides production cost, the module efficiency appears to be the main metrics for Photovoltaic modules used in several applications, in terms of efficiency, crystalline silicon still ranks highest in efficiency at the module level followed by CIGS thin-film [40]. The material composition of the module, as well as the energy gap of the semiconductor materials, is very important, as solar cell made of semiconductors, which has energy gaps lying between 1.3 and 1.6eV stands to yield maximum performance [41]. Increase in module efficiency, as well as power output, increases with an increase in the use of solar cells made of materials with high energy conversion efficiency.

2.5.2 PV system devices

The devices use for the installation of a solar energy system for the electricity generation purpose are very useful but they also have their drawbacks. Once they are not utilized effectively or their performance is being retarded due to equipment failure or other factors, the efficiency of the modules reduces. These factors are as shown below:

2.5.2.1 Size of inverters, batteries and charge controller

The PV module efficiency is driven by the efficiency of the inverter, which is responsible for the conversion of direct current (DC) to alternating current (AC). On the other hand, the charge controller keeps the battery from overcharging, and also ensures that the batteries do not return the charge to the charging source while the charges are stored in the batteries. In a situation where the inverter is under-sized, a fraction of the module 's power output will be clipped by the inverter in order to ensure that the inverter's rated capacity is not exceeded. Conversely, over-sizing the inverter implies installing an inverter whose capacity is more than the PV module nominal capacity, this is usually implemented for future expansion purpose but it is not usually recommended. Using the wrong size of inverters, batteries and charge controller will result in poor performance or failure of the system and this reduces the efficiency of the system [42].

2.5.2.2 Effect of Inverter power conversion efficiency on PV performance

The power conversion efficiency of the inverter used in a PV installation for DC to AC conversion is very important. The efficiency of the inverter determines the amount of DC power from the panel that is converted to AC power, as a fraction of the power may be lost as heat energy, besides some power is also used up when the inverter is left in powered mode [43]. In [44] several Photovoltaic systems make use of inverters, whose power rating is lower than that of the solar panel, as it has been observed that the PV panel may not give out power at its rated efficiency for a long duration of time. This system is adapted to ensure the initial input voltage and maximum point voltage range are met oftentimes. The PV performance increases with the use of an inverter with high power conversion efficiency. The power conversion efficiency of the inverter as in [45] reduces in the following ways:

- Installing the inverter in a manner that it is exposed to sunlight directly
- Exposing the inverter to insufficient ventilation
- Installing the inverter near or on a combustible surface

2.5.2.3 Effect of incorrect size/ type of conductor.

Conductors such as the cables used for PV installations as [46] are usually designed to:

- Withstand exposure to U.V rays, which comes from sunlight,
- Be water resistant
- Withstand extreme temperatures

The solar energy systems designed to utilize standard color-coded solar cable and interconnect sizes. During the installation of the PV system, the cables or conductors are exposed to high level of twisting, abrasions, and flexing as they are passed via the conduits as these may affect the insulation on the cable. The use of the incorrect size/type of cable conductor may affect the performance of the installation or cause the installation to fail.

2.5.2.4 Effect of extent of voltage drop on PV performance

Voltage drop refers to the amount of the electrical potential loss that occurs inevitably when current passes through a conductor between the source and the load. Voltage drop depends on the total length of the conductor through which the current passes. The voltage drop must not exceed the allowable amount of voltage drop for a cable installation, for instance, the voltage drop on the cable connected from the PV panel to the inverter should be about 3% ie 2% on the DC side and 1% on the AC side. The PV system cabling work should be done in a manner that minimizes resistive loss to a value < 3% for efficiency purpose [47]. It is necessary to

minimize losses from PV energy system as it leads to a waste of energy and hence a reduction in the efficiency of the system [48].

2.5.2.5 Odd wiring technique

Wrong wiring technique is one of the factors, which reduces the performance of solar panel installations. When PV modules produced by different manufacturers or of different wattage or voltage are joined together, the challenge is not the vendors, but the challenge lies with the differences in the performance degradation and the characteristics of the different PV modules combined. To combine PV modules together, only PV modules of similar or exact current should be connected together. If you join a 5A PV module to another PV module of 5.8A, the overall current reduces to 5A, this reduction in the total current also results in a decrease in the output power and hence a reduction in the performance of the system. Conversely, If you join a 20V PV module with a 30V PV module, the total voltage reduces to 20V, this reduction in voltage results in the reduction in the output power hence, a drop in the performance of the system [49].

2.5.2.6 Insufficient use of disconnect

The PV energy system requires an adequate amount of disconnects in order to protect the system from failing, a heavy load connected to the solar system requires a separate disconnect to aid its isolation from the system when it is not supposed to be supplied with electricity. As suggested in a past research work [50], the design should be able to protect the components of the system from short circuits, reverse polarity connections and electrical storms. Fuses or circuit breaker should be installed on the positive line close to the battery. A lighting surge protection and other relevant devices must be fixed with the required means of disconnection. Fitting solar systems with the required number of disconnect helps to minimise failure, but installing less than the required number of disconnects put the system at a high risk of failure and poor performance becomes inevitable. The use of the required number disconnects and over-current protection is a significant safety aspect of the system electrical design.

2.5.2.7 Effect of Incorrect grounding on PV performance.

The performance of the solar energy installation is also at a risk of failure or poor performance if it is not properly grounded. Some of the challenges as in [45], could be due to the followings

- Lack of lightning protection
- Allowing the grounding conductor to make contact with the module frames and the aluminium rails

- Installation of PV energy system in an exposed location.

Incorrect grounding affects the entire solar energy installations as it leads to poor performance and hence, the eventual failure of the installation.

2.5.2.8 Underrated component usage

In order for the PV installation to start out right, and keep running at peak efficiency, it is important for us to make use of the right size and type of cables and components used in the installation. Failure to use the right components implies usage of inferior or faulty components for installation. This will reduce the overall performance of the installation and consequently results in system collapse.

2.5.3 Environmental factors

Several environmental factors are responsible for the reduction in the performance of PV modules, and the effect of these environmental factors can be minimised to enable the PV module to function better. Some of the key environmental factors, which retards the efficiency of the PV modules are as discussed below:

2.5.3.1 Effect of dust on PV module efficiency

Dust particles have also been found to affect the efficiency of the PV module. In a recent research [51], an experiment was conducted to ascertain the performance of the PV module exposed to dust. The result of the experiments shows that an installed PV module without cleaning for more than six months can record about 50% reduction in its power output. In [29], it was observed that it is during the dry season that the PV module experiences dust accumulation the most. Accumulation of dust on the surface of the PV module reduces the power output of the PV module, and this makes the PV module less efficient, hence for the module to perform efficiently, it is advisable to keep the module surface free from dust particles.

2.5.3.2 The effect of solar radiation on PV module efficiency

The amount of power output generated from the PV module is affected by the irradiance, several other factors of influence are related and these are the angle of incidence and the tilt angle of the PV module. Since solar radiation is required to enable electricity generation by the solar cell, the idea is the more the solar irradiation, the more the power output but in reality, the result is different. This is because, about 15% of the irradiation obtained from the sun is what is transformed into electricity for use, and 85% is converted to heat energy. The heat

energy increases the module temperature and hence reduces the efficiency of the PV module [33]. According to a recent research [52], the amount of solar radiation incident on the surface of the PV module differs as it depends on the position of the panel and the time interval within the day.

The amount of solar radiation incident on a module surface also depends on the type of PV system in place as the radiation depends on the orientation and inclination for a fixed PV system, the kind of tracker for the tracking system while the concentrating PV utilizes normal radiation directly [28].

A report from a past research [53] indicates that as the irradiance increase, the output current increases and hence the greater the amount of electricity generated provided all the relevant parameters are kept constant

2.5.3.3 The effect of humidity on PV modules

The relative humidity of the atmosphere is expressed in terms of its moisture content; it is usually expressed as the ratio of the exact amount of water vapour in the air to the saturated water vapour pressure present at that same temperature. The moment air, which has a constant water vapour experiences a rise in temperature, the relative humidity, reduces as reported by a previous research [54]. This water vapour does not appear visible to the eye but does have an effect on the solar cells. The principal consequence of humidity on the solar panel is corrosion, this corrosion results in the deterioration of the solar cells titanium – silver contact and hence a reduction in the efficiency of the PV module

2.5.3.4 The effect of ambient temperature on PV module efficiency

The ambient temperature, in this case, refers to the air temperature surrounding the installed PV. The temperature of the PV module affects its efficiency and power output tremendously. A recent research [55] shows that Wind speed, cloud patterns, and ambient temperature influence the temperature of the PV module, but its rate of temperature change is influenced by the frame position and PV material. The module generates higher voltages at low temperatures and at high temperature, a reduction in voltage is experienced. As the temperature of the PV module rises, the semiconductor bandgap shrinks and this leads to a reduction in the open circuit voltage, due to the dependence of the p-n junction voltage on temperature [56]. The PV power output tends to decrease as the temperature of the module increases, this is because, at high temperatures, the bulk of the incident radiation is converted

to heat energy and wasted. The module works better at low temperature, hence there is the need for heat extraction from the surface of the PV module during a sunny day.

Heat energy, which increases the module surface temperature is also generated at the same time as electricity generation. The PV module produces heat alongside electricity when exposed to sunlight in several ways as in [57] as shown in figure 2-30

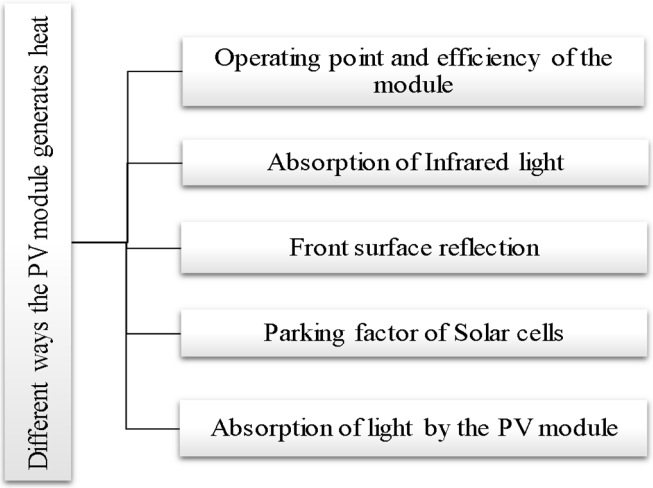

Figure 2-30 several ways PV module generates heat

2.5.3.4.1 The operating point and efficiency of the PV module

The amount of light absorbed by the PV module, which is transformed into usable electricity depends on the solar cell efficiency and operating point. Operating the PV module to obtain the open-circuit voltage or short-circuit current implies that no form of electricity is being generated from the PV module, at such conditions, the solar radiation absorbed by the PV module only produces heat.

2.5.3.4.2 Absorption of infrared light

The smallest amount of energy required by the electron in order to break free is referred to as the band gap of a semiconductor as in [58]. Any light incident on the PV module whose energy is lower than that of the band gap does contribute to electricity generation, but can only add to heating when it is absorbed by the PV module or solar cells. This infrared light is usually absorbed by the aluminium, which forms part of the rear of the panel, but for PV modules whose rear is without aluminium coverage, the infrared passes via the solar cell and goes out.

2.5.3.4.3 Front surface reflection

When a PV module is exposed to sunlight, some of the light rays incidents on the PV module surface are reflected away from the module surface, such reflected ray of light is referred to as electrical loss as they do not add to the electricity generated from the PV module neither do they add to the PV module heating. The module maximum temperature rise is achieved from the product of the reflection and the incident power as reported in [57]

2.5.3.4.4 Parking factor of the solar cells

Solar radiation is absorbed efficiently by solar cells by design. During the absorption, a sizeable amount of heat greater than the required specification is generated by the PV module cells. This generated heat per unit area increases with an increase in the solar cells parking factor.

2.5.3.4.5 Absorption of light by the PV module

The quantity of light, which other parts of the PV Module other than the solar cells absorb, also add to the module heating. The material composition and colour of the rear are the factors which determine the quantity of light to be absorbed.

2.5.3.5 Effect of shading on the PV module efficiency

Shading appears to be one of the many factors, which affects the power output from PV module, the PV modules experience shading from the clouds passing over the installed PV module, electricity poles, trees, buildings within the neighbourhood of the installation and many other means [59]. Shading is experienced, the moment any form of shadow or obstruction appears on any portion of the module surface. According to past research [29], it's a common practice that the PV module is installed to face the sun, and should be positioned in a manner that does not give room for shading as shading reduces the power output and hence the efficiency of the solar panel.

2.5.3.6 Effect of wind direction and wind Speed.

Wind direction and wind speed are important factors, which affects the performance of the PV module. Past research effort shows that [55] the wind direction has less effect on the temperature of the PV module than wind speed and that the wind speed affects the module temperature rise greatly. It was also reported in the same research that the temperature difference between the ambient temperature and the PV cell temperature reduces as the wind speed increases. It was reported in another research [60], that with increasing wind speed, the

efficiency of the PV module rises as the elevation increases, and that the efficiency of the PV module approaches its maximal level when the wind direction is from the north to the rear of the PV module and it creates room for a better heat extraction.

2.5.3.7 Effect of Tilt angle on PV module efficiency

The PV module gets solar radiation from the sky, from the sun directly and also from reflected sunlight from the ground and objects surrounding the module. Mounting the PV module in the appropriate tilt angle and direction will enhance the efficiency. In [61], the PV module tilt angle is an essential variable to consider to ensure the module receives maximum radiation from the sun. This tilt angle depends on the site where the PV installation will be carried out as it is influenced by the sun position; the parameters of interest are the daily position of the sun as well as the monthly and yearly position. In order to achieve maximum power from the sun, it is advisable to ensure that the module is mounted at the optimal tilt angle appropriate for the location. The module is mounted with its plain facing the pole when at a negative tilt angle while it is mounted with its plane facing the equator when the tilt angle is positive.

A recent research [53] reports that generally, during summer, electricity generation is favoured by mounting the module at a tilt angle that is lower while during winter, where a lower irradiance is experienced compared to the summer months, the irradiance is favoured with a higher tilt angle. For better performance in summer, the tilting of the PV module should be lower than the latitude of the location by 15° while for the winter months, it should be at a tilt angle of 15° above that of the location.

Due to the unstable nature of renewable energy resources, wind energy is used as part of the hybrid energy system to help stabilize energy supply from solar energy.

2.6 Wind energy system

The wind energy system comprises generators, wind turbines, interconnection apparatus, control system, etc. It performs an important function of converting the energy in wind movement to mechanical power, and the wind power obtained is converted to electrical energy with the help of the wind turbine. This energy is used to perform useful work, such as in mill grains, water pumping, and to drive machines. The unequal heating of the earth's surface by the sun is what gives rise to wind and wind has Kinetic energy, this kinetic energy is what is converted to electricity by wind turbines [62] [63].

The wind energy system has recorded a tremendous growth than the other sources of energy for the past years and this is majorly due to the interest of the key stakeholders on the reduction of emission, diversification of energy as well as security in the supply of electricity. The global

annual installed wind capacity and the global cumulative installed wind capacity from the year 2001 to 2017 is as shown in figure 2-31 and 2-32 respectively.

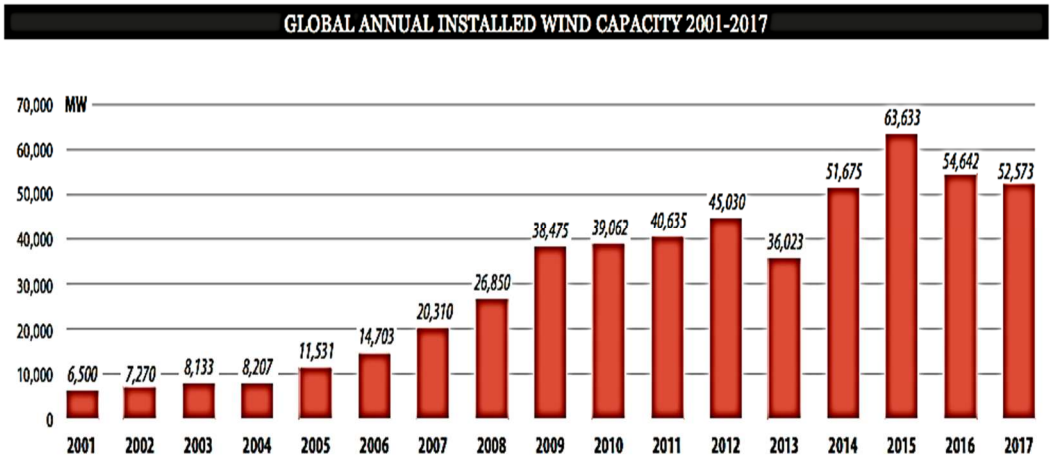

Figure 2-31 Global annual installed wind capacity 2001-2017 [64]

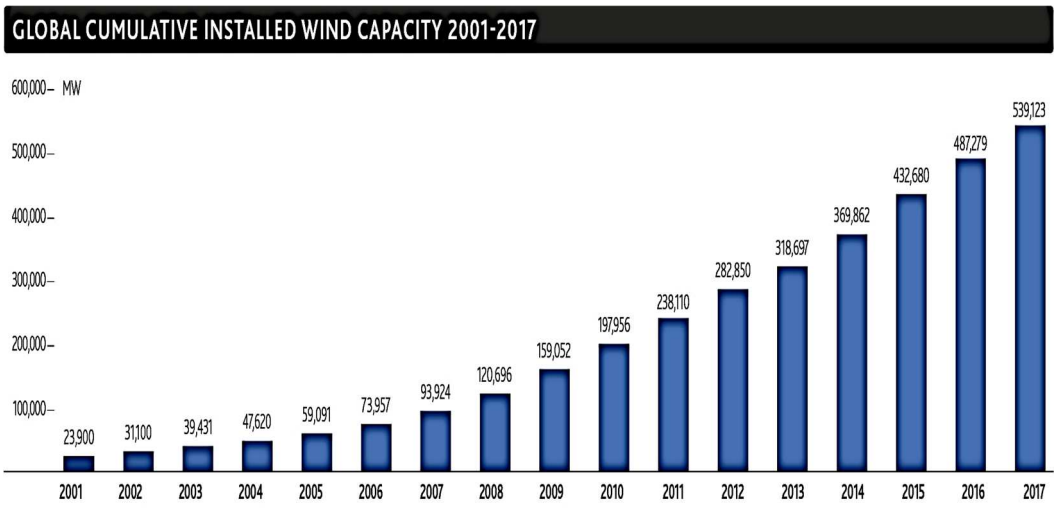

Figure 2-32 Global cumulative installed wind capacity 2001-2017 [64].

According to past research [62], the main factor, which affects the quantity of energy that is converted to electricity by the wind turbine, is the wind speed. The amount of air mass that passes the turbine rotor increases with an increase in wind velocity, the amount of energy in the wind is proportional to the cube of the average speed of the wind. Electricity generation from wind as a renewable energy source as in [65] has the following benefits as in:

- Wind energy is a natural and unpolluted source of power unlike power plants which generate energy from fossil fuel through combustion
- Wind turbines do not produce emissions

- Wind energy can be found in several countries globally as a useful source of energy unlike energy from fossil fuel, which is obtainable in countries with oil deposits.
- Wind turbine installation consumes less space of land and as such landowners can still make good use of their land.
- The wind energy sector provides employment opportunities.
- The wind energy system is a sustainable source of energy.

Despite the numerous benefits associated with the wind as a source of energy, it also faces the following setbacks

- Wind supply though natural and unpolluted is usually irregular
- Wind may not even blow at a time when electricity is in need, it is somehow difficult to store wind energy.
- Conversely, some of the winds cannot be utilized to meet up with electricity demand.
- Sites with good wind speeds are usually in remote areas, and not close to areas which are in need of electricity
- Blades of wind turbine serve as a potential source of risk to birds.

2.6.1 Elements of a wind energy conversion system (WECS)

The elements of the wind energy conversion system according to a past research is made up of the rotor, support tower, Instrumentation, nacelle, gearbox, and control system. The diagram of the key components of the wind energy conversion system as in [62] is shown in figure 2-33.

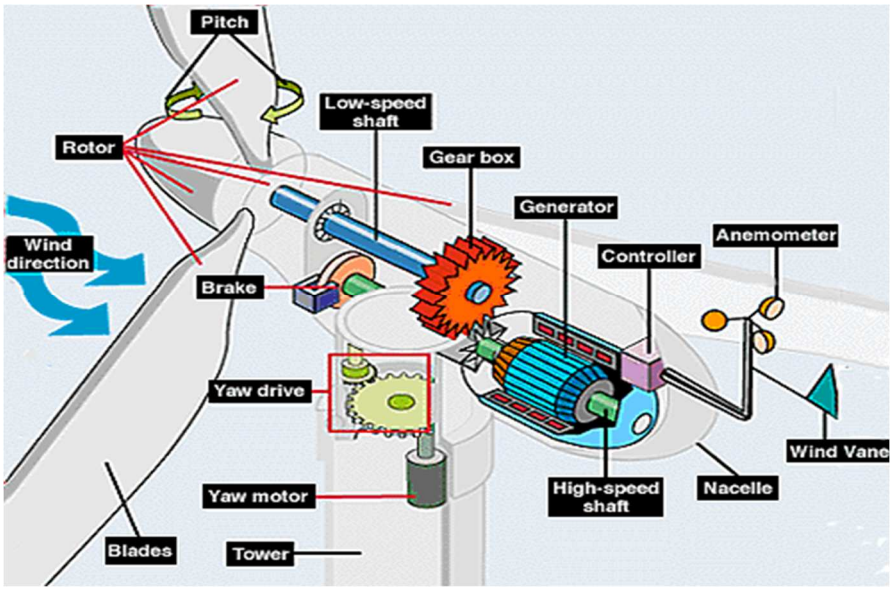

Figure 2-33 Basic components of the WECS [62]

2.6.2 Choice of wind turbine for this project.

A variable speed wind turbine was selected for this research project for the following reasons:

- There is an increase in the amount of energy captured
- Power quality is enhanced
- The wind turbine experiences a reduction in mechanical stress.

Conversely, a variable speed wind turbine also has some disadvantages and these are

- As a result of the use of power electronics, an additional cost is required
- Losses in the power electronics cannot be completely avoided
- More devices are required

This research work used the variable speed wind turbine with a fully rated power converter, equipped with permanent magnet synchronous generator (PMSG).

2.6.3 PMSG driven wind turbine

In [66] the permanent magnet synchronous generator is defined as a type of generator that a permanent magnet provides the excitation field instead of a coil. The PMSG wind turbine became the choice of this research because of its numerous advantages reported in past research works [67], [67], [68] and these are:

- It does not require an external DC excitation
- The absence of slip rings, mechanical commutators and brushes makes maintenance low and less frequent
- It is small in size and its weight is light
- The avoidance of gearbox is possible
- The PMSG wind turbine is more stable than the DFIG wind turbine
- It is relatively easy and simple to implement its control schemes
- Ability to control active and reactive power completely.
- Full speed regulation is achievable
- It does not experience heat dissipation due to the absence of field winding and hence it has high reliability and efficiency

The PMSG also experiences some drawbacks as in [67] and these are:

- It is an expensive option due to the cost of permanent magnets
- Its output voltage varies with load
- It has a fixed excitation
- Maintenance, assembling, and manufacturing are difficult

- High temperatures and large opposing magneto-motive-force (m.mf) can demagnetize the permanent magnet.
- Because its power converters have a full-scale power rating, it attracts high cost, high losses and conversely, high harmonic components are generated.

The sign of the torque input of the PMSG is what determines its mode of operation. If its sign is negative, the PMSG operates as a generator and if its sign is positive, the PMSG operates as a motor [69].

The bulk of wind turbines have a gearbox, but as a result, of the high rate of failure associated with the gearbox, the direct driven wind turbine is now becoming the preferred choice due to its advantages over wind turbines, which contains a gearbox. The advantages of direct driven wind turbines include; its maintenance is lower especially with offshore, reduced losses in the drive drain, reduced noise, besides, it has a simpler structure [70].

The block diagram of the PMSG driven wind turbine is as shown in figure 2-34

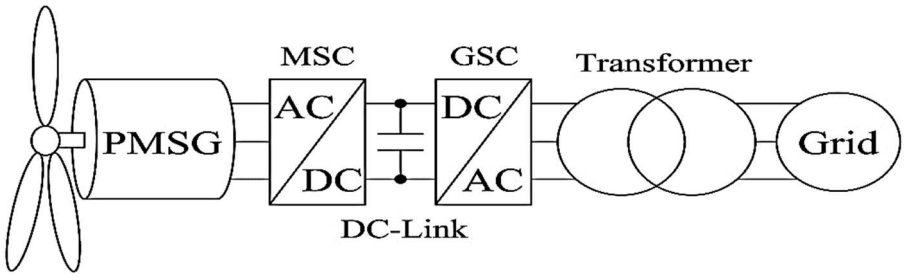

Figure 2-34. Block diagram of a PMSG driven wind turbine generator [71]

This research work utilized a 50kW Polaris wind turbine with the following specification sheet

Polaris AMERICA LLC

P19-50 Specification Sheet WS-0005

General	
Type	Horizontal Axis, Upwind
Rated power	50kW
Model	P19-50
Design Class	IEC SWT Class II
Design Standard	IEC 61400-1
Cut-in Speed	2.7m/s (6.0 mph)
Rated Speed	11.0m/s (24.6 mph)
Cut-out Speed	25m/s (55.9 mph)

Design Class	
IEC Class II Standard	Air density 1.225kg/m³,
	Avg annual wind below 8.5m/s
	50 yr peak gustbelow 59.5 m/s

Generator	
Type	Permanent Magnet
Rated Power	62W, 3 Phase
Voltage	460VAC

Pitch System	
Type	Variable Pitch
Drive	Centralized Pitching Mechanism

Yaw System	
Type	Active
Drive	AC
Brake	Electric
Yaw Bearing	Ball Bearing

Power Inverter	
Type	Variable Frequency Drive
	AC/DC

Power Coverter	
Type	DC/AC
	Pulse-width modulated IGBT
	frequency converter
Voltage	230VAC - (1) or 460VAC - (3)
Frequency/Phase	60Hz or 50Hz/ (1) or (3)

Environmental Limits	
Survival Wind Speed	59 m/s (132 mph)

Rotor	
Diameter	19.6m (64.3ft)
Material	Fiberglass/Resin
Operation RPM	68 RPM

Drive Train	
Type	Direct Drive

Braking Systems	
Emergency Back Up Speed Reg	Regenerative Brake
GridLoss Power/DC Bus over voltage	Dynamic Resistive Brake
Emergency Shutdown/parking	Caliper Disc Brake

Controller	
Processor	PLC
User Interface	HMI
Communications	Ethernet
Monitoring System	Web Based

Speed Regulation	
Generator	Torque Control from Drive

Tower	
Type	Tubular
Hub Height	21.3m (70ft)
	30.5m (100ft)
	36.6m (120ft)

Lightning Protection	
Standard	Surge Suppression on Generator

Weight	
Nacelle	6150kg

Temperature Conditions	
Standard Operation	-10°C to 40°C (14°F to 104°F)
Extreme Range	-25°C to 50°C (-13°F to 122°F)

Noise Performance	
Apparent Noise Level	50-55 db at 30m (100ft)

The wind power curve for the selected wind turbine is as shown in figure 2-35

Polaris AMERICA LLC

Power Curve - P21-60 WP-0012

Wind Velocity (m/s)	Wind Velocity (mph)	Grid Power (kW)
1	2.2	0.0
2	4.5	0.0
3	6.7	2.2
4	8.9	5.2
5	11.2	10.1
6	13.4	17.5
7	15.7	27.7
8	17.9	41.4
9	20.1	58.9
10	22.4	60.0
11	24.6	60.0
12	26.8	60.0
13	29.1	60.0
14	31.3	60.0
15	33.6	60.0
16	35.8	60.0
17	38.0	60.0
18	40.3	60.0
19	42.5	60.0
20	44.7	60.0
21	47.0	60.0
22	49.2	60.0
23	51.4	60.0
24	53.7	60.0
25	55.9	60.0

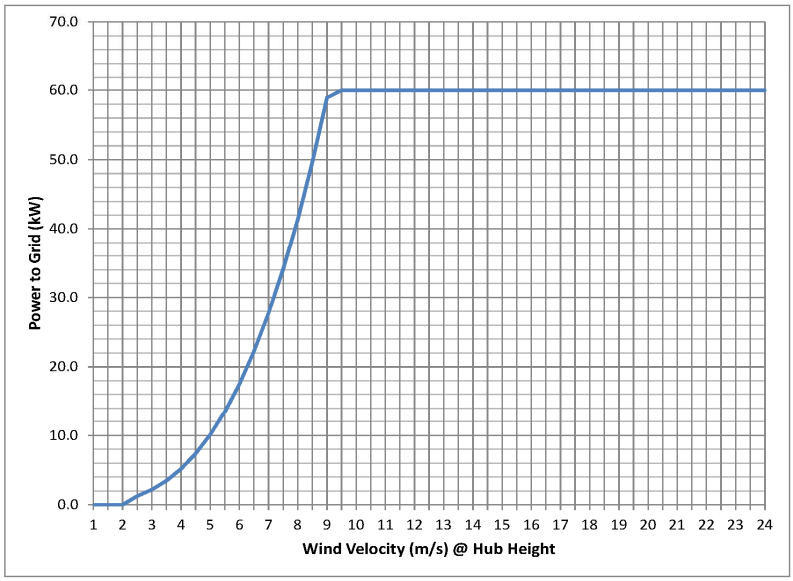

Figure 2-35. Wind power curve of the 50kW Polaris variable speed wind turbine [72].

This is the closest 50kW wind turbine available which has a range from 0 to 60kW. It can be operated at 50kW tops either by modifying the pitch angle control or by using a 50kW converter. The power characteristics of the wind turbine are as shown in figure 2-36.

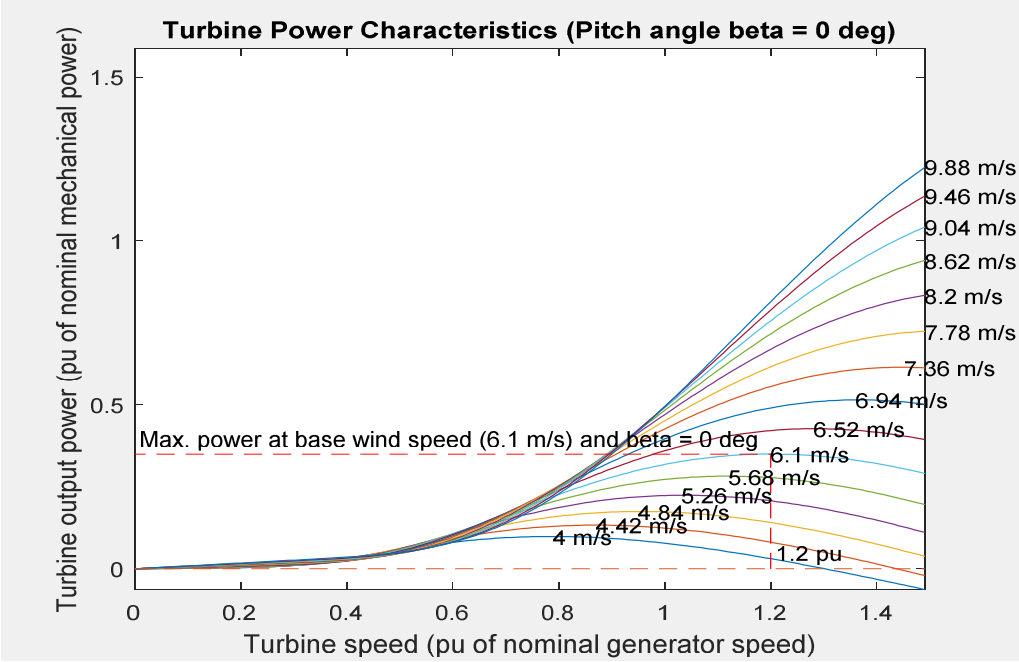

Figure 2-36 Wind turbine power characteristics

The usefulness of power electronic converters continues to gain more importance as the wind turbine technology advances as it serves as the link between the grid and the wind turbine generators. Essentially, three kinds of converters are in the wind market and these are matrix converter, multilevel converter and back-to-back converter [73] [74]

2.7 Power electronic converters used with PMSG driven WECS

A number of power electronic converters are used with the PMSG generator, but the most widely used is the diode bridge-VSC and the back-to-back VSCs.

2.7.1 Voltage source converter (VSC) with a diode bridge.

This type of converter is as shown in figure 2-37.

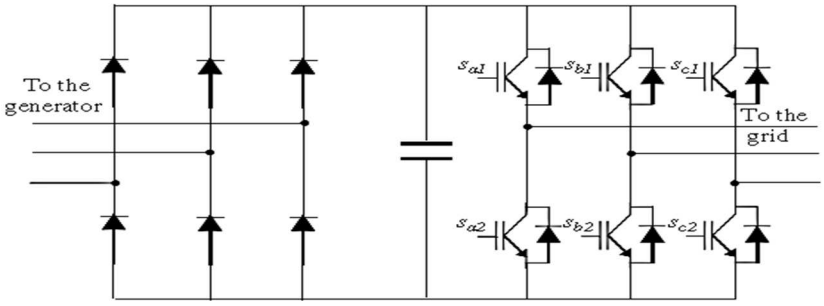

Figure 2-37. Voltage source converter with a 3-phase diode bridge.

For this power electronic converter topology, power flow only in one direction, ie from the generator side to grid. The diode bridge converts the power generated to DC power while the VSC converts the DC power to 50 Hz AC power. Decoupling between the grid-side converter and the generator side converter is provided by the DC link and hence both converters enjoy separate control flexibilities. The voltage of DC link capacitor is maintained constant with the help of the VSC control, to ensure the movement of power between the DC link capacitor and grid, but in a situation where the power from the generator-side does not flow to the grid, the voltage of the DC link rises. In order to reduce the DC ripple, a filter is introduced into the system, this is achieved by adding a series inductor to the DC link capacitor. Conversely, the DC link is protected from overvoltage by introducing a DC chopper [70].

2.7.2 The back-to-back Voltage source converter

According to a past research [75], this topology is made of two PWM voltage source converters, unlike VSC with a 3-phase diode bridge, a controlled rectifier is used at the rectification stage instead of a diode rectifier alongside a chopper. Functionalities such as the bi-directional electricity flow ability, reduction in harmonic losses, and input harmonic current

are provided by the controlled rectifier. The grid-side converters perform the following functions.

- It controls the movement of reactive and reactive power to the grid
- It ensures the voltage at the DC link is kept constant
- It helps to reduce harmonic distortion and in the process, improve the quality of the output power

On the other hand, the magnetisation demand, as well as the desired rotor speed for the generator, is controlled by the generator-side converter. The independent control ability of both converters is provided by the decoupling capacity between both converters.

The back-to-back VSC is as shown in figure 2-38.

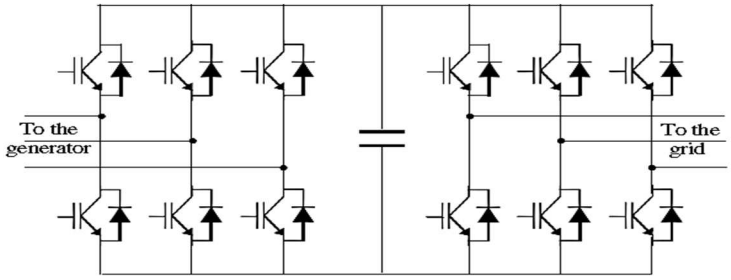

Figure 2-38. Back-to-back voltage source converter [70].

2.7.3 Matrix converter

This is another type of converter topology, which is used with the PMSG driven WECS, it is used basically for AC-AC power conversion that does not require DC conversion and its associated filters.

DC part is completed eliminated from the system and the incoming AC voltage is modified to match the AC power output required ie it embraces AC-AC conversion. A total of nine power electronic switches constitutes this converter with three switches in each of the legs. A diagram of this type of converter is as shown in fig31c, because, the DC capacitor stage is not required in this design, there is an improvement in size, reliability and in its efficiency, even the cost is reduced. Some of its disadvantages include: the conducting power loss is high, it is sensitive to grid disturbance, and its voltage is limited to about 86% of the input voltage [74] [75]

2.8 Hybrid PV/wind/diesel generator system operation

The battery bank performs two roles in this project as it serves a sink, and also as a source, hence it charges or discharges when the network experiences surplus or lack of power from the sources of energy due to the situation of the weather. When the amount of electricity supplied by the sources of power is greater than the load on the network, the battery controller

charges the battery and when the load on the network is more than the electricity supply from the sources, the controller causes the battery bank to discharge [76]. The control of the battery storage is done in such a way as to ensure the DC voltage is stabilized and this is achieved through the control of the DC/DC bidirectional converter in the network.

When there is a shortage of power from the sources, the bidirectional converter serves as a boost converter to provide power by discharging the battery and when the power supplied from the sources is in excess, it operates as a buck converter to charge the battery 77].

The hybrid system is also, incorporated with a dump load, the dump load is made up of a bank of resistors and a power converter, the capacity of the dump load power is such that it exceeds the amount of power produced by the wind, PV and diesel generator by 30%. It is to ensure the control of the network should, a condition arises when there is no load and the battery storage fails or is fully charged.

The energy storage helps to compensate the mismatch in power, which exist between the load and the energy sources. Energy from the PV array flows through the charge controller to charge the battery and also to provide electricity to the load through the inverter simultaneously. The charge controller ensures that the charging and discharging of the battery are monitored and controlled to protect the battery from damage due to over-discharging and over-charging. When the Wind, PV, and the battery can no longer meet the load demand, the Diesel generator provides electricity to the load and at the same time charges the battery through the rectifier. When the power generated is greater than the demand and the battery is fully charged, the excess power is passed to the dump load. For the periods in which the electricity provided by the renewable energy sources is low, the Diesel generator is usually ON to supply electricity, hence charging and discharging as well as the losses involved (this is as a result of charge and discharge efficiencies) are very high since the diesel generator is always switched ON.

2.9 The evolution of wind turbine size and the advancement in power electronics coverage

Electricity generation from renewable energy has achieved a lot of improvement due to increasing advancement in power electronics technology in the past decades. The emerging power electronic devices alongside intelligent control strategies made it possible for power from renewable energy sources of energy to be easily controlled and reliable. The future promises better advancement in power electronics and hence a more flexible and better

integration with grid power. In terms of coverage of wind turbine technology, power electronics converters have recorded 100% achievement since 2005 [78]. The evolution of the wind turbine systems shown in figure 2-39 shows the advancement in power electronics coverage with advancement in wind turbine technology.

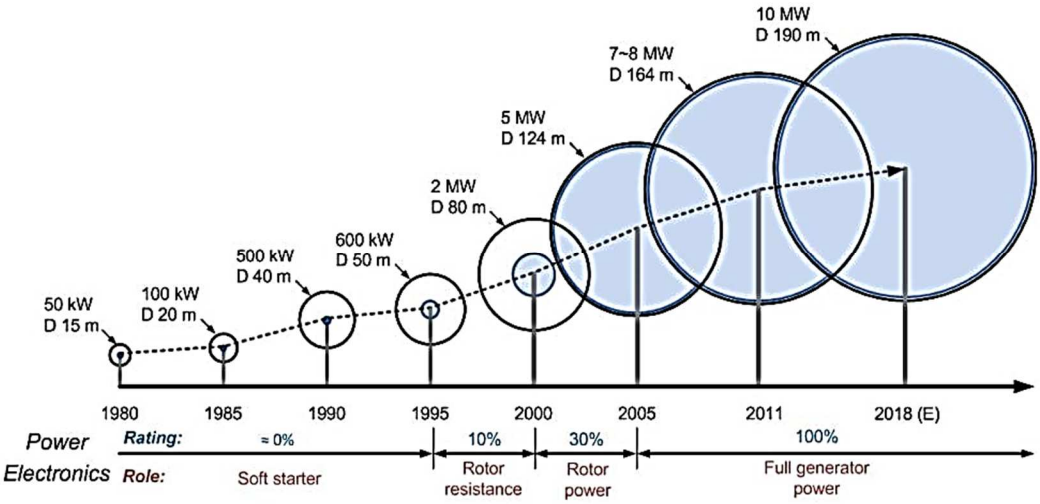

Figure 2-39. The evolution of wind turbine size and power electronics coverage [79].

2.10 References

[1] B. Schinke, J. Klawitter, M. Doring, N. Komendantova, J. Irshaid, and J. Bayer, "Energy Planning for sustainable development in the MENA region," 2017.

[2] A. S. Sambo, I. H. Zarma, P. E. Ugwuoke, I. J. Dioha, and Y. M. Ganda, "Implementation of Standard Solar PV Projects in Nigeria," *ISSN*, vol. 4, no. 9, pp. 2224–3232, 2014.

[3] J. O. Oji, N. Idusuyi, T. O. Aliu, M. O. Petinrin, O. A. Odejobi, and A. R. Adetunji, "Utilization of Solar Energy for Power Generation in Nigeria," *Int. J. Energy Eng.*, vol. 2, no. 2, pp. 54–59, 2012.

[4] Y. S. Bijjargi, K. SS, and S. K A, "Cooling Techniques for Photovoltaic Module for Improving Its Conversion Efficiency: a Review," *Int. J. Mech. Eng. Technol.*, vol. 7, no. 4, pp. 22–28, 2016.

[5] D. Khetarpal, "World Energy Resources: Solar 2016," *World Energy Counc.*, p. 78, 2016.

[6] E. Franklin, *Types of Solar Photovoltaic Systems*. 2017.

[7] SaveYourEnergy, "Types of solar PV modules," 2007. [Online]. Available: http://www.staffordarea.saveyourenergy.org.uk/what/solar/PVtypes. [Accessed: 29-Apr-2018].

[8] University of Central Florida, "Types of PV Systems," *Florida Solar Energy Center*, 2014. [Online]. Available: http://www.fsec.ucf.edu/en/consumer/solar_electricity/basics/types_of_pv.htm. [Accessed: 01-May-2018].

[9] "Types of Solar PV Systems." [Online]. Available: http://www.enerzytech.com/resources/articles/13-types-of-solar-pv-systems. [Accessed: 03-May-2018].

[10] G. K. Singh, "Solar power generation by PV (photovoltaic) technology: A review," *Energy*, vol. 53, pp. 1–13, 2013.

[11] I. El-mohr and A. Anas, "Hybrid Energy Systems Applications," 2014.

[12] E. Franklin, "Mounting Your Solar Photovoltaic (PV) System," 2017.

[13] L. Idoko, O. Anaya-Lara, and D. Campos-Gaona, "Voltage control ancillary services for low voltage distributed generation," *Int. J. smart grid clean energy*, vol. 7, no. 2, pp. 98–108, 2018.

[14] M. Farman, A. Alam, and M. P. Sharma, "Off-Grid Hybrid Energy Systems for Rural Electrification," in *National Conference on Power and Energy Systems (NCPES-2011) April 23-24, 2011*, 2011, no. April, pp. 51–57.

[15] F. J. Vivas, A. De las Heras, F. Segura, and J. M. Andújar, "A review of energy management strategies for renewable hybrid energy systems with hydrogen backup," *Renew. Sustain. Energy Rev.*, vol. 82, no. 1, pp. 126–155, Feb. 2018.

[16] R. Al Badwawi, M. Abusara, and T. Mallick, "A Review of Hybrid Solar PV and Wind Energy System," *Smart Sci.*, vol. 3, no. 3, pp. 127–138, 2015.

[17] M. Ibrahim, A. Khair, and S. Ansari, "A Review of Hybrid Renewable Energy Systems for Electric Power Generation," *J. Eng. Res. Appl. www.ijera.com ISSN*, vol. 5, no. 81, pp. 2248–962242, 2015.

[18] C. V. Nayar, S. M. Islam, H. Dehbonei, K. Tan, and H. Sharma, *Power electronics for renewable energy sources*, Third Edit. Elsevier Inc., 2011.

[19] P. Balachander, "AC Coupling," 2012.

[20] A. Chauhan and R. P. Saini, "A review on Integrated Renewable Energy System based power generation for stand- alone applications : Configurations , storage ...," *Renew. Sustain. Energy Rev.*, vol. 38, pp. 99–120, 2014.

[21] S. Elster and K. Moutawakkil, "RE hybrid systems: Coupling of Renewable Energy Sources on the AC and DC Side of the Inverter," *Refocus*, vol. 7, no. 5, pp. 46–48, 2006.

[22] R. Sedaghati, "Optimal design and Intelligent Management of Hybrid Power System,"

Int. J. Energy Power Eng., vol. 10, no. 6, pp. 835–848, 2016.

[23] S. Negi and L. Mathew, "Hybrid Renewable Energy System: A Review," *Int. J. Electron. Electr. Eng.*, vol. 7, no. 5, pp. 535–542, 2014.

[24] K. . Divya and J. Østergaard, "Battery energy storage technology for power systems-an overview," *Electr. Power Syst. Res.*, vol. 29, pp. 511–520, 2009.

[25] "Grid-Tied, Off-Grid and Hybrid Solar Systems - Energy Informative." [Online]. Available: http://energyinformative.org/grid-tied-off-grid-and-hybrid-solar-systems/. [Accessed: 11-Jun-2018].

[26] T. Ma, H. Yang, and L. Lu, "Development of hybrid battery–supercapacitor energy storage for remote area renewable energy systems," *Appl. Energy*, vol. 153, pp. 56–62, Sep. 2015.

[27] S. Mekhilef, R. Saidur, and M. Kamalisarvestani, "Effect of dust, humidity and air velocity on efficiency of photovoltaic cells," *Renew. Sustain. Energy Rev.*, vol. 16, no. 5, pp. 2920–2925, 2012.

[28] M. I. Yusoff, S. Ibrahim, A. R. Amelia, Y. M. Irwan, W. Z. Leow, M. Irwanto, I. Safwati, and M. Zhafarina, "Investigation of the Effect Temperature on Photovoltaic (PV) Panel Output Performance," *Int. J. Adv. Sci. Eng. Inf. Technol.*, vol. 6, no. 5, 2016.

[29] P. Mohanty and A. Tyagi, *Introduction to Solar Photovoltaic Technology*. Elsevier Inc., 2015.

[30] L. El Chaar, *Photovoltaic System Conversion*, Third Edit. Elsevier Inc., 2011.

[31] L. Idoko, O. Anaya-Lara, and A. McDonald, "Enhancing PV modules efficiency and power output using multi-concept cooling technique," *Energy Reports*, no. 4, pp. 357–369, 2018.

[32] "Corrosion 101: What Is Corrosion? | EonCoat, LLC." [Online]. Available: https://eoncoat.com/corrosion-101-what-is-corrosion/. [Accessed: 17-Jun-2018].

[33] M. T. Chaichan and H. A. Kazem, *Generating Electricity Using Photovoltaic Solar Plants in Iraq*. 2018.

[34] J.-H. Kim, J. Park, D. Kim, and N. Park, "Study on Mitigation Method of Solder Corrosion for Crystalline Silicon Photovoltaic Modules," *Int. J. Photoenergy*, vol. 2014, pp. 1–9, Dec. 2014.

[35] M. Saadsaoud, A. H. Ahmed, Z. Er, and Z. Rouabah, "Experimental Study of Degradation Modes and Their Effects on Reliability of Photovoltaic Modules after 12 Years of Field Operation in the Steppe Region," vol. 13240, no. 88, pp. 930–935, 2017.

[36] J. Larrivee, "An analysis of degradation rates of PV power plants at the system level [M.Sc Thesis]," 2013.

[37] M. Köntges, S. Kajari-Schröder, I. Kunze, and U. Jahn, “Crack Statistic of Crystalline Silicon Photovoltaic Modules,” in *26th EUPVSEC, Hamburg, Germany*, 2011, no. September, pp. 1–5.

[38] M. Dhimish, V. Holmes, B. Mehrdadi, and M. Dales, “The impact of cracks on photovoltaic power performance,” *J. Sci. Adv. Mater. Devices*, vol. 2, no. 2, pp. 199–209, Jun. 2017.

[39] S. Pingel, Y. Zemen, O. Frank, T. Geipel, and J. Berghold, “mechanical stability of solar cells within solar panels.”

[40] “Final Report Summary - solar design (On-the-fly alterable thin-film solar modules for design driven applications).” [Online]. Available: https://cordis.europa.eu/result/rcn/187148_en.html. [Accessed: 17-Jul-2018].

[41] R. C. Neville, *Solar energy conversion : the solar cell*. Elsevier, 1995.

[42] “Sizing inverters to optimise solar panel system efficiency - Solar Choice.” [Online]. Available: https://www.solarchoice.net.au/blog/optimizing-solar-panel-system-efficiency-through-inverter-sizing/. [Accessed: 18-Jul-2018].

[43] M. Fedkin and J. A, “Efficiency of Inverters | Utility Solar Power and Concentration.” [Online]. Available: https://www.e-education.psu.edu/eme812/node/738. [Accessed: 19-Jul-2018].

[44] A. string Inverters, “Solar inverters TRIO-20.0/27.6-TL-OUTD,” *Abb*, pp. 0–3, 2014.

[45] EPIA, “Catalogue of common failures and improper practices on PV installations and maintenance,” 2011.

[46] “Installation and Maintenance of Solar Photovoltaic Systems Using handheld and benchtop solutions for solar energy applications,” 2017.

[47] “Voltage Drop |Commercial Solar Electric Systems.” [Online]. Available: https://www.e-education.psu.edu/ae868/node/967. [Accessed: 19-Jul-2018].

[48] S. Ekici and A. Kopru, “Investigation of PV System Cable Losses,” *Int. J. Renew. ENERGY Res. S.Ekici M.A.Kopru*, vol. 7, no. 2, 2017.

[49] “Mixing solar panels – Dos and Don’ts.” [Online]. Available: http://solarpanelsvenue.com/mixing-solar-panels/. [Accessed: 19-Jul-2018].

[50] “Solar power system for compression-cycle vaccine refrigerator or combined refrigerator-icepack freezer.,” 2007.

[51] M. J. Adinoyi and S. a M. Said, “Effect of dust accumulation on the power outputs of solar photovoltaic modules,” *Renew. Energy*, vol. 60, pp. 633–636, 2013.

[52] A. Karafil, H. Ozbay, and M. Kesler, “Temperature and Solar Radiation Effects on Photovoltaic Panel Power,” *J. New Results Sci.*, vol. 5, no. 12, pp. 48–58, 2016.

[53] “Irradiance and PV Performance Optimization | AE 868: Commercial Solar Electric Systems.” [Online]. Available: https://www.e-education.psu.edu/ae868/node/877. [Accessed: 14-Jun-2018].

[54] H. K. Elminir, V. Benda, and J. Toušek, “effects of solar irradiation conditions and other factors on the outdoor performance of photovoltaic modules,” *J. Electr. Eng.*, vol. 52, pp. 5–6, 2001.

[55] J. K. Kaldellis, M. Kapsali, and K. a. Kavadias, “Temperature and wind speed impact on the efficiency of PV installations. Experience obtained from outdoor measurements in Greece,” *Renew. Energy*, vol. 66, pp. 612–624, 2014.

[56] B. V Chikate and Y. A. Sadawarte, “The Factors Affecting the Performance of Solar Cell,” in *International Journal of Computer Applications Science and Technology*, 2015, pp. 975–8887.

[57] “Heat Generation in PV Modules | PVEducation.” [Online]. Available: https://www.pveducation.org/pvcdrom/modules/heat-generation-in-pv-modules. [Accessed: 12-Jun-2018].

[58] Y. Baghzouz, “EE 446/646 Photovoltaic Devices I.” [Online]. Available: http://www.egr.unlv.edu/~eebag/Photovoltaic Devices I.pdf. [Accessed: 12-Jun-2018].

[59] N. Gupta and M. Khatri, “An Experimental Analysis of Shading on Solar Photovoltaic System,” vol. 8, no. 1, pp. 226–228, 2017.

[60] A. M. Homadi, “Effect of elevation and wind direction on silicon solar panel efficiency,” *Int. J. Energy Power Eng.*, vol. 10, no. 9, pp. 1205–1212, 2016.

[61] M. A. A. Mamun, M. Hasanuzzaman, and J. Selvaraj, “Impact of tilt angle on the performance of photovoltaic modules in Malaysia: A review,” in *IET Conference Publications*, 2016, vol. 2016, no. CP688, p. 97 (8 .)-97 (8 .).

[62] Z. Salameh, *Renewable Energy System Design*, 1st ed. 2014.

[63] N. R. Babu and P. Arulmozhivarman, “Wind energy conversion systems - A technical review,” *J. Eng. Sci. Technol.*, vol. 8, no. 4, pp. 493–507, 2013.

[64] “Global Wind Statistics 2017,” 2018. [Online]. Available: http://gwec.net/wp-content/uploads/vip/GWEC_PRstats2017_EN-003_FINAL.pdf. [Accessed: 09-Jul-2018].

[65] “Advantages and Challenges of Wind Energy | Department of Energy.” [Online]. Available: https://www.energy.gov/eere/wind/advantages-and-challenges-wind-energy. [Accessed: 09-Jul-2018].

[66] L. Kumar Gautam and M. Mishra, “Permanent Magnet Synchronous Generator Based Wind Energy Conversion System,” *Int. J. Electr. Electron. Comput. Sci. Eng.*, vol. 1,

no. 1, pp. 2348–2273, 2014.

[67] A. Gupta, D. K. Jain, and S. Dahiya, “Some Investigations on Recent Advances in Wind Energy Conversion Systems,” 2012, vol. 28, pp. 47–52.

[68] “Permanent Magnet Synchronous Generator Configuration in Wind Turbines – Technological status review, survey and market trends.” [Online]. Available: https://www.ijser.org/paper/Permanent-Magnet-Synchronous-Generator-Configuration-in-Wind-Turbines.html. [Accessed: 13-Jul-2018].

[69] S. Mishra, M. Gupta, A. Garg, R. Goel, and V. K. Mishra, “Modeling and Simulation of Solar Photo-Voltaic and PMSG Based Wind Hybrid System,” in *lEEE Students' Conference on Electrical, Electronics and Computer Science*, 2014.

[70] O. Anaya-Lara, N. Jenkins, J. Ekanayake, P. Cartwright, and M. Hughes, *Wind energy generation : modelling and control*, vol. 54, no. 2. 2009.

[71] H. Matayoshi, A. M. Howlader, M. Datta, and T. Senjyu, “Control strategy of PMSG based wind energy conversion system under strong wind conditions,” *Energy Sustain. Dev.*, vol. 45, pp. 211–218, Aug. 2018.

[72] “50kW Variable Pitch.” [Online]. Available: http://www.polarisamerica.com/turbines/50kw-variablepitch-wind-turbines/. [Accessed: 09-Dec-2018].

[73] H. S. Kim and D. D. Lu, “Wind Energy Conversion System from Electrical Perspective — A Survey,” vol. 2010, no. November, pp. 119–131, 2010.

[74] W. Cao, Y. Xie, and Z. Tan, *Wind Turbine Generator Technologies*. .

[75] R. Islam, Y. Guo, and J. Zhu, “Power converters for wind turbines : Current and future development,” pp. 559–571, 2013.

[76] N. H. Samrat, N. Bin Ahmad, I. A. Choudhury, and Z. Bin Taha, “Modeling , Control , and Simulation of Battery Storage Photovoltaic-Wave Energy Hybrid Renewable Power Generation Systems for Island Electrification in Malaysia Modeling , Control , and Simulation of Battery Storage Photovoltaic-Wave Energy Hybrid Renewab,” *Sci. World J.*, vol. 2014, no. February 2016, p. 22, 2014.

[77] A. Yasin, G. Napoli, M. Ferraro, and V. Antonucci, “Modelling and control of a residential wind/PV/battery hybrid power system with performance analysis,” *J. Appl. Sci.*, vol. 11, no. 22, pp. 3663–3676, 2011.

[78] F. Blaabjerg, K. Ma, and Y. Yang, “Power Electronics for Renewable Energy Systems - Status and Trends,” in *Integrated Power Systems (CIPS), 2014 8th International Conference on : date 25-27 Feb. 2014*, 2014, p. 11.

[79] “Power electronics technology in wind turbine system.” [Online]. Available:

https://www.slideshare.net/pranavikasina/power-electronics-technology-in-wind-turbine-system. [Accessed: 15-Jul-2018].

Chapter 3:

Sizing of hybrid PV/wind/diesel generator system

In order to carry out the modeling of this energy system, the sizing of the different energy sources was first carried out using HOMER software simulator and the capacity of the different energy sources was achieved and the desired configuration was also selected. The primary focus is to use the HOMER software to design an energy system that will provide adequate power to 120 residential apartments in the location.

This chapter embraces the benefits of the hybrid energy system, the different types of the standalone energy system, sizing of the hybrid energy units, and the methods of unit sizing. The different types of simulation software used for sizing a hybrid energy system treated. The design of the load profile for the research location, the available wind and solar energy resources in the location and finally, the result of the simulation treated.

In order to conclude on the type of hybrid energy system required for this project, the following decisions as in [1], were taken during the design stage.

- The capacity and number of units of renewable that will be installed
- The choice of backup power, for example, fuel cell, diesel generator etc to be incorporated in the hybrid energy system.
- To include a battery storage in the hybrid energy system or not
- The choice to adopt a grid-connected or a standalone system
- The kind of renewable sources of energy that will make up the hybrid energy system

The choice of the type of hybrid energy system to be adopted depends on the renewable energy resources available in the chosen location and the decision depends on the condition of the weather in the location. Due to the fact that the location of interest in this research does not require a connection to the grid, a standalone system was adopted. The hybrid energy system has the following benefits as in [2] [1]:

- The design of a hybrid system can be done with deep penetration of renewable energy and in the process cut down emissions
- Since the different sources can complement each other, the performance and efficiency of the system are increased

- A design at the lowest cost is achievable.
- It creates room for flexibility in the use of renewable energy resources.

A standalone system also referred to as an off-grid system, is an electrical system that provides electricity to locations separated completely or partly from the electricity grid. A past research [3], reports that it can be grouped on the basis of energy sources into different types a shown in figure 3-1.

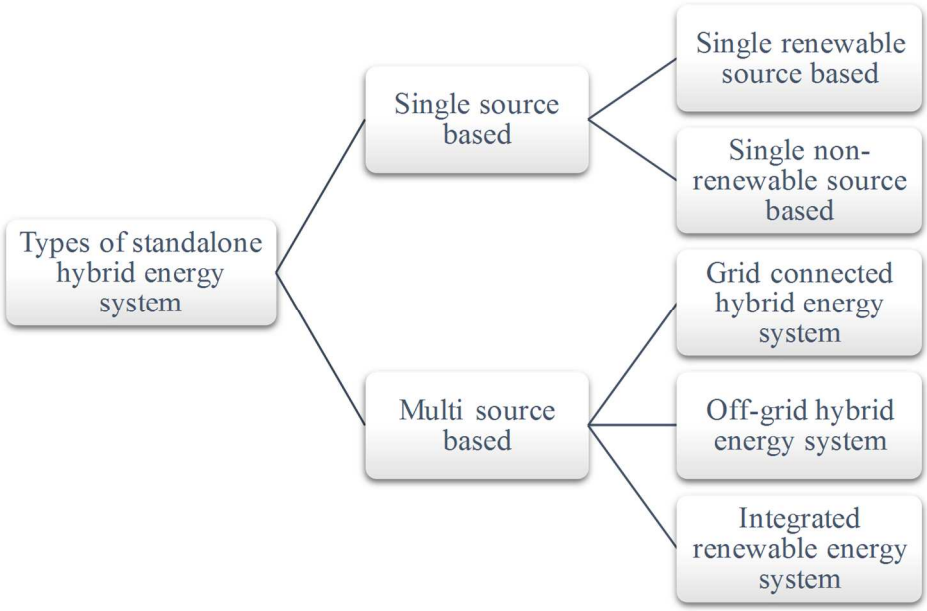

Figure 3-1. Types of standalone hybrid energy system

This research work embraces the multi-source based off-grid hybrid energy system. Applications of hybrid energy systems include hospitals, villages, schools, residential buildings, desalination system, irrigation schemes, hotels, farmhouses etc. The research location selected for this project experiences a long period of intense sunlight but the wind speed is low when compared to wind speed experienced in the UK and other countries, which experiences high wind speed.

3.1 Sizing of hybrid PV/wind/diesel generator energy system.

The cost of energy and demand for electricity is both rising while the reserve for the sources is reduced e.g. fossil fuel globally is actually diminishing. This gives us the idea that in years to come, the demand for electricity might exceed the supply of electricity from fossil fuel such that other sources of energy may be required, and asides energy generation from fossil fuel gives rise to the emission of pollutants. As a result of the quest to cut down on pollution and prepare for the future energy demand requirement, the use of available renewable energy resources in every location for the provision of electricity is a necessity [4]. To enable us to meet the electrical load demand using renewable energy sources, a hybrid energy system is required, this will help us to employ the use of wind and solar resources to provide power and in the process overcome the challenge which energy generation from a single renewable energy source experiences [5].

Nigeria, popularly known as the giant of Africa, has many minerals and renewable resources; it experiences a daily average sunshine of 6.25 hours, the period of sunshine hours varies from 3.5 hours in locations in the coast of the country to 9 hours towards the north end. As a result of the long duration of sunshine hours, the value of its annual average daily radiation ranges from 7.0kW/m2/day at the north end to 3.5kWh/m2/d at the coastal area with annual average daily radiation of 5.25kWh/m2/d and as such a high amount of energy can be generated from the sun. Consequently, the potential for the use of renewable resources to provide alternative power supply is high provided the maximum use of the available renewable resources is adopted [6].

3.2 Sizing of the hybrid energy system units.

The sizing of the hybrid energy system is an important aspect of this hybrid energy system, it is a process which helps to ascertain the exact components of the hybrid energy system, the process ensures the cost of the system is minimized while the reliability of the system is being maintained as in [7]. The cost of the system tends to increase when the system is oversized but under sizing may result in power supply failure or the load may be supplied with inadequate power. Sizing can be achieved using any of the methods as shown in figure 3-2.

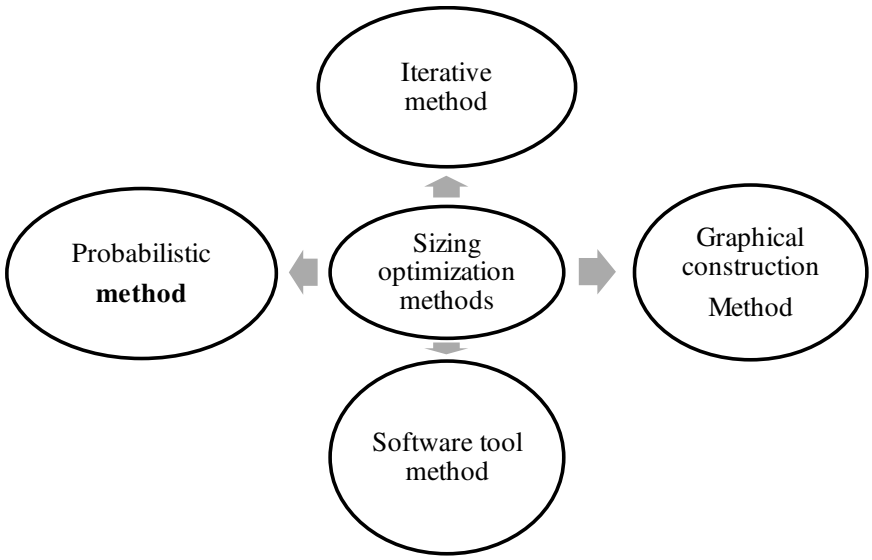

Figure 3-2. Methods of unit sizing optimization.

This research adopted the use of the software tool method of sizing and the software tool method involves the use of computer simulations to achieve the desired results, examples of simulator software for sizing the hybrid energy system include HYBRIDS, PVSYST, RAPSIM, SOMES, PVF-chart, RETSCREEN, HOMER etc as in [8].

HYBRIDS

This soft utilizes the Microsoft Excel software for its operation, it requires data from the environment estimated for every month of the year and the daily average load for its analysis. the software development was achieved at the National Renewable Energy Laboratory and the University of Massachusetts. This software demands for high knowledge of system configuration as its content regarding optimization variables is very comprehensive. It utilizes the combination of time series/probabilistic approach, which is very helpful for long-term predictions as in [9]

PVSYST

This is a software designed to aid photovoltaic systems evaluation, simulation, sizing and data analysis. It works based on the available user information provided to the battery capacity and the PV size for the design and this user information include the allowable time frame that load cannot be met and the load profile of the user. It is a useful software, which provides a sizeable database for meteorological locations, Photovoltaic devices, an expert system coupled with a 3-D tool to support shading work. The software was built by Geneva University in Switzerland [8]

RAPSIM

The Remote Area Power Supply Simulator is a software built at the energy research institute at Murdoch University, Australia. The software performs the simulation of available alternative energy supply and this includes wind turbine, PV, diesel, and battery system. A system and an operating strategy of choice are selected by the user of the software. The selection is usually made out of the available pre-defined options in the software after which the optimization is done using the control variables and also varying the sizes of the components [10].

SOMES

This abbreviation represents simulation and optimization model for renewable energy systems and it has the ability to simulate renewable energy system performance comprising of wind, PV, and other sources of power, such as diesel generator, grid, different types of converters and battery storage. The reliability of the power and system performance is obtained by analyzing the results and its simulation is performed on an hourly basis within the period of simulation [3].

PVF-CHART

This is another useful tool for PV system sizing, with this software as [8], the long-term prediction of the average performance of the PV and its utility interface, systems with battery storage, and systems, which do not have an interface or battery storage are easily achieved. This programme gives a comprehensive photovoltaic system design and analysis. Its results give monthly average analysis showing the performance estimates for each of the hours in a day

RETSCREEN

This is another useful software that its operation is based on Microsoft Excel application software tools. A Typical attribute of this software is the ability to reduce life-cycle cost, energy generation and emission of greenhouse gas. This software has the ability to carry out calculations on energy efficiency and the assessment of risk associated with each of the renewable energy types, energy-efficient technologies and as well as the analysis of the designed system cost function including the feasibility of the hybrid system. The software is built and managed by the Canadian government [11].

HOMER

HOMER means Hybrid optimization model for Electric renewables, it appears to one of the most used software for hybrid renewable energy systems. It can be used for the integration and optimization of a hybrid renewable energy system which comprises Wind generator, PV generators, Hydrogen tanks, hydraulic turbines, fuel cells, AC generators, boilers, electrolyzers, and AC-DC bi-directional converters. The loads can be thermal load, DC or AC load and /or hydrogen loads. It can be downloaded and use free of charge. It is a user-friendly software and usually used for optimization, sensitivity analysis and pre-feasibility [10][11].
It makes the evaluation of both grid-connected and off-grid designs simple. To carry out a power system design, decisions such as system configuration, the number as well as the size of component to include in the design, energy resources availability, differences in the cost of technology, the technology options and the numerous system configurations possible are easily evaluated with the help of the HOMER software simulator.

In order to be able to use HOMER for system design, you are required to provide inputs to the model, the inputs are such that identifies the cost of components, availability of resources as well as the technology options. HOMER performs simulations on all the different configurations possible and produce a list of possible configurations as its result. HOMER also displays the results of his simulation in a form of tables and graphs to aid the comparison of the various configurations. Their evaluations are based on the technical or economic merits and the operation of the system to be simulated by HOMER, this is achieved by performing an energy balance calculation in each time step of that particular year. Conversely, HOMER ensures that the electric and thermal demand in each of the time step is compared to the amount of energy that can be supplied by the system in that particular time step, then the movement of energy to and from each of the components is computed [12]

The outputs from HOMER software simulator as in [13] usually are the renewable fraction, fuel consumption, excess energy unmet load, cost of energy and net present cost
Net present cost, cost of energy, capital cost, unmet load, excess energy, fuel consumption, renewable energy fraction. HOMER and SOMES are applicable to this research since both have the ability to provide an optimal hybrid system design. This research made use of Hybrid Optimization Model for Electric Renewables (HOMER) for sizing the hybrid system and this is because it utilizes data from the location under investigation to carry out hourly simulations, it is a user-friendly software which has been adopted by several researchers.

3.3 The requirements for the optimization of hybrid energy system

In order for the system load profile to be satisfied, an optimal mix of hybrid energy system has to be chosen and the selection is done based on the life-cycle cost of the system and power reliability.

3.3.1 System cost analysis

The system cost analysis of the system is also very important and involves several criteria for example Levelized cost of energy, Net present cost, and life-cycle cost. The annual total cost of the system divided by the annual electricity generated by the systems is referred to as the levelised cost. The net present cost refers to "the total present value, which includes the initial cost of all the system components, the cost of any component's replacement that occurs within the project lifetime and the cost of maintenance" [14].

3.3.2 Analysis of power reliability.

Power reliability is an essential part of the process of hybrid energy design; this is because it is mandatory for the load, to be satisfied in the most cost-effective and economical manner. There are a number of ways to compute the reliability of the hybrid energy system and these involve the use of loss of load probability (LOLP), loss of load hours (LOLH), loss of power supply probability (LPSP), and system performance level (SPL). The LOLP measures the probability that the load requirement of the system will exceed the power supply ability of the system in a specific period. Conversely, LPSP measures the probability that an inadequate power is evident when the power supplied by the hybrid energy system cannot satisfy the load requirement of the system [15].

In developing countries, about 80% of the population resides in the rural areas, where a large population of people does not have access to the required electricity services to enable them to meet their essential needs, etc. Energy resources from wind or PV may stand a good chance to provide uninterrupted power supply. During the winter and the periods of no sun, the solar energy is not able to provide a steady power supply. Conversely, during the summer, the wind energy system is not able to supply constant power and this is because of the variations in wind speed hourly. The use of each of the renewable energy does not produce steady electricity, but combining the two sources creates room for an elevated availability of electricity. The combination of both renewable energy is also associated with problems such as the selection of the appropriate capacity of each of them etc [16]. This problem was addressed with the help of HOMER simulator software.

3.4 Selection of integration configuration

In order to select the structure for integrating the different components of the hybrid energy system, the major methods of integration were considered, these are AC coupling, DC coupling, and Hybrid coupling. This hybrid energy consists of both sources, i.e. sources, which generate AC power as well as sources, which generate DC power. The hybrid system consists of Photovoltaic modules and battery storage, which give out DC power, while the wind energy, diesel generator systems incorporated into the network produces AC power. In order, for the diesel generator to be able to charge the battery in times of excess supply and also provide power supply to the entire network in the event of power failure from the renewable sources. A hybrid DC-AC coupled hybrid energy system is used, where all the DC sources are connected to the DC bus while the AC sources as well the AC load are connected to the AC bus. This helps to minimize the number of converters as well as their associated losses. Conversely, this configuration gives room for a greater efficiency when compared with the use of DC coupled or AC coupled hybrid system and the cost involved is lower [11].

3.5 Description of research location and data

The major source of electric power in developing countries, for example Nigeria, is usually the national grid, which in most cases has limitations, as some areas cannot have access to the grid due to the geographical location of the place like many areas in Gusau in Nigeria situated at Longitude: 6.77 Degrees East and Latitude: 12.17 Degrees North. Hence an independent and reliable source of power is essential, as the majority of the inhabitants depend on fuel-based generators for power supply which is usually associated with the heavy cost of maintenance and environmental pollution [17]. Gusau, the capital of Zamfara state discovered to be one of the states in the country with a good potential for wind-generated electricity also has the potential for solar-generated electricity and this is because the location experiences high temperature and a long period of sunshine hours.

Gusau, a city with similar weather conditions in Sokoto state, Nigeria is faced with the challenge of the inadequate power supply as electricity supply from the national grid is unstable and inadequate, besides the majority of those in the remote areas are isolated from the grid. The location has a potential for renewable resources, to overcome this challenge of inadequate power supply, a hybrid electric power system, which employs the use of battery storage, solar and wind energy system with a diesel generator as reserve to provide adequate power to 120 residential apartments in a settlement isolated from the grid is been designed.

The data for the average sunshine hours alongside the minimum and maximum temperature in Gusau for the year 2015 obtained from the Nigerian Meteorological Agency, NIMET as shown in figure 3-3 and 3-4 respectively.

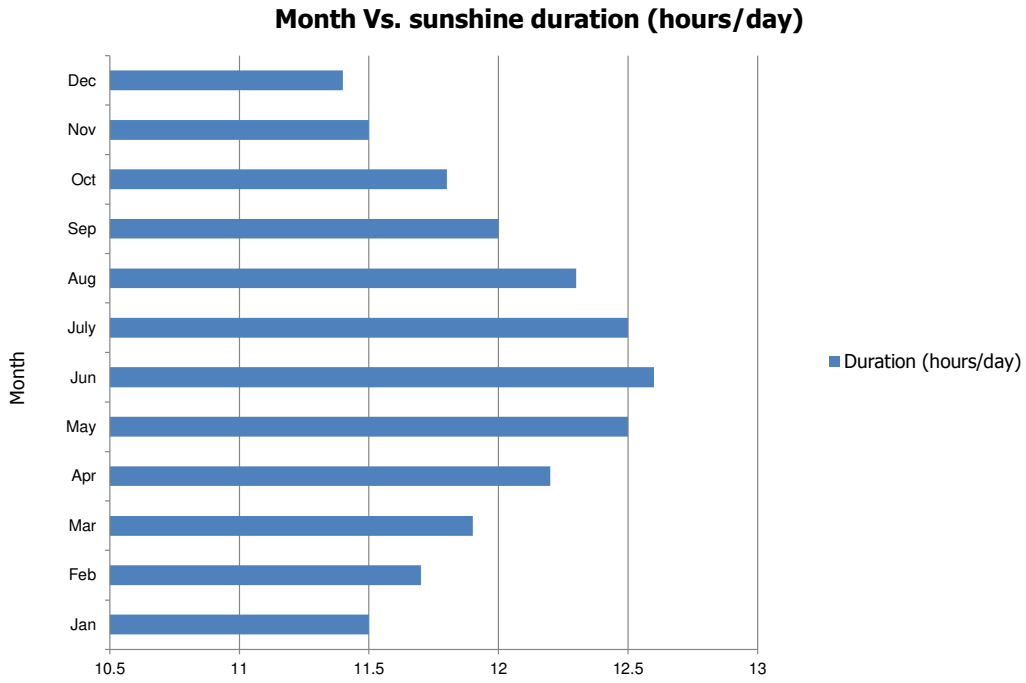

Figure 3-3. Average Monthly Sunshine hours per day for Gusau in 2015.

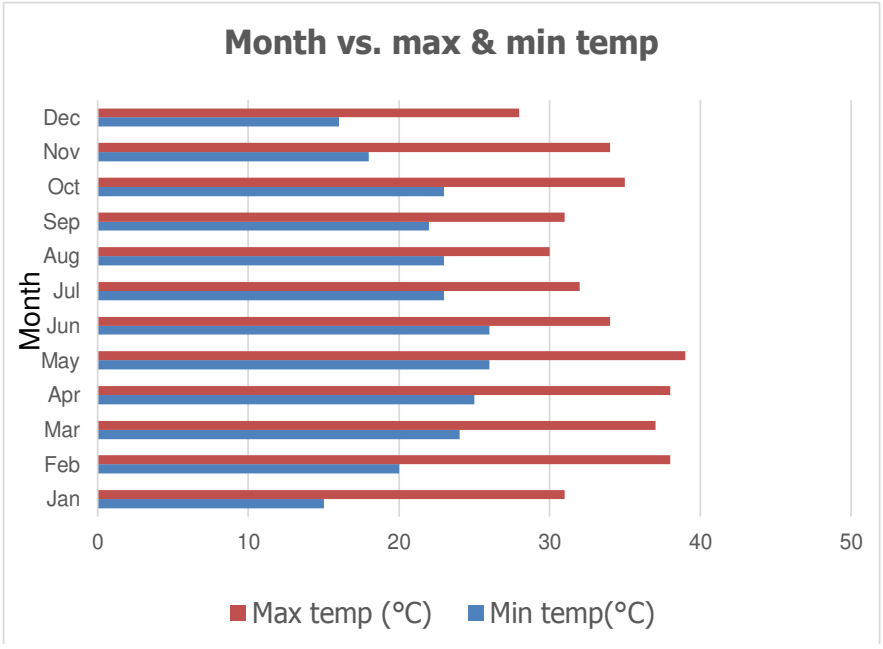

Figure 3-4. Minimum & maximum temperature for Gusau in 2015.

As shown in figure 3-3, the least of the sunshine hours are above 11 hours and the peak of the sunshine hours is slightly above 12.5 hours, which implies there is an abundance of sunlight in the area. Conversely, from figure 3-4, the peak of temperature in this location is around 38°C, which puts the temperature of the location high. Other data obtained from NIMET include the monthly solar radiation for Gusau in the year 2015 as shown in table 3.1

Table 3.1 Monthly solar radiation in Gusau in the year, 2015

Month	Jan	Feb	Mar	Apr	May	Jun	Jul	Aug	Sep	Oct	Nov	Dec
Monthly solar Radiation ($KWh/m^2/day$)	6.70	7.39	6.63	6.38	5.87	5.12	4.58	4.66	5.24	5.87	6.76	5.75

Unlike in Europe, wind resources are low in several areas of Nigeria but the distribution is appreciable in some part of the country, including the location of study as shown in figure 3-5.

The areas in green in the figure are the areas in the country where there is good potential for wind energy.

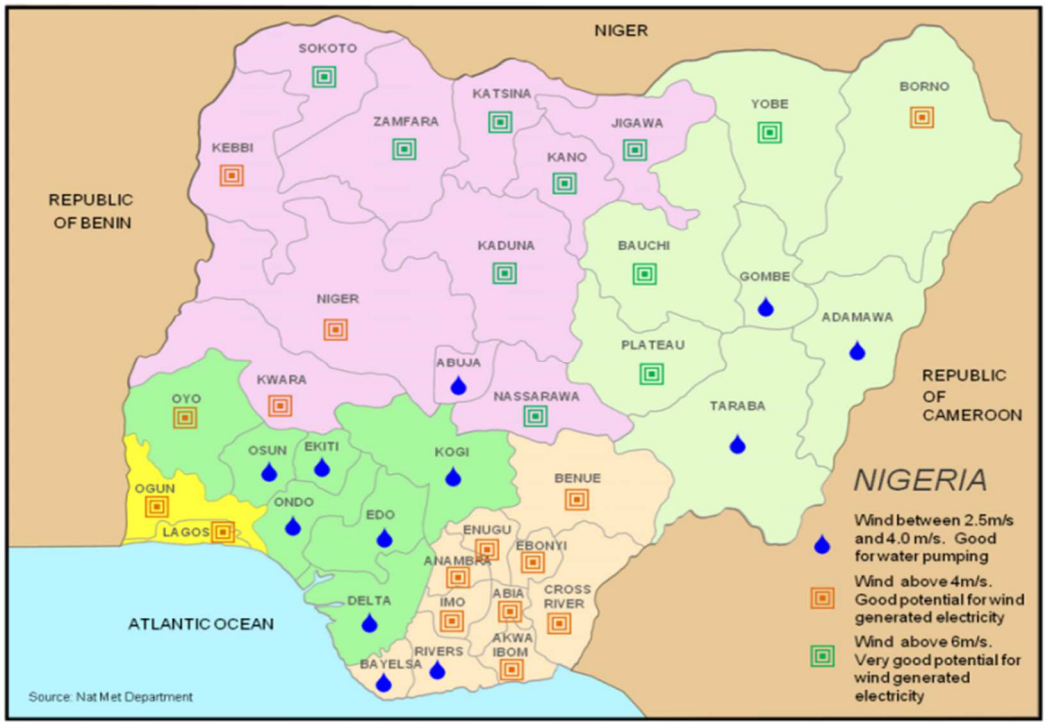

Figure 3-5. wind energy potential in Gusau, Zamfara state and other states in Nigeria [18]

Wind speed and solar radiation data for the research location obtained and implemented to estimate the electric potential at the location. The wind speed data were obtained from a research in the past [19]. The solar energy resources and clearness index for Gusau in the year 2015 is as shown in figure 3-6, and table 3.2 shows the clearness index, daily solar radiation, and wind speed values for each of the different months.

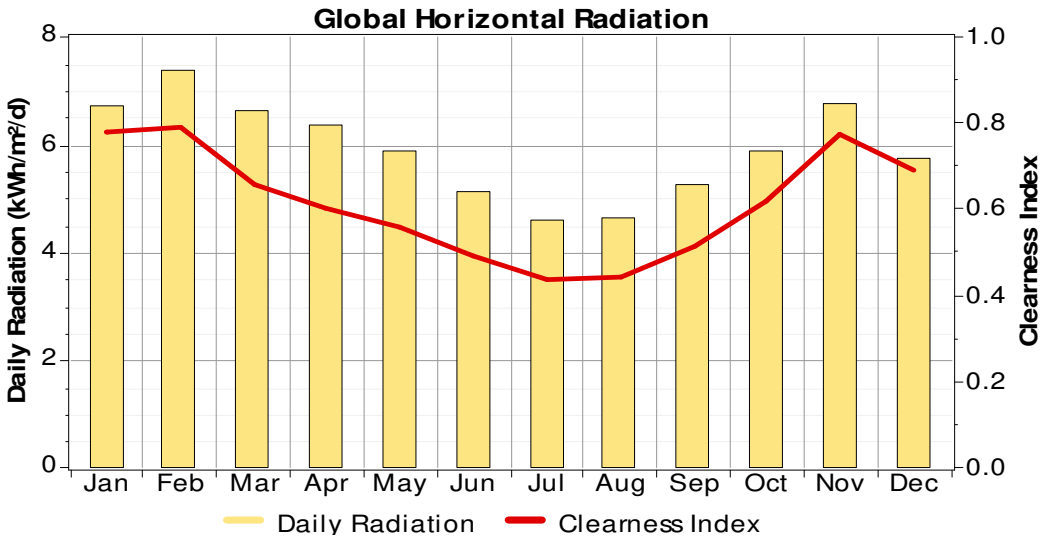

Figure 3-6. Solar energy resources in Gusau in 2015

Table 3.2 Solar and wind resources in Gusau in 2015

Month	Clearness Index	Daily Radiation (kWh/m2/d)	Wind Speed (m/s)
January	0.780	6.700	7.500
February	0.791	7.390	7.000
March	0.655	6.630	7.000
April	0.605	6.380	7.100
May	0.556	5.870	7.200
June	0.490	5.120	7.000
July	0.438	4.580	5.900
August	0.444	4.660	5.000
September	0.513	5.240	4.000
October	0.616	5.870	3.600
November	0.775	6.760	5.000
December	0.692	5.750	7.400
Annual Average		5.94899	6.139

The month, which experiences the highest sunlight is February with a daily radiation of 7.390kWh/m2/d, on the other hand, July had a daily radiation of 4.580kWh/m2/d, which is the least, from the month of March to July, the daily radiation reduces progressively with the following differences: (0.25), (051), (0.75), and (0.54). During this period of reduction in daily radiation, energy from the wind energy system can be of tremendous support, besides during the nights, the energy stored in the battery alongside the wind energy can support the system. Conversely, the daily radiation increases progressively from the month of August to November with the following differences: (0.08), (0.58), (0.63), (0.89), after which it reduces in December by (1.01) followed by another increase in January and February by (0.95) and (0.69) respectively. A plot of the wind speed, solar radiation, maximum, and minimum temperatures in Gusau is as shown in figure 3-7.

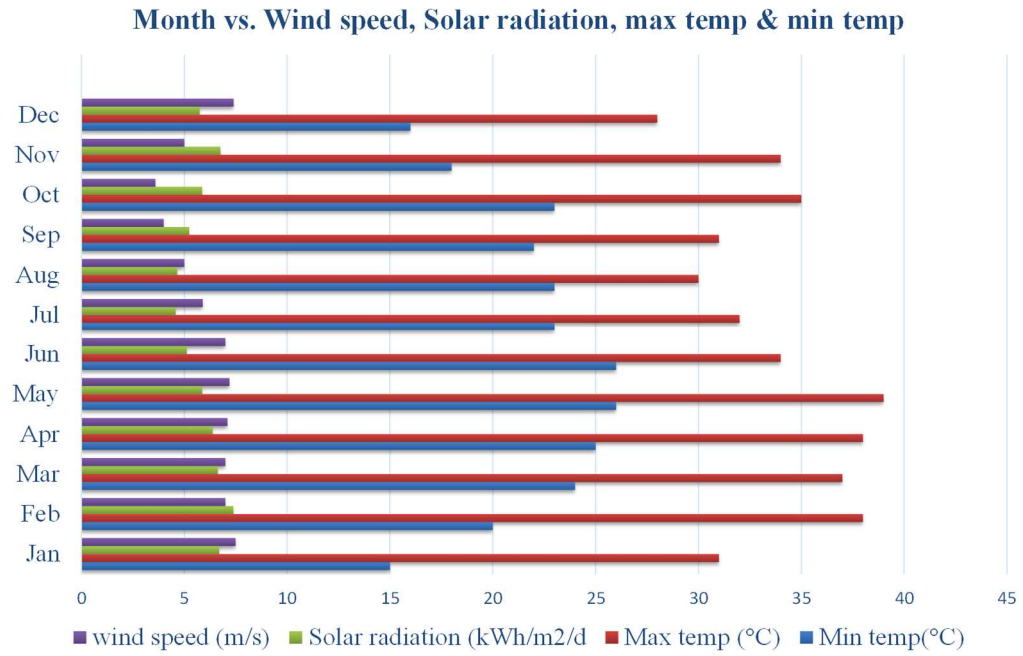

Figure 3-7. Month Vs solar radiation, max & min temperature

The wind and solar energy resources in the location have the potential to provide adequate power supply to the community, but remains yet untapped and as a result, the area is faced with inadequate power supply. Other reasons behind the challenge of inadequate supply in the area include:

- The power supply is majorly from fossil fuel, which is inadequate and capital intensive
- Several people don't have electricity as they are being isolated from the grid

- The efficiency of the Photovoltaic module reduces at the peak of the sun for those who can afford it.

In most households in rural areas including Gusau, fuelwood appears to be the major source of energy for cooking, and this leads to indiscriminate cutting down of trees since access to adequate electricity becomes more difficult. People realized they can access fuelwood resources with ease, hence the use of fuelwood as an energy source became their choice, besides for lighting, kerosene appears to be in high demand [20].

In a research carried out in the past [21], There has been no proof to confirm that those who live in remote locations make use of electricity supply from the grid. Solar and wind energy systems are still gaining awareness in the country as hydropower, energy from fossil fuel and fuelwood constitute the major source of energy consumed [22]. In order to find a solution to this lingering electricity crisis, the use of island mode of the hybrid energy system is a necessity. The main essence of employing renewable energy to provide electricity to the affected areas is due to the fact that the use of renewable energy resources for power generation provides security of supply, it reduces the number of pollutants, there is a power quality enhancement and in the process create some form of employment to those in the area [7]. The contribution of this work is to develop a new strategy to eradicate inadequate power supply in areas faced with such challenges. Hence, a hybrid energy system is designed to provide stable and adequate power to a hundred and twenty residential buildings in the area.

3.6 Method

The specific aim of this project is to provide electricity to people isolated from the grid and also, to those connected to the grid but are dissatisfied with the use of electricity from the grid. A general description of the hybrid system is as shown in figure 3-8. The design requires energy majorly from renewable energy applications such as wind turbine and PV, which requires battery storage, and a diesel generator as a reserve. The diesel generator is to serve in a situation where there is a failure of one of the sources. When power generation exceeds demand and the battery is fully charged, the excess load is channelled through to the load dump, although it is not shown explicitly in figure 3-8.

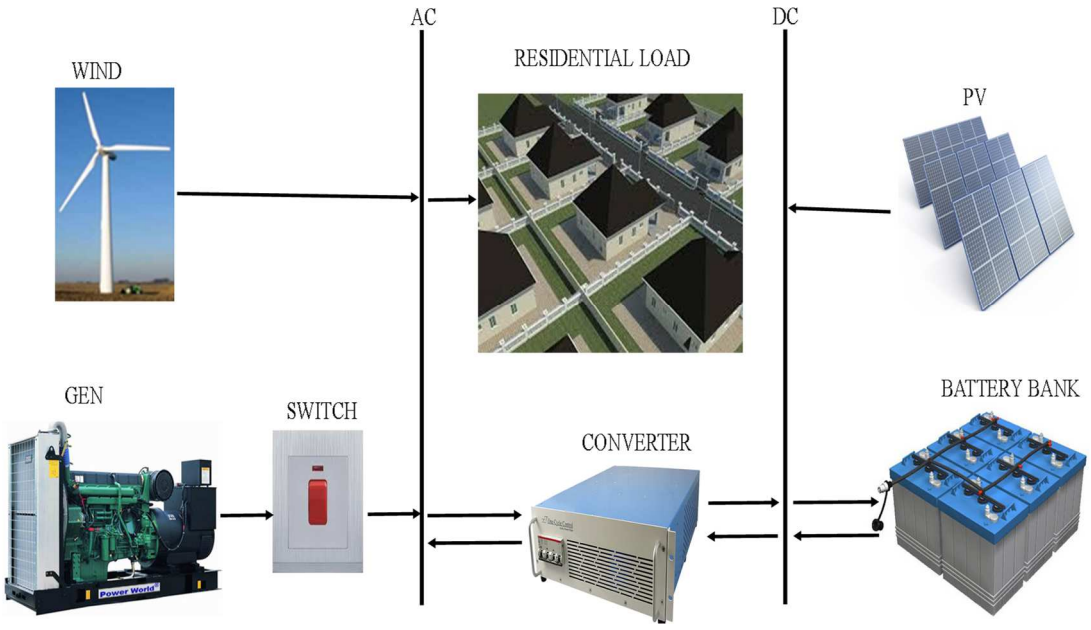

Figure 3-8. A general description of the hybrid system

The method involves the general assessment of the location to identify the gravity of the power failure challenge in the area, the unavailability of the electricity grid, the extent of environmental pollution experienced because of constant use of diesel generator as a source of power supply.

The design of the load requirement of the selected location done, the data from the available renewable energy resources in the area, coupled with the geographical information of the study location were also gathered. The method adopted the use of HOMER software simulator to enable an efficient and reliable analysis of the energy requirement of the site in question, and the use of a systematic procedure for the implementation of the simulator software.

The wind turbine and diesel generator are connected to the AC Busbar while the PV array, battery bank are all connected to the DC Busbar. With this arrangement in place, energy storage is obtainable from any of the electrical sources with the help of the converter. The control of the diesel generator is achievable with the help of the electrical switch as it serves as a reserve; its usage is in the event of total power failure. When both the Wind turbine and PV array is ON, the battery bank charges and stores energy for use when the load demand is more than supply, the battery also supplies power to the system.

3.7 Load estimation of one hundred and twenty residential apartments.

The design of the system load achieved and represented as shown in figure 3-9 and table 3.3, it is a design for 120 residential apartments and as such, to aid the accurate determination of

the total demand, the design used a diversity factor of 0.4. A diversity factor is used because all loads such as fridge, fan etc connected to the system are not operating simultaneously or are not operating at their maximum rating simultaneously [23].

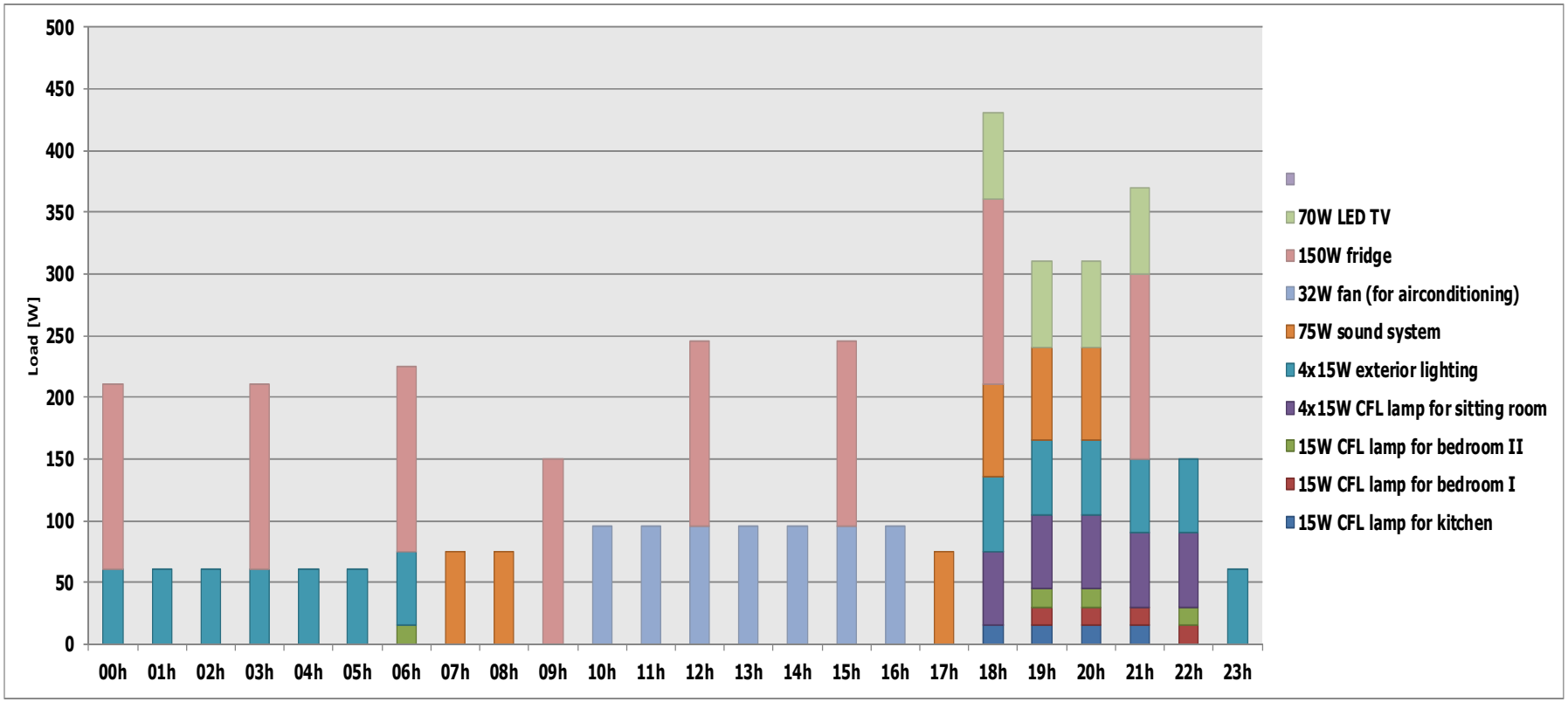

Figure 3-9. The load profile of a house

The detailed analysis of the load profile of figure 3-9 is as shown in Table 3.3 where a diversity factor of 0.4 was used, this is because, all the loads such as fridges, fan etc are not operating simultaneously.

Table 3.3 System load requirement

HOURLY LOAD [W]	00h	01h	02h	03h	04h	05h	06h	07h	08h	09h	10h	11h	12h	13h	14h	15h	16h	17h	18h	19h	20h	21h	22h	23h	Energy [Wh]
15W CFL lamp for kitchen																			15	15	15	15			60
15W CFL lamp for bedroom I																				15	15	15	15		60
15W CFL lamp for bedroom II							15													15	15		15		60
4x15W CFL lamp for sitting room																			60	60	60	60	60		300
4x15W exterior lighting	60	60	60	60	60	60	60												60	60	60	60	60	60	780
75W sound system								75	75									75	75	75	75				450
32W fan (for airconditioning)											96	96	96	96	96	96	96								672
150W fridge	150			150			150			150			150			150			150			150			1200
70W LED TV																			70	70	70	70			280
																									0
TOTAL [W]	210	60	60	210	60	60	225	75	75	150	96	96	246	96	96	246	96	75	430	310	310	370	150	60	3862 [Wh]
Number of users	120																								
TOTAL USERS [kW]	25.2	7.2	7.2	25.2	7.2	7.2	27	9	9	18	11.52	11.52	29.52	11.52	11.52	29.52	11.52	9	51.6	37.2	37.2	44.4	18	7.2	463.44 [kWh]
Demand factor	0.4																								
TOTAL DEMAND [kW]	10.08	2.88	2.88	10.08	2.88	2.88	10.8	3.6	3.6	7.2	4.608	4.608	11.81	4.608	4.608	11.81	4.608	3.6	20.64	14.88	14.88	17.76	7.2	2.88	185.38 [kWh]

Table 3.4 represents a diversity factor table for a residential apartment as specified by French standards NFC14-100 implemented for a residential apartment that does not require electrical heating. This standard is applicable to the majority of the states in Nigeria but in a situation where electrical heat-storage is required for space heating, then irrespective of the number of residential apartments involved, a factor of 0.8 is used.

Table 3.4 Diversity factor for residential apartments [23]

Apartment	Diversity factor (ks)
2-4	1
5-9	0.78
10-14	0.63
15-19	0.53
20-24	0.49
25-29	0.46
30-34	0.44
35-39	0.42
40-49	0.41
50 and above	0.40

3.8 System load variations

The load demand for this design varies from time to time during the day, from 11 pm in the night to 6 am in the morning as shown in table 3.3. The load demand is low, this is because most of the electrical devices are OFF and only the exterior lights and fridge are ON and during this period, the least load is obtainable when the fridge is not consuming energy, though there is a slight increase experienced by 6 pm. The load demand between the hours of 7 am and 5 pm is still low owing to less use of electrical devices, but the moment the time is 6 pm, the load demand is observed to be at its peak (20.64kW) as most devices are in use since most individuals would have returned back home either from work, school etc. The load remains high from 6 pm to 9 pm and begins to reduce since most people are preparing to go to sleep. The procedure used to implement the design using a HOMER software simulator is as shown in figure 3-10.

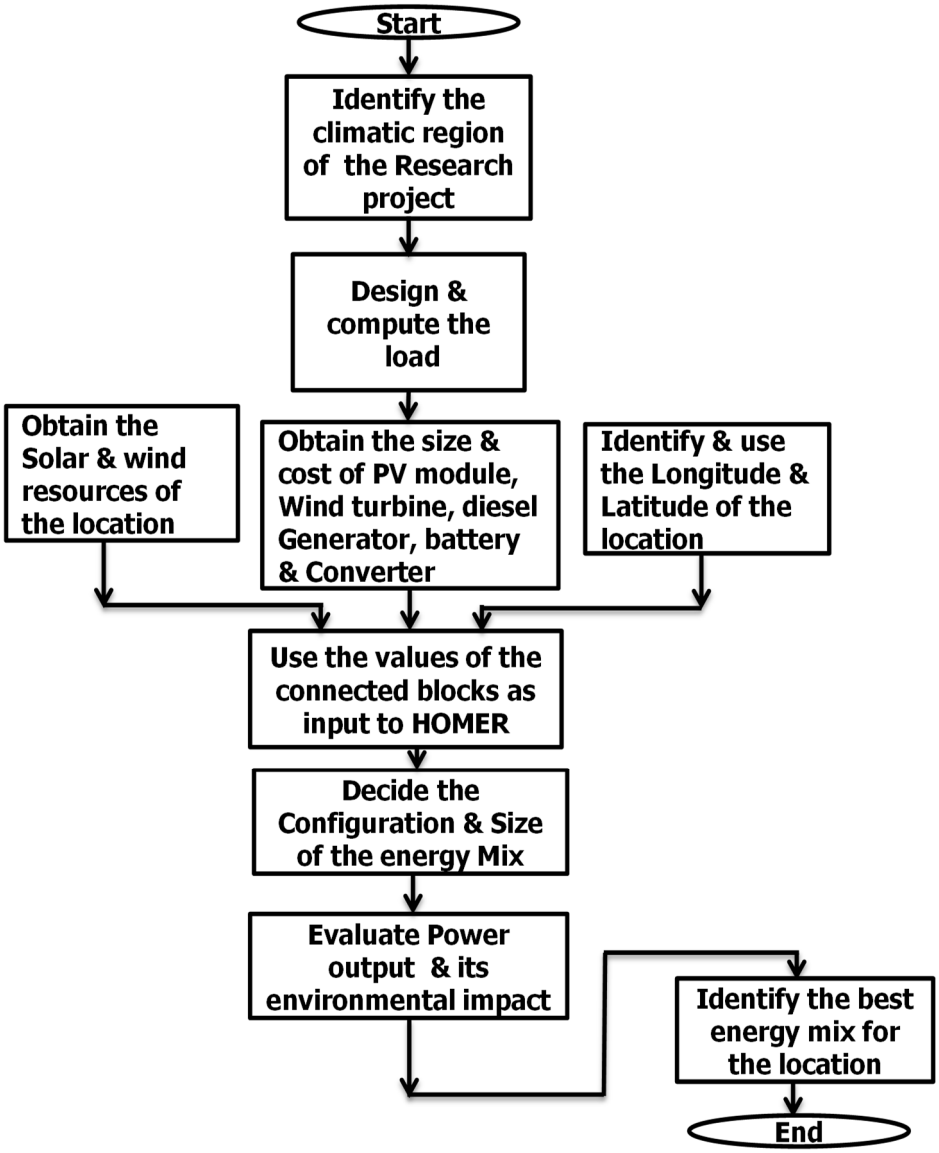

Figure 3-10. Systematic procedure

3.9 Results

The required inputs fed into the HOMER software simulator using the systematic procedure in figure 3-10 made the desired system configuration achievable. In order to ensure a reliable and efficient system sizing, I performed several simulations and gathered the results.

3.9.1 System configuration

The system configuration comprises of a wind turbine, PV array, diesel generator, battery bank, the converter, the load requirements, DC and AC buses for connection, several values of the different energy sources and devices were used as input to ensure that the best energy mix for the project under consideration is obtained. The system configuration is as shown in figure 3-11.

The simulated hybrid energy system is made of different sums of PV module of 250W up to 120kW (but the range of PV sizes varies from 0kW – 120kW), 50kW diesel generator, 50kW wind turbine and a set of converters, which range from 0kW – 80kW. The outcome of the simulation displays a number of the appropriate mix of the hybrid systems with the potential to cater for the required load demand. Based on my design, the peak load of the residential apartments is 20.64kW, but the HOMER software simulator also considers other loads, which may arise during system operation that is not accounted for in my design for example, during charging, the battery serves as load, hence, the HOMER software simulator infers a peak load of 35kW. A diesel generator slightly higher than the peak load demand was selected to match the load demand and also provide an avenue for the storage of excess energy [24]

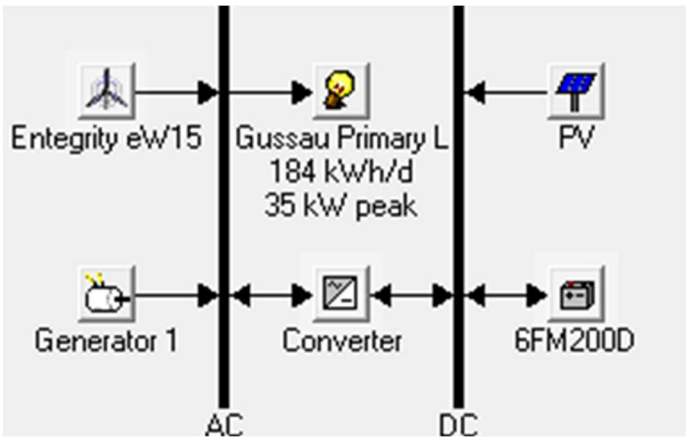

Figure 3-11. System configuration

3.9.2 Simulation results

Among the numerous simulations carried out, a section of the simulation results for sensitivity values of 5kWh/m2/d and 5m/s considered are as shown in table 3.5, 3.7 and 3.9, as the result is achievable.

Table 3.5 Option 1 Simulation result

Global Solar (kWh/m²/d) 5 Wind Speed (m/s) 5

Double click on a system below for simulation results.

PV (kW)	eW15	Label (kW)	6FM200D	Conv. (kW)	Initial Capital	Operating Cost ($/yr)	Total NPC	COE ($/kWh)	Ren. Frac.	Diesel (L)	Label (hrs)
45	1	50	540	55	$ 70,862	2,460	$ 102,314	0.119	0.97	1,623	101
40	1	50	480	46	$ 63,385	3,046	$ 102,324	0.119	0.95	2,433	150
60	1		720	44	$ 84,760	1,375	$ 102,333	0.119	1.00		
35	1	50	540	48	$ 57,891	3,477	$ 102,338	0.119	0.94	2,950	181
50	1	50	300	46	$ 74,265	2,197	$ 102,349	0.119	0.97	1,368	85
35	1	50	540	47	$ 57,798	3,487	$ 102,376	0.119	0.94	2,965	183
40	1	50	360	60	$ 63,727	3,023	$ 102,377	0.119	0.95	2,409	148
35	1	50	180	44	$ 54,640	3,734	$ 102,378	0.119	0.93	3,301	207
55	1	50	600	44	$ 82,640	1,545	$ 102,391	0.119	0.99	446	27
45	1	50	300	60	$ 69,407	2,582	$ 102,408	0.119	0.96	1,821	113
45	1	50	360	55	$ 69,422	2,581	$ 102,418	0.119	0.96	1,856	113
35	1	50	600	44	$ 58,000	3,475	$ 102,418	0.119	0.94	2,927	178
40	1	50	480	47	$ 63,478	3,050	$ 102,461	0.119	0.95	2,433	150
55	1		1140	50	$ 82,517	1,561	$ 102,474	0.119	1.00		
50	1	50	540	50	$ 76,557	2,028	$ 102,483	0.119	0.98	1,080	66
55	1	50	360	50	$ 81,277	1,659	$ 102,485	0.119	0.99	683	43
50	1	50	300	47	$ 74,358	2,200	$ 102,486	0.119	0.97	1,368	85
30	1	50	420	44	$ 50,400	4,075	$ 102,492	0.119	0.92	3,791	234
60	1		540	65	$ 85,272	1,348	$ 102,507	0.119	1.00		
55	1	50	720	44	$ 83,600	1,480	$ 102,519	0.119	0.99	297	18
35	1	50	360	65	$ 58,032	3,483	$ 102,551	0.119	0.94	2,984	184
40	1	50	600	55	$ 65,182	2,923	$ 102,553	0.119	0.95	2,185	134
55	1		1200	44	$ 82,440	1,573	$ 102,554	0.119	1.00		
30	1	50	420	50	$ 50,957	4,038	$ 102,575	0.119	0.92	3,725	230
60	1	50	480	44	$ 87,840	1,153	$ 102,585	0.119	1.00		0

The simulation results of table 3.5 present us with several alternative solutions to provide adequate power to the location. Three alternative solutions were considered out of the numerous options provided by the HOMER simulator software.

Option 1: This option of the simulation is highlighted in blue in table 3.5. This option does not generate electricity from the diesel generator. It has the diesel generator in the design as a backup in the event of power failure. The system architecture is as shown in table 3.6.

Table 3.6. Option 1 system architecture.

60kW PV, 50kW Wind turbine, 50kW Diesel Gen, 480 Vision 6FM200D battery, 44kW Inverter & Rectifier					
Production	**kWh/yr**	**%**	**Consumption**	**kWh/yr**	**%**
PV array	90,638	54	AC Primary load	67160	100
Wind turbine	77,907	46	Total	67160	100
Generator	0	0			
Total	168545	100	Excess Electricity	88581	52.6
			Unmet electrical load	0.00000226	0.0
			Capacity shortage	0.00	0.0
Quantity		**Value**			
Renewable fraction		1.00			

More electricity is generated from the PV array than wind as it appears to be the most abundant source of renewable energy in the location hence the renewable energy fraction is 1.0. The electric production for this option is as shown in figure 3-12.

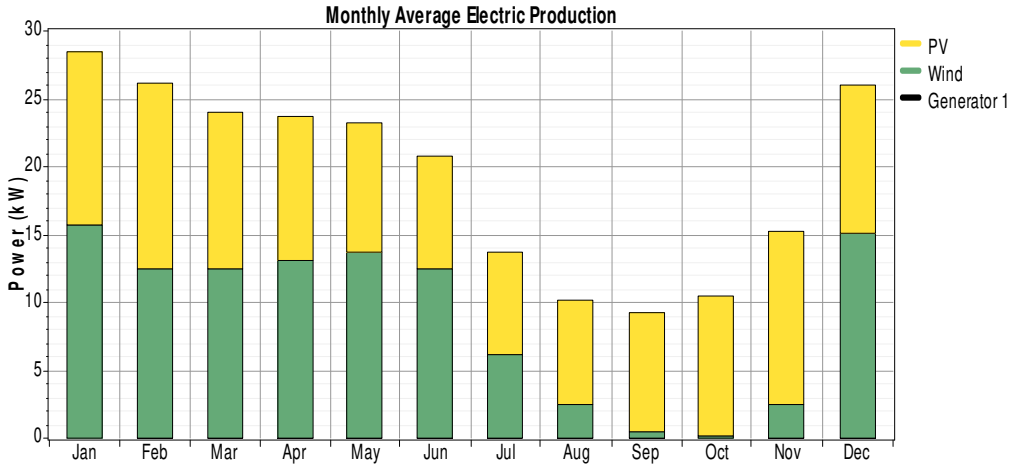

Figure 3-12 Option 1 monthly averages electric production

Figure 3-12 shows that the peak period of electricity production is in January, with December, January, and February as the periods of abundant renewable energy resources, the electrical output reduces progressively from the month of February to September, after which it begins to rise gradually. In this hybrid energy system, the sizing was done in such a way that it favours the wind and PV system relative to diesel generation. In order to overcome the challenge of climate changes and also accommodate the load demand for all the months, excess electricity is generated by the wind and PV system. The excess electricity generated differ from month to month depending on the incident solar and available wind energy resources.

The AC primary load monthly averages is as shown in figure 3-13.

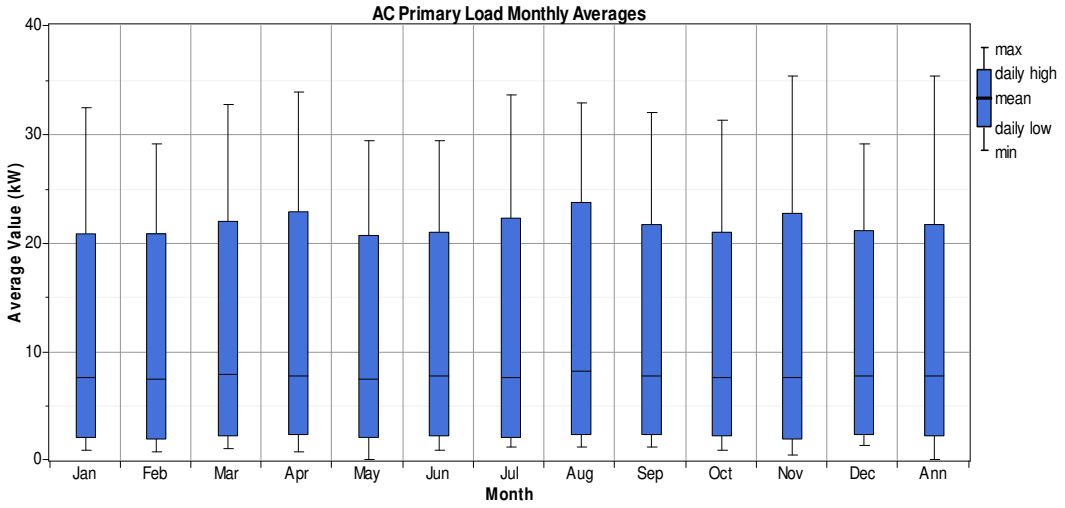

Figure 3-13 AC primary load monthly averages

The electrical energy generated is also stored in the solar energy battery bank, which also gives back the energy to the system, and because of the energy stored by the battery system; the AC production achieves a big boost to enable it to serve the AC primary load. After simulation, the AC primary load served is as shown in figure 3-14. Comparing the mean of figure 3-13, and the mean of figure 3-14, implies that the demand is being met by supply, the deficit is met by the battery and the surplus is dumped.

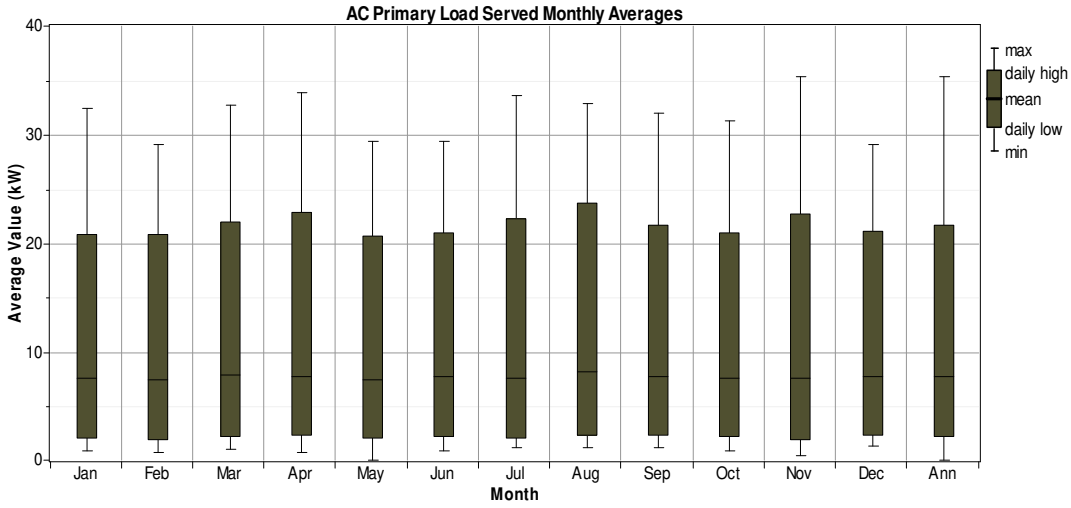

Figure 3.14 AC primary load served monthly averages

Option 2: The simulation result of this option is highlighted in blue as shown in table 3.7 and its system architecture consists of the components shown in table 3.8

Table 3.7 Option 2 simulation result

Global Solar (kWh/m²/d) 5 Wind Speed (m/s) 5

Double click on a system below for simulation results.

	PV (kW)	eW15	Label (kW)	6FM200D	Conv. (kW)	Initial Capital	Operating Cost ($/yr)	Total NPC	COE ($/kWh)	Ren. Frac.	Diesel (L)	Label (hrs)
	60	1		480	46	$ 83,025	1,249	$ 98,994	0.115	1.00		
	60	1		480	47	$ 83,118	1,253	$ 99,131	0.115	1.00		
	35	1	50	300	44	$ 55,600	3,412	$ 99,219	0.116	0.94	2,972	185

Table 3.8 Option 2 system architecture.

35kW PV, 50kW Wind turbine, 50kW Diesel Gen, 300 Vision 6FM200D battery, 44kW Inverter & Rectifier					
Production	**kWh/yr**	**%**	**Consumption**	**kWh/yr**	**%**
PV array	52,872	38	AC Primary load	67160	100
Wind turbine	77,907	56	Total	67160	100
Generator	8,928	6			
Total	139,707	100	Excess Electricity	58,379	41.8
			Unmet electrical load	0.00000584	0.0
			Capacity shortage	0.00	0.0
Quantity		**Value**			
Renewable fraction		0.936			

In this case, energy generation is from the PV array, wind turbine, and a diesel generator. The renewable energy fraction is 0.936, which also shows a deep penetration of renewable energy, but the challenge with this option is that the diesel generator is under-utilized. Whenever a diesel generator is required, it operates at full capacity, hence under-utilizing the diesel generator reduces the performance as well as the efficiency of the diesel generator with time. The electric production from this configuration is as shown in figure 3-15.

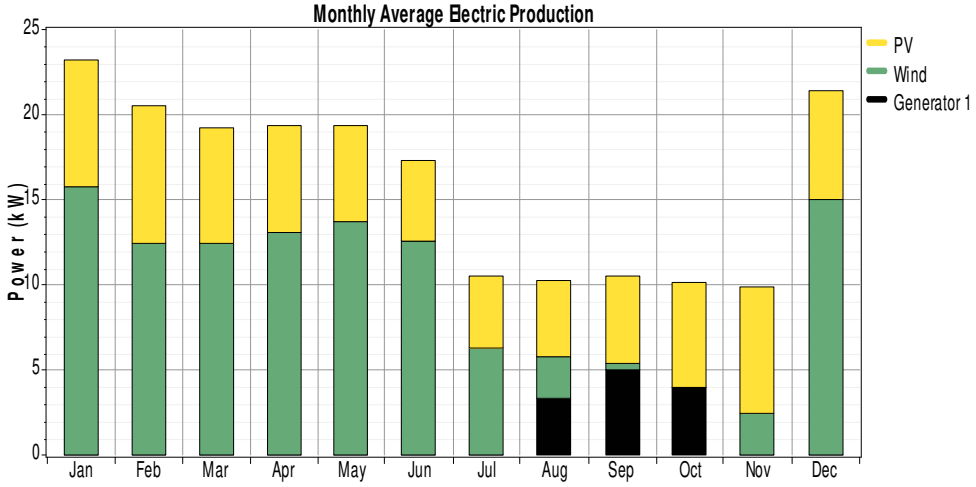

Figure 3-15 Option 2 monthly averages electric production.

The results generated from the HOMER software simulator infer the monthly production shown in figure 3-15. Electricity generation from wind and PV in August, September, and October are low. Hence, the diesel generator is required to supply electricity to the load and also charge the battery (which also serves in the event of a shortage of power). Other months such as March, April, May, June, July and November require battery support. The use of diesel generator faces the risk of being under-utilised in the month of August, September, and October. Electricity from wind and PV cannot replace the need for diesel generator in the month of August, September, and October, but could offset a portion of the diesel fuel used.

Option 3: The simulation result of this option is highlighted in blue as shown in table 3.9. Its system architecture does not include the use of the PV array, electricity generation is achieved from the wind turbine and the diesel generator as shown in table 3.10.

Table 3.9 Option 3 simulation result

Global Solar (kWh/m²/d) 5 Wind Speed (m/s) 5

Double click on a system below for simulation results.

PV (kW)	eW15	Label (kW)	6FM200D	Conv. (kW)	Initial Capital	Operating Cost ($/yr)	Total NPC	COE ($/kWh)	Ren. Frac.	Diesel (L)	Label (hrs)
60	1		420	44	$ 82,360	1,209	$ 97,817	0.114	1.00		
35	1	50	300	44	$ 55,600	3,412	$ 99,219	0.116	0.94	2,972	185
	1	50	300	46	$ 12,665	9,393	$ 132,741	0.155	0.72	10,219	630

Table 3.10 Option 3 system architecture.

50kW Wind turbine, 50kW Diesel Gen, 300 Vision 6FM200D battery, 46kW Inverter & Rectifier					
Production	**kWh/yr**	**%**	**Consumption**	**kWh/yr**	**%**
Wind turbine	77,907	72	AC Primary load	67160	100
Generator	30,794	28	Total	67160	100
Total	108702	100	Excess Electricity	22,775	21.0
			Unmet electrical load	-0.00000226	0.0
			Capacity shortage	0.00	0.0
Quantity		**Value**			
Renewable fraction		0.717			

The renewable fraction, in this case, is 0.717 and is less compared to option one. The challenge with this option is that it does not utilize energy from the PV array, which appears to be the most available source of renewable energy in the research location. The electric production, in this case, is as shown in figure 3-16.

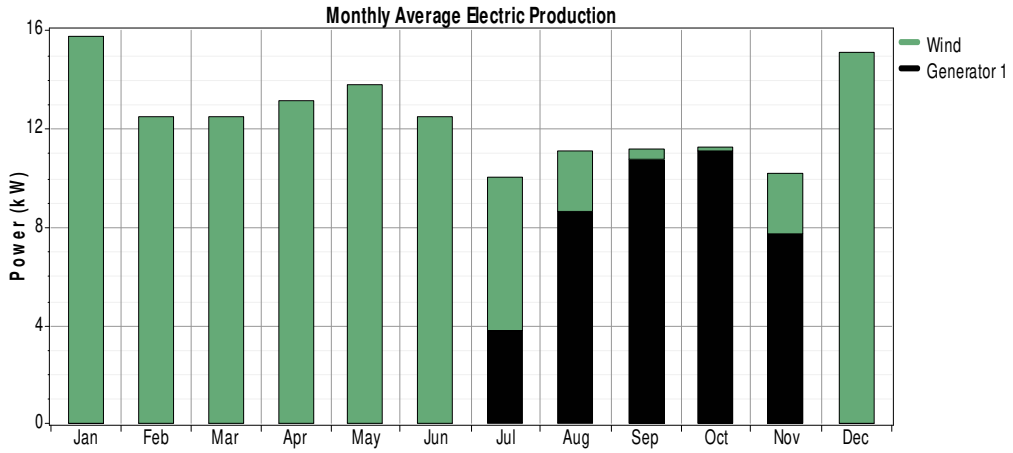

Figure 3-16 Option 3 monthly averages electric production.

In this option, electricity generation from the wind energy in the month of January, February, March, April, May, June, and December is high, any deficit is provided by the battery storage. For the month of July, August, September, October and November, electricity production from the diesel generator supports the electricity generated from the wind to serve the load. In the months of August, September, October, and November, the average production from diesel is well above the average demand for these months, the surplus production from diesel is not dumped but stored in the batteries leaving the system with no excess energy in those months as shown in figure 3-17. This architecture relies on battery support and the electricity supply from the diesel generator to meet the load

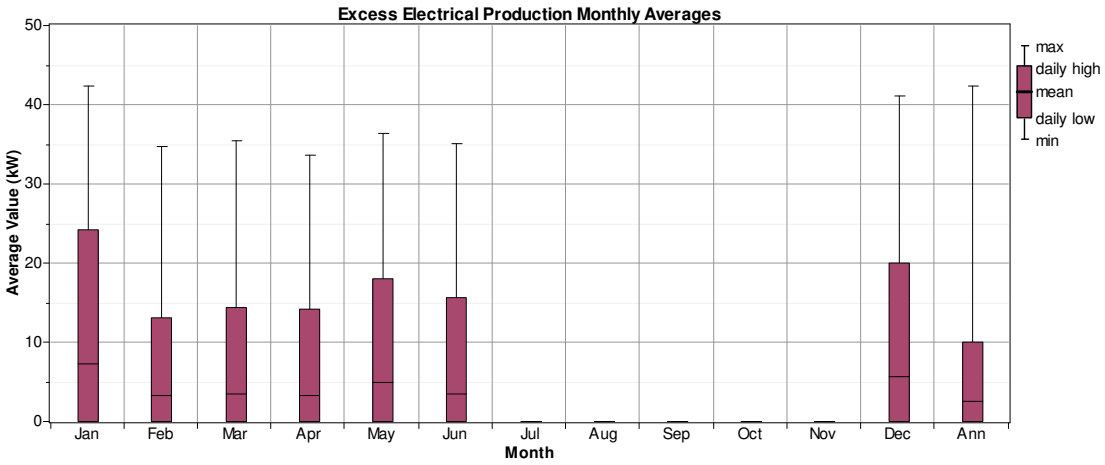

Figure 3-17 Excess Electrical production monthly averages

Cost consideration was not an issue in this research, hence it was not included in the criterion. The interest in this research is to provide electricity with deep penetration of renewable energy, even if the required starting capital is high as the operating cost is low and there is little or no cost for fuelling compared to those with a diesel generator. Option 1 can serve without the use of the diesel generator, but due to the unstable nature of renewable energy resources, it was included as a backup source of power. After careful consideration of several system architectures obtained from the simulation result, Option 1 was selected as more electricity is generated from the PV array, which appears to be the most abundant source of renewable energy in the location. Conversely, option 1 allows for the highest penetration of renewable energy among the three options.

3.9.3 Capacity of energy storage

The selected hybrid energy system configuration (option 1) shows that a total of 480 batteries, each with a nominal voltage of 12V, and a nominal capacity of 200Ah (2.4kWh) is required for this project. It comprises a string size of 30 with 16 battery strings in parallel.

Batteries added up in series to increase the voltage while the amperage remains the same. Conversely, they add up in parallel to increase current while the voltage remains the same. A string size of 30 implies connecting 30 batteries in series. This generates 30(12V), at an amperage of 200Ah, and hence, the bus voltage is 360V. A battery string size of 30 generates 360V, 200Ah. 16 parallel strings of the battery connected in parallel yields 360V, 16 (200Ah). Therefore, the 480 batteries required for this research work generate a bus voltage of 360V and an amperage of 3200Ah.

During the operation of the system, the battery is either in the charging mode or in storage mode or in discharging mode. When the amount of energy generated by the hybrid system is more than the energy required by the load, there is excess energy, which is stored in the battery, during this state, the battery is in the charging mode. When the amount of energy generated is less than the amount of energy required by the load, the battery supplies power to the system and therefore in the discharging mode. The battery is in the storage mode when the battery stores energy for future use, this happens when the amount of energy generated by the system equals the amount of energy required by the load.

The minimum state of charge of the battery is slightly above 40%, the battery bank has a nominal capacity of 1,152kW and autonomy of 90.2 hours, the battery bank gives out 31,149kWh/yr, with losses of about 7700kWh/yr and an expected life of 10years. The batteries monthly statistics show that in the month of January, February, March, April, May, June, July, November and December, the battery bank state of charge remains high and this is because there is enough energy produced by the mix that the battery does not need to be used up. However, in the month of August, the state of charge of the battery drops and with the least obtained in September and that is, the month with the least electricity production as shown in figure 3-18. In those months in which the energy generated is more than the load demand, the batteries serve as a storage of the excess energy.

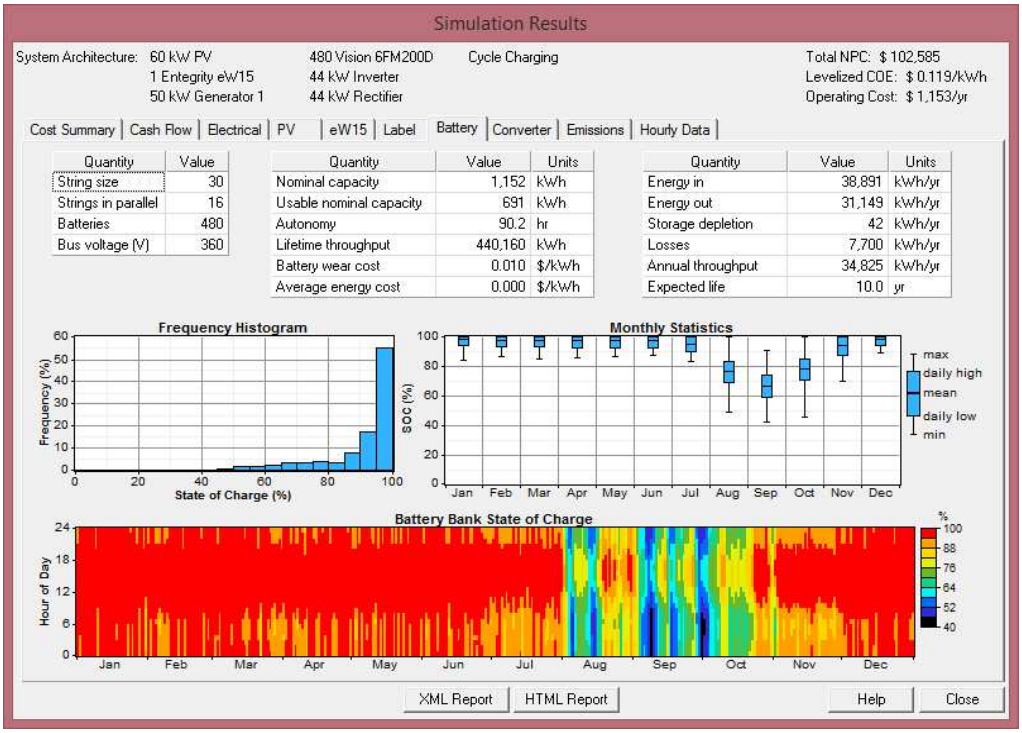

Figure 3-18. Battery bank state of charge

The monthly electricity output generated by the wind turbine and the PV array is as shown in figure 3-19 and 3-20 respectively.

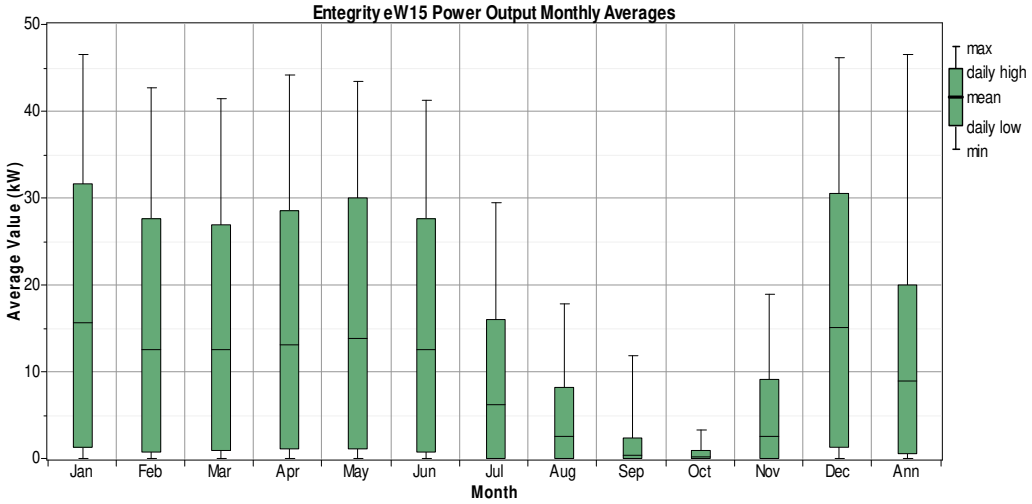

Figure 3-19. Wind turbine power output

As shown in the figure 3-19, this research location experiences low wind speed in the month of July, August, September, October, and November, after which, the wind speed begins to rise again with the peak wind speed in the month of December.

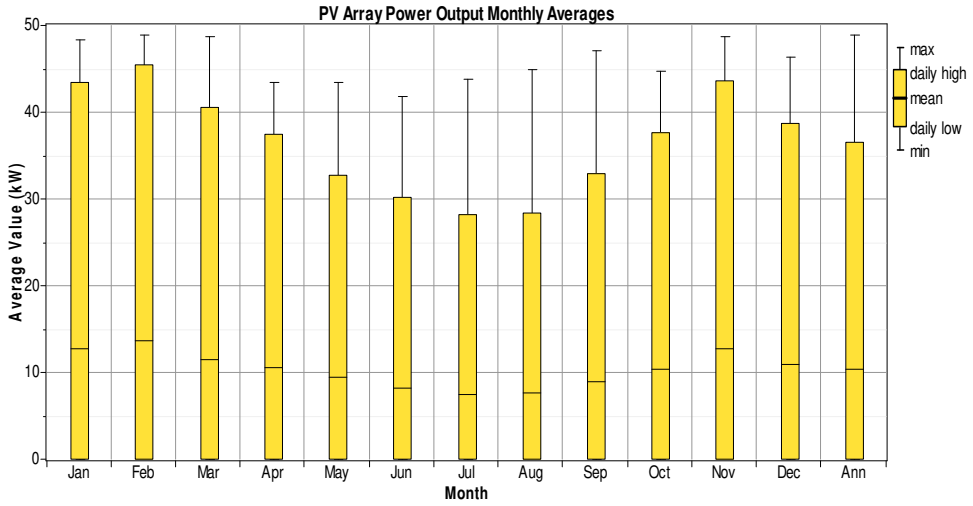

Figure 3-20. PV array power output.

Conversely, in this location, the solar energy is more promising than wind energy; the peak solar energy is generated in the month of February.

3.9.4 Summary

From the Homer Software simulator output, the total yearly electricity production is 168,545kWh/yr., the yearly AC primary load consumption is 67160 kWh. In addition, the excess electricity is 88581kWh/yr. The excess electricity accounts for 52.6% of the total electricity generated. Conversely, table 3-3 shows that the peak demand is 20.64kW, and the AC primary served as shown in figure 3-16 shows that the AC primary load for each month was met. Therefore, the hybrid energy system has the potential to provide the affected area with an adequate power supply that is environmentally friendly.

3.10 References

[1] M. Ibrahim, A. Khair, and S. Ansari, "A Review of Hybrid Renewable Energy Systems for Electric Power Generation," *J. Eng. Res. Appl. www.ijera.com ISSN*, vol. 5, no. 81, pp. 2248–962242, 2015.

[2] "Feasibility Study of Solar-Wind Hybrid Power System," *Int. J. Emerg. Technol. Adv. Eng.*, vol. 2, no. 3, pp. 125–128, 2012.

[3] M. Farman, A. Alam, and M. P. Sharma, "Off-Grid Hybrid Energy Systems for Rural Electrification," in *National Conference on Power and Energy Systems (NCPES-2011) April 23-24, 2011*, 2011, no. April, pp. 51–57.

[4] V. Bakić, M. Pezo, Ž. Stevanović, M. Živković, and B. Grubor, "Dynamical simulation of PV/Wind hybrid energy conversion system," *Energy*, vol. 45, no. 1, pp. 324–328, 2012.

[5] F. Jahanbani and G. H. Riahy, "Optimum Design of a Hybrid Renewable Energy System," *Renew. Energy - Trends Appl.*, pp. 231–250, 2008.

[6] A. V. Anayochukwu, "Simulation of Photovoltaic / Diesel Hybrid Power Generation System with Energy Storage and Supervisory Control," vol. 3, no. 3, 2013.

[7] S. Negi and L. Mathew, "Hybrid Renewable Energy System : A Review," vol. 7, no. 5, pp. 535–542, 2014.

[8] Y. Sawle, S. C. Gupta, and A. Kumar Bohre, "PV-wind hybrid system: A review with case study," *Cogent Eng.*, vol. 18, no. 3, pp. 1–31, 2016.

[9] H. Belmili, M. Haddadi, S. Bacha, M. F. Almi, and B. Bendib, "Sizing stand-alone photovoltaic-wind hybrid system: Techno-economic analysis and optimization," *Renew. Sustain. Energy Rev.*, vol. 30, pp. 821–832, 2014.

[10] J. L. Bernal-Agustín and R. Dufo-López, "Simulation and optimization of stand-alone hybrid renewable energy systems," *Renew. Sustain. Energy Rev.*, vol. 13, no. 8, pp. 2111–2118, 2009.

[11] A. Chauhan and R. P. Saini, "A review on Integrated Renewable Energy System based power generation for stand-alone applications : Configurations, storage ...," *Renew. Sustain. Energy Rev.*, vol. 38, pp. 99–120, 2014.

[12] "HOMER Help Manual."

[13] A. Chauhan and R. P. Saini, "A review on Integrated Renewable Energy System based power generation for stand-alone applications: Configurations, storage options, sizing methodologies and control," *Renew. Sustain. Energy Rev.*, vol. 38, pp. 99–120, 2014.

[14] S. Negi and L. Mathew, "Hybrid Renewable Energy System: A Review," *Int. J. Electron. Electr. Eng.*, vol. 7, no. 5, pp. 535–542, 2014.

[15] M. Abdolzadeh and M. Ameri, "Improving the effectiveness of a photovoltaic water pumping system by spraying water over the front of photovoltaic cells," *Renew. Energy*, vol. 34, no. 1, pp. 91–96, 2009.

[16] G. Notton, S. Diaf, and L. Stoyanov, “Hybrid photovoltaic/wind energy systems for remote locations,” *Energy Procedia*, vol. 6, pp. 666–677, 2011.

[17] A. V. Anayochukwu, “Energy Optimization Map for Off-Grid Health Clinics in Nigeria,” vol. 4, no. 1, 2014.

[18] N. V. Emodi, *Energy Policies for Sustainable Development Strategies*. 2016.

[19] O. O. Ajayi, R. O. Fagbenle, J. Katende, J. O. Okeniyi, and O. a. Omotosho, “Wind Energy Potential for Power Generation of a Local Site in Gusau, Nigeria,” *Int. J. Energy a Clean Environ.*, vol. 11, no. 1–4, pp. 99–116, 2010.

[20] a. S. Sambo, “Renewable Energy for Rural Development: The Nigerian Perspective,” *ISESCO Sci. Technol. Vis.*, vol. 1, pp. 12–22, 2005.

[21] H. M. Muye, “Adoption of Solar Energy Systems in Remote and Rural Communities of Nigeria (A Review),” vol. 4, no. 1, pp. 23–28, 2016.

[22] D. Maijama, A. L. Maijama, and A. M. Umar, “Renewable sources of energy for economic development in Nigeria,” vol. 4, no. 2, pp. 49–63, 2015.

[23] S. Schneider Electric, Electrical installation guide - According to IEC international standards. Schneider electric, Merlin Gerin, 2007.

[24] S. M. Shaahid, “Review of research on autonomous wind farms and solar parks and their feasibility for commercial loads in hot regions,” *Renew. Sustain. Energy Rev.*, vol. 15, no. 8, pp. 3877–3887, 2011.

Chapter 4:

Enhancing PV modules efficiency and power output using the multi-concept cooling technique.

Nigeria is a country, which experiences high Sunlight throughout the year, and as a result, every effort of Nigerian government focuses on taking advantage of the availability of intense sunlight to end the problem of shortage of power supply in the country. The idea is to reduce over-dependence on the hydroelectric energy power source, which is inadequate and requires huge capital every year. Due to the abundance of sunlight in Nigeria, electricity generation from solar energy resources appears more prominent than energy generation from wind. Electricity generation from solar energy resources does not produce pollutants, and also fuelling is not required, as a result, it makes it a very favourable source of energy [1]. Generation of electricity from solar energy sources is a function of the efficiency of the PV module, and several factors influence module efficiency. Temperature among the numerous factors affecting the efficiency of the PV module is the major factor affecting PV module efficiency and power output in Sokoto, Gusau, and other locations with similar weather condition. This is because the location experiences high temperature, long period of sunshine and setback from the use of PV power when the temperature is at its peak

This chapter contains the survey of past efforts made by researchers to tackle the effect of temperature on the efficiency of the PV module. Other areas covered in this chapter include the temperature effect on PV module, PV module temperature coefficient of power, the effect of heat on PV module, cooling of PV module, concept, features, and advantages of the proposed method of cooling. Conversely, the result of experiments to demonstrate the improvement in efficiency of the PV module using multi-concept cooling technique also analysed. In one of the experiments, effort was made to improve the efficiency of the PV module, and also increase the power output using a derating factor of 80%. In the second experiment, the emphasis is on increasing the power output. The module manufacturer's rating is being considered and a derating factor of 95%, which considers a loss of power by 5% was used. Cooling is again applied to the PV module to increase his power output via increased module efficiency

4.1 Literature survey

With the exposure of PV module to sunlight, the amount of energy from the sun converted to useful energy is about 31%, a greater percentage change to heat energy, which tends to make the temperature of the module to rise, and this leads to a reduction in electricity produced by the module. An increase in the temperature of the module as a result of this energy wasted as heat can damage the material used to fabricate the PV module and hence reduce the cell lifespan as well as its conversion efficiency [2].

A review of past research effort to identify a solution to the challenge of overheating of PV modules shows that a single concept cooling technique has been employed. In [3] an attempt was carried out to provide active cooling, a pipe whose role was to serve as a spiral exchanger was stationed on the module, the result indicates 13% increase in the efficiency of the module with this cooling approach.

In a recent research, [4] effort was made to cool the PV module using water spraying, and an attempt was also made to ascertain how long it takes to reduce the temperature of the module to 35°C, the result indicates the module energy output was highest when cooling commenced at 45°C. In order to reduce the temperature of the module from the rear, an attempt was made in [5] where an efficiency of 9% was achieved, in this experiment an active cooling system was adopted where a heat exchanger was mounted at the back of the PV module and this helped to reduce the module temperature appreciably.

Conversely, another effort was also made to extract heat from the rear of the PV module in [6], here a sheet of clay was added to the rear of the module and a provision was made for an insubstantial amount of water to evaporate and in the process, the power output increased by 19.4%. Still on the rear of the panel, in [7] a cooling system was carried out with the help of a fan for air cooling and an appreciable amount of energy was achieved.

A hybrid solar/thermal system was carried out in [8] to reduce the temperature of PV modules, in this experiment, the rear of the PV module was fitted with an arrangement of the air channel, an increase in efficiency of around 14% was achieved. A past research, [9] focuses on the use of active water cooling on concentrated CPV and the result shows that as the module temperature dropped below 60°C, the power output improved. Several other efforts are ongoing to tackle the challenge posed by overheating of PV module. To achieve a more efficient use of the energy from the sun, an experiment was designed and performed in [10] where the energy extracted through the use of a small arrangement of the water used in cooling

is being channelled for another purpose so as to avoid wastage, the efficiency obtained in general was more than the regular arrangement.

Some years ago, an attempt was made in [11], to reduce the PV module temperature using an installed water pumped. In this experiment, the pump water serves as the source of cooling water to the module. The results show that the power output from the PV module and the overall efficiency improved substantially. Furthermore, the performance of the PV module when immersed in water was carried out in [12], an appreciable rise in the output power was achieved. The surface cooling approach was adopted in [13], an effort was made here to lower the temperature at the surface of the panel, a water arrangement was installed to provide water drizzling on the PV module surface, the experiment yielded 15% rise in output at the height of solar radiation. In [14], cooling of the PV module surface to reduce the temperature became the primary focus, a water pump was used for spraying the PV module as well as enhancing the operation of the pump framework. The experiment recorded a rise in the power of the cell, which causes the efficiency of the system as well as the rate at which the pump flows to increase.

A cooling medium, which employs the use of siphonage was carried out in [15], the cooling medium was fastened to the solar module rear side of a number of PV modules connected together, cooling was achieved with the help of a number of small openings in the cooling medium at the rear of each panel through which water flows. The siphonage helped to channel water into the PV module. Cooling of the PV module improves the efficiency of the PV module, as well as the power output and, the experiment, helped to generate hot water for use. In another research [16] effort made to help improve the PV module efficiency using water as the cooling medium, with the spraying of the water facilitated by a fan. The results show that out of the two PV modules used in this experiment, the PV module sprayed with water facilitated with the help of a fan produced a higher power output. An observation worthy of note is that using the fan for spraying was not effective as some part of the PV module that cannot be reached were left out of the cooling process.

Furthermore, a researcher attempts to reduce the overheating of a concentrating PV module in [17], the experiment involves a concentrated solar energy obtained from the PV module and a heat pipe made of copper with water as the working fluid. Conversely, attached to the heat

pipe are fins made of aluminium to aid cooling, the result shows that the heat pipe helped to channel the heat away from the PV module.
In a recent research [18] an effort was made to reduce overheating of PV cell by applying free running water at the surface of the panel. Asides cooling, the free running water washed away the dirt deposit on the surface of the panel. The experiment recorded 8.4% rise in its power output, but there was nothing to show the quantity of used pump water for cooling. Another research carried out recently, [19] involves a wind collecting apparatus based cooling system built to reduce PV cell temperature in a hybrid Wind/PV system. The cooling system performs two functions: it reduces the PV cell temperature and generates power. The outcome of the experiment shows that both the wind and PV module recorded a 36% rise in power.

A review of the possibility of using Nanofluids for cooling PV cells was carried out in [20], the result indicates that the temperature of the Solar thermal system can be reduced with the help of Nanofluids. A Recent research work, [21] employed the use of Peltier effect to reduce the temperature of PV modules, at the rear of the single PV cell was attached a thermo-electric unit with an assumption that the PV cell will provide the energy to operate the thermoelectric unit. A MATLAB model was developed to ascertain the system temperature, the experiment considered two techniques and the outcome shows that the temperature of a solar cell in a PV module can be kept low with the help of a thermo-electric cooling unit.

Another research effort was made in [22] to cool the temperature of the PV module with water or air using a micro-heat-pipe. The experimental setup is made of a PV module, which embraced air-cooling, and another PV module, which embraced water-cooling. The heat-pipe, which is attached to the rear of the module has two major parts namely the condenser part and the evaporator part. The experiment achieved cooling of the condenser part using water or air as the medium. The result of this setup attained a rise in the module efficiency by 2.6% with air, as the medium for cooling while a 3% rise in the efficiency of the PV module was achieved using water as the medium for cooling the module.

This research aims at using the multi-concept cooling technique to help reduce overheating of the PV module. This is to increase the PV module efficiency and power output by cooling the module surface with water and attaching an Aluminium heat sink to the rear of the module for heat extraction. This research attempts to solve the following research questions:

- PV module efficiency/Power output reduces as the surface temperature of the PV module increases due to overheating; how do we solve the challenge of overheating?
- How can the PV module generate peak power continuously at the peak of sunlight?

4.2 PV module efficiency

Ambient temperature, as well as the temperature of the module, affects a PV module efficiency and this is because the module voltage and current depend on temperature. The PV module maximum power as expressed in [23][24] is

$$P_{mp} = V_{mp}.\mathrm{I}_{m\ p} = V_{oc}.I_{sc}.FF \quad (1)$$

Where P_{mp} stands for the PV module maximum power, V_{mp} stands for the maximum voltage, I_{mp} stands for maximum current, FF stands for fill factor while V_{oc} and I_{sc} stand for open circuit voltage and short circuit current respectively. As the module temperature increases, the I_{sc} rises a little bit while the fill factor and V_{oc} reduce in magnitude.

The efficiency of a PV cell as in [25] is the ratio of energy output obtained from the PV cell divided by the energy input provided by the sun as represented in equation (2).

$$\eta = E_{out} / E_{in} \quad (2)$$

The PV module efficiency can also take the form of equation (3)

$$\eta = P_{\max} / E.A \quad (3)$$

Where $P_{\max}$ is the maximum power, E is the solar irradiance under STC (W/m^2) and A is the surface area of the module in m^2.

The efficiency of a solar cell can also be expressed using the relation in [26] as

$$\eta_{pv} = \eta_{rT}[1-\beta(T_{pv}-T_{rT})] \quad (4)$$

Where η_{pv} represents the efficiency of the PV cell, η_{rT} is the PV module efficiency at the reference temperature, which is usually 25°C, T_{pv} is the temperature of the PV module cell, β represents the temperature coefficient of power and T_{rT} is the reference temperature of the PV module or module cell.

4.2.1 Temperature effect of PV module

The temperature effect of a PV module can be expressed using the equation for PV array power output as in [27] as

$$P_{pv} = Y_{pv}.f_{pv}(G_T / G_{T,STC})[1+\alpha_p(T_C - T_{C,STC})] \quad (5)$$

Where

Y_{pv} is the rated capacity of the PV array, which implies that its output power under standard test conditions (kW)

f_{pv} is the PV derating factor (%),

G_T is the solar radiation incident on the PV array in the current time step (kW/m^2)

$G_{T,STC}$ is the incident radiation at Standard Test Conditions (1Km/m^2)

α_p is the temperature coefficient of power (%/°C)

T_c is the PV cell temperature in the current time step (°C)

$T_{C,STC}$ is the PV cell temperature under standard test conditions (25°C)

The PV module temperature coefficient of power is essential as it helps in the determination of the deviation of power produced by the module from its values at STC [28], the temperature coefficient of power for this PV module is -0.44%/°C. Furthermore, the experiment considered the derating factor of PV module; this is because, PV modules, measurement in the field may indicate that the module powers obtained are different from that of the nameplate reading. Some environmental factors such as cloud, high dust concentration, shadow, etc. can reduce the efficiencies of the PV module [29]. Performing a PV module experiment with a derating factor of 0.95 implies that the test yielded power readings at STC, which are 5% lower than the nameplate rating of the PV manufacturer. The power output equation of the PV array uses this factor to account for factors like wiring losses, shading, soiling of the module, etc. This experiment used a derating factor of 0.8 to account for the losses and a derating factor of 1.0 for an installation done in an ideal situation.

The efficiency of the PV module can be expressed as in [27] as

$$\eta_{mp,STC} = Y_{pv}/(A_{pv}.G_{T,STC}) \quad (6)$$

Where

$\eta_{mp,STC}$ is the PV module's efficiency under standard test condition (%).

Y_{pv} Represents the PV module's rated power output at STC (kW)

A_{pv} Is the PV module's surface area (m^2)

$G_{T,STC}$ Represents the radiation at STC (1kW/m^2)

By substituting, for $A_{pv}.\eta_{mp,STC} = Y_{pv}/(G_{T,STC})$, in equation (5), the efficiency of the PV module becomes

$$\eta mp = P_{pv}/((A_{pv}.f_{pv}.G_T)[1+\alpha_p(T_C - T_{C,STC}]) \quad (7)$$

4.2.2 Photovoltaic module temperature coefficient of power.

For a PV module, this coefficient shows the extent to which the temperature of the PV cell affects the power generated from the module. This temperature coefficient is assigned a negative value and this is because as the temperature of the PV cell increases, the power output reduces [30]. The temperature coefficient of the model of 250 Watt PV module used in this experiment is -0.44%/°C [31], this implies that for every degree rise in temperature above 25°C, the module maximum power experiences -0.44% reduction. When the temperature increases above 25°C, the power output reduces and when the temperature of the module surface reduces below 25°C, power output increase above the module rated value is expected [32].

4.2.3 Effect of heat on the PV module.

As the temperature of the PV module increases due to exposure to sunlight, heat generation commences in the process. When this heat reaches a point where the output of the PV module drops, overheating becomes evident. This overheating is one of the major challenges, which confronts the Photovoltaic module's smooth operation and it is because of exposure to more than required solar radiation and high-level ambient temperatures. The overheating decreases the efficiency as well as the power output of the module. The efficiency, as well as the output power, reduces substantially as temperature rises, the extent of the reduction is a function of the material used to fabricate the solar cell [33]

In order to find a solution to this challenge of overheating and loss of valuable energy as heat, cooling of PV modules is required.

4.3 Proposed cooling of Photovoltaic module

A lot of research took place in the past and several others are ongoing on ways to tackle this challenge of overheating. Heat energy can be lost from a Photovoltaic module through conduction, radiation and convection, two major cooling techniques can be identified, namely Passive cooling, which requires natural means for heat removal without energy consumption and active cooling where energy consumption is needed for heat removal [33]. For the purpose of energy conservation, this research work embraces the concept of passive cooling. Passive cooling grouped into three major types is as shown in Figure 4-1.

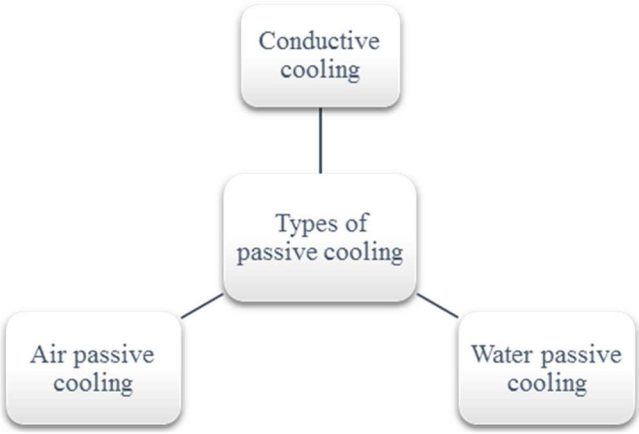

Figure 4-1. Types of passive cooling.

The method of cooling adopted by this research involves the different methods of passive cooling, hence it is referred to as multi-concept cooling technique.

4.4 Multi-concept cooling technique

The multi-concept cooling technique was also used to help reduce the energy wasted as heat energy when a PV module is placed under sunlight. The aim is to extract the excess energy, which causes the temperature of the PV module surface to rise to a level, where the power output reduces due to a reduction in the conversion efficiency of the module. The concept involves:

- Cooling the surface of the PV module to a temperature of 20°C using water
- Attaching aluminium heat sink at the rear of the PV module.
- Mounting of the module at a height of 137cm above the ground to enhance air-cooling.

Cooling of the module surface with water helps to reduce the temperature of the module surface considerably; this helps to increase the conversion efficiency of the PV module. Conversely, the aluminium heat sink attached to the rear of the module serves two functions: it helps to extract heat from the rear of the module and, it also helps the module to maintain a uniform temperature.

4.4.1 New features and advantages of the proposed method.

The new features of the proposed method include the followings: cooling of the module is achieved using the multi-concept cooling technique, ice blocks are added to the cooling water to reduce its temperature and cooling is applied at the surface as well as the rear of the module. Past research effort shows cooling is achieved with the single concept of cooling the PV module surface or cooling the rear of the PV module. The concept of cooling adopted by this

research employs both the concept of cooling the surface of the PV module and the concept of cooling the rear of the PV module. Conversely, past researchers employ water passive cooling alone, or air passive cooling alone or conductive cooling alone, but this research incorporates the different types and the following experiments were carried out:

- PV module attached with Aluminium heat sink compared with the PV module without an Aluminium heat sink.
- PV module attached with Al heat sink + water-cooling compared with PV module without Al heat sink + water-cooling.
- PV module attached with Al heat sink with module temperature reduced to 20°C compared with the PV module without Aluminium heat sink with module temperature reduced to 20°C.

Water-cooling of the PV module was carried out at 12:45 pm, 13:45 pm, 14:45 pm, and 15:45 pm. Before the first water-cooling of the module surface was carried out, the effect of Aluminium cooling can be felt from the readings obtained between 9: am and 12:30 pm as shown in table 4.7. The readings show a reduction in the temperature of the PV module and it also recorded an increase in power with the use of the Aluminium heat sink. Both evidence shows the usefulness of the Aluminium heat sink.

With the different comparisons carried out, it is evident that more power was achieved with the PV module + Aluminium heat sink and water-cooling of the PV surface to 20°C than PV module + Aluminium heat sink + water-cooling, hence an increase in efficiency was achieved. Also evident is that, there is an increase in power output when the result of the PV module + Aluminium heat sink is compared with the PV module without Aluminium heat sink before water-cooling started (at 12:45 pm).

Conversely, the main advantages of this method are as follows: maintaining the temperature of the module surface at 20°C ensures the module yields a steady increase in power output. At an irradiance of 1000w/m^2, more power than the module rated capacity is achieved and in the absence of water-cooling, a certain amount of cooling can be achieved.

4.5 Materials and methods

A flowchart of the procedure used to conduct the experiment is as shown in figure 4-2.

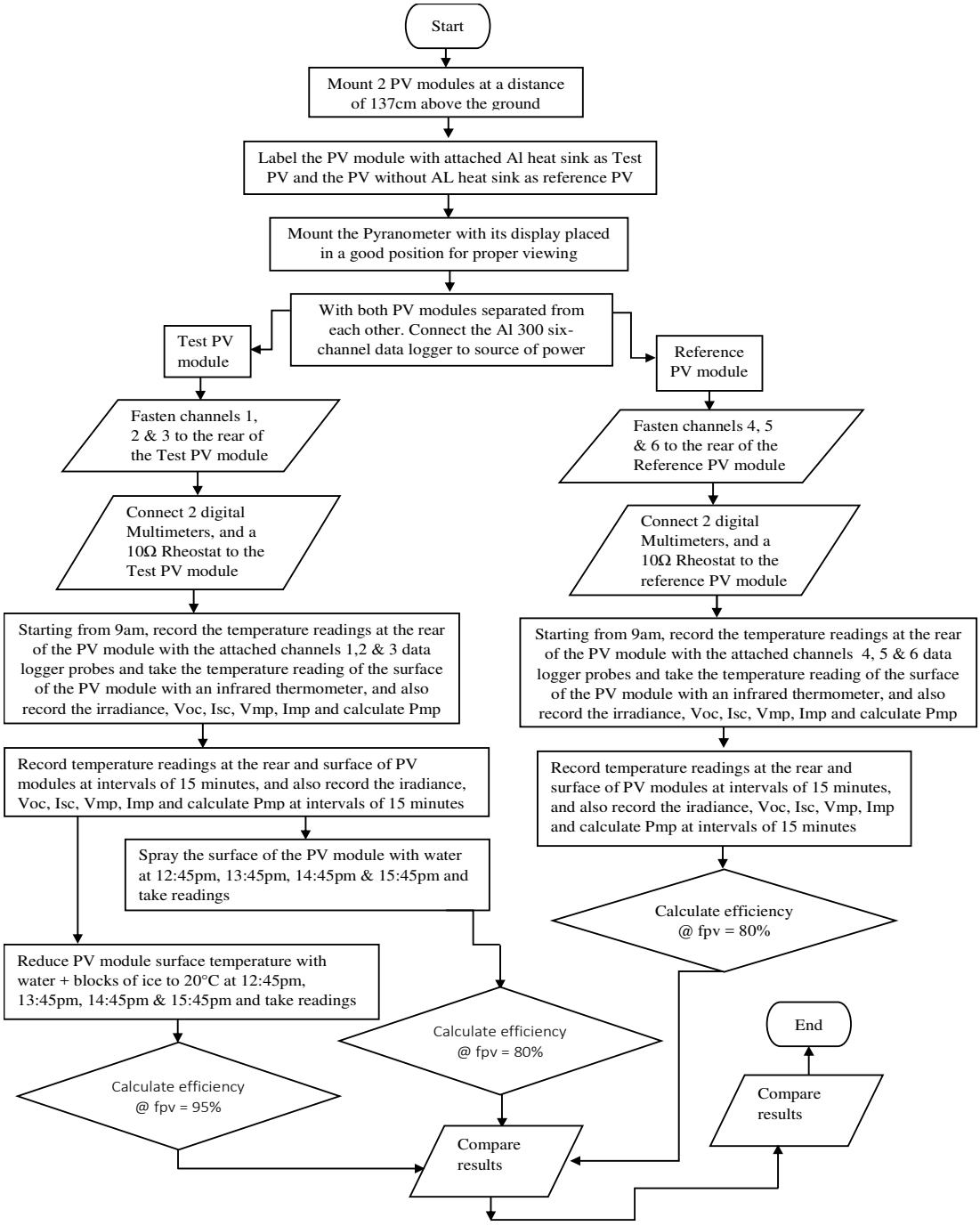

Figure 4-2. Flowchart of the experiment

All necessary precautions observed during the conduct of this experiment, the method adopted and the materials used in the process are as shown below.

4.5.1 Materials

The materials used in this experiment consist of the following:

i. Two Suntech 250 watts solar PV module with the specifications shown in table 4.1

Table 4.1 Suntech 250watts PV module [31].

250 Watts Suntech PV module	
Maximum Power at STC Pmax	250 W
Optimum operating voltage (Vmp)	30.7V
Optimum operating current (Imp)	8.15A
Operating circuit voltage (Voc)	37.4
Short circuit current (Isc)	8.63A
Operating module temperature	-40°C to +85°C
Temperature coefficient of Pmax	-0.44%/°C
Temperature coefficient of Voc	-0.34%/°C
The temperature coefficient of Isc	-0.060%/°C
Solar cell	Monocrystalline silicon 156 x156mm (6 inches)
No of cells	60 (6x10)
Dimensions	1640x992 x35mm (64.6 x 39.1 x1.4 inches)

ii. The Aluminium heat sink used in this work is made of Aluminium sheet, which serves as the base of the heat sink attached with 56 Aluminium sheets as fins. Aluminium material became the choice for this design because it has lightweight and high thermal conductivity. Thermal grease was applied to the base of the aluminium heat sink to help eliminate air gaps and improve thermal conductivity. The fins have openings to aid the passage of pipes for future heat extraction from the rear of the module and for generation of hot water. Furthermore, the module mounted at a height of 137cm keeps the heat sink at a considerable height for proper air-cooling. The Aluminium heat sink is fabricated using an Aluminium sheet with a dimension of 154 cm x 93cm x 0.1cm on which several Aluminium fins with fin base of 2.4cm each, were mounted. The dimension of the heat sink is as shown in table 4.2

Table 4.2 Aluminium, AL heatsink dimensions.

Parameter	**Value**
Length of Aluminium sheet	154cm
Length/height of Aluminium Fin	84cm
The depth of Aluminium Fin	10cm
The thickness of Aluminium Fin	1mm
The width of the Fin base	2.4cm
Spacing between fins	3.12cm

The fabrication of the aluminium heat sink took place in the mechanical workshop of the University of Strathclyde, Glasgow. A snapshot of the fabrication process is as shown in Figure 4-3.

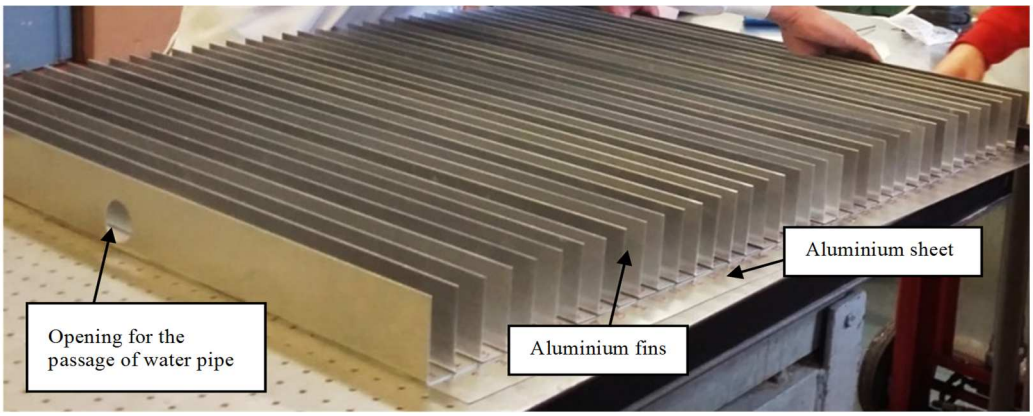

Figure 4-3. Aluminium heat sink fabrication at the mechanical workshop University of Strathclyde in Glasgow UK.

iii. Other equipment used include:

10 litres watering can, Infrared thermometer, Al 300 data logger (6 channels), a set of Spanners, measuring tape, combination plier, long nose plier, four multimeters, two for each of the PV modules, Meteon Irradiance meter with Pyranometer, PV module stand, flexible cable, ice blocks and 2 variable resistors, one for each module.

4.5.2 Experimental setup

Each of the PV modules used in the experiment was initially mounted without an Al heat sink connected to any one of them. This was done to compare the state and rating of both PV modules. The result of the measurements is as shown in table 4.3.

Table 4.3 Parameters of the PV modules without Al heat sink attachment

PV parameters	**PV 1**	**PV 2**
Open circuit voltage, Voc (V)	36.67	36.67
Short circuit current, Isc (A)	8.03	8.02
Optimum operating voltage, Vmp (V)	29.60	29.63
Optimum operating current, Imp (A)	7.03	7.02
Maximum power, Pmp (W)	208.09	208.00

The measurement obtained for the Voc, Isc, Vmp and Imp for both PV modules were found to be approximately the same. Mounting of both 250 W, PV modules carried out as shown in

Figure 4-4 with one module mounted without any form of cooling, referred to as the reference PV module while the other with an attached aluminium heat sink served as the efficiency test PV module.

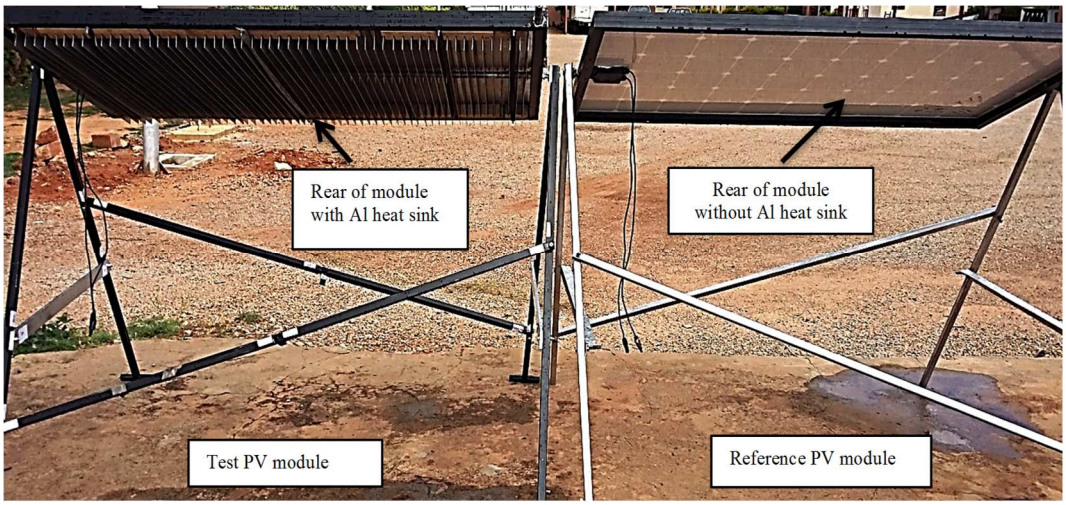

Figure 4-4. Test PV module and Reference PV module.

With the Pyranometer properly mounted, and the Al 300 six-channel data logger connected to the PV module, channels, four, five and six temperature probes were connected and fastened to the rear of the PV module without Al heat sink with the help of a tape. Conversely, with channels, one, two and three temperature probes connected to the rear of the PV module attached with aluminium heat sink; completes the first stage of the setup. With the modules, data logger and Pyranometer in place, two out of the four multimeters and a rheostat connected to the PV module without Al heat sink while the remaining two multimeters and the second rheostat connected to the PV module with attached Al heat sink makes up the second stage as shown in Figure 4-5.

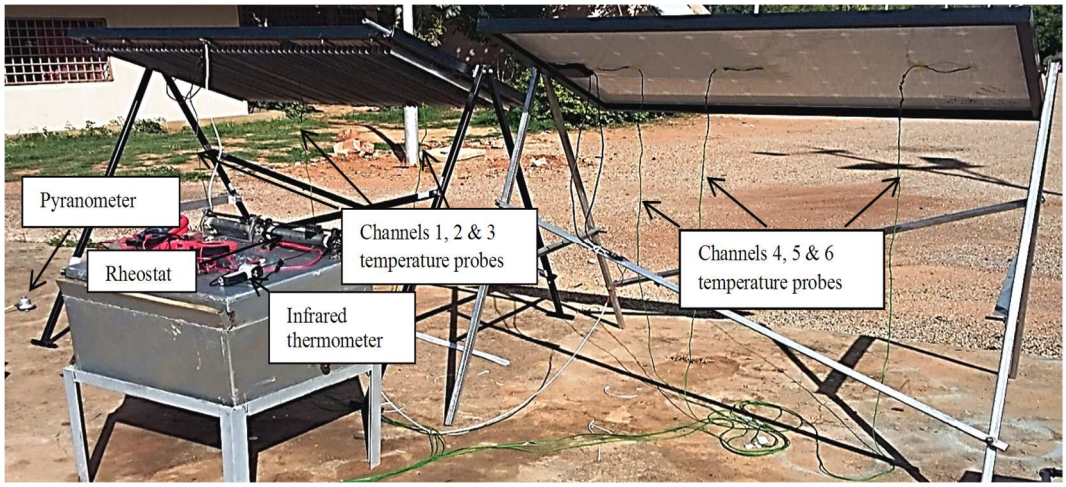

Figure 4-5. Experimental setup.

4.5.3 Site selection

This experiment took place in Sokoto State, Nigeria located within Latitude 13.1274 and longitude 5.2046 with the PV module tilted properly to ensure maximum reception of radiation from the sun. The PV modules and Pyranometer did not experience any form of shading each day from the rising of the sun to the setting of the sun. The sunshine hours data for Sokoto, Sokoto State, Nigeria is as shown in Figure 4-6.

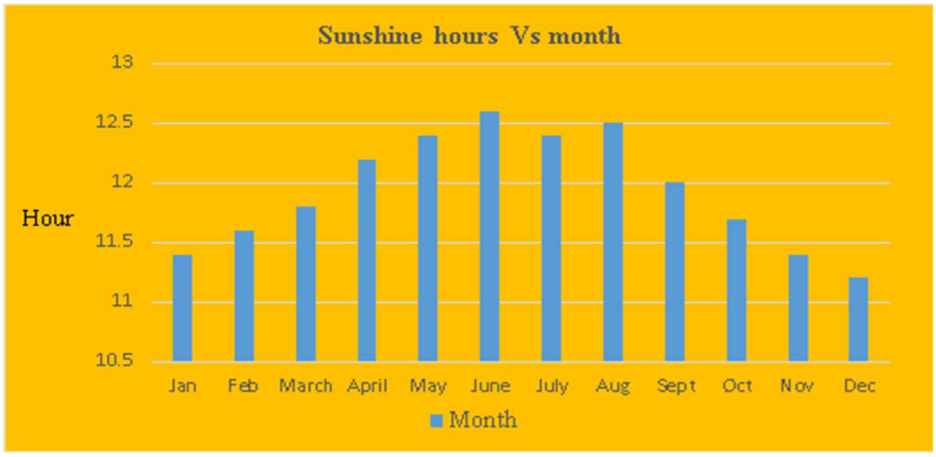

Figure 4-6 Sunshine hours in Sokoto in 2016.

4.5.4 PV module Orientation and tilting

The PV modules were initially mounted without Aluminium heat sink attached to any at two different tilt angles, one module was tilted at an angle of 13° facing due south while the other

was tilted at an angle of 15° facing due south so as to determine the best tilt angle for the PV module at the research location. After comparison, the result of the module tilted at an angle of 15° was better, which is the recommended tilt angle for a fixed system in site latitude between 0° and 15°.

Mounting of the PV module with attached Aluminium heat sink and that without Aluminium heat sink carried out facing due south and tilted at an angle of 15°. With the help of the Pyranometer, recording of the solar irradiance data in W/m^2 took place successfully and all the readings taken at an interval of 15 minutes.

4.5.5 PV module temperature

In this experiment, several temperature readings were taken, the temperatures in the rear of both PV modules were taken with the help of Al 300 six channels data logger while the temperatures at the surface of both PV modules were taken with the help of an infrared thermometer. I had the temperature probes of the data logger attached to the rear of the panel with the help of a tape, to aid accurate determination of the rear temperature of the PV module. On the other hand, an infrared thermometer was used to take the surface temperature of the PV module. This is because, attaching a data logger temperature probe at points on the surface of the PV modules, as I did with the rear of the module, will cast a shade on some part of the module surface and in the process, lead to energy loss due to shading. Another step taken was the spraying of water on the PV module surface carried out at intervals, to help reduce the temperature of the panel to enhance its energy conversion efficiency as shown in Figure 4-7.

Figure 4-7 Manual water spraying of the module.

Temperature readings during the experiment were taken at intervals of 15 minutes, it was observed after spraying the module with water, because of the high ambient temperature in the location, the surface temperature of the module rises almost immediately. Ice blocks became useful in this work when added to the cooling water as it helps to reduce the temperature of the cooling water and the quantity of water used for cooling. Ice blocks are cheap and affordable in this community, and as such, a number of blocks of ice added to the cooling water helped to reduce the temperature as using cold water-cooling would go a long way to enhance the energy conversion efficiency of the PV module. Samples of Ice blocks and ice blocks in the watering can are as shown in Figure 4-8 (a) and (b) respectively.

Figure 4-8. (a) Ice blocks and watering can. (b) Ice blocks in a watering can.

4.5.6 Output current and voltage

The voltage and current of each of the modules were obtained with the help of the multimeters, which were used as voltmeters and ammeters respectively, two variable resistors of 10 Ω each was used in this experiment. With the output terminal of each of the PV modules short-circuited with a wire, the short circuit voltage and the module output voltage measured with ease. Conversely, a variable resistor of 10 Ω was connected to each of the modules, and readings for the current and voltage were taken starting from the lowest resistance to the highest. Other readings taken include current and voltage when the module is in open circuit, voltage and current for the following values of resistance, 1.43Ω, 2.86Ω, 4.29Ω, 5.27Ω, 7.15Ω, 8.58Ω and 10.0Ω.

4.5.7 PV module power output

The setup achieved electricity production via the ability of the PV modules to generate a current through the 10.0Ω variable resistor and voltage across the same variable resistor

simultaneously at constant Irradiance. The expression for the module output power is as given in equation 1.

4.6 Results and discussion

4.6.1 Solar radiation

Recording of the Pyranometer readings took place between 9: am and 4: pm on a daily basis at an interval of 15 minutes as shown in Figure 4-9.

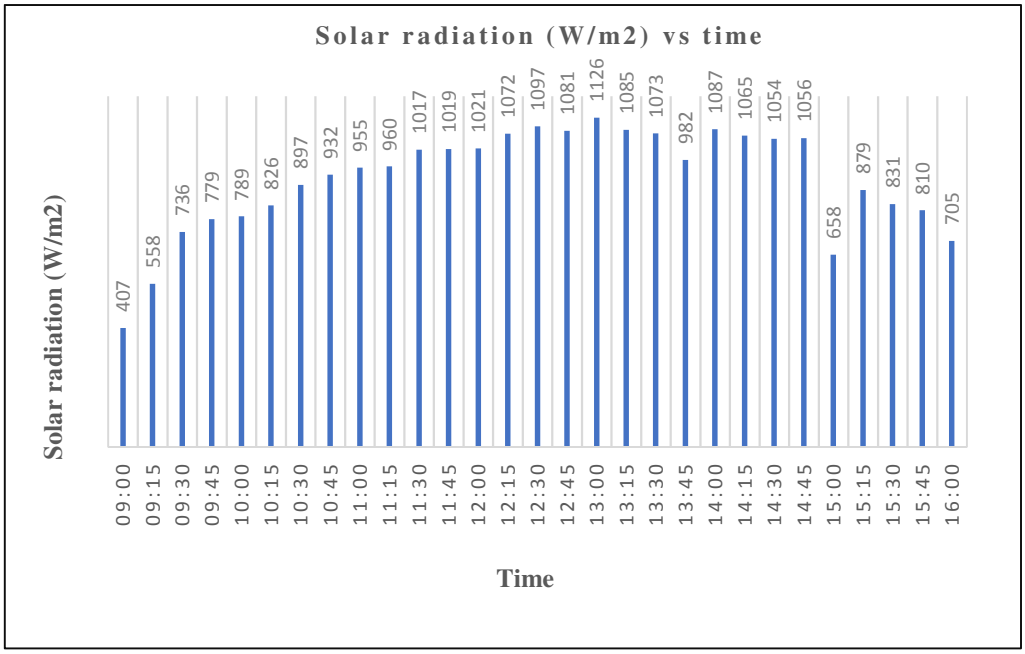

Figure 4-9. A graph of solar radiation Vs time.

During the rising of the sun in the morning, the radiation from the sun is low and it increases as the intensity of the sunlight increases, but with little drops until 13.00pm when the solar radiation reaches its peak, after which there are some fluctuations in the radiation, but as the setting of the sun approaches, the radiation reduces progressively.

4.6.2 Temperature readings

The temperature readings such as ambient temperature, the temperature at different sections of the two modules alongside the solar radiation taken at intervals of 15 minutes are as shown in Figure 4-10, 4-11, 4-12, and 4-13.

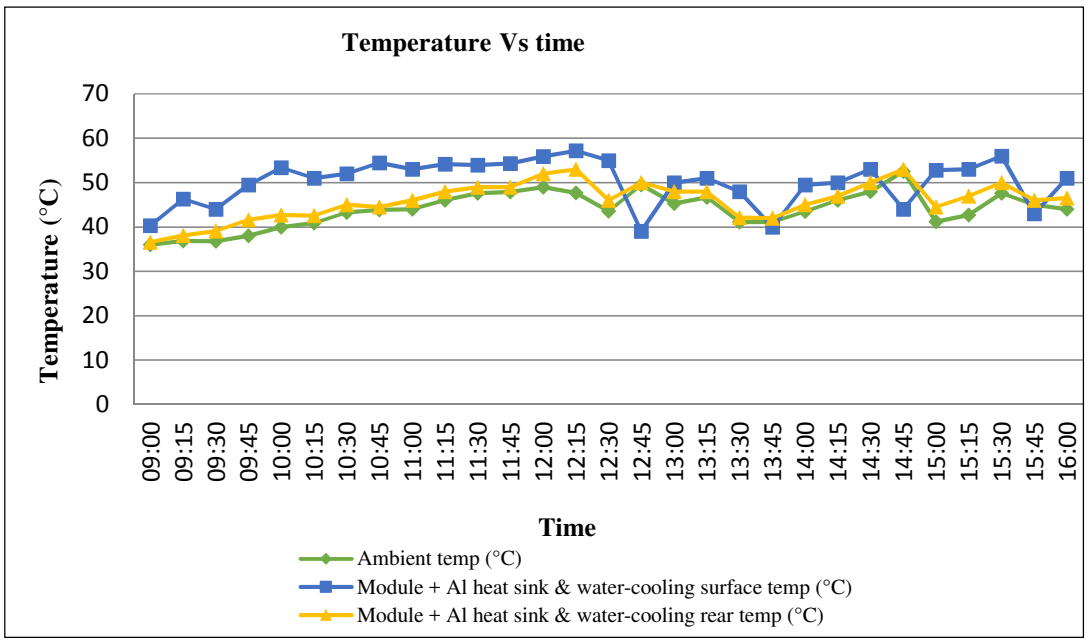

Figure 4-10. A plot of ambient temperature, module + Al heat sink & water cooling surface and rear temperature (°C) Vs time.

The ambient temperature increases with an increase in the intensity of the sun and as a result, there is an increase in both the surface and rear temperature of the PV. The surface of the PV module experiences the effect of sun intensity mainly; as a result, the temperature on the module surface is higher. Heat usually flows from the hotter object or surface to the cooler object or surface, there was heat transfer from the module surface to the rear of the module attached with Aluminium heat sink, this makes the temperature of the rear of the PV module, higher than the ambient temperature. At the start of the experiment, the module surface temperature was 40.3°*C,* after which, it rises with few fluctuations. The module surface temperature remains higher than that of the rear and the ambient temperature, but at 12:45 pm, 13:45 pm, 14:45 pm and 15:45 pm, the module surface temperature was lower than the ambient temperature and its rear temperature, and this is because the module surface was sprayed with water during those periods. The module surface reached a peak temperature of 57.2°*C* at 12:15 pm as shown in Figure 4-11.

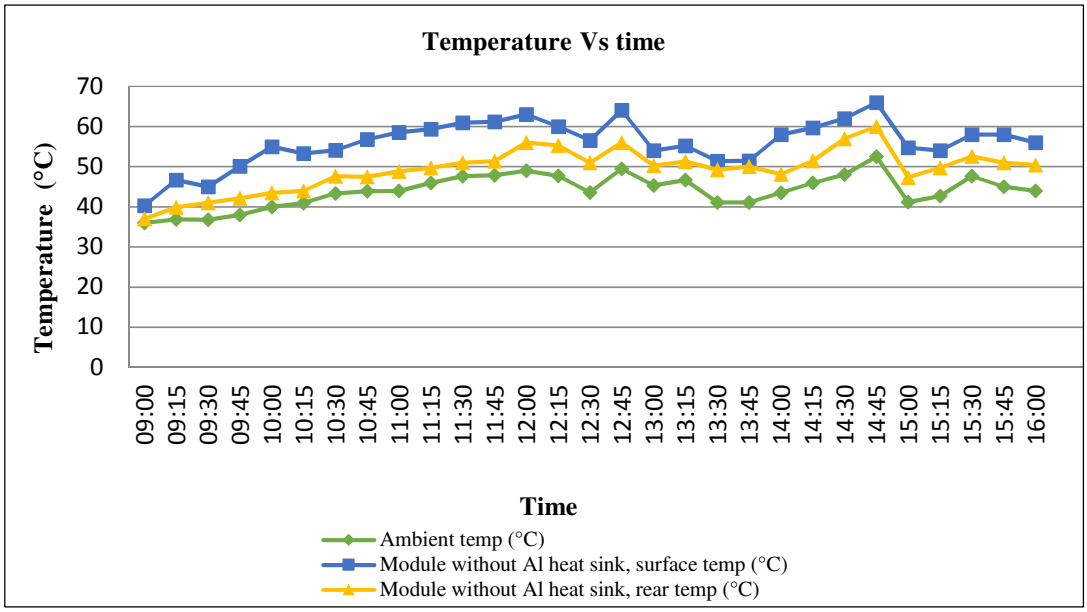

Figure 4-11. A plot of ambient temperature, module without Al heat sink's surface and rear temperature (°C) Vs time.

Unlike Figure 4-10, the peak temperature of the module surface was 66°C while the peak temperature of the rear of the module was 60°C, and this module is not fitted with aluminium heat sink, and not sprayed with water. The graph shows that the module surface temperature is highest, followed by the module rear temperature, the rear temperature is higher than the ambient temperature because of the heat transfer from the module surface to the rear.

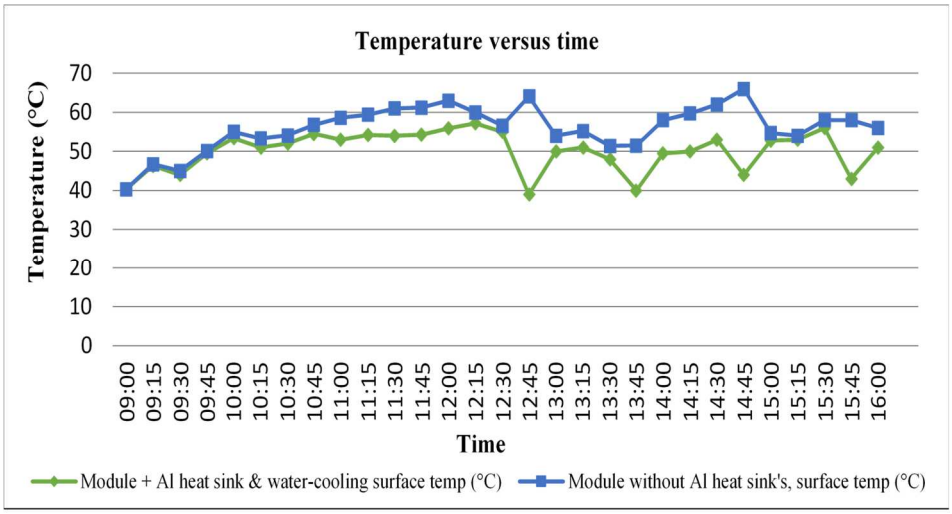

Figure 4-12. A plot of module + Al heat sink & water-cooling and the module without Al heat sink's surface temperatures (°C) versus time.

The temperature of both modules was the same at the start of the experiment, but as time progresses, there was a progressive difference in temperature between the two modules. The temperature reading obtained from the module without attaching aluminium heat sink, at each interval appears higher than the values obtained from the module attached with the heat sink. The difference in temperature progresses gradually, the difference becomes more at 12:45 pm, 13:45 pm, 14:45 pm and 15:45 pm after spraying the module with water to reduce the module temperature.

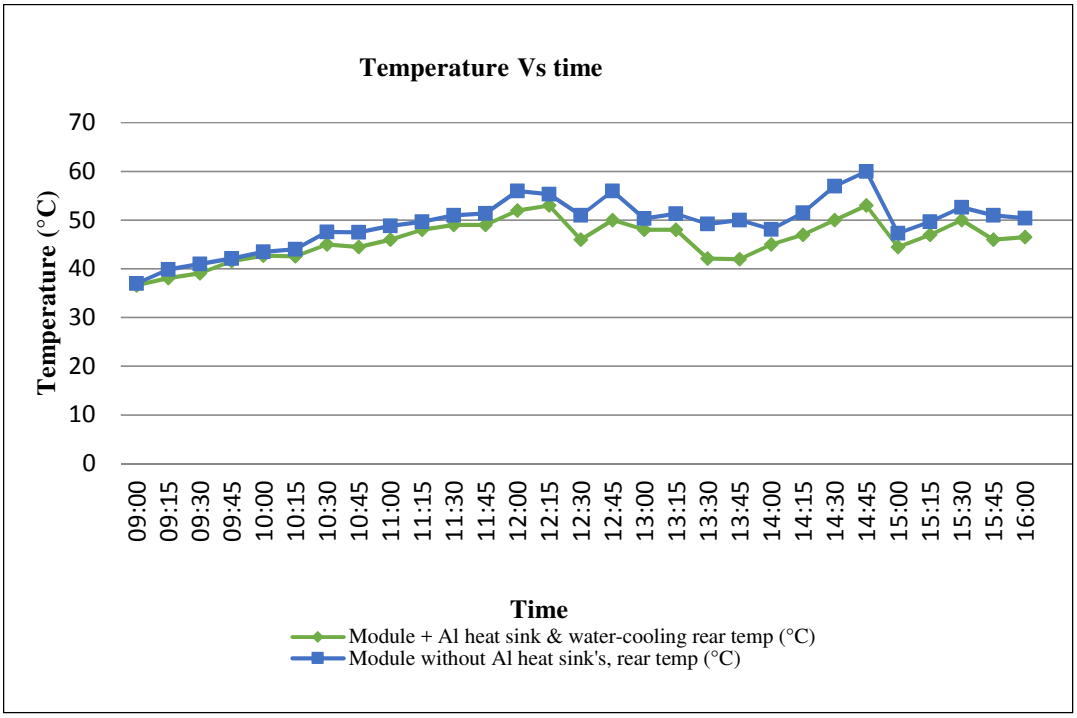

Figure 4-13. A plot of module + Al heat sink & water-cooling and the module without Al heat sink's rear temperatures (°C).

Temperature readings from the module without attaching aluminium heat sink, appear higher than the readings obtained from the module with attached aluminium heat sink & water-cooling, this is because heat energy is extracted from the rear of the module with the help of the attached aluminium heat sink.

4.6.3 Maximum voltage, maximum current and maximum power output.

Cooling of the PV module with well water at a temperature of 35°C and cooling of the PV module surface temperature to 20°C by introducing blocks of ice into the cooling water

performed with readings taken. A plot of resistance against maximum Voltage, maximum current and maximum power is as shown in Figure 4-14 (a), (b) and (c) respectively.

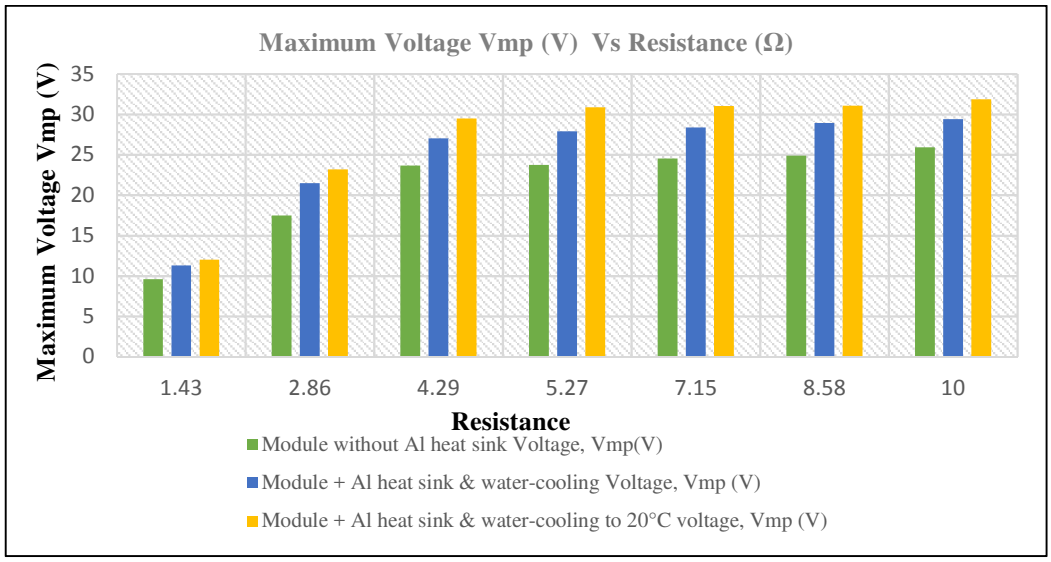

(a) The maximum voltage measured.

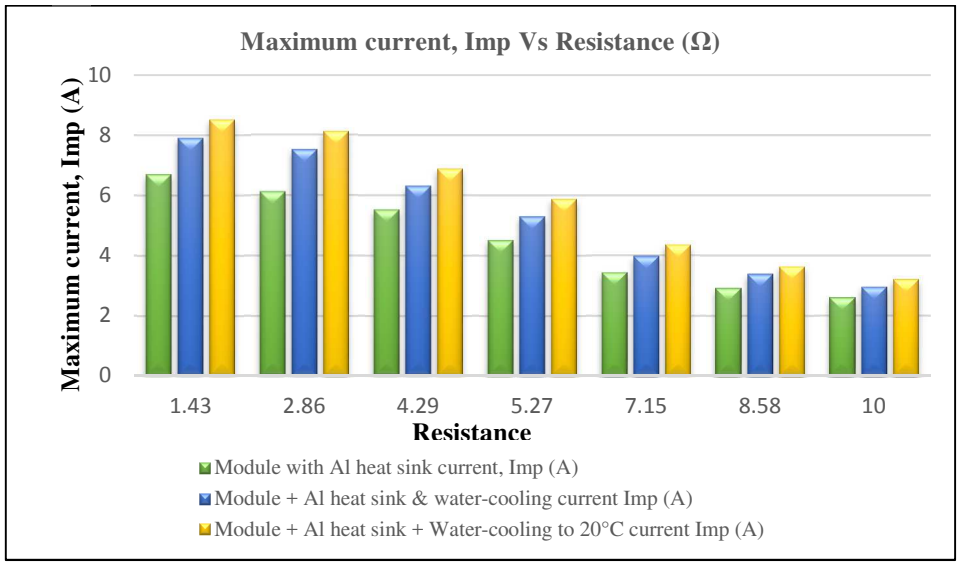

(b) Maximum current measured.

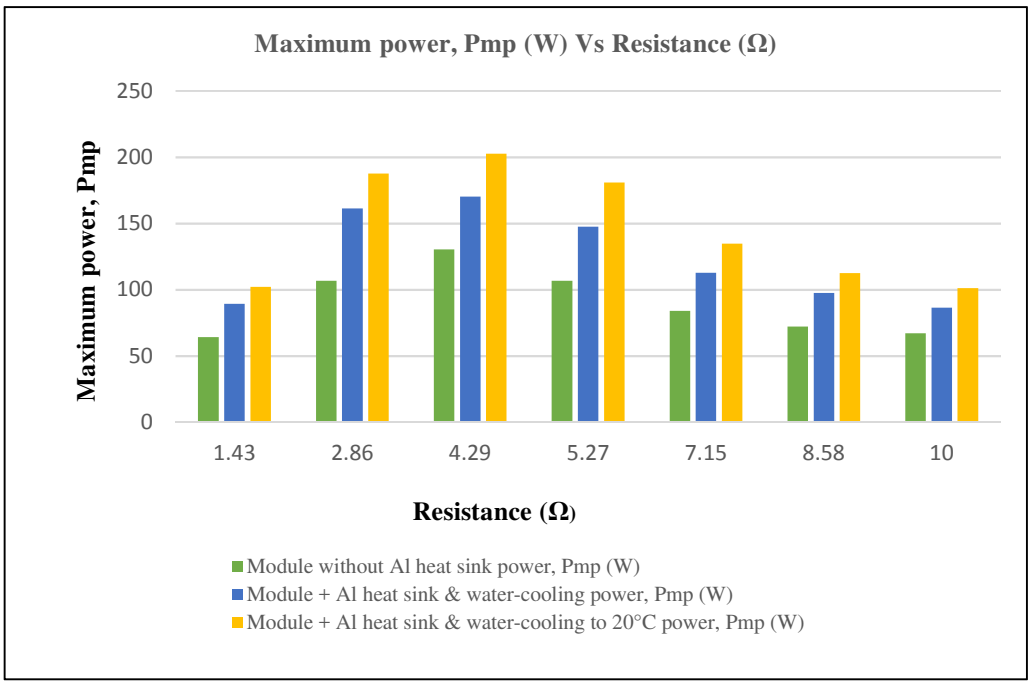

(c) Maximum power measured.

Figure 4-14. (a) maximum voltage Vs load (b) maximum current Vs load (c) maximum power Vs load.

From Figure 4-14, in (a) the maximum voltage increases progressively as the load increases, in any of the three cases, it can be seen that the maximum voltage obtained increases with an increase in the load. Conversely, the maximum voltage obtained cooling the module with water to a temperature of 20°C is more, and that obtained from the module + heat sink & water-cooling is more than that obtained from the module without a heat sink & water-cooling. In (b) the value of the current obtained in each case, reduces as the load increases, but with the highest values for current obtained with water cooling of the module to a temperature of 20°C, this is followed by the values of the current obtained from module + Al heat sink & water cooling.

Conversely, the maximum power measured as shown in (c), increases with the peak power obtained at a load of 4.29 Ω, the power shows that the power output obtained with the module + Al heat sink & water-cooling is more than the power output achieved with module without Al heat sink and also. The highest power output was achieved with module + Al heat sink & water-cooling of module surface to a temperature of 20°C.

In order to consider the temperature coefficient of power, the calculation of the power output considered a derating factor of 0.8 and 1 using equation 5, the results are as shown in Figure 4-15 and 4-16.

In Figure 4-15, the temperature of the module increases as the intensity of the sun increases, but with a reduction at 12:45 pm, 13:45 pm, 14:45 pm and 15:45 pm during which cooling of the module with water took place. Conversely, as shown in figure 4-15, the experiment recorded an increase in power output at each stage of cooling except at 13:45 pm where it recorded a decrease in the power output even with water-cooling and this was because of a reduction in solar radiation experienced at that time. The reduction in solar radiation experienced at 13:45 pm is as shown in Figure 4-16.

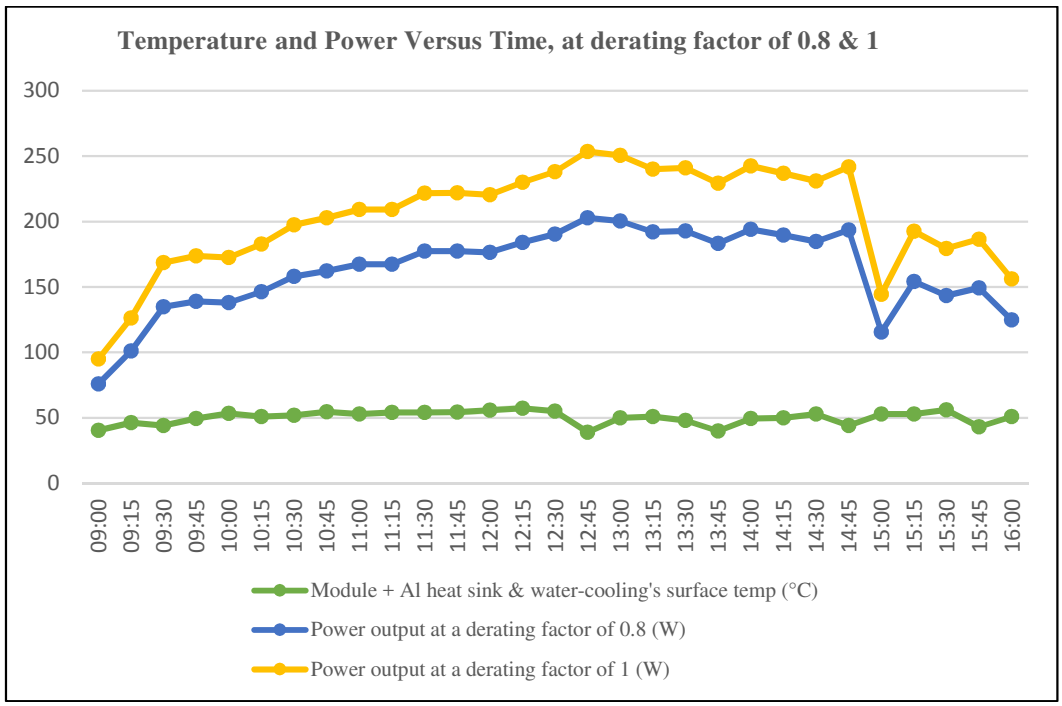

Figure 4-15. A plot of temperature and power versus time at derating factor of 0.8 & 1.

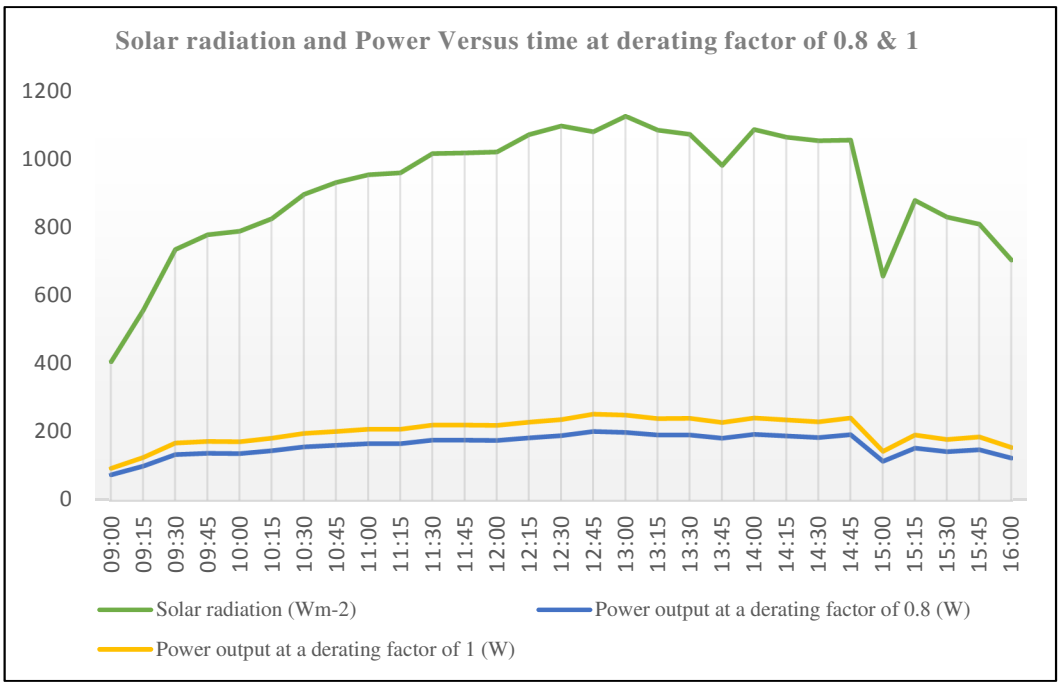

Figure 4-16. A plot of solar radiation and power versus time at derating factor of 0.8 & 1.

The power output at a derating factor of 0.8 and 1 as shown in Figure 4-15 and 4-16 indicate that the experiment considers losses for the setup at a derating factor of 0.8 and no losses at a derating factor of 1. The graphs show that power output increases with time, but with fluctuations due to changes in the intensity of the sun or ambient temperature. The setup achieved peak power both at a derating factor of 0.8 and 1 at 12:45 noon, this is because the solar irradiation was high at the time and the temperature of the module was 39°C. This experiment considers the values of power output obtained with a derating factor of 0.8 to account for losses.

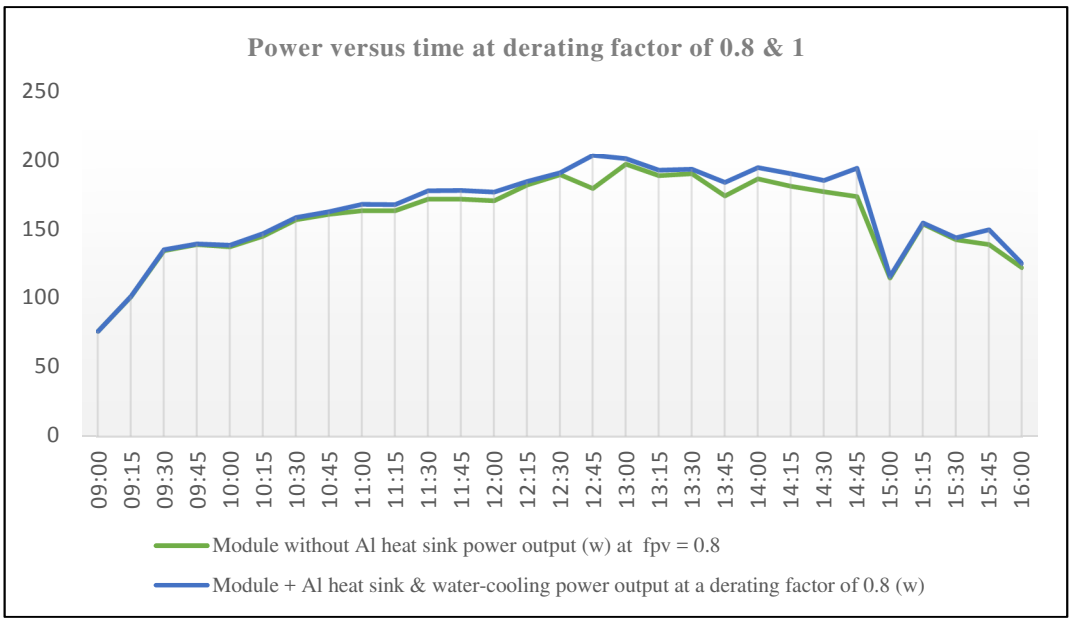

Figure 4-17. A plot of power versus time at a derating factor of 0.8 for module with cooling and module without cooling.

Figure 4-17 shows the effect of using the Aluminium heat sink at the rear of the module. The first attempt to cool the module using water took place at exactly 12:45 pm; before this time, the power output obtained from the module + Al heat sink & water-cooling gradually increases above that of the module without a heat sink and water-cooling. This implies there is a slight improvement in the module efficiency.

Water flow on the module surface may act as a reflecting mirror and reflect the solar radiation away from the module during water spraying on the surface of the module, in order to minimize this, spraying of water on the module surface was not done continuously, instead, it was done intermittently. Furthermore, in order to improve the efficiency of the PV module during water flow on the module surface, I used a semi-transparent PV module for the experiment [34]. The PV modules stand the risk of experiencing increased leakage current, which will result in potential induced degradation of the PV modules as [35]. The measures to help minimize potential induced degradation of the PV modules include:

- The use of certified PID resistant PV modules
- The use of strings with negative terminal grounded
- The use of isolation transformers between the strings and inverters
- Early installation of anti-PID equipment.

- Ensuring reduced accumulation of water on the module to avoid leakage of charges

Water-cooling of the PV module and the cooling of the PV module surface to 20°C performed at 12:45 pm, 13:45 pm, 14:45 pm and 15:45 pm generated the result shown in table 4.4

Table 4.4 Module power output at a derating factor, f_{pv} = 80%

Time	**Module without Al heat sink power output (w) @ a f_{pv} = 80%**	**Module + Al heat sink & water-cooling, power output (w) @ a f_{pv} = 80%**	**Module + Al heat sink & water-cooling of module surface to 20 °C, *power output* (w) @ a f_{pv} = 80%**
12:45	179	202.9	220.96
13:45	173.5	183.4	200.72
14:45	173.1	193.5	215.85
15:45	138.48	149	165.56

A 250W PV module considered with a derating factor of 80% implies that the power output expected from the module in an ideal situation is 200 W. Since the maximum power expected from the PV module is 200W, power output in excess of 200W is an addition. In table 4.4, module + Al heat sink & water-cooling generated more power than the module without Al heat sink and the higher power output generated by the PV module was achieved with module + Al heat sink & water-cooling of module surface to 20°C. At 12:45 pm, 13:45 pm and 14:45 pm, power output exceeded 200W by 20.96W, 0.72W and 15.85W respectively.

Equation (7) for PV module efficiency was used with the following values Ppv=250 watt, fpv=1, T_C = 25°C and $T_{C,STC}$ = 25°C and an efficiency of 15.4% were achieved. This 15.4% is the value of the SUNTECH 250 watt module efficiency as stated in the manufacturer's specification sheet. Using a module surface temperature, T_C = 20°C, with an irradiation of 1081 at a derating factor of 0.8 yields an efficiency of 18.8%. Conversely, using equation 4 at a temperature of 20°C gives an efficiency of 18.48%.

4.6.4 Cost of cooling the PV module

The application of ice blocks to the cooling water, used for the reduction of the module temperature to 20°C was performed at 12:45 pm, 13:45 pm, 14:45 pm and 15:45 pm each day. Each of the cooling processes used a small bag of ice blocks made of 20 blocks of ice at a cost of N100 per bag. A total of 4 bags of ice was used for cooling each day. The cost of using ice blocks for cooling is as shown in table 4.5

Table 4.5 Cost of cooling the PV module

Bags of Ice blocks used/day	Days	Cost/bag (Naira)	Total cost (Naira)	Total cost (GBP)
4	21	100	8400	17.99

Conversely, the Aluminium heat sink used for this research work was fabricated at the electrical workshop and the cost of the materials used in fabricating the Aluminium heat sink is as shown in table 4.6

Table 4.6 Cost of materials for Al heat sink fabrication.

Materials	Cost/material (£)	Total cost (£)
Two sheets of Aluminium	42	84
Speed frame	32	32
Sundries	18	18
Wood	8	8
Copper tube	39	39
Total cost of materials	**£181**	

The total cost of providing cooling for the PV module $\Rightarrow £17.99 + £181 = £198.99$

From figure 4.10, measurements were taken at an interval of 15 minutes, there are four periods of cooling at a maximum of 15 minutes over the day, i.e. 1 hour. From table 4.4, the increase in power with ice cooling compared to without ice cooling when approximated to the nearest tenth is 20W. The extra energy is 1hour x 0.02kW = 0.02kWh. The cost of cooling with Ice blocks is 17.99/0.02kWh = £899.5/kWh.

Considering the high cost involved in cooling the PV with the use of Ice blocks, the excess energy is channelled towards producing the Ice blocks required for cooling.

The simulation of the hybrid energy system using the HOMER software simulator in chapter three shows that an excess amount of energy was produced by the selected hybrid architecture. In [36] the excess electricity obtained is that surplus amount of electrical energy, which has to be dumped as it cannot be used to charge the batteries or serve a load. Excess electricity becomes available when either one of the renewable sources or the diesel generator produces more power such that its minimum power output exceeds the load and the batteries are unable to absorb it all. This excess energy can be used to run an ice machine in order to make ice

available for cooling the surface of the PV module, for sale, and also for cooling the house. This can be achieved with the use of the Ice bear energy storage technology.

4.6.5 Summary of experiments conducted at a derating factor of 80%

This experiment, conducted at the Sokoto Energy Research Centre, Sokoto State achieved the following results:

- An appreciable increase in the module output power with module + Al hint sink & water-cooling of the module surface temperature to 20°C.
- An output power increase of 20.96W at 12:45 pm at 80% derating factor used in order to account for losses. This increase in output exceeds 250Watts with 0% losses.
- An increase in efficiency above 3%, hence the PV module and the power output were enhanced using the multi-concept cooling technique.

4.7 Details of experiments performed at a derating factor of 95%

The experiment was set up as shown in Figure 4-18 and readings were taken.

Figure 4-18 Project setup

The function of the Al heat sink attached to the rear of one the module is to extract heat from the module and keep the temperature uniform while cooling of the surface of the PV module was carried out by spraying the surface of the PV module with water as done in the previous experiment. Ice blocks were introduced into the cooling water to reduce the temperature of the cooling water, spraying of the module was done with the cold water and a module surface

temperature of about 20°C was achieved. Spraying of the module was carried out as shown in Figure 4-19.

Figure 4-19 Spraying of PV module with cold water.

The results of the experiment are as shown in Table 4-7; the power output of the PV module at a derating factor of 95% was calculated using equation (5). The calculation was carried out for the module without an aluminium heat sink and cooling, the module with Aluminium heat sink + water-cooling, and finally it was used to compute the power output of the module when the module surface temperature was reduced to 20°C.

Using a derating factor of 95% to comply with the PV manufacturer's data sheet, which has a power tolerance of ± 5% gives Table 4.7.

Table 4.7 Module power output at a derating factor of 95%.

Time	Ambient temp (°C)	Panel without Al heat sink, surface temp (°C)	Module + Al heat sink & water-cooling surface temp (°C)	Solar radiation (Wm-2)	Module without Al heat sink power output (w) at f_{pv} = 95%	Module + Al heat sink & water-cooling, power output (w) at f_{pv} = 95%	Module + Al heat sink & water-cooling of module surface to 20°C power output (w) at f_{pv} = 95%
09:00	36	40.3	40.3	407	90.16	90.16	
09:15	36.9	46.7	46.3	558	119.9	120.1	
09:30	36.8	45	44	736	159.4	160.2	
09:45	38	50.1	49.5	779	164.6	165.1	
10:00	40	55	53.4	789	162.7	164	
10:15	40.9	53.3	51	826	171.7	173.7	
10:30	43.3	54.1	52	897	185.8	187.7	
10:45	43.9	56.8	54.5	932	190.4	192.6	
11:00	44	58.6	53	955	193.3	198.9	
11:15	46	59.4	54.2	960	193.5	198.7	
11:30	47.6	61	54	1017	203.3	210.7	
11:45	47.9	61.2	54.3	1019	203.5	210.8	
12:00	49	63	55.9	1021	201.9	209.5	
12:15	47.7	60	57.2	1072	215.4	218.5	
12:30	43.6	56.6	55	1097	224.3	226.1	
12:45	49.5	64.1	39	1081	212.6	240.9	262.4
13:00	45.3	54	50	1126	233.3	238	
13:15	46.7	55.2	51	1085	223.4	228.2	
13:30	41.1	51.4	48	1073	225.2	229	
13:45	41.1	51.5	40	982	206	217.8	238.4
14:00	43.5	58	49.5	1087	220.7	230.3	
14:15	46	59.7	50	1065	214.3	225.1	
14:30	48	62	53	1054	209.6	219.5	
14:45	52.5	66	44	1056	205.6	229.8	256.3
15:00	41.2	54.7	52.8	658	135.9	137.2	
15:15	42.7	54	53	879	182.1	183	
15:30	47.6	58	56	831	168.7	170.4	
15:45	45	58	43	810	164.4	177.1	196.6
16:00	44	56	51	705	144.6	148.3	

A section of table 4.7, which shows the difference in the power output from the PV module without Al heat sink and the PV module + Al heat sink & water-cooling of the module surface, is as shown in figure 4-20.

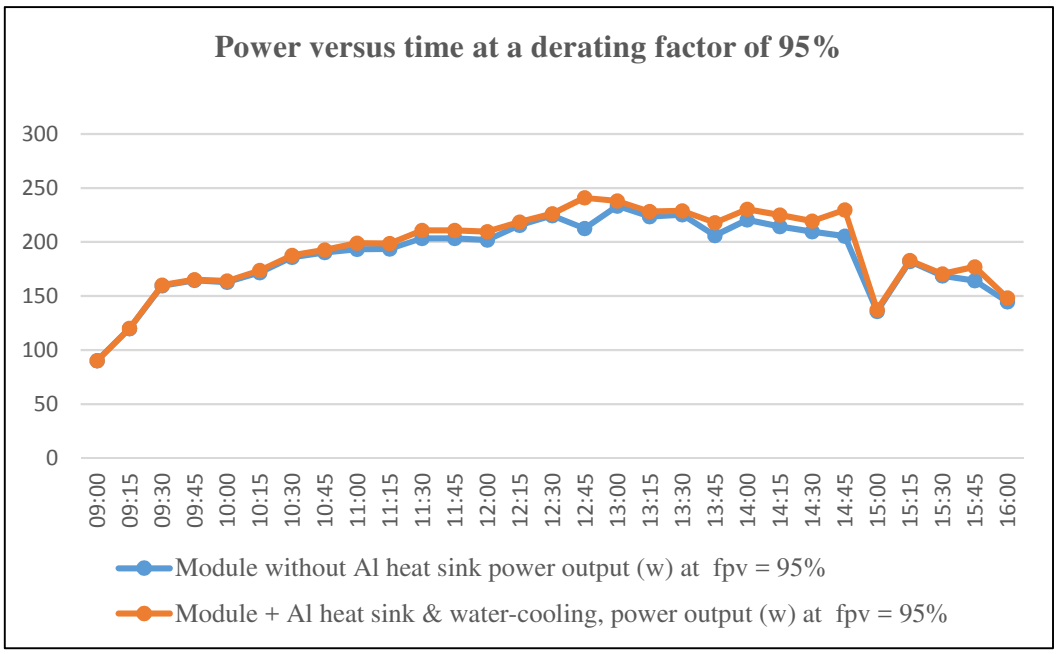

Figure 4-20 A plot of power versus time at a derating factor of 95% for PV module without Al heat sink and PV module + Al heat sink & water-cooling of module surface.

4.7.1 Summary of experiments conducted at a derating factor of 95%

The plot shows that more power is generated with the application of a heat sink to the rear of the module and water-cooling on the module surface than using the PV module without cooling. Conversely, another section through table 4.7, which indicates the difference in the power output produced by the module when subjected to different conditions, is as shown in Table 4.8.

Table 4.8 Power outputs obtained from the experiment

Time	Module without Al heat sink power output (W) at f_{pv} = 95%	Module + Al heat sink & water-cooling, power output (W) at f_{pv} = 95%	Module + Al heat sink & water-cooling of module surface to 20°C power output (W) at f_{pv} = 95%
12:45	212.6	240.9	262.4
13:45	206	217.8	238.4
14:45	205.6	229.8	256.3
15:45	164.4	177.1	196.6

From table 4.8 above, more power is obtained with the module + Al heat sink & water cooling, but maximum power output of 262.4 w was achieved by cooling the PV module + Al heat sink & water-cooling of module surface to 20°C. In order to implement the effect of the increase in power output using MATLAB, the module operating temperature set to 20°C, is used as an input to the PV array MATLAB Simulink block.

4.8 References

[1] M. E. Meral and F. Diner, "A review of the factors affecting operation and efficiency of photovoltaic based electricity generation systems," *Renew. Sustain. Energy Rev.*, vol. 15, no. 5, pp. 2176–2184, 2011.

[2] B. Koteswararao, K. Radha, P. Vijay, and N. Raja, "Experimental Analysis of solar panel efficiency with different modes of cooling," vol. 8, no. 3, pp. 1451–1456, 2016.

[3] I. Ceylan, A. E. Gürel, H. Demircan, and B. Aksu, "Cooling of a photovoltaic module with temperature controlled solar collector," *Energy Build.*, vol. 72, pp. 96–101, 2014.

[4] K. a. Moharram, M. S. Abd-Elhady, H. a. Kandil, and H. El-Sherif, "Enhancing the performance of photovoltaic panels by water cooling," *Ain Shams Eng. J.*, vol. 4, no. 4, pp. 869–877, 2013.

[5] H. Bahaidarah, A. Subhan, P. Gandhidasan, and S. Rehman, "Performance evaluation of a PV (photovoltaic) module by back surface water cooling for hot climatic conditions," *Energy*, vol. 59, pp. 445–453, 2013.

[6] A. H. Alami, "Effects of evaporative cooling on efficiency of photovoltaic modules," *Energy Convers. Manag.*, vol. 77, pp. 668–679, 2014.

[7] Y. M. Irwan, I. Daut, I. Safwati, M. Irwanto, N. Gomesh, and M. Fitra, "A new technique of photovoltaic/wind hybrid system in Perlis," *Energy Procedia*, vol. 36, pp. 492–501, 2013.

[8] H. G. Teo, P. S. Lee, and M. N. a Hawlader, "An active cooling system for photovoltaic modules," *Appl. Energy*, vol. 90, no. 1, pp. 309–315, 2012.

[9] B. Du, E. Hu, and M. Kolhe, "Performance analysis of water-cooled concentrated photovoltaic (CPV) system," *Renew. Sustain. Energy Rev.*, vol. 16, no. 9, pp. 6732–6736, 2012.

[10] R. Hosseini, N. Hosseini, and H. Khorasanizadeh, "An Experimental Study of Combining a Photovoltaic System with a Heating System," *World Renew. Energy Congr. Linköping, Sweden*, pp. 2993–3000, 2011.

[11] A. Kordzadeh, "The effects of nominal power of array and system head on the

operation of photovoltaic water pumping set with array surface covered by a film of water," *Renew. Energy*, vol. 35, no. 5, pp. 1098–1102, 2010.

[12] M. Rosa-clot, P. Rosa-clot, G. M. Tina, and P. F. Scandura, "Submerged photovoltaic solar panel : SP2," *Renew. Energy*, vol. 35, no. 8, pp. 1862–1865, 2010.

[13] S. Odeh and M. Behnia, "Improving Photovoltaic Module Efficiency Using Water Cooling," *Heat Transf. Eng.*, vol. 30, no. 6, pp. 499–505, 2009.

[14] M. Abdolzadeh and M. Ameri, "Improving the effectiveness of a photovoltaic water pumping system by spraying water over the front of photovoltaic cells," *Renew. Energy*, vol. 34, no. 1, pp. 91–96, 2009.

[15] K. Furushima and Y. Nawata, "Performance Evaluation of Photovoltaic Power-Generation System Equipped With a Cooling Device Utilizing Siphonage," *Journal of Solar Energy Engineering*, vol. 128, no. 2. p. 146, 2006.

[16] A. Kluth, "Using Water as a Coolant to Increase Solar Panel Efficiency," p. 2008, 2008.

[17] W. G. Anderson, P. M. Dussinger, D. B. Sarraf, and S. Tamanna, "Heat pipe cooling of concentrating photovoltaic cells," *Conf. Rec. IEEE Photovolt. Spec. Conf.*, pp. 1641–1647, 2008.

[18] L. Dorobanțu, M. O. Popescu, C. L. Popescu, and A. Crăciunescu, "Experimental Assessment of PV Panels Front Water Cooling Strategy," vol. 1, no. 11, pp. 1–4, 2013.

[19] M. Rahimi, P. Valeh-e-sheyda, and M. Amin, "Design of a self-adjusted jet impingement system for cooling of photovoltaic cells," *Energy Convers. Manag.*, vol. 83, pp. 48–57, 2014.

[20] A. N. Al-shamani, M. H. Yazdi, M. A. Alghoul, A. M. Abed, M. H. Ruslan, S. Mat, and K. Sopian, "Nanofluids for improved efficiency in cooling solar collectors – A review," vol. 38, pp. 348–367, 2014.

[21] H. Najafi and K. A. Woodbury, "Optimization of a cooling system based on Peltier effect for photovoltaic cells," *Sol. Energy*, vol. 91, pp. 152–160, 2013.

[22] X. Tang, Z. Quan, and Y. Zhao, "Experimental Investigation of Solar Panel Cooling by a Novel Micro Heat Pipe Array," vol. 2010, no. August, pp. 171–174, 2010.

[23] V. P. Sethi, K. Sumathy, S. Yuvarajan, and D. S. Pal, "Mathematical Model for Computing Maximum Power Output of a PV Solar Module and Experimental Validation," *Ashdin Publ. J. Fundam. Renew. Energy Appl.*, vol. 2, no. 5, p. pp 1-5, 2012.

[24] S. Dubey, J. N. Sarvaiya, and B. Seshadri, "Temperature-dependent photovoltaic (PV) efficiency and its effect on PV production in the world - A review," in *Energy*

Procedia, 2013, vol. 33, pp. 311–321.

[25] B. V Chikate and Y. A. Sadawarte, "The Factors Affecting the Performance of Solar Cell," in *International Journal of Computer Applications Science and Technology*, 2015, pp. 975–8887.

[26] J. K. Kaldellis, M. Kapsali, and K. a. Kavadias, "Temperature and wind speed impact on the efficiency of PV installations. Experience obtained from outdoor measurements in Greece," *Renew. Energy*, vol. 66, pp. 612–624, 2014.

[27] Homer Energy, "How homer calculates the PV array power output," *Homer Energy Support*, 2014. [Online]. Available: https://www.homerenergy.com/support/docs/3.10/how_homer_calculates_the_pv_array_power_output.html. [Accessed: 31-Oct-2017].

[28] R. Hren, "Understanding PV Module Specifications," *Home Power*, 2011. [Online]. Available: https://www.homepower.com/articles/solar-electricity/equipment-products/understanding-pv-module-specifications?v=print. [Accessed: 03-Oct-2017].

[29] B. Yerli, M. K. Kaymak, E. Izgi, A. Oztopal, and A. D. Sahin, "Effect of Derating Factors on Photovoltaics under Climatic Conditions of Istanbul," *World Acad. Sci. Eng. Technol.*, vol. 4, no. 8, pp. 1303–1307, 2010.

[30] "PV Temperature Coefficient of Power." [Online]. Available: https://www.homerenergy.com/support/docs/3.10/pv_temperature_coefficient_of_power.html. [Accessed: 11-Oct-2017].

[31] "SUNTECH 250 Watt Monocrystalline Solar module datasheet." [Online]. Available: https://es-media-prod.s3.amazonaws.com/media/u/bad/9e9/d9b/4a377fac554a5266604e7b20285d4e78/SuntechWd mono(MC4_250_255_260_265)_EN_web.pdf. [Accessed: 11-Oct-2017].

[32] "Solar Panel Temperature – Facts and Tips." [Online]. Available: http://www.solar-facts-and-advice.com/solar-panel-temperature.html. [Accessed: 10-Oct-2017].

[33] T. G. Grubisić-Čabo, F., Nizetić, S., & Marco, "Photovoltaic Panels: A Review of the Cooling Techniques," *Trans. FAMENA*, vol. 40, no. 1, p. p63–74. 12p., 2016.

[34] G. N. Tiwari, S. Tiwari, V. K. Dwivedi, S. Sharma, and V. Tiwari, "Effect of water flow on PV module: A case study," in *International Conference on Energy Economics and Environment - 1st IEEE Uttar Pradesh Section Conference, UPCON-ICEEE 2015*, 2015, pp. 1–7.

[35] W. Luo, Y. S. Khoo, P. Hacke, V. Naumann, D. Lausch, S. P. Harvey, J. P. Singh, J. Chai, Y. Wang, A. G. Aberle, and S. Ramakrishna, "Potential-induced degradation in

photovoltaic modules: a critical review," *Energy Environ. Sci.*, vol. 10, no. 1, pp. 43–68, 2017.

[36] "Excess Electricity." [Online]. Available: https://www.homerenergy.com/products/pro/docs/3.10/excess_electricity.html. [Accessed: 03-Dec-2018].

Chapter 5:

Increasing hybrid PV/wind/diesel generator power output with increased PV module efficiency

The growth of any developing nation depends largely on the accessibility of adequate Power, as the availability of adequate power is a necessity, for an appreciable economic and technological development to be achieved. Sources of energy supply from natural resources such as wind and sunlight provide a clean alternative source of power in locations which experience high sunshine and high wind speed and as a result, energy from renewable sources can compete favourably with energy generation from fossil fuel, which usually introduce pollution to the environment [1]. The PV module is a good source of energy in Nigeria and other parts of the world, which experiences long periods of sunshine. In locations where a long period of sunshine hours is experienced during the day, the excess sunlight is not fully utilized due to the effect of temperature on the PV module.
As the intensity of the sun increases, the temperature of the module surface also increases. Temperatures above 25°C causes the power output from the solar panel to reduce.

This chapter deals with the application of the enhanced PV module to the hybrid PV/wind/diesel generator power system, the model composition of the hybrid micro-grid, the design of the PV battery, boost converter, modelling of diesel generator, wind energy conversion system, as well as the control of the hybrid energy system, are illustrated. In order to implement the effect of the increase, in power output using MATLAB, the module operating temperature set to 20°C, is used as an input to the PV array MATLAB Simulink block.

5.1 The model composition of hybrid PV/wind/diesel generator

The research project comprises of 60kW PV array, 50kW diesel generator, 50kW PMSG driven wind turbine, 480 Vision 6FM200D batteries made up of a string size of 30 with 16 strings in parallel, each battery have a nominal voltage of 12volts and a nominal capacity of 200AH (2.4kWh). The configuration of the hybrid energy system and the complete MATLAB model of the hybrid energy system are as shown in figure 5-1 and 5-2 respectively.

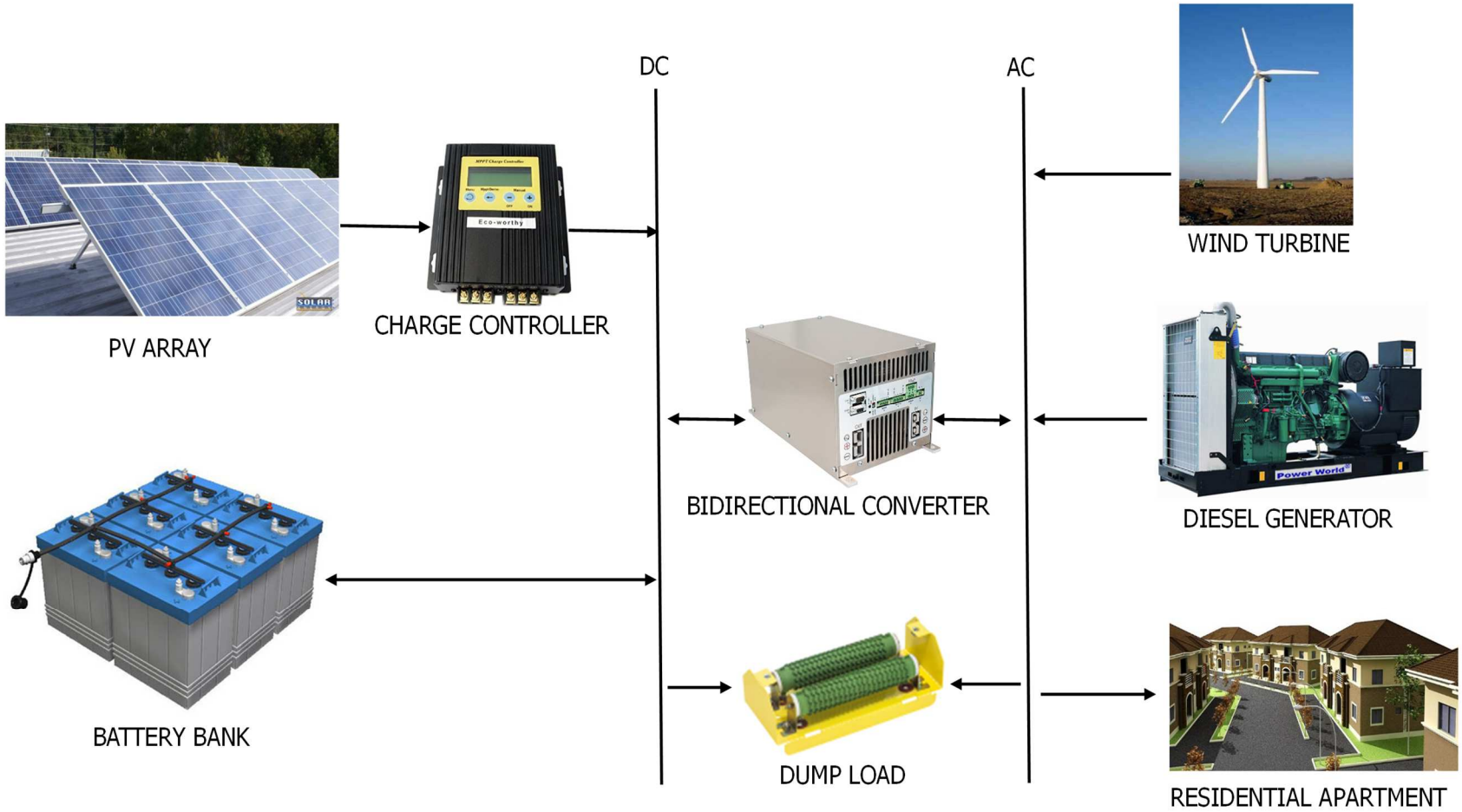

Figure 5-1 Hybrid energy system configuration

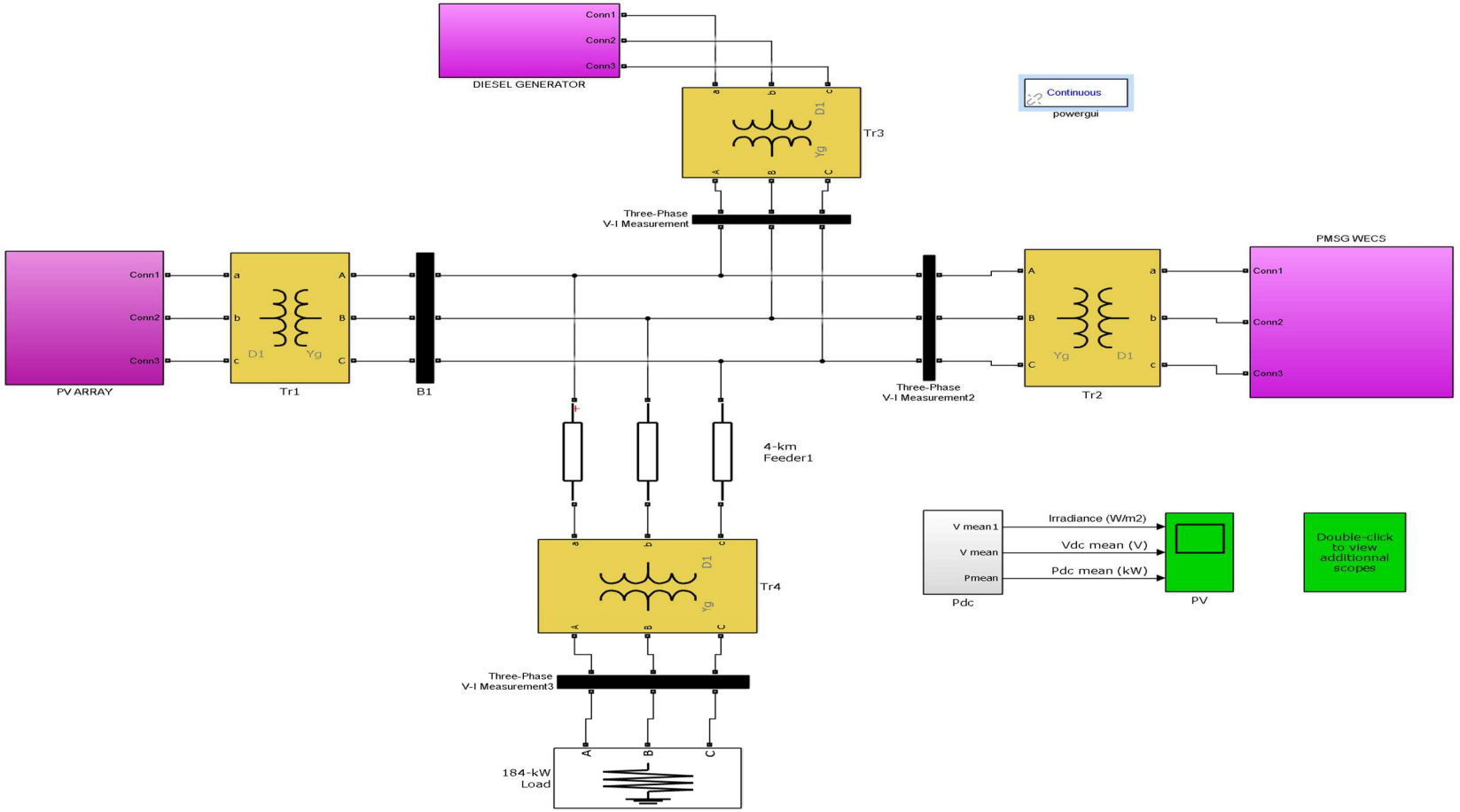

Figure 5-2 Complete MATLAB model of the hybrid energy system

5.1.1 Design of 60kW PV array

The maximum power delivered by a photovoltaic array as in [5] is given by the expression

$$P_{mp} = (N_p \times I_{mp}).(N_s \times V_{mp}). \quad (4)$$

Where the N_p and N_s stand for the number PV modules connected in parallel and in series respectively. I_{mp} and V_{mp} stand for the maximum current and voltage at MPPT respectively. This is because adding PV modules in series increases the voltage while adding PV modules in parallel increases the current.

In order to achieve a PV array with a capacity of 60kW, a PV array voltage of 614V was considered by connecting 20 PV modules in series, conversely, 12 PV modules are connected in parallel and each module has a maximum voltage, V_{mp} of 30.7v and a maximum current, I_{mp} of 8.15A at maximum power.

5.1.1.1 Sizing of the battery bank

The size of the battery bank can be calculated as in [6] using equation (5).

$$B_{cp} = \frac{D_d . D_A}{\eta . V_{sys} . DoD} \quad (5)$$

Where DoD, η, V_{sys}, B_{cp}, D_d, and D_A stand for depth of discharge, efficiency, Battery capacity, daily load demand and battery days of autonomy respectively. Battery round-trip efficiency of 85% was selected for this project.

Sizing of battery bank for this project does not require any further design as the sizing was achieved with the help of HOMER software simulator. A total of 480 batteries, each with a nominal voltage of 12V and a nominal capacity of 200Ah (2.4kWh) is required for this project and it comprises of a string size of 30 with 16 battery strings in parallel.

Batteries add up in series to increase the voltage while the amperage remains the same, conversely, they add up in parallel to increase current while the voltage remains the same. A string size of 30 implies connecting 30 batteries in series.

This generates 30 (12V), at an amperage of 200Ah and hence, the bus voltage is 360V, hence a battery string size of 30 generates 360V, 200Ah. Sixteen, 16 parallel strings of the battery connected in parallel yields 360V, 16 (200Ah). Therefore, the 480 batteries required for this research work generate a bus voltage of 360V and an amperage of 3200Ah.

5.1.1.2 Boost converter design

In this case, the boost converter is used to give the PV voltage, Vpv a boost from 614V to 700V, which is the selected V_{dc} of the VSC DC bus.

The boost converter duty cycle (D) is expressed as in [7] as

$$D = \left(\frac{V_{dc} - V_{pv}}{V_{dc}} \right) = \left(\frac{700 - 614}{614} \right) = 0.12 \quad (6)$$

The capacity of the boost converter inductor is given as

$$L_{bc} = \left(\frac{V_{in} D}{f_{sw} \triangle I_{pv}} \right) = \left(\frac{614 \times 0.12}{10 \times 10^3 \times \frac{5}{100} \left(\frac{60 \times 10^3}{614} \right)} \right) = 1.508 mH \quad (7)$$

Where $\triangle I_{pv}$ is considered as the input current ripples (5%) of I_{pv} and f_{sw} represents the switching frequency in hertz, the value of the inductance, L_{bc} is selected as 1.6mH.

5.1.1.3 DC link capacitor design

The size of the DC link capacitor can be calculated as in [7] using the expression

$$C_1 = C_2 = \left(\frac{I_d}{2(2 \times \omega \times \triangle V_{dcrip}} \right) = \left(\frac{P / V_{dc}}{2(2 \times \omega \times \triangle V_{dcrip})} \right) = 4875 \mu F \quad (8)$$

Where V_{dcrip} is the ripple voltage, its value is 2% of the $V_{dc,}$ I_d represents the VSC DC link current, the angular frequency is represented by ω, the value of the selected DC link capacitors is C1=C2=500μF

Interfacing Inductor design and selection

The value of the interfacing inductor is achieved using the expression in [7] as

$$L_{\text{int}} = \left(\frac{\sqrt{3} \times m \times V_{dc}}{12 \times O_f \times f_{sw} \times I_{Rr}} \right) = \left(\frac{\sqrt{3} \times 0.90 \times 700}{12 \times 1.2 \times 900 \times 0.25 \times 86.60} \right) = 3.89 mH \quad (9)$$

Where O_f represents the overloading factor, m represents the modulation index, fsw represents the switching frequency, Vdc represents the DC link voltage, I_{Rr} represents the ripple in the grid current, its value is 25% of the grid current, IR.

$$I_R = \left(\frac{60 \times 10^3}{\sqrt{3} \times 400} \right) = 86.60 A \quad (10)$$

5.1.2 Modelling of diesel generator

The diesel generator is made up a diesel engine and an alternator for electricity generation; it consists of a diesel engine, a synchronous generator, an excitation system, and speed controller. The diesel engine and governor system exert control on the speed of the governor

to supply mechanical power. Its diesel engine comprises of the governor and an internal combustion (IC) engine.

The diesel generator ensures the conversion of energy from a fuel such as diesel or bio-diesel into mechanical energy with the help of its internal combustion engine, after which, this mechanical energy is converted into electrical energy with the help of its electric machine operating as a generator. The governor is made up of actuator and speed controller, the maintenance of a constant speed during the period of operation of a diesel generator is maintained by the governor [8] [9]

The transfer function of the actuator, as well as that of the regulator as in [8], is as shown in equation 11 and 12 respectively

$$H_a = \frac{(1 + T_{a1}s)}{s(1 + T_{a2}s) + (1 + T_{a3}s)} \tag{11}$$

$$H_r = \frac{\Upsilon_r(1 + T_{ra}s)}{(1 + T_{r1}s + T_{r2}s^2)} \tag{12}$$

Where, T_{a1}, $T_{a2,}$ and T_{a3} represent the time constants of the actuator, Υ_r represents the gain of the regulator while, the time constants of the regulator is represented by T_{r1}, $T_{r2,}$ and T_{r3}.

Conversely, the speed regulation and diesel engine of the diesel generator can be described using differential equations as in [8] as equation (13) and equation (14).

$$\frac{dm_B}{dt} = \frac{1}{\tau_2}(K_2 P_c - \frac{K_2}{\omega_{ref} R}\Delta\omega - m_B) \tag{13}$$

$$\frac{dPc}{dt} = \frac{-K1}{\omega_{ref}}\Delta\omega \tag{14}$$

Where the rate of fuel consumption of the diesel engine is denoted m_B, ω_{ref} is the engine reference speed in rad/sec, R is the permanent speed drop of the diesel engine, K_1 is the summing loop amplification factor of the governor, the gain and dead time of the engine is represented by K_2 and τ_2 respectively.

The dead time, τ_2 can be represented as in [8] as equation (15).

$$\tau_2 = \frac{60 S_t}{2Nn} + \frac{60}{4N} \tag{15}$$

N refers to the speed in rev/min, n is the number of cylinders, S_t represents the number of stroke engine, in this case, S_t=4 and due to combustion, the generated mechanical power is expressed as equation (16)

$$P = E_1 m_B \eta \tag{16}$$

η represents the efficiency and E_1 represents the proportionality constant.

5.1.3 Modelling of wind energy conversion system

With the help of the wind turbine, wind energy is converted into mechanical power and hence. The mechanical power is transformed into electrical power. The value of the mechanical power can be computed using the equation (17) [10]

$$P_m = 0.5 \rho A C_p(\lambda, \beta) V_{wind} \tag{17}$$

Where ρ represents the density of air, its value is within the range of 1.22-1.3Kg/ms, V_{wind} refers to the speed of the wind in m/s. A represents the swept area of the turbine blades (m^2), the coefficient of power is denoted by $C_p(\lambda,\beta)$, it's influenced by two factors, the pitch angle of the blade, β and the speed slip ratio, mathematically, the tip speed ratio is defined as

$$\lambda = \Omega R / V_{wind} \tag{18}$$

R is the radius of the blade (m) and Ω refers to the angular speed (m/s)

The coefficient of power is defined as in [10] as

$$C_p(\lambda,\beta) = C_1\left(\frac{C_2}{\lambda_1} - C_3\beta - C_4\right)\exp\left(\frac{-C_5}{\lambda_1}\right) + C_6\lambda \tag{19}$$

Where

$$\frac{1}{\lambda 1} = \left(\frac{1}{\lambda + 0.08\beta} - \frac{0.035}{\beta^3 + 1}\right) \tag{20}$$

The rotational torque can be expressed as

$$T_m = P_m / \Omega \tag{21}$$

And the optimal angular speed is represented by the relation

$$\Omega opt = \lambda_{opt} V_{wind} / R \tag{22}$$

In order to achieve the maximum mechanical power, the following relation is used

$$P_{m\_\max} = 0.5\rho A C_{p\max} V^3{}_{wind} \tag{23}$$

5.1.3.1 PMSG driven wind turbine

The PMSG driven wind turbine was chosen for this project as a result of certain advantages in [11] as follows:

- There is the absence of brush/slip ring.
- The mechanical stress is low
- The rotor does not experience any form of copper loss

- Reactive/active power controllability is higher

The sign of the torque input of the PMSG is what determines its mode of operation if its sign is negative, the PMSG operates as a generator and if its sign is positive, the PMSG operates as a motor [12].

The implementation of PMSG model is done in the dq-coordinates, which implies AC states does not exist in the model. Its mathematical equation is developed from the synchronously rotating reference frame by ensuring that the d-axis aligns with the rotor flux direction [10] [13].

$$V_q = R_s i_q + L_q \frac{d i_q}{d t} - \omega_e L_d i_d + \omega_e \varphi_m \tag{24}$$

$$V_d = R_s i_a + L_d \frac{d i_a}{d t} - \omega_e L_q i_q \tag{25}$$

Where V_q and V_d represent the q and d components of the voltages in the stator, i_q and i_d represent the q and d components of the currents in the stator, L_q and L_d represent the inductances (H) of the machine, φ_m represents the magnetic flux (wb), ω_e represents the electrical speed (rad/s).

In order to obtain the electrical torque, the following expression is used.

$$Te = \frac{3}{2} P \left\{ \varphi_m i_q + \left(L_d - L_q \right) L_d i_q \right\} \tag{26}$$

P in the expression above represents the poles pair and the machine rotor dynamics can be represented by the following expression

$$T_m - T_e = B \omega_r + J \frac{d \omega_r}{d t} \tag{27}$$

Where J represents the inertia of the rotor (kgm^2), ω_r is the speed of the rotor (rad/s), B represents the friction in the rotor Kgm^2/s, the mechanical torque that was produced by the wind is represented by T_m

Assuming $L_d=L_q=0$, and the d-reference current, $id^*=0$, then the $(L_d-L_q)i_d i_q$ becomes negligible.

5.2 Control of the hybrid energy system

The battery bank performs two roles in this project as it serves a sink, and also as a source, hence it charges or discharges when the network experiences surplus or lack of power from the sources of energy due to the situation of the weather. When the amount of electricity supplied by the sources of power is greater the load on the network, the battery controller

charges the battery and when the load on the network is more than the electricity supply from the sources, the controller causes the battery bank to discharge [14]. The control of the battery storage is done in such a way as to ensure the DC voltage is stabilized and this is achieved through the control of the DC/DC bidirectional converter in the network.

When there is a shortage of power from the sources, the bidirectional converter serves as a boost converter to provide power by discharging the battery and when the power supplied from the sources is in excess, it operates as a buck converter to charge the battery [15].

The hybrid system is also, incorporated with a dump load, the dump load is made up of a bank of resistors and a power converter, the capacity of the dump load power is such that it exceeds the amount of power produced by the wind, PV and diesel generator by 30%. It is to ensure the control of the network should, a condition arises when there is no load and the battery storage fails or is fully charged.

The flow of power in the network can be represented as

$$P_{network} = P_{pv} + P_{wt} + P_{diesel} - P_{load} \quad (28)$$

Where the net power generated is represented by $P_{network}$, P_{pv} is the amount of power supplied by the PV, P_{wt} represents the power supplied by the wind turbine and P_{load} is the power to the load.

When $P_{network} < 0$, it means the power supplied by the energy sources is not enough and the battery provides power to make up for the shortage of power. When $P_{network} > 0$, it implies the amount of power produced by the energy sources is in excess, the excess power is stored in the battery, but the moment it becomes more than the rated power of the batteries in the battery bank, a fraction of the excess power is transferred to the system dump load.

5.3 Results

The results obtained from the simulations carried out from the project implementation using MATLAB Simulink are as shown in figure 5-3.

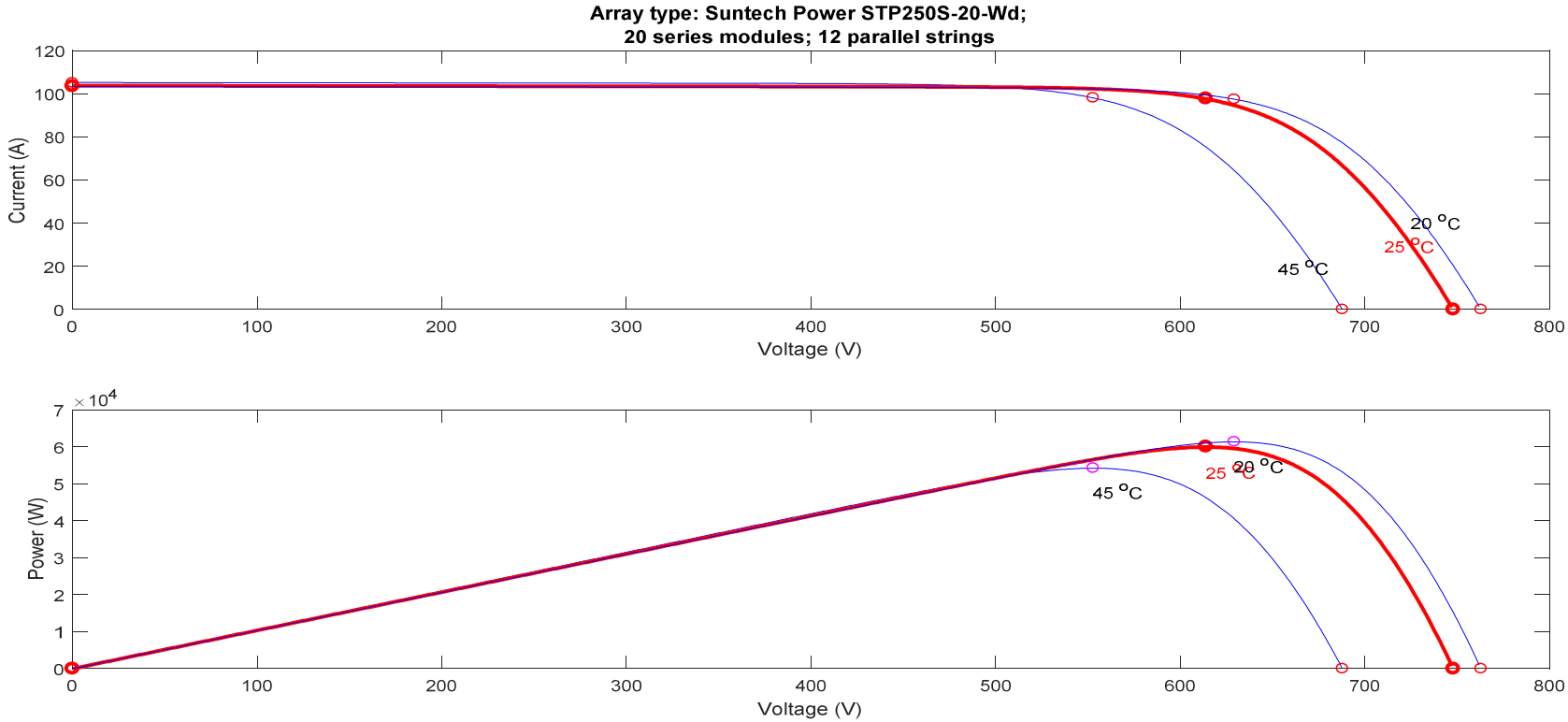

Figure 5-3 I-V and P-V curve of 60kW PV array.

The I-V and P-V curve below shows the usual characteristic of a PV module, which generates less power as the temperature of the module increases. The research location for this project usually experiences low wind speed unlike some part of Europe where the wind speed is high and as a result, the simulation was carried out at a wind speed of 6.1m/s. The input radiation is as shown, between 0 and 5minutes, the radiation is 1000W/m^2, between 5 and 10 minutes, the radiation is 800W/m^2 while 10 and 15 minutes, the radiation is 1000W/m^2. The result is as shown in figure 5-4 and figure 5-5.

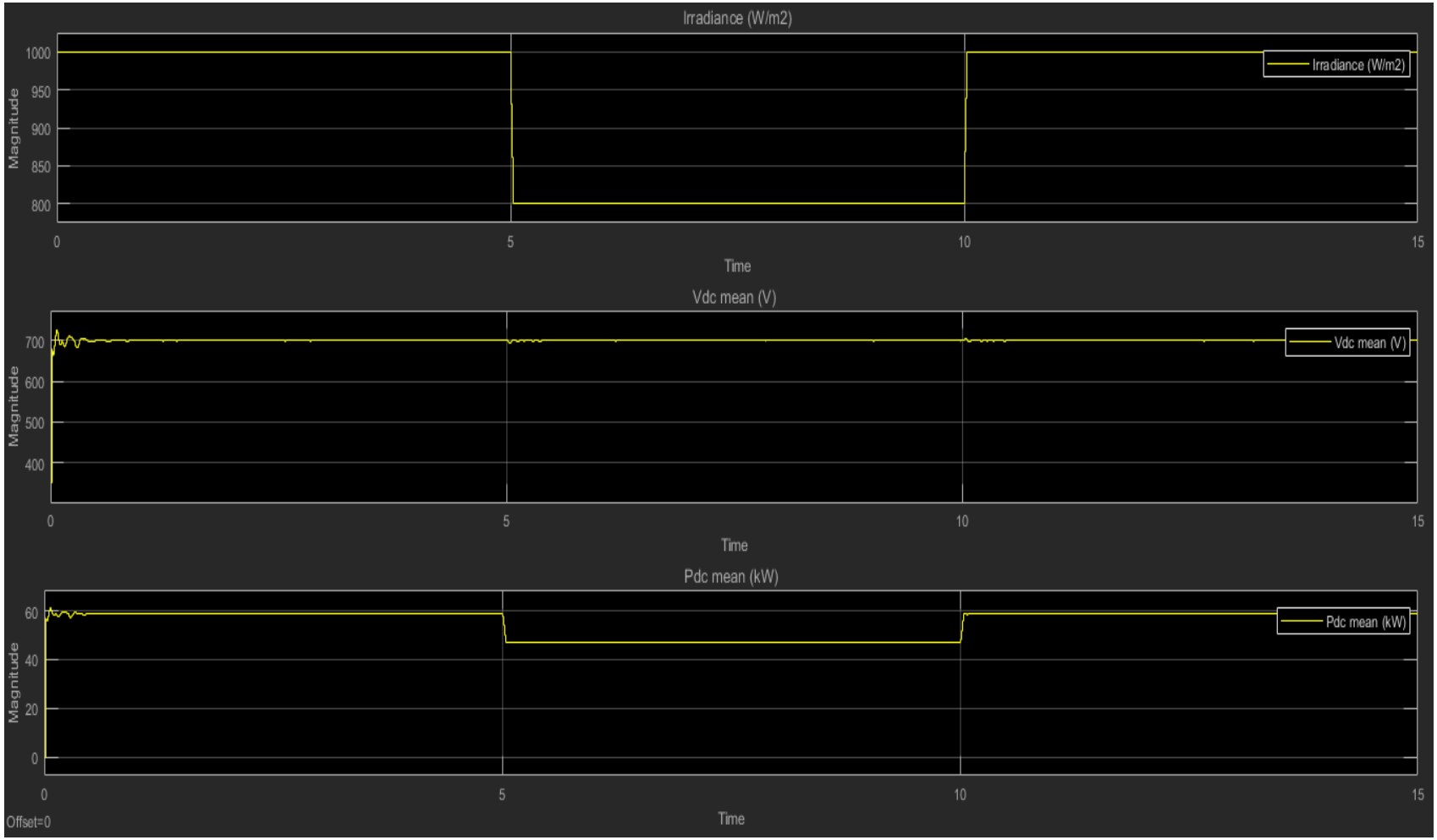

Figure 5-4. 60kW PV array power output at 45°C

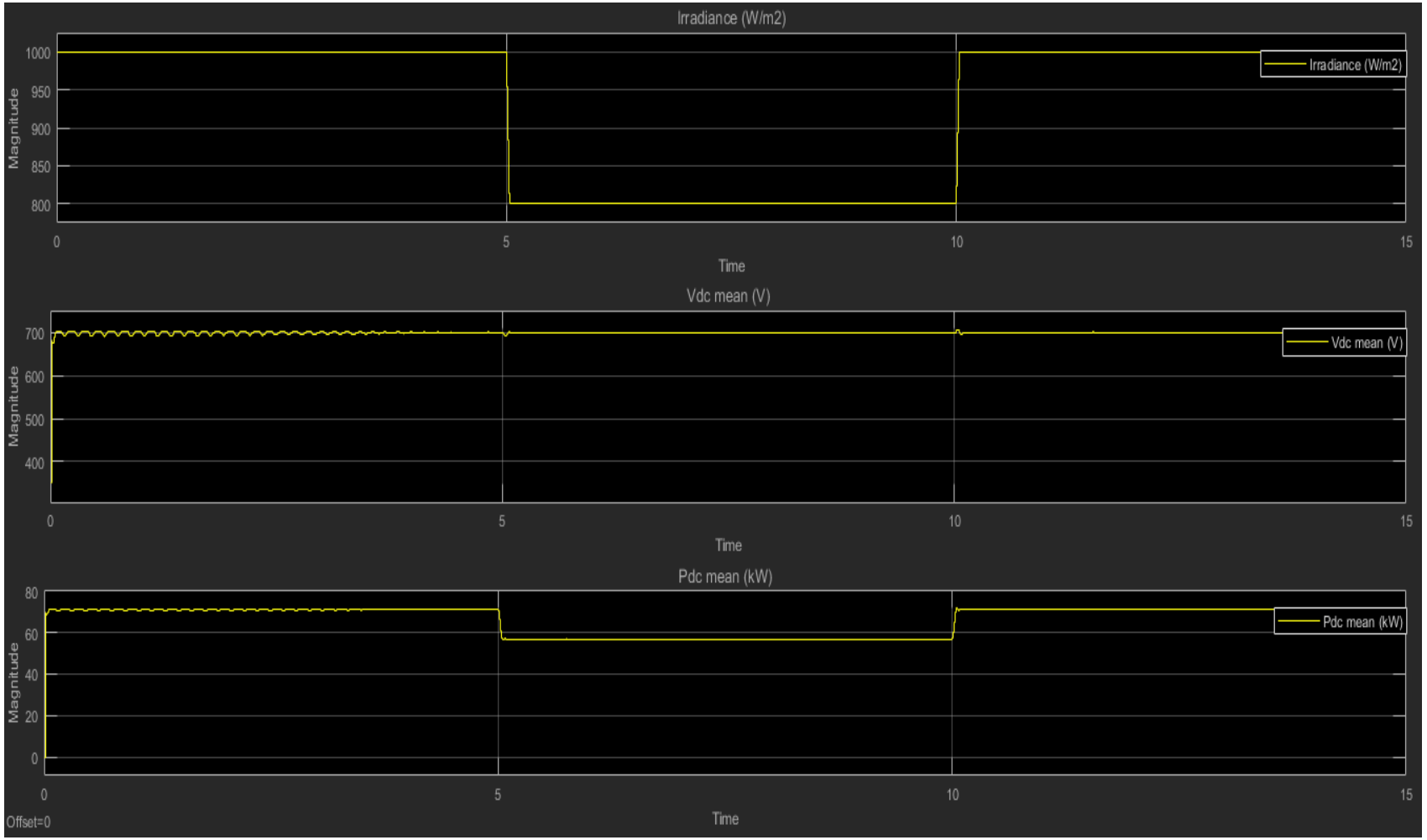

Figure 5-5. 60kW PV array power output at 20°C

From figure 5-4 and 5-5, it can be observed that the power output produced by the PV array at a temperature of 20°C is more, this is because the PV module works better when the module surface temperature is low. The measured Vdc and the reference Vdc of the network were compared and the values obtained are very close as shown in figure 5-6. This shows the system is working well.

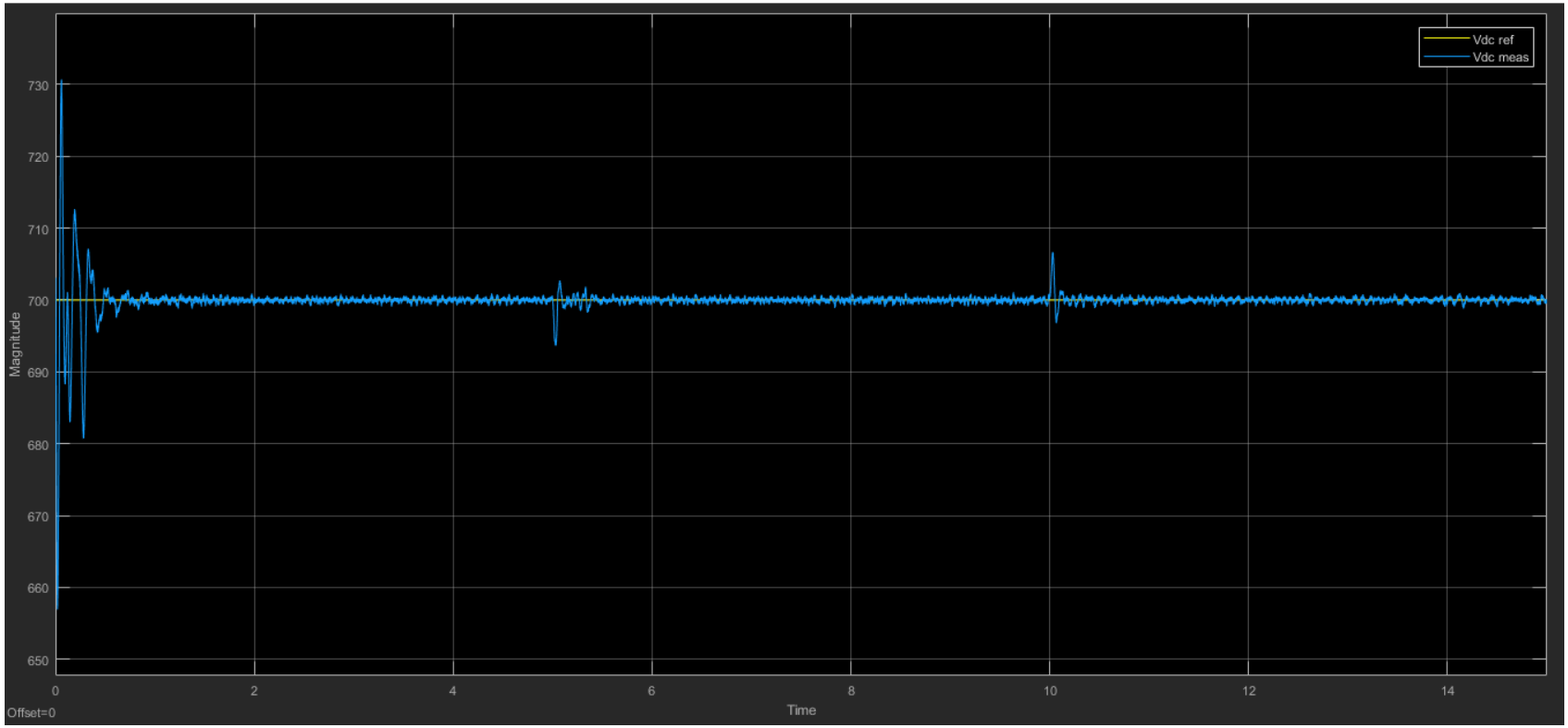

Figure 5-6 Vdc reference and Vdc measured

The diesel generator, rotor speed in pu and the stator currents are as shown in figure 5-7 and 5-8 respectively

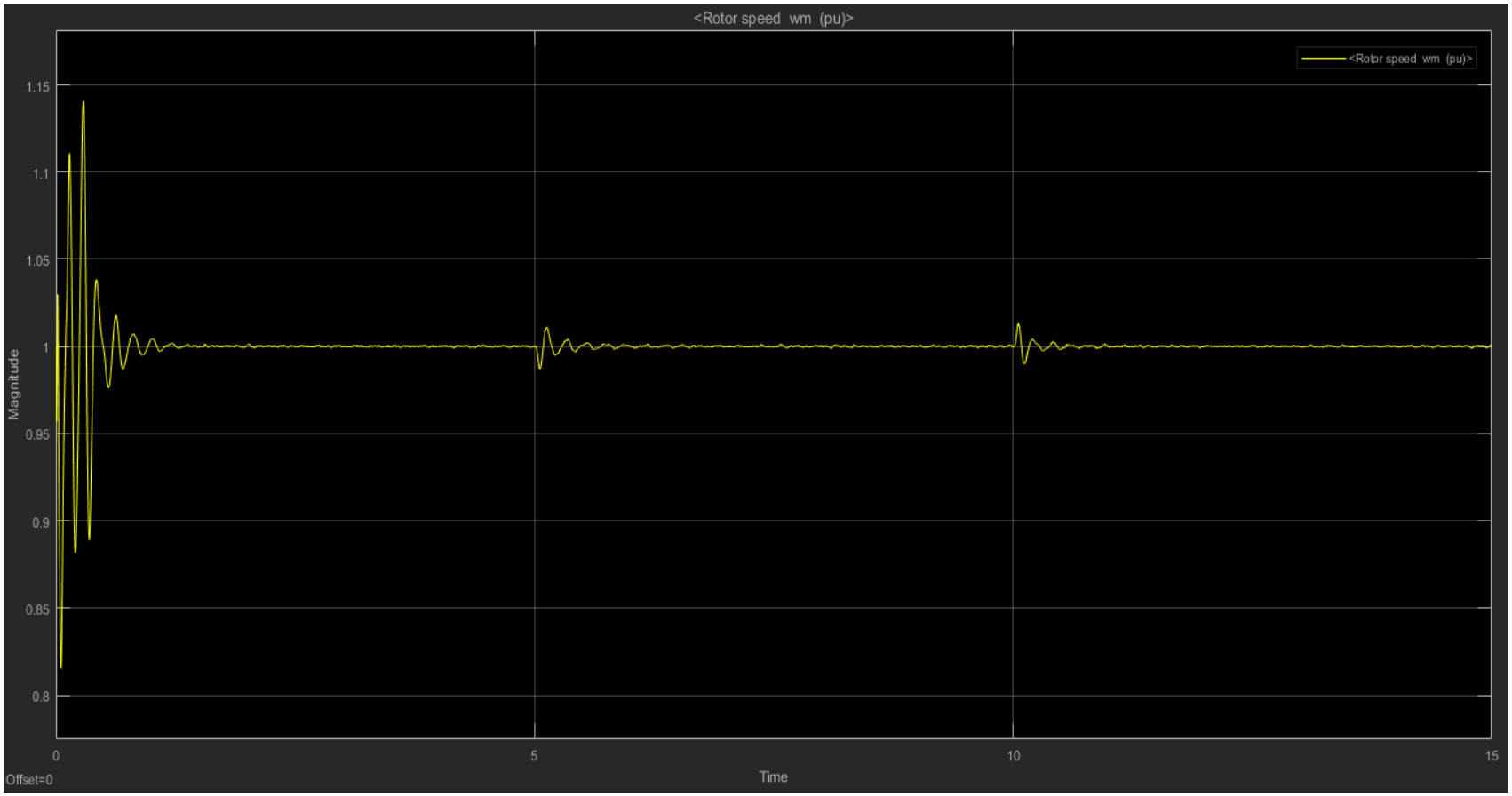

Figure 5-7 Diesel generator rotor speed.

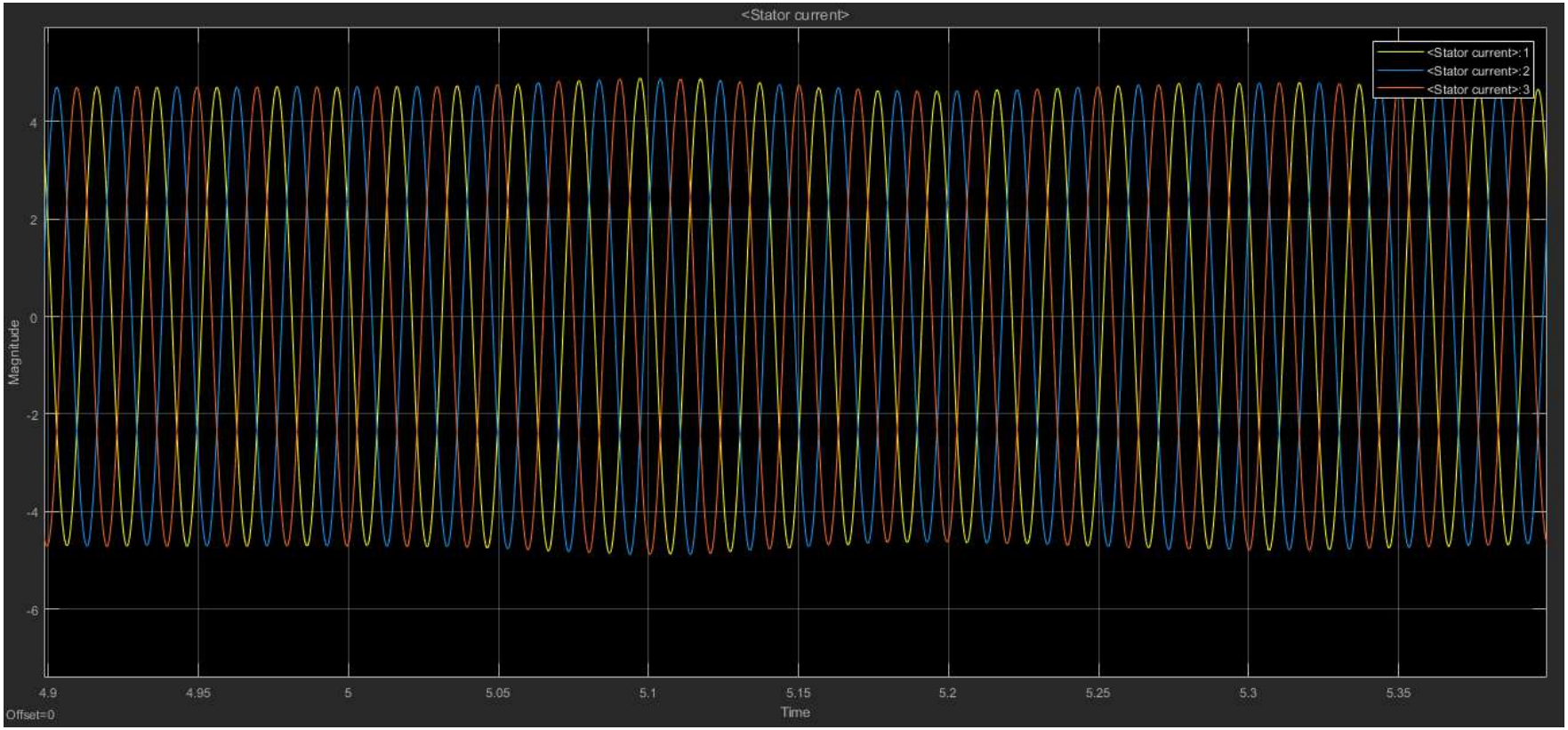

Figure 5-8 Diesel generator stator current

The PMSG driven wind turbine variables showing the voltages and currents expressed in dq values, the electrical torque, mechanical torque etc are as shown in figure 5-9.

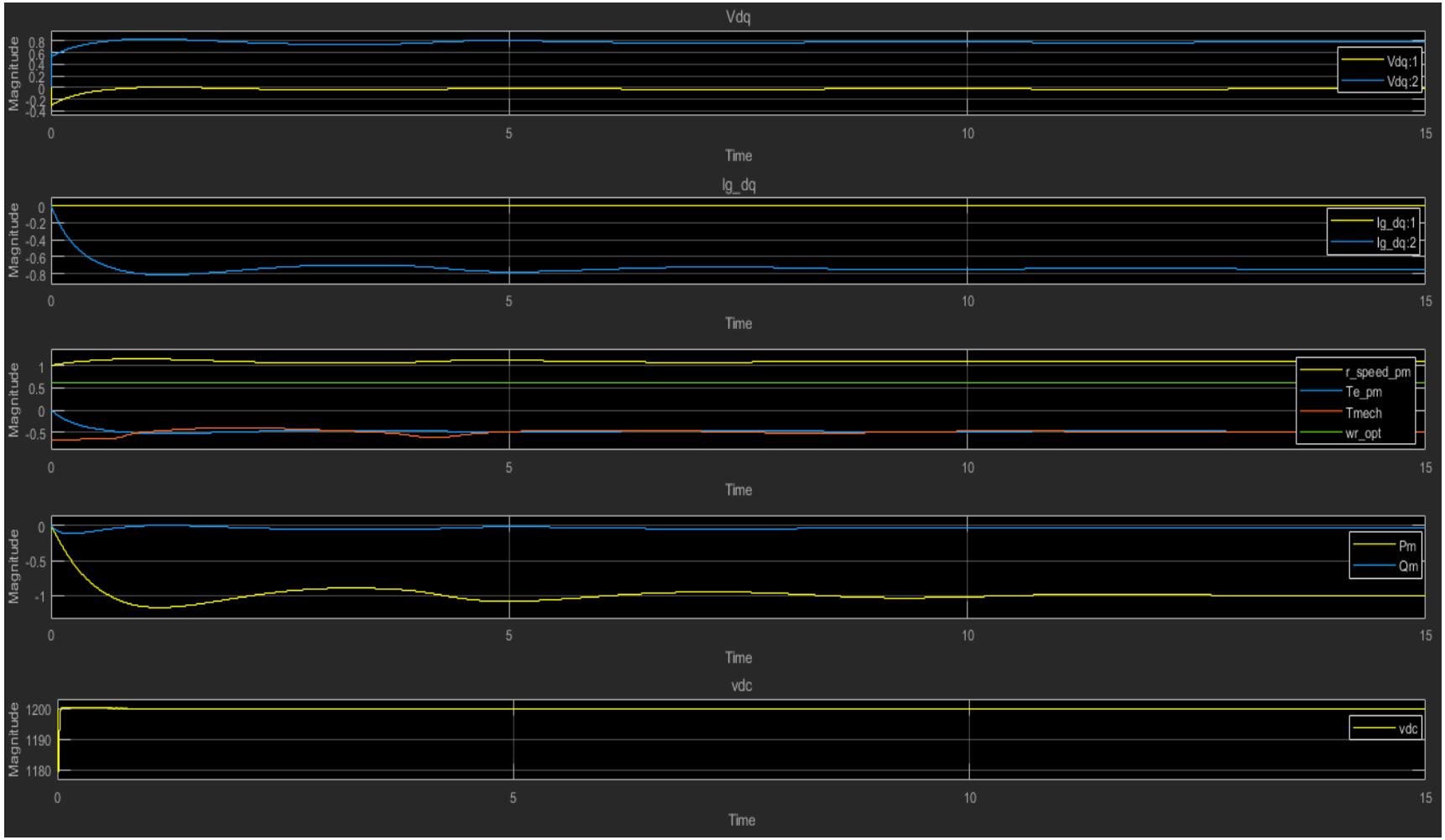

Figure 5-9 PMSG Wind turbine variables

The graph shows that the turbine controller is working properly, adjusting the electrical torque to match the mechanical torque for a steady control of the turbine speed. The speed of the turbine is set by the maximum power point tracking controller for a maximum extraction of wind power at the given speed. The accurate control of the electrical torque of the PMSG implies that the current control loops of the back-to-back converter are also working in a stable manner

5.4 Summary

The reduction in the surface temperature of the PV module increases the efficiency of the PV module, this results in an increase in the power output obtained from the experiment. The experiment shows that an increase in power output from 250watts to 262.4 watts is achievable. The result of the simulation also shows that at a temperature of 20°C, the PV module contributes more power to the hybrid energy system than at a temperature of 45°C. Hence, there is an increase in the hybrid PV/Wind/Diesel generator power output with increased module efficiency. Future works in this project involve the provision of voltage control of the hybrid energy system.

5.5 References

[1] Engin M. Sizing and simulation of PV-wind hybrid power system. Int J Photoenergy. 2013;2013

[2] Chikate B V, Sadawarte Y A. The Factors Affecting the Performance of Solar Cell. Int J Comput Appl Sci Technol [Internet]. 2015 [cited 2017 Sep 16];975–8887. Available from: http://research.ijcaonline.org/icquest2015/number1/icquest2776.pdf

[3] Koteswararao B, Radha K, Vijay P and Raja N. Experimental Analysis of solar panel efficiency with different modes of cooling. 2016;8(3):1451–6.

[4] Homer Energy. How homer calculates the PV array power output [Internet]. Homer Energy Support. 2014 [cited 2017 Oct 31]. p. 1. Available from: https://www.homerenergy.com/support/docs/3.10/how_homer_calculates_the_pv_array_power_output.html

[5] Kumar S, Verma A K, Hussain I and Singh B. Performance of Grid Interfaced Solar PV System under Variable Solar Intensity. [cited 2017 Nov 22]; Available from: https://www.researchgate.net/profile/Ikhlaq_Hussain/publication/280562137_Performance_of_grid_interfaced_solar_PV_system_under_variable_solar_intensity/links/55

b9c8c608aed621de0879dc/Performance-of-grid-interfaced-solar-PV-system-under-variable-solar-inte

[6] Akinyele D O and Rayudu R K. Community-based hybrid electricity supply system: A practical and comparative approach. Appl Energy [Internet]. Elsevier Ltd; 2016;171:608–28. Available from: http://dx.doi.org/10.1016/j.apenergy.2016.03.031

[7] Mohan N, Undeland T M and Robbins W P. Power electronics : converters, applications, and design. 3rd ed. John Wiley & Sons; 2003. 824 p.

[8] Faten Hosney Fahmy. PV/Diesel Hybrid System for Fuel Production from Waste Plastics Recycling. Ijmer [Internet]. 2014;4(12):68–79. Available from: http://www.ijmer.com/papers/Vol4_Issue11/Version-1/H04011_01-6879.pdf

[9] Pachori A, Suhane P and Scholar P. Design and modelling of standalone hybrid power system with MATLAB/Simulink. Int J Sci Res Manag Stud [Internet]. [cited 2017 Dec 3];1(2):2349–3771. Available from: http://www.ijsrms.com/media/3n2-IJSRMS0102116_v1_is2_65-71.pdf

[10] Babu N R and Arulmozhivarman P. Wind energy conversion systems - A technical review. J Eng Sci Technol. 2013;8(4):493–507.

[11] Kim H S and Lu D D. Wind Energy Conversion System from Electrical Perspective — A Survey. 2010;2010(November):119–31. Available from: http://www.scirp.org/journal/PaperInformation.aspx?PaperID=3324

[12] Mishra S, Gupta M, Garg A, Goel R and Mishra V K. Modeling and Simulation of Solar Photo-Voltaic and PMSG Based Wind Hybrid System. IEEE Students' Conference on Electrical, Electronics and Computer Science [Internet]. 2014 [cited 2017 Nov 19]. Available from: http://ieeexplore.ieee.org/stamp/stamp.jsp?arnumber=6804430

[13] Gajewski P and Pieńkowski K. Analysis of a wind energy converter system with PMSG generator. 2015;

[14] Samrat N H, Ahmad N Bin, Choudhury I A and Taha Z B. Modeling, Control, and Simulation of Battery Storage Photovoltaic-Wave Energy Hybrid Renewable Power Generation Systems for Island Electrification in Malaysia Modeling, Control, and Simulation of Battery Storage Photovoltaic-Wave Energy Hybrid Renewab. Sci World

J. 2014;2014(February 2016):22.

[15] Yasin A, Napoli G, Ferraro M and Antonucci V. Modelling and control of a residential wind/PV/battery hybrid power system with performance analysis. J Appl Sci [Internet]. 2011 [cited 2017 Sep 6];11(22):3663–76. Available from: http://www.scialert.net/qredirect.php?doi=jas.2011.3663.3676&linkid=pdf

Chapter 6:
Voltage control ancillary services for low-voltage distributed generation

This chapter of the thesis makes recommendations to support the creation of microgrid ancillary services market, and the provision of voltage control ancillary services to low voltage distributed generation since it is currently applicable to large power networks. It sheds light on the provision of voltage control ancillary services for low-voltage distributed generation (DG) and the need for the creation of a microgrid ancillary services market since the ancillary service network operations do not include small-size energy generation. The limitations facing the participation of DG in the provision of ancillary services, the basis of the creation of microgrid ancillary services market, the gap between large power plants and small power networks, and the useful recommendations to help suggest a solution to the problem have been considered herein. This work also embraces the types of ancillary services, microgrids, DG units, voltage control ancillary services, and various types of voltage control services and their usefulness to power system networks. Various techniques for voltage control, the relationship between reactive power and voltage control, the power factor (PF) and PF corrections, and their effects on power systems have been illustrated.

This chapter covers the different types of ancillary services in the power system, including their basis of classification, provision of ancillary services to the microgrid, distributed generation (DG) and the different types of DG classifications. Other areas covered are microgrid ancillary services, market prospects for microgrid voltage control ancillary services, types and techniques of voltage control, reactive power, and power factor.

6.1 Introduction

Ancillary services are the specialty services and functions provided by electric grids that facilitate and support the continuous flow of electricity to ensure that the supply will continually meet the demand. Ancillary services refer to a variety of operations beyond generation and transmission that are required to maintain grid stability and security. These services refer to those mandatory services that are required to provide support to grid operations. A number of ancillary services exist; they are supplied by different authorities and may not certainly be the same; however, some ancillary services, e.g. black start, voltage

control, and frequency control are accepted by virtually all the authorities [1]. According to previous research [2], ancillary services refer to all essential services that are usually provided by the grid and which the DSO or TSO also need so as to sustain the stability, integrity, and power quality of the distribution or transmission system.

Conversely, another research study [3] showed that customers usually demand for energy and capacity, for the power system to work effectively, in addition to these factors, a number of grid support services are essential because they equip the system operators with the resources required to sustain the immediate and continual balance between load and generation. This is to ensure that the transmission line flows are appropriately coordinated and the control schemes implemented. Under normal conditions and during emergencies, these ancillary services are in demand as they also make provisions for the necessary amenities required for the power system to restart when a situation wherein the balance between generation and load could not be maintained arises, resulting in a system breakdown. Figure 6-1 shows the types of ancillary services used in power systems based on the mode of delivery.

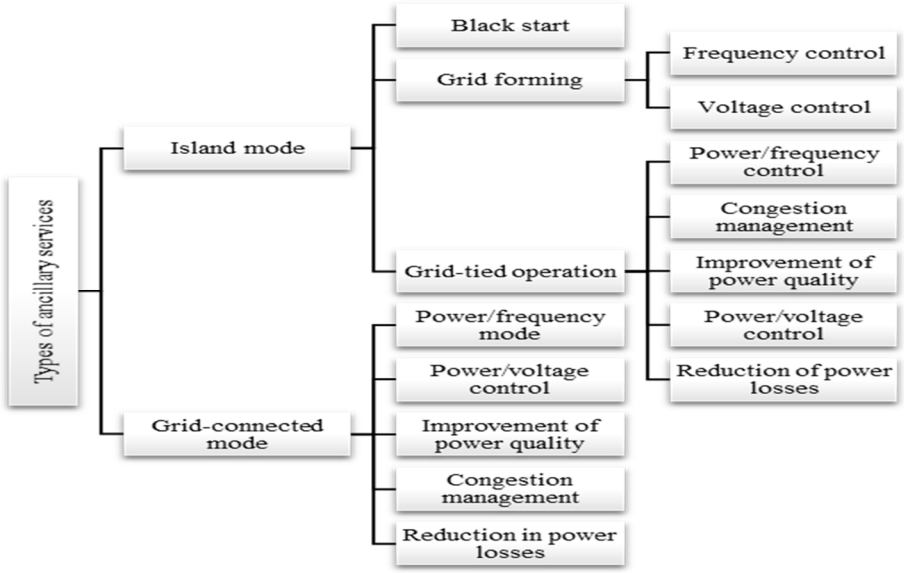

Figure 6-1 Types of ancillary services used in power systems.

On the other hand, based on types of services rendered, ancillary services are classified as shown in figure 6-2

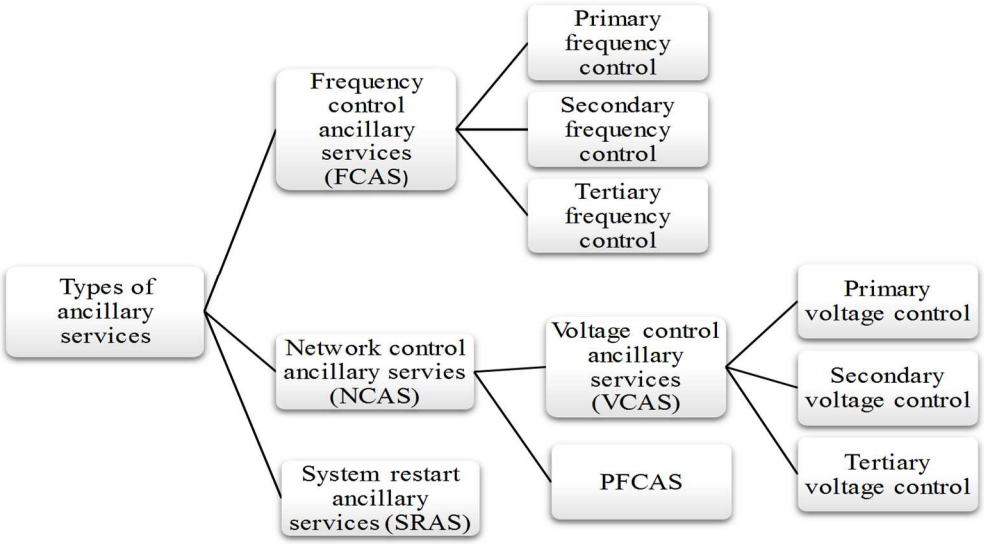

Figure 6-2 types of ancillary services.

In a past research [4], Transmission operators, load serving entities, and generators, usually provide ancillary services and a number of technologies used for the provision of ancillary services are as shown in table 6.1.

Ancillary services	**Technologies used**
NCAS	Capacitors, Generators, Distributed energy resources (DERs), FACTS controllers, inductors, Synchronous condensers
FCAS	Distributed energy resources (DERs), Demand-side management, Rapid unit loading, Rapid unit unloading, AGC, Governor
SRAS	Generators and Distributed energy resources

Table 6.1 Ancillary services provision technologies

6.2 Provision of ancillary services to the microgrid

A microgrid is a small-scale electricity grid that can function separately or simultaneously with the major electricity grid in its location; it usually requires different sources of energy. The distribution system of a microgrid is usually composed of the sources of energy, often referred to as micro-sources, a storage system alongside loads that are controllable [5]. Different types of microgrids exist, and these are shown in figure 6-3.

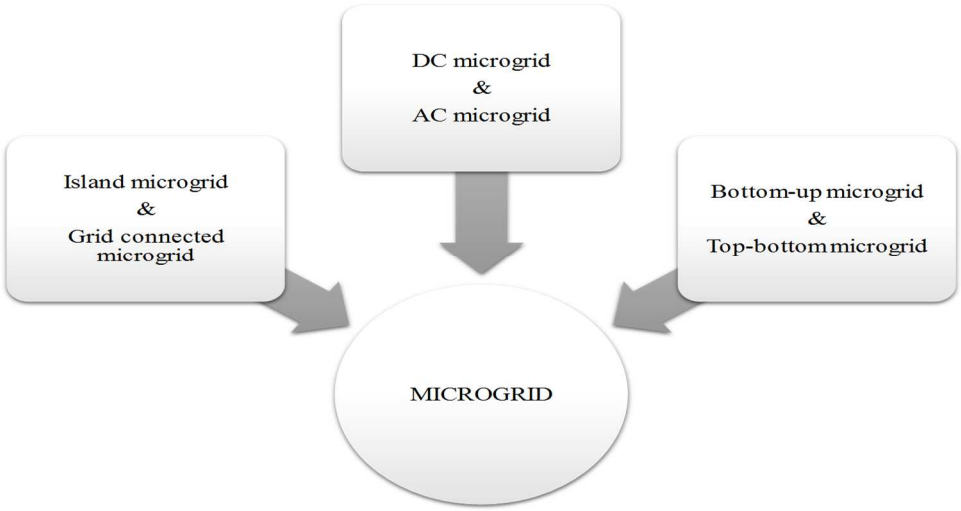

Figure 6-3 Types of microgrids.

In a previous study [6], the microgrid is made up of electrical power generators, some of whose power was sourced from renewable resources, e.g., sunlight and wind, and these power generators are referred to as distributed generation (DG). Depending on the size and capacity, a microgrid as in [7] has some basic functionalities, as shown in Figure 6-4.

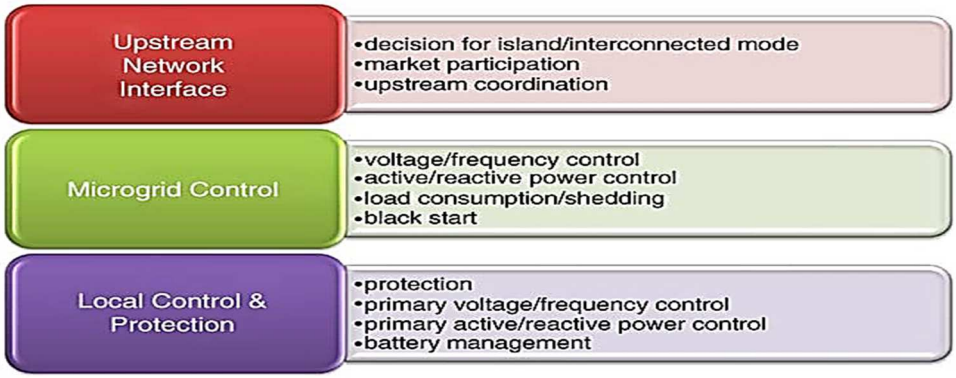

Figure 6-4. Microgrid functionalities [7].

Ancillary services can be provided by microgrids, as shown in Figure 6.3, and this is possible when the technical requirements to provide the ancillary services are satisfied by the microgrid [1]. We anticipate that in the future, the supply of electricity will depend more on DG, especially from renewable energy sources, but now, the power contribution to distribution from DG, such as wind and PV, is limited and does not participate in network operations. DG units are excluded from network operations because of their unstable nature, operational cost, and size [8].

6.3 Distributed generation (DG)

DG refers to a system or mechanism that produces electricity near the users with the use of small-scale power systems. In a previous research [9], the energy sources of the DG technology comprised non-renewable and renewable energy sources as well as battery storage. Using renewable DG, the stability of the power supply cannot be predicted since the resources are usually unstable, as reported in previous research [10]. The energy sources are as shown in Figure 6-5.

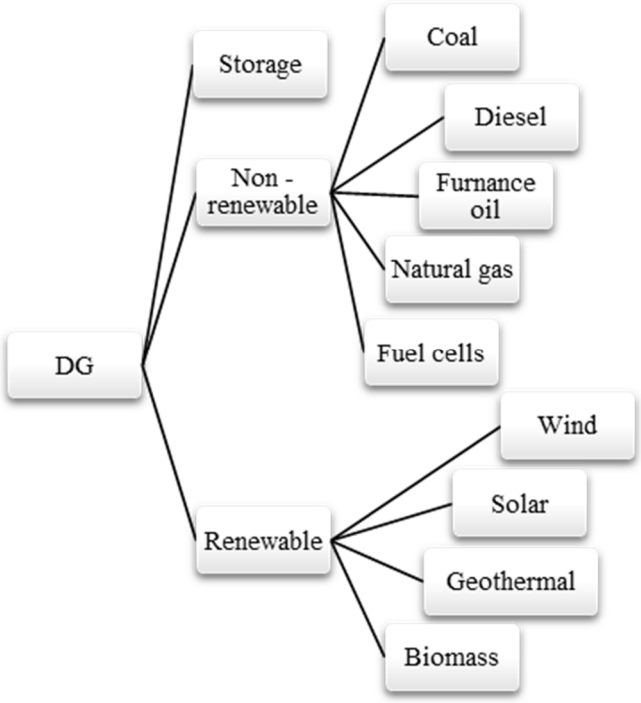

Figure 6-5. Distributed generation (DG) energy sources.

DG mainly comprises of energy sources that are modular in nature and usually comprises renewable energy sources. Because DG is usually constituted by energy from renewable sources, it has the following advantages: It is friendly to the environment, it can be made available at a much lower cost than the conventional power generators and is more reliable and secured [11]. Each of the DG sources has the capabilities of providing ancillary services. The capabilities of renewable and non-renewable DG sources to provide ancillary services are as shown in table 6.2 and 6.3 respectively.

Table 6.2. The capabilities of renewable DG sources to provide ancillary services.

Ancillary services	Wind Non-DFIG	Wind DFIG	Biomass	Land fill Gas	Solar PV	Hydro
Size	**<50MW**	**> 50MW**	**1-100MW**	**1-10MW**	**<100kW**	**>1MW**
Frequency	HF only	√	HF only	HF only	X	√
Reserve	X	√	√	√	√	√
Reactive power	X	√	√	√	√	√
Network Support	√	√	√	√	Limited	√
Black start	X	X	Future Islanding?	Future Islanding?	X	Future Islanding?

Table 6.3. The capabilities of non-renewable DG sources to provide ancillary services.

Ancillary services	CCGT	Large CHP	Micro CHP	DIESEL & OCGT (STANDBY)
Size	**>100MW**	**1-100MW**	**1-5kW**	**<50MW**
Frequency	√√	Limited	X	Limited
Reserve	√√	Possible	Possible: High penetration	√√
Reactive power	√√	√	X	√
Network Support	√	√	Possible: High penetration	√
Black start	Possible	Future Islanding opportunity ?	X	Future Islanding opportunity?

The major stakeholders in the business of ancillary services as in [12] are academics, Ofgem, Micro-CHP developers, distribution network operators, transmission system operators, renewable and non-renewable plant developers and operators. The summary of the ancillary services provided by the national grid company in Wales and England is as shown in figure 6-6.

Ancillary Service	Product Types	Service Providers	Loading & Control	Contract Types	Payment Arrangement	Market Value (per annum)
Frequency Response	**Mandatory** • Primary • Secondary • High **Commercial**	• Large generators • Demand side • BM & non-BM	• Part loaded generators • Dynamic controlled • Automatic initiation	**Mandatory**: • Firm **Commercial** • Firm & • Optional	• Holding Payments (£/MW/h) • Response Energy payments (£/MWh)	**Mandatory**: • £19 million **Commercial**: • £26 million **Total:** • **£45 million**
Reserve	• **Regulating** • **Standing** • **Fast** • **Warming & Hot Standby**	• BM • Non-BM • Large & small generators • Demand side	**Regulating** • Part loaded **Others** • Off-load • Single point of contact	**Standing Res:** **BM** • Committed **Non-BM** • Committed • Flexible	**Regulating**: • BOAs • **Others** • Availability (£/MW/h) • Utilisation (£/MWh)	**Standing** • £41 million **Fast** • £21 million **Warming** • £ 21 million
Reactive Power	**Default** **Commercial** • Obligatory • Enhanced	**Generators** • BM or • Non-BM (non participate) **NGC SVCs**	Generators both • Partly loaded • Fully loaded	**Default** • Grid Code • Firm **Commercial** • Bilateral • Firm	**Default** • Utilisation (£/MVArh) **Commercial** • Utilisation • Availability (£/MVArh)	**Default** • £16 million **Commercial** • £17 million **Total** • £33 million
Fast Start	Fast Start	OCGT	Off Load Remote	Bilateral	Availability: £/h	• £3 million
Black Start	Black Start	OCGT	Off load	Bilateral	Availability	•£10 million

Figure 6-6 The summary of the major ancillary services provided by Wales and England [12]

Generally, DG classification done on several bases is as shown in Figure 6-7.

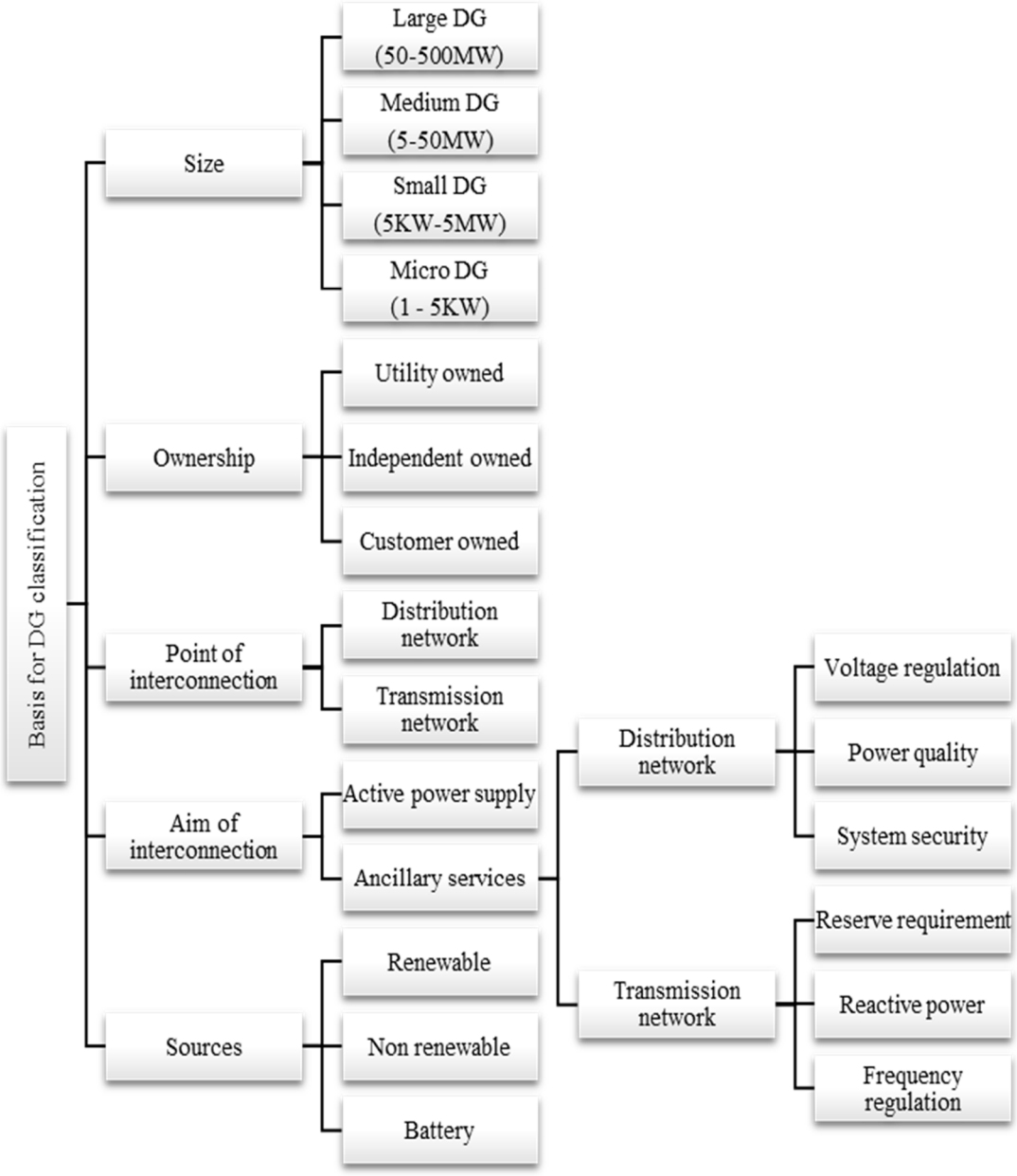

Figure 6-7 Classification of DG.

DG operates as a utility-connected system or a standalone system and usually installed in an isolated location, such as rural areas, where used to provide power supply to small buildings, large buildings, industrial sites, and estates. Generally, individuals operate it. DG units generate DC power or AC power, and these two forms of power do not connect together directly. As such, the required frequency, voltage magnitude, and phase angle are derived by means of power electronics interfaces. With the aid of a suitable power electronics interface,

each of the various DG units can be linked to the main grid. In some designs, a number of power electronic units are employed, whereas some designs make use of a single power electronics unit to reap some benefits, such as minimized losses, simpler design than those with a number of power electronics, and reduced cost, in terms of system control.

It has been observed that DG units comprising renewable energy sources are better than those comprising of non-renewable energy sources because, In the former type of DG units, energy sources will not be exhausted in the long run. They are environmentally friendly, and energy from the individual sources can be combined to produce a DC voltage as an input to a DC/AC inverter, which is required for grid connection or connection to a low-voltage distribution network [13]. DG has the potential to provide active power as well as ancillary services to the electrical network. In a low-voltage network, DG can operate at a power factor (PF) of unity. As such, it can be used to proffer solution to the challenges of voltage regulation, as reported in previous research [14].

Other numerous benefits of DG identified by the proponents of DG as reported by past research [15], includes the following:

- DG system technologies have the potential to provide a more dependable power supply to organisations in demand for uninterrupted power supply.
- Since DG produce power to users locally, it reduces the demand for power during peak demand and by reducing power congestion on the electrical network, power transmission is enhanced
- DG as a decentralized source of power is less, exposed to terrorist targets than large power stations.
- The widespread use of DG technologies has the potential to reduce emissions considerably
- Because, DG technologies do not depend on the grid, they serve as a source of emergency power to hospitals, military bases, airports etc.
- It helps a nation to increase the diversity of its sources of energy.

The Distributed generation services and benefits matrix are as shown in figure 6-8

		Benefit Categories							
		Energy Cost Savings	Savings in T&D Losses and Congestion Costs	Deferred Generation Capacity	Deferred T&D Capacity	System Reliability Benefits	Power Quality Benefits	Land Use Effects	Reduced Vulnerability to Terrorism
DG Services	Reduction in Peak Power Requirements	✓	✓	✓	✓	✓	✓	✓	✓
	Provision of Ancillary Services –Operating Reserves – Regulation – Blackstart –Reactive Power	✓	✓	✓	✓	✓	✓	✓	✓
	Emergency Power Supply	✓	✓			✓	✓		

T&D= transmission and distribution.

Figure 6-8 The matrix of DG services and benefits [15]

This research focuses on the application of a voltage control ancillary service to a low-voltage distribution network in a hybrid microgrid and the creation of a microgrid ancillary services market.

6.4 Microgrid ancillary services market

To support efficiency and encourage improvement in electrical power services, there is a need for competition among the stakeholders. The participation of distributed energy resources in power generation and the provision of ancillary services need to be supported. Currently, distributed energy resources have several limitations. Some factors responsible for the limitations, as reported in previous research [16], include the following:

- The requirements and naming of the voltage control services within European countries is not homogenous as the voltage control layers are not differentiated.
- The existing market structure for ancillary services supports the supply of ancillary services via programmable generation units, i.e., non-renewable energy sources.
- There is a technological limitation to the participation of renewable energy sources due to the existing regulations.
- The access to participation is limited to the size of the plant because access is only restricted to plants with a capacity above 10 MVA.

6.4.1 The need for the creation of a microgrid ancillary services market

Some of the reasons why it is important for us to create a market for microgrid ancillary services include the followings:

- A market for microgrid ancillary services can create room for competition among the players, and this will result in an increase in the quality of service
- Network operations are required for both low- and high-voltage distribution systems.
- Power quality and stability is a necessity for every electrical power network.
- To create more Job and investment opportunities.
- To create a basis for DG and microgrid structures.
- To increase flexibility

6.4.2 The basis for the creation of a microgrid ancillary services market.

A microgrid ancillary services market is grouped based on the connectivity, offering, vertical, region, and grid type. The different groups also have divisions, as shown in Figure 6-9.

Figure 6-9 The basis for the classification of the ancillary services market.

6.4.3 Recommendations

Some of the recommendations made to proffer solutions to the inability of distributed energy resources to participate in the provision of ancillary services are shown below:

- The procurement process should be enhanced and additional power sources activated.

- Renewable energy sources should be allowed to participate in the provision of ancillary services whenever technically possible.
- The combination of smaller energy units should be engaged and not only large-scale power units
- The gradient should be expressed based on the percentage of the maximum power output and not in absolute values, e.g., 10 MW.
- Harmonization of the rules for balancing and using ancillary services across countries in a geographical region, e.g., Europe, should be conducted.

For a reliable microgrid ancillary services market to function effectively, there must be an audience, usually referred to as the business target audience. The targets, in this case, are government agencies, transmission system operators, raw materials and equipment suppliers, investors, utilities, photovoltaic companies, smart grid software vendors, energy storage vendors, and microgrid system integrators and suppliers.

6.5 Market prospects for microgrid voltage control ancillary services

In the ancillary services market, volt-ampere reactive (var) utilization is the major product for voltage control. To satisfy the needs of the reactive power, the distribution system operator operates a voltage control ancillary services market so that the var needs are distributed between the numerous players whose var bids are accommodated by the distribution system. In this case, the DSO performs the role of the buyer and ensures that the market is settled. The major sources of var include the microgrids, MV-connected DG units, and HV network (if available) [8].

6.6 Voltage control ancillary services

Voltage control as an ancillary service involves maintaining the set points of the reactive power or the voltage in a network. To this end, the conditions required for obtaining a balance between the reactive power demand of the customers and that of the network have to be reached [16]. Voltage control is achieved through the management of reactive power in an AC electrical network. In an electrical network, the transmission and distribution equipment absorb and produce reactive power. For power systems to operate reliably and effectively, the voltage and reactive power must be controlled to meet the following objectives, as reported in the literature [17] [18]:

- The movement of reactive power in an electrical system from one point to another is reduced in order to reasonably minimize the XI^2 and RI^2 losses.
- The system stability is improved to ensure that the transmission system utilization is maximized.
- The voltages are within an allowable limit at the terminals of each equipment in the system.

The function of voltage control is related to the fluctuating load conditions and the corresponding reactive power compensation requirements. The voltage control ancillary services include a fault ride-through (FRT) capability, congestion management, primary voltage control, secondary voltage control, and tertiary voltage control. This can be grouped into two categories, as reported in the literature [19]:

- Distribution system voltage control.
- Transmission system voltage control.

6.6.1 Distribution voltage control

Distribution voltage control, also known as volt/var, refers to voltage control at the distribution level, and its main aim is to ensure the energy losses and peak power are reduced while maintaining the voltage within the allowable limits for a number of different nominal load systems. The variables of interest include the sizes and locations of the tap changer voltage regulator and capacitor control dead bands. The voltage on the secondary side of a transformer is measured or regulated with the help of tap changers, and the tap changers are usually controlled with the help of relay controllers.

6.6.2 Transmission voltage control

On the contrary, transmission system voltage control can be categorized with respect to activation time, as shown in Figure 6-10.

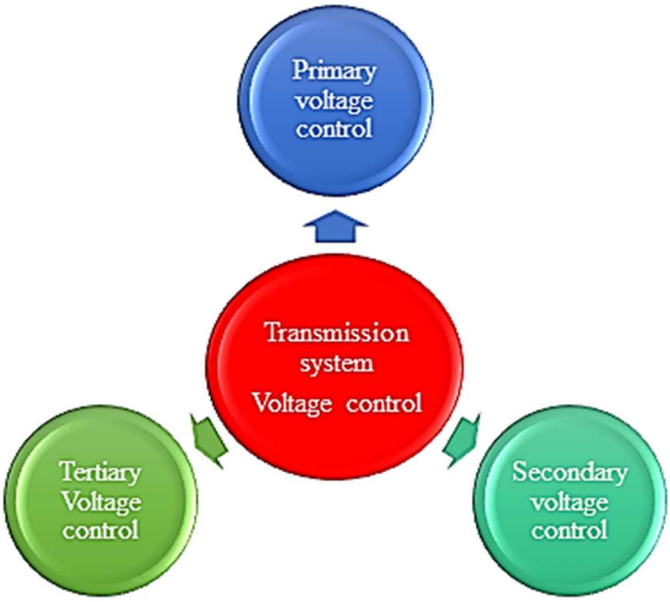

Figure 6-10 The categories of transmission voltage control.

6.6.2.1 Primary voltage control

This involves the use of automatic voltage regulators (AVRs) to ensure the voltage of the electrical devices is maintained with respect to their reference value at the point of common coupling. The values involved are normally fixed based on several factors, e.g., the maximum amount of reactive power to be supplied from any of the devices, voltage drops, and security requirements. This type of voltage control can be in operation for 1 min.

6.6.2.2 Secondary voltage control

Unlike primary voltage control, this type of voltage control can progress for 1 min and continue for several minutes. The voltage is maintained at specific pilot nodes by coordinating the reactive power resources from different segments of the network. Once the voltage at the buses becomes out of scope, the voltage regulator set points are adjusted by the system operator to ensure a voltage profile is recovered.

6.6.2.3 Tertiary voltage control

This type of voltage control has the longest duration of operation (10–30 min). It operates in the entire system. Its primary purpose is to ensure that the losses are minimized, the required voltage is maintained, reactive reserves are replaced. The secondary voltage control setpoint values are provided for the operation of the network to be optimized [16]. In a distribution system, the variation in voltage across the line is given by equation (1) as follows:

$$\Delta V = \frac{(P_R + Q_X)}{V}, \quad (1)$$

Where P and Q represent the active power and reactive power generated by a power source, respectively, while the resistance and reactance of the electrical line linking the power source are represented by R and X, respectively. V represents the nominal voltage at the power source terminal [20]. With respect to equation (1), any meaningful amount of electrical power introduced by a power source, e.g., a DG unit, will result in an increase/decrease in the voltage of the power distribution system, especially if the distribution feeder is weak and its impedance is high. The variation in the voltage is also influenced by the size of the DG unit, the voltage regulation method adopted, and the location.

6.7 Techniques for voltage control

Some of the numerous techniques used for voltage control applied in several applications are shown in Figure 6-11.

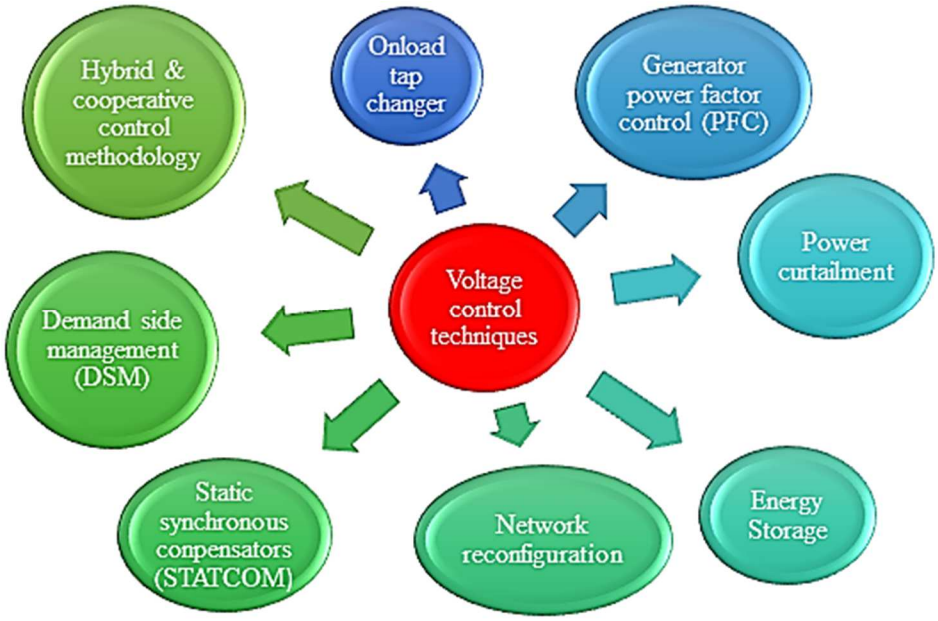

Figure 6-11 Techniques used for voltage control.

Over time, ancillary services have been provided by conventional generators because of the need for power generation from distributed energy resources; however, there is a need for the creation of microgrid ancillary services.

6.8 Reactive power and voltage control

In a power system network, when the voltage and current are not in phase, the reactive power is said to be present. It is evident that reactive power exists in a power network when (a) one waveform leads the other waveform, (b) PF of the network is less than unity, and (c) the phase

angle between the current and voltage is not equal to 0°. Reactive power is produced when the waveform of the current leads that of the voltage (often referred to as the leading PF) and consumed when the waveform of the current lags that of the voltage (usually referred to as the lagging PF) [21]. A device that consumes power in a manner such that the waveform of the voltage and that of the current are in phase with each other is said to have consumed real power and zero reactive power, but if the current waveform lags that of the voltage, reactive power is said to be consumed. The quantity of the reactive power consumed by the device is determined based on the phase shift between the current and the voltage.

The relationship between the real power P and the reactive power Q is given in equation (2) as follows:

$$S = P + JQ = V.I^* = VI\cos\varphi + jVI\sin\varphi \quad (2)$$

Where S represents the apparent power, P is measured in watts, and Q is measured in var [22]. Reactive power exists as a result of a phase shift between the current and voltage curves in a power system [23]. The operation of a power system network is affected by reactive power in numerous ways, as reported in previous research [24]:

- Loads absorb reactive power, which has to be supplied from some source.
- Transformers and transmission lines absorb reactive power, which has to be supplied from some source, but note that every transmission line does generate a certain amount of reactive power from the charging of their shunt line, which affects their ability to consume reactive power.
- The movement of reactive power from its source to sink creates extra heating in the lines and drops the voltage of the network.
- The production of real power can be restricted by the production of reactive power.

6.8.1 Usefulness of reactive power in a power system

In an electrical power network, voltage control is very useful as it ensures that power system devices operate properly to (a) help stops problems, such as excessive heating of motors and generators, in order to minimize losses from transmission and (b) sustain the capacity of the electrical system to prevent as well as withstand voltage collapse. Electrical power often witness under-voltage and over-voltage during operation; this challenge can be checked with the help of voltage/var control. Voltage/var control ensures that the movement of reactive power and its absorption and production at different levels in the power system are controlled. It also ensures that the voltage profile is maintained within the allowable range and that the

transmission losses are minimized. A reduction in reactive power leads to a reduction in the voltage. Conversely, increasing the reactive power increases the voltage. When a power system experiences a situation wherein the load exceeds that which the voltage can support, a voltage collapse takes place.

In the event of a reduction in the supply of reactive power, the supply voltage also reduces; there has to be an increase in the current in order to maintain the power supply. This results in the absorption of more reactive power by the system, leading to a further reduction in the voltage. If the increase in current is in excess, the transmission line will go off and overload other lines in this process, thereby cascading failure results. Conversely, if the reduction in voltage is very low, it will give rise to a situation wherein a number of generators will have to be disconnected from the network automatically to avoid being damaged. When a power system experiences a reduction in voltage of this nature that is progressive and uncontrollable, it implies that the power system network cannot supply appropriate reactive power that is needed by the power system [19].

Other uses of reactive power, as reported in the literature [21], are as follows:

- For the movement of electrons to be converted to useful work, reactive power is required by motor loads and other loads.
- For active power to perform useful work, the necessary voltage level required is provided by reactive power.
- It helps to regulate voltage.
- For active power to move to a consumer through the distribution and transmission system, reactive power is required.

6.8.2 Limitations of reactive power

- It cannot travel far.
- Production of reactive power closest to the area of need is a necessity.
- Its supply is tied closely to its capacity to provide active power.
- A source of reactive power at a close proximity to the area of need is in better condition to deliver reactive power than a source at a far distance from the area of need.

The consumption and generation of reactive power are attainable with several devices, as shown in Figure 6-12.

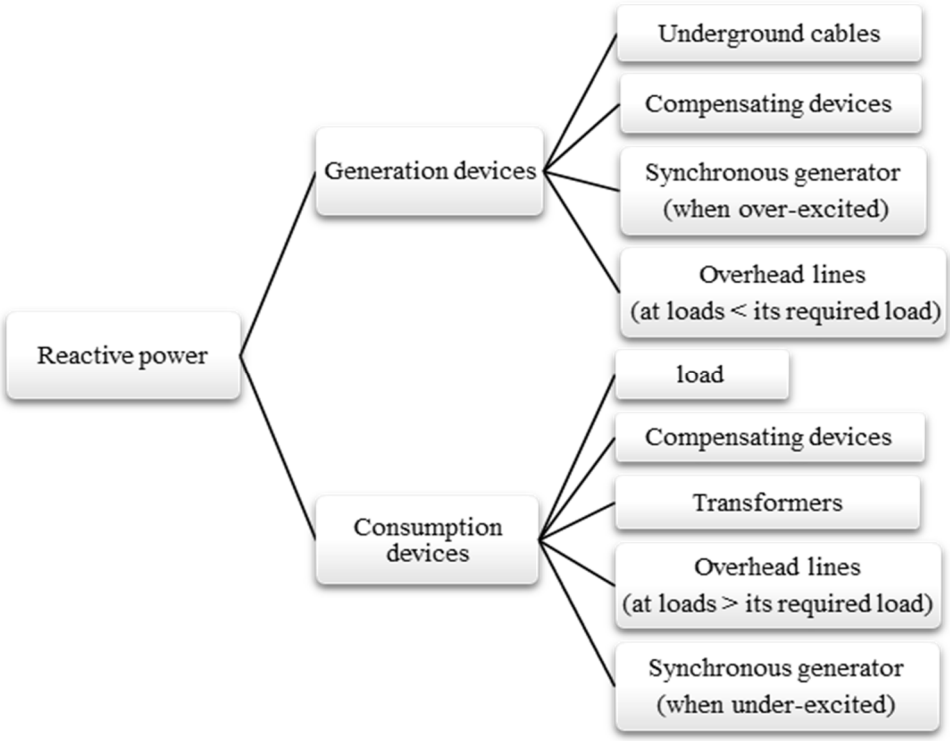

Figure 6-12 The absorption and generation of reactive power.

6.9 Power factor (PF)

For an electrical appliance, which operates using an AC supply, e.g., a fan or a refrigerator, its specification is usually given in wattage, voltage, and PF. The voltage rating of an appliance represents its nominal operating voltage, the wattage rating shows the amount of power required for the appliance when it is switched on, and PF is usually a value between 0.6 and 1. Electrical appliances usually consume power while they in operation. A large portion of the used power is converted to useful energy for its intended activity, while the remaining portion is wasted as heat. As reported in a previous study [25], PF is defined as the true power (kW) divided by the apparent power (KVA) consumed by an AC electrical appliance. A PF value of unity is the ideal PF, but in most cases, PF is less than unity. Once it is less than 1, the implication is that more power will be required to accomplish the task. When PF is less than 1, the remaining fraction accounts for the reactive power.

PF measures the fraction of electrical power that is actually useful in performing tasks. Mathematically, there are two ways of achieving PF:

- PF can be calculated using the following expression:

$PF = \cos\theta =$ the cosine of the angle between real power and apparent power.

- PF can also be calculated as follows:

$$PF = \left(\frac{Real\_power(KW)}{Apparent\_Power(KVA)} \right)$$

Recalling equation (2),

$S = P + JQ$, to find the magnitude of apparent power, equation (2) becomes

$$|S|^2 = P^2 + Q^2, \text{ where } |S| = \sqrt{P^2 + Q^2} \quad (3)$$

$$PF = \cos\theta = \left(\frac{P(KW)}{|S|(KVA)} \right). \quad (4)$$

A network with a PF value of unity is an efficient network. This means there is no reactive power and that the power is ideal for transmission, but it is practically unattainable. There are multiple variations in PF because the several types of electrical devices that supply or absorb reactive power are connected to a microgrid [26]. Poor PF in a network indicates a high presence of inductive loads e.g., air-conditioning units and AC motors on the network, hence, requires a high demand for reactive power. The PF in an AC system can be unity, lagging or leading depending on the electrical devices in the network.

Unity PF: This implies that the current and voltage are in phase, which means the angle between the current and voltage, in this case, is zero. As a result, the cosine of the angle or PF is unity. A load with a unity PF means that the load is purely resistive.

Lagging PF: This is the case with an inductive load in which, the current vector lags the voltage vector and the PF varies with the angle of the lead. Because PF is inductive, its sign is positive.

Leading PF: A network PF is referred to as a leading PF when the current leads the voltage, and this is the case with capacitive loads in which PF varies with the angle of lead. Because PF is capacitive, its sign is negative.

6.9.1 PF correction

This refers to a technology that helps to bring the PF of an AC power system close to unity by providing the reactive power of the opposite sign. This involves introducing capacitors and inductors that can help to neutralize the capacitive and inductive effects on the system load, respectively. For instance, a motor-load inductive effect may be canceled by connecting a capacitor locally. Similarly, the effect of a capacitive load may be offset by connecting an

inductor (reactor) for PF correction [25] [26].

6.9.2 Usefulness of PF correction

As reported in previous research [26], PF correction has several benefits as shown in figure 6-13.

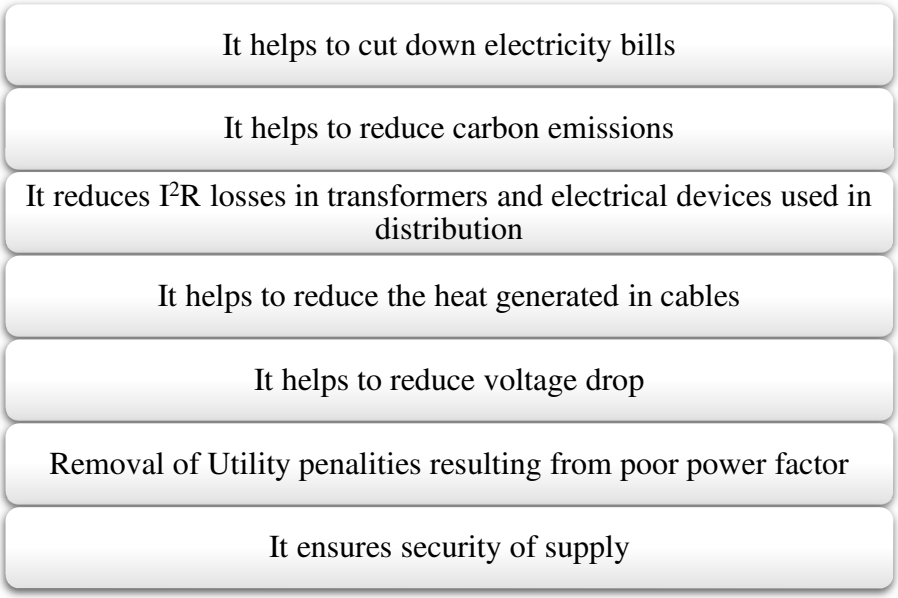

Figure 6-13 Benefits of power factor (PF) correction.

6.9.3 Summary

Voltage control ancillary services for low-voltage distributed DG should be allowed and the possibility of creating a microgrid ancillary services market should be explored. The limitations concerning the participation of low voltage DG in the ancillary services were explored and useful recommendations to suggest a solution for addressing these challenges were provided. Future work will involve the design of market models for microgrid ancillary services.

6.10 References

[1] S. Qin, "Quantification of Ancillary Service Provision by Microgrid," McGill University Montreal, Canada, 2015.

[2] M. Faiella, T. Hennig, F. Iwes, N. A. Cutululis, and F. Van Hulle, "Capabilities and

costs for ancillary services provision by wind power plants," 2013.

[3] J. M. Bert, "Ancillary services : Technical and Commercial Insights," *Orthop. Clin. North Am.*, vol. 39, no. 1, p. 1–4, v, 2008.

[4] "Drivers of Ancillary Services in India." [Online]. Available: https://www.slideshare.net/IPPAI/drivers-of-ancillary-servicesinindia?from_action=save. [Accessed: 05-Jul-2018].

[5] I. Luís and A. Nascimento, "Voltage and Reactive Power Control in Autonomous Microgrids," 2017.

[6] K. Abo-Al-Ez, X. Xia, and J. Zhang, "Smart interconnection of a PV/wind DG Micro Grid with the utility distribution network," in *2012 Proceedings of the 9th Industrial and Commercial Use of Energy Conference*, 2012, pp. 243–250.

[7] A.. Fallis, "Microgrid: Architectures and Control - Front Matter," *J. Chem. Inf. Model.*, vol. 53, no. 9, pp. 1689–1699, 2013.

[8] A. G. Madureira and J. A. Peças Lopes, "Ancillary services market framework for voltage control in distribution networks with microgrids," *Electr. Power Syst. Res.*, vol. 86, no. 5, pp. 1–7, 2012.

[9] M. A. Hossain, H. R. Pota, W. Issa, and M. J. Hossain, "Overview of AC microgrid controls with inverter-interfaced generations," *Energies*, vol. 10, no. 9, pp. 1–27, 2017.

[10] B. Starfield, "State of the Art in Research on Equity in Health," *J. Health Polit. Policy Law*, vol. 31, no. 1, pp. 11–32, 2006.

[11] "Introduction to Distributed Generation." [Online]. Available: http://www.dg.history.vt.edu/ch1/introduction.html. [Accessed: 24-Oct-2017].

[12] D. Porter, G. Strbac, and J. Mutale, "Ancillary service provision from distributed generation," *Electr. Distrib. 2005. CIRED 2005. 18th Int. Conf. Exhib.*, no. 4, pp. 1–4, 2005.

[13] J. J. Justo, F. Mwasilu, J. Lee, and J.-W. Jung, "AC-microgrids versus DC-microgrids with distributed energy resources: A review," *Renew. Sustain. Energy Rev.*, vol. 24, no. April, pp. 387–405, 2013.

[14] F. Sulla, J. Björnstedt, and O. Samuelsson, "Distributed Generation with Voltage

Control Capability in the Low Voltage Network," in *International Conference on Renewable Energies and Power Quality (ICREPQ'10)*, 2010, pp. 206–211.

[15] "Benefits of Distributed Generation." [Online]. Available: http://www.dg.history.vt.edu/ch1/benefits.html. [Accessed: 05-Jul-2018].

[16] J. Merino, G. Inés, E. Turienzo, M. Carlos, I. Cobelo, M. Andrei, S. Hanne, V. Koen, H. Enrique, Rivero Puente Seppo, K. Pekka, E. Corentin, N. Helistö, D. Siface, and A. Zani, "Ancillary service provision by RES and DSM connected at distribution level in the future power system," 2016.

[17] B. Kirby and E. Hirst, "Ancillary Service Details : Voltage Control," 1997.

[18] Kundur P, *Power System Stability and Control*, 1st edition. McGraw-Hill: New York, NY, USA., 1994.

[19] I. O. Akwukwaegbu and O. G. Ibe, "Concepts of Reactive Power Control and Voltage Stability Methods in Power System Network," *IOSR J. Comput. Eng.*, vol. 11, no. 2, pp. 15–25, 2013.

[20] T. Xu and P. C. Taylor, "Voltage Control Techniques for Electrical Distribution Networks Including Distributed Generation," in *17th IFAC World Congress - the International Federation of Automatic Control Conference, Seoul, Korea, July 6-11,* 2008, pp. 11967–11971.

[21] R. Fetea and A. Petroianu, "Can the reactive power be used?," *PowerCon 2000 - 2000 Int. Conf. Power Syst. Technol. Proc.*, vol. 3, no. 2, pp. 1251–1255, 2000.

[22] A. Kumar and S. Vyas, "Reactive Power Control in Electrical Power Transmission System," *Int. J. Eng. Trends Technol.*, vol. 4, no. 5, pp. 1707–1717, 2013.

[23] a. J. Von Appen, B. C. Marnay, C. M. Stadler, D. I. Momber, E. D. Klapp, and F. A. Von Scheven, "Assessment of the economic potential of microgrids for reactive power supply," *8th Int. Conf. Power Electron. - ECCE Asia*, no. June, pp. 809–816, 2011.

[24] P. Sauer, "Reactive power and voltage control issues in electric power systems," ... *Math. Restructured Electr. Power Syst.*, vol. Chapter 2, pp. 11–24, 2005.

[25] J. Ware, "Power Factor Correction," *IEE Wiring Matters 18*, vol. 18, pp. 22–24, 2006.

[26] A. Kouzou, *Power Factor Correction Circuits*, 4th ed. Elsevier Inc., 2018.

Chapter 7:

Conclusions and future works

This thesis carried out a research on how to develop a new strategy to eradicate inadequate power supply in areas faced with such challenges and to make the PV module more efficient in terms of energy yield. The PV module efficiency was enhanced, a hybrid PV/wind/diesel generator system also designed to provide power to 120 residential apartments. Finally, recommendations were made to support the participation of distributed generation in the provision of ancillary services. The idea is to provide adequate power to a location, which faces the challenge of the inadequate power supply with the renewable energy resources from sunlight and wind present in the location. The location experiences long periods of intense sunlight, which makes the energy generation from the sun very promising hence, it is a necessity to improve the efficiency of the PV module in order to increase the amount of power generated from the sun with the help of the PV module.

7.1 General conclusions

Power shortage appears to be the bane of industrial, social and economic development in Nigeria and countries faced with similar challenges. The use of renewable energy solely to provide power in those areas, faced with shortage power supply, is the way out of this challenge. The thesis intends to revolutionize the electricity sector in Nigeria, entire Africa and other nations faced with a lack of adequate power by embracing the use of renewable energy to provide electricity in every location.

The first part of this thesis (chapter 2) concentrated on reviewing the state of the art of solar energy technologies, cooling techniques and hybrid energy systems. It talks about the different classifications of hybrid energy systems and their features, energy storage systems and their classifications, PV module efficiency and the various factors that affect the efficiency of a PV module. Conversely, it describes the wind energy system and the permanent magnet synchronous generator driven wind turbines. The general conclusion of this review is that the efficiency of the PV module is affected by several factors and that temperature appears to be

the major factor, which affects the efficiency of PV module in this part of Nigeria and other countries with similar weather conditions.

Chapter 3 of this thesis presented energy generation form different energy sources in order to provide electricity to the research location, which consists of 120 residential apartments. The wind energy and solar energy resources for the location were gathered from the Nigerian Meteorological Agency, NIMET; this data, as well as the load design, were used as input to the HOMER simulator software. The electrical load design of 120 residential apartments carried out, shows the result of the total energy capacity of the hybrid energy system, the total amount of load on demand by the system. The sizing of the hybrid energy system carried out using HOMER software simulation shows that the renewable energy in the research location has the potential to provide adequate power to the 120 residential apartments with room for expansion. The chapter helps to create more awareness that energy can be generated from the renewable energy resources in the location to provide adequate power to the location. The excess energy generated from the hybrid energy system in this research work, which is channelled to the dump load can be used to generate ice blocks in order to provide cooling to the PV module, however.

In chapter 4 of this thesis, experiments to improve the efficiency and power output of the PV module were carried out. A novel approach to provide cooling to the PV module when mounted in a location, which experiences a long period of intense sunlight is presented. The thesis provides a new knowledge in increasing the power output obtained from the PV module via cooling. The investigation of the cooling of PV module with an Aluminium heat sink attached to the rear of the PV module carried out alongside water-cooling with the PV module mounted at a height of 137cm above the ground to aid air-cooling showed that the efficiency of the PV module, as well as the power output, recorded an increase. This increase in efficiency and the power output form the basis for the use of the multi-concept cooling technique for heat extraction from the PV module in order to make energy generation via the PV module a more useful and reliable means of energy generation.
The results of the experiments show that:

- The multi-concept cooling technique increased the power output of the PV module by 20.96W at a derating factor of 80%
- The technique also recorded above 3% increase in the efficiency of the PV module.

Furthermore, another investigation was carried out to ascertain the amount of power output that can be generated from the PV module by reducing the temperature of the module surface to 20°C at a derating factor of 95% unlike that done at a derating factor of 80%. The 250W PV module generated an output power of 262.4W at a derating factor of 95% after reducing the temperature of the module surface to 20°C. More effort was made on the PV since the research location experiences more sunlight that wind energy resources.

The concept of cooling has new features and advantages; the new features are

- Cooling is achieved via air-cooling, water-cooling and the attachment of Aluminium heat sink at the rear of the module, unlike the single concept of cooling embraced by past researchers.
- Ice blocks are added to the cooling water to reduce its temperature and cooling is applied at the surface of the module as well as the rear of the module.

Conversely, the advantages are as follows:

- Maintaining the temperature of the module surface at 20°C ensures the module yields a steady increase in power output.
- At an irradiance of 1000w/m^2, more power than the module rated capacity is achieved.
- In the absence of water-cooling, a certain amount of cooling can be achieved.

Chapter 5 deals with the modelling and simulation of the hybrid energy system. The wind speed at the location is low as such, the simulation of the MATLAB model of the Hybrid PV/wind/diesel energy was done with the wind speed set at 6.1m/s and the module temperature set at a temperature of 20°C. This made the PV system to contribute more power to the hybrid energy system, thereby given a boost to the generated power. The hybrid system architecture selected from the result of the HOMER software simulator was discussed in this chapter. The result shows that with enhanced PV module efficiency as demonstrated by this research, the PV can serve as an efficient source of energy generation, as even in the peak of intense sunlight, it will generate high amount power.

Chapter 6 of this thesis throws light on the importance of the creation of a market for microgrid ancillary services and offered useful recommendations. The emerging trend indicates the need for the provision of ancillary services from renewable energy sources and the current ancillary services market is favoured by large power plants alone. The factors limiting the participation of renewable energy resources or distributed energy resources in the provision of ancillary

services were considered. The need and basis for the creation of a market for microgrid ancillary services were explored, recommendations were made to support distributed energy resources to participate in the market for ancillary services and these are:

- The procurement process should be enhanced and additional power sources activated.
- Renewable energy sources should be allowed to participate in the provision of ancillary services whenever technically possible.
- The combination of smaller energy units should be engaged and not only large-scale power units
- The gradient should be expressed based on the percentage of the maximum power output and not in absolute values, e.g., 10 MW.
- Harmonization of the rules for balancing and using ancillary services across countries in a geographical region, e.g., Europe, should be conducted.

7.2 Contributions of the thesis

The major contributions of this thesis are:

- Development of a new concept for cooling the PV module as the multi-concept cooling technique ensures that the module experiences cooling at all times. This is so because cooling of the module still takes place even in the absence of water-cooling.
- The system allows the module to continue to provide increased power output even at the peak of sunlight
- Creation of the awareness that individuals who live in regions that experience a long period of sunshine has an opportunity to utilize energy from PV module, as their major source of power, provided there is an efficient PV module cooling system in place.
- Recommendations for the participation of distributed generation in the provision of ancillary services
- Application of Voltage control ancillary services to low voltage distributed generation.

7.3 Future works

The research work in this thesis contributes to the impact of energy efficiency in power generation, with improved efficiency of the PV module, power generation from PV module as a single source of energy or as a part of a hybrid energy system as in this case is made more reliable, efficient and useful. This thesis has fulfilled all its initially defined research aims. Nevertheless, there are several drawbacks to energy generation

from Photovoltaic module used alone or in a hybrid energy system, hence, further research is required to develop the established methods and ideas.

- The pipe extension in the designed Aluminium heat sink was fashioned to extract heat from the rear of the panel by allowing the passage of water through it, but it was not utilized in the experiment. Further research can be done on how to extract more heat from the PV module via the pipe extension in the Aluminium heat sink.
- A multi-concept cooling technique, which embraces forced air convection at the rear of the PV module using a fan, should be considered in future, to remove the distributed heat energy and further improve the efficiency of the PV module for better performance.
- Water spraying of the PV module was done manually, future research can include a design of an automatic water spraying system, to ensure the timely spraying of the PV module, conversely the water sprayed on the panel can be connected to a reservoir as a source of hot water
- The role of the Aluminium heat sink is to extract heat from the rear of the PV module, a further investigation could include the use of a more efficient thermal grease at the point of contact between the Aluminium heat sink and the rear of the PV module. This is important to increase the amount of heat extracted from the rear of the PV module.
- The Al 300 six-channel data logger used for temperature reading was monotonous as it was not connected to a computer system with readings recorded simultaneously. Further investigation could include the use of a better temperature sensing equipment connected to a computer with the ability to record the temperature readings simultaneously for an instant and more accurate results
- Further research work is required for the creation of business models for microgrid ancillary services market as in the energy market presently, those who are able to negotiate the prices of energy and related conditions in the supply of electricity are large consumers. Hence, consumers occupy a passive

position and are unable to take advantage of the current liberalization of the energy market.

Appendix A:

Modelling of hybrid PV/wind/diesel generator system

This chapter consists of the model composition of the hybrid PV/wind/diesel energy system and the modelling of the individual units that make up the model, such as the modelling of the solar energy system, battery storage, wind energy system, diesel generator energy system, etc.

From the system architecture in table 3.6 of chapter three shown below:

60kW PV, 50kW Wind turbine, 50kW Diesel Gen, 480 Vision 6FM200D battery, 44kW Inverter & Rectifier					
Production	**kWh/yr**	**%**	**Consumption**	**kWh/yr**	**%**
PV array	90,638	54	AC Primary load	67160	100
Wind turbine	77,907	46	Total	67160	100
Generator	0	0			
Total	168545	100	Excess Electricity	88581	52.6
			Unmet electrical load	0.00000226	0.0
			Capacity shortage	0.00	0.0
Quantity	**Value**				
Renewable fraction	1.00				

The model configuration of the hybrid energy system requires the followings:

- 60kW PV array, which is made up of a collection of 250W PV modules.
- 50kW diesel generator
- 50kW wind turbine
- 480 Vision 6FM200D battery, which is made up of a string size of 30 with 16 strings in parallel as shown in fig 12.
- 44kW Inverter & Rectifier.

A.1 Modeling of PV module

The Photovoltaic module is a collection of solar cells, and the solar cell can be represented by a simple equivalent circuit as shown in figure A-1.

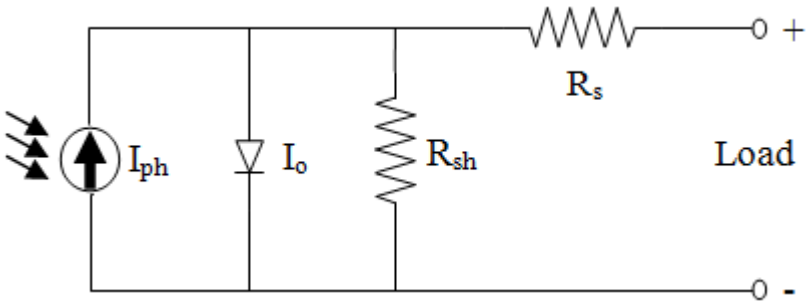

Figure A-1. Equivalent circuit of a solar cell [1]

The equivalent circuit shows that a solar cell is made up of a current source such that a diode and a shunt resistance, R_{sh} is both connected in parallel to the current source while the other resistance, R_S is connected in series with it.

In order to make the analysis simple, the value of $R_{s,}$ which usually is very small and the value of $R_{sh,}$ which usually is very large are both neglected.

A collection of Photovoltaic cells makes up a PV module and a number of Photovoltaic modules can be connected together in series and also in parallel to provide the desired amount of current or voltage.

For PV module modeling, some basic equations are required, and these are:

The photo-current equation of the Photovoltaic module as represented in equation (1)

$$I_{ph} = \{I_{SCrf} + K_i(T - 298)\} * \lambda / 1000 \quad (1)$$

Where I_{ph} is the photocurrent of the module, I_{SCrf} is the short-circuit current of the module at the reference temperature (Rf_{temp}) of 25°C, K_i = 0.0017A, and it represents the short-circuit current temperature coefficient. T is the operating temperature (Op_{temp}) of the module, and **λ=1000**W/m^2, and refers to the illumination of the module [2]

A temperature conversion from Celsius scale to Kelvin is required, both for the reference temperature and the operating temperature.

$$Rf_{tempK} = 273 + 25 \quad (2)$$

$$Op_{tempK} = 273 + T \quad (3)$$

Where Rf_{tempK} is the reference temperature in Kelvin, Rf_{temp} is the reference temperature in degree Celsius, Op_{tempK} is the operating temperature in Kelvin while Op_{temp} is the operating temperature in degree Celsius.

The MATLAB model of the temperature conversion equation is as shown in figure A-2

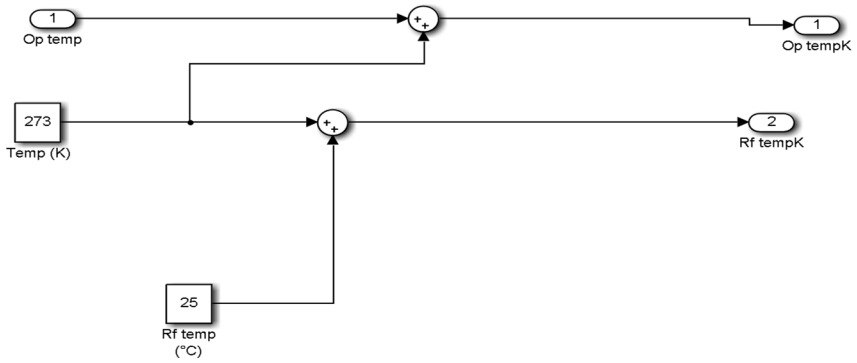

Figure A-2 Temperature conversion from degree Celsius to Kelvin.

The subsystem of the temperature conversion, equation model is as represented in figure A-3

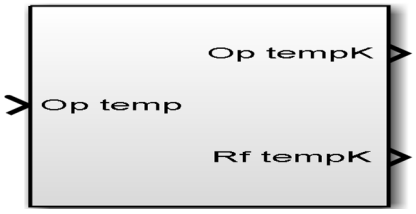

Figure A-3 Temperature conversion subsystem

The Matlab model of the module Photocurrent in equation 1 is as shown in figure A-4

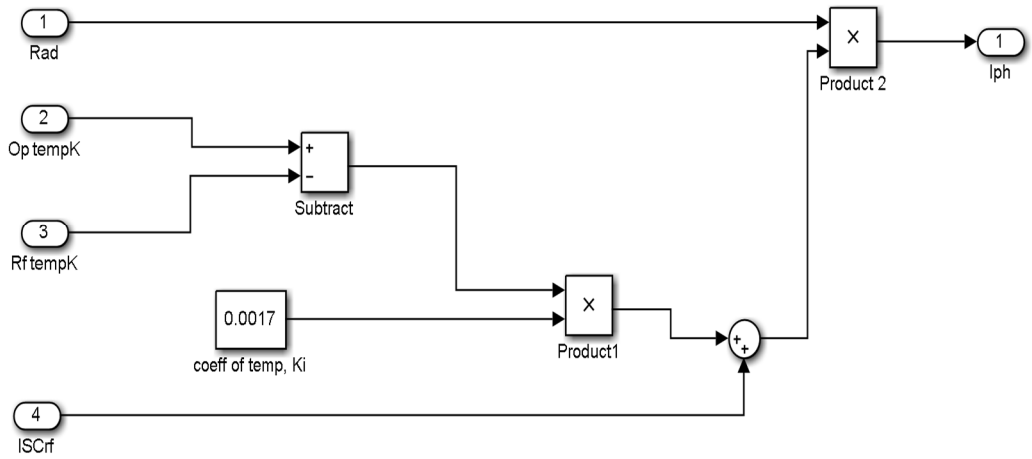

Figure A-4 MATLAB model of the Photocurrent I_{ph} equation

This model uses the following inputs:

Operating temperature of the PV module, Op_{tempK} = 30°C to 75°C

Reference temperature of the PV module, Rf_{tempK} = 25°C

Irradiation/insolation $= \frac{G}{1000} = 1kW/m^2 = 1$ and at the reference temperature, the short-circuit current, I_{SCrf} = 8.63A

The subsystem of figure A-4 is as shown in figure A-5

Figure A.5 Subsystem for Photocurrent equation model

The reverse saturation current of the PV module is given as

$$I_{rvs} = \frac{I_{scrf}}{[\,e\,(\frac{q\,V_{oc}}{N_S\,A\,K\,T})\,-\,1\,]} \tag{4}$$

Where $q = 1.6x10^{-19}C$, stands for the electron charge, V_{oc} is the open-circuit voltage of the module, the ideality factor = B = A = 1.6, the Boltzmann constant, K = 1.3805 x 10^{-23} J/K, N_S refers to the number of cells in series, V_{oc} is the open circuit voltage of the module [2][3].

The model and subsystem of equation (4) are represented in figure A-6 and A-7 respectively.

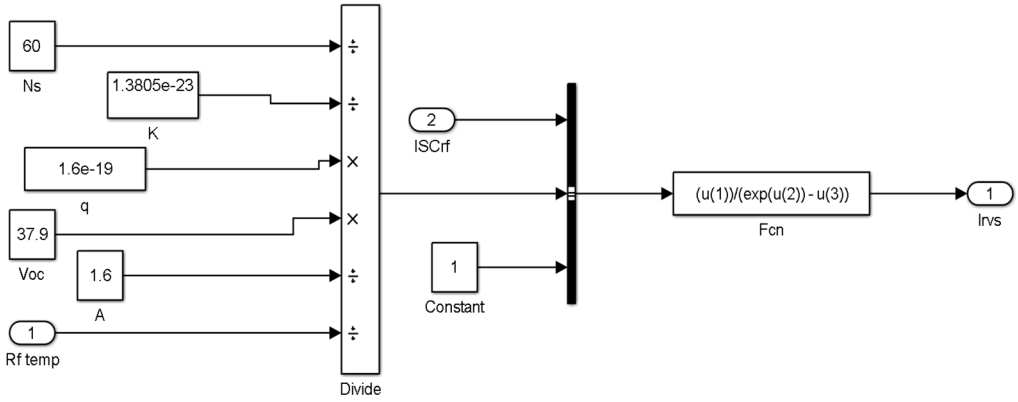

Figure A-6 MATLAB model of reverse saturation current, I_{rvs}.

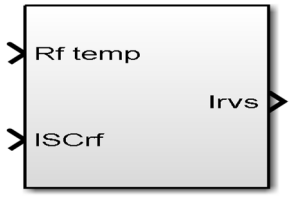

Figure A-7 Subsystem for reverse saturation current equation model

The relationship between the temperature of the solar cell and the saturation current of the module is given in equation (5).

$$I_o = I_{rvs}[\frac{T}{Tr}]^3 \exp[\frac{q * Ego}{B_k}\left\{\frac{1}{Tr} - \frac{1}{T}\right\}] \quad (5)$$

Where I_0 is the saturation current of the module, T and Tr are the operating temperatures and the reference temperature (25℃) of the module respectively, E_{go} is the value of the band gap of silicon. Equation (5) can be modeled as shown in figure A-8. Conversely, its subsystem is represented in figure A-9.

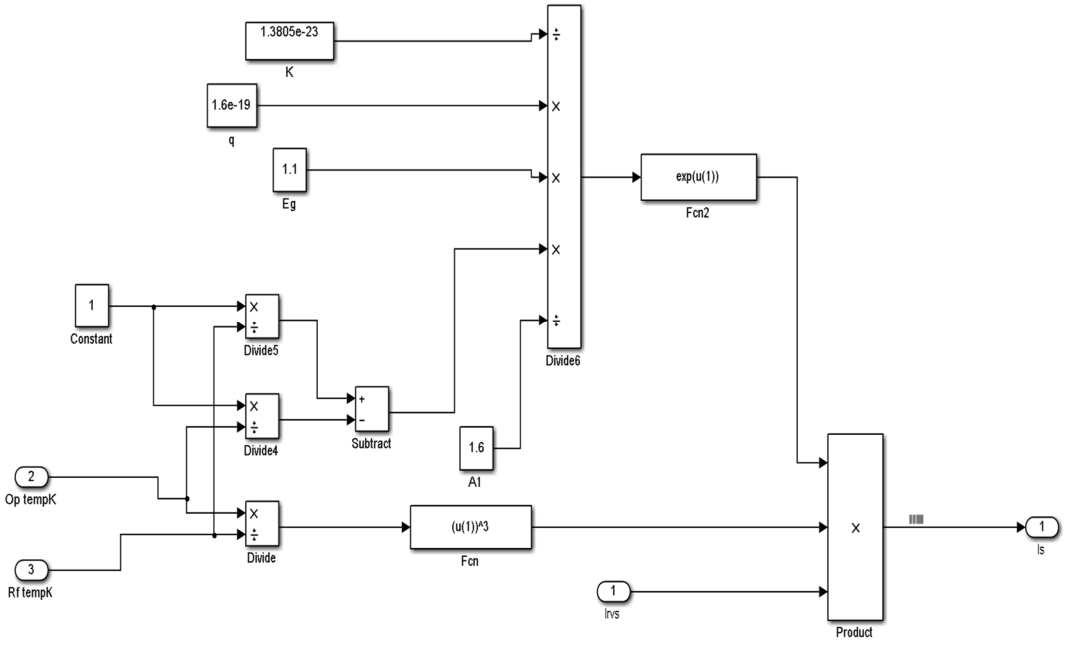

Figure A-8 Model of the saturation current equation.

Figure A-9 Subsystem of the saturation current equation model.

The Photovoltaic module output current, I_{PV} is given as

$$I_{pv} = N_p * I_{pv} - N_p * I_o[\exp\left\{\frac{q*(V_{pv}+I_{pv}R_s}{N_S AKT}\right\} - 1 \quad (6)$$

Since this is for a single Photovoltaic module, the number of cells in parallel, $N_P = 1$ and also since the Photovoltaic module is made of 60 cells in series $N_S = 60$, the open circuit voltage, $V_{OC} = V_{PV}$.

Equation (6) is modeled as figure A-10, and its subsystem is represented as figure A-11.

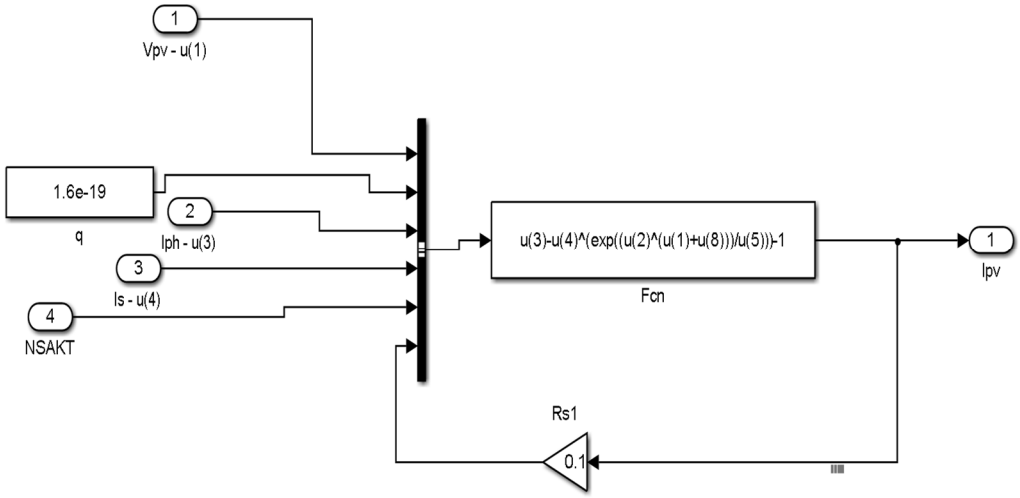

Figure A-10. Photovoltaic module output current equation model

This model implements the function in equation (6) and the function equation used is represented as

I_{PV} = u(3)-u(4)*(exp((u(2)*(u(1)+u(8)))/u(5)))-1 (7)

Figure A-11. The subsystem of figure A-10.

N_SAKT, which appears in equation (6) as the exponential function denominator utilizes the number of cells in series, operating temperature of the module in Kelvin, and other parameters to produce the model of figure A-12

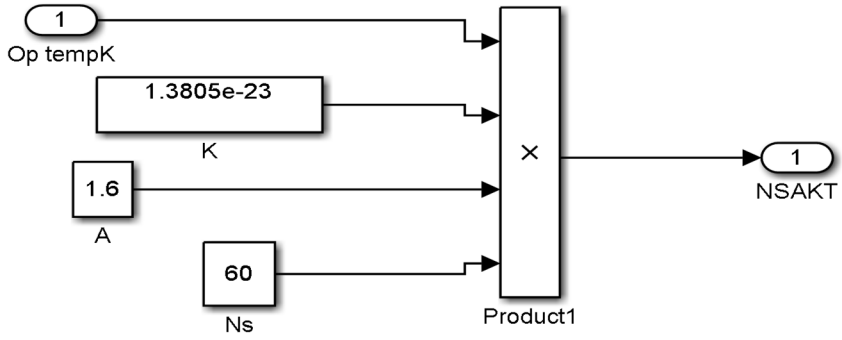

Figure A-12. Model of N_SAKT

The subsystem of figure A-12 is represented as figure A-13.

Figure A-13. Subsystem of N_SAKT

The connection of the different models and its final subsystem is as shown figure A-14 and A-15 respectively.

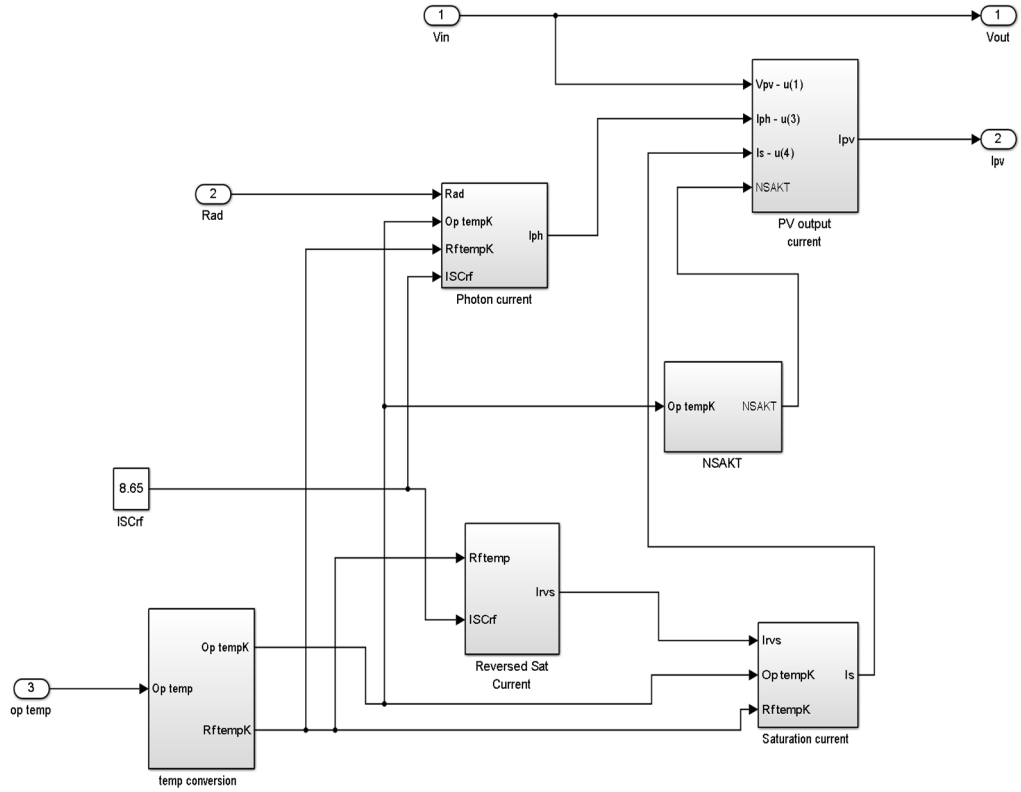

Figure A-14. The connections of all the models

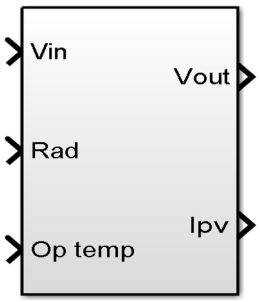

Figure A-15. PV module final subsystem.

The complete model is as shown in figure A-16 where the workspace was included to aid the measurement of P_{PV}, $V_{PV,}$ and I_{PV}.

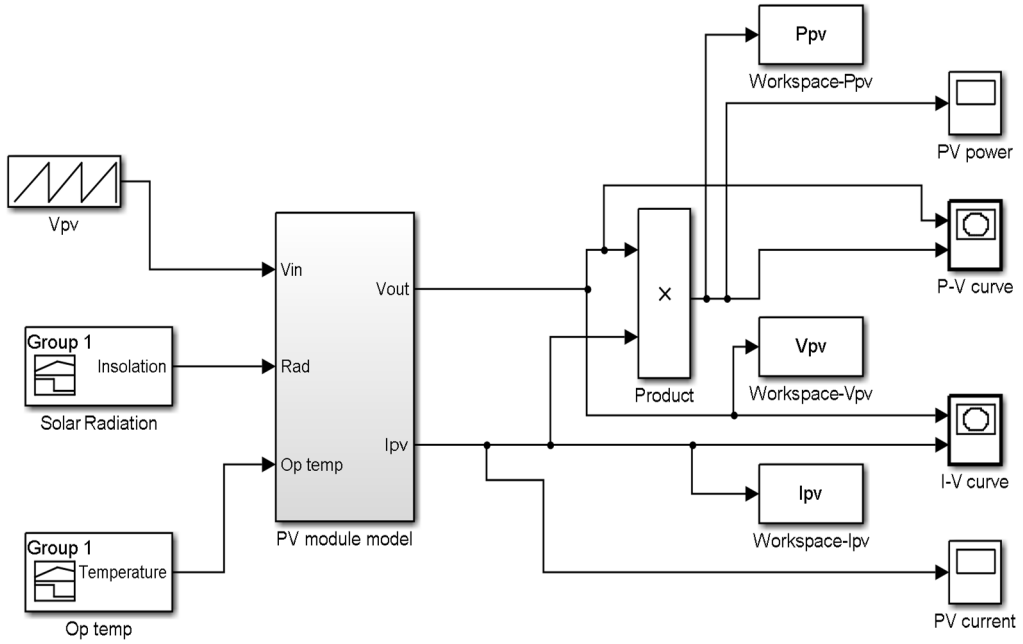

Figure A-16. A complete model of the Photovoltaic module.

The complete Photovoltaic module model above takes the module voltage, operating temperature (in Celsius) and irradiation as input in order to give out the output voltage, V_{PV} and output current I_{PV}.

Suntech 250W solar PV Module with the specifications as shown in table 4.1 of chapter 4 was used for the purpose of this project.

Maximum Power at STC Pmax	**250 W**
Optimum operating voltage (Vmp)	**30.7V**
Optimum operating current (Imp)	**8.15A**
Operating circuit voltage (Voc)	**37.4**
Short circuit current (Isc)	**8.63A**
Operating module temperature	**-40°C to +85°C**
Temperature coefficient of Pmax	**-0.44%/°C**
Temperature coefficient of Voc	**-0.34%/°C**
Temperature coefficient of Isc	**-0.060%/°C**
Solar cell	**Monocrystalline silicon 156x156mm(6 inches)**
No of cells	**60 (6x10)**
Dimensions	**1640 x992 x35mm (64.6 x 39.1 x1.4 inches)**

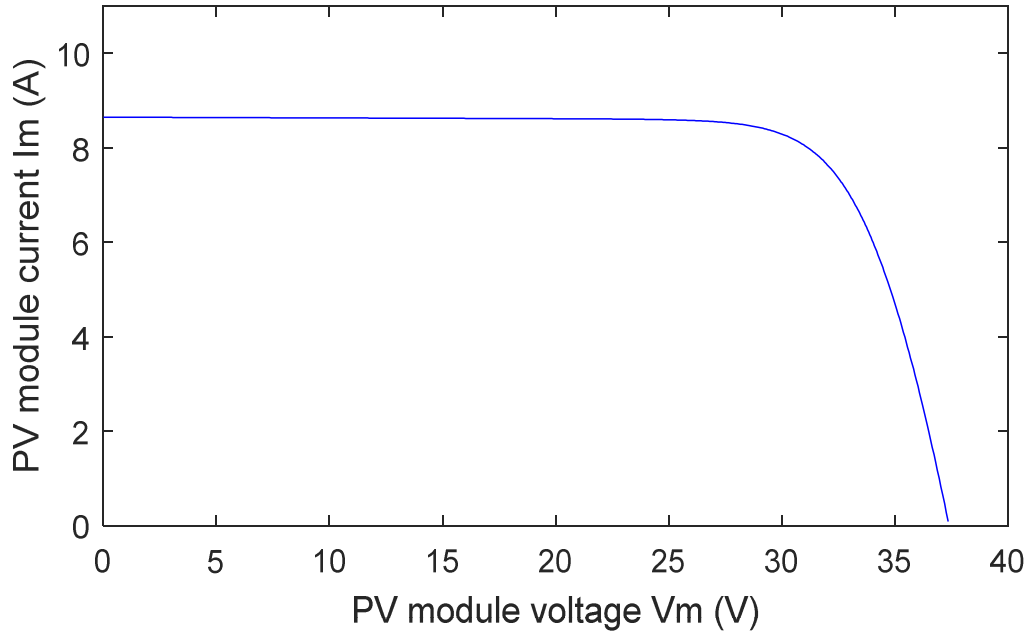

Figure A-17. I-V curve of the PV module

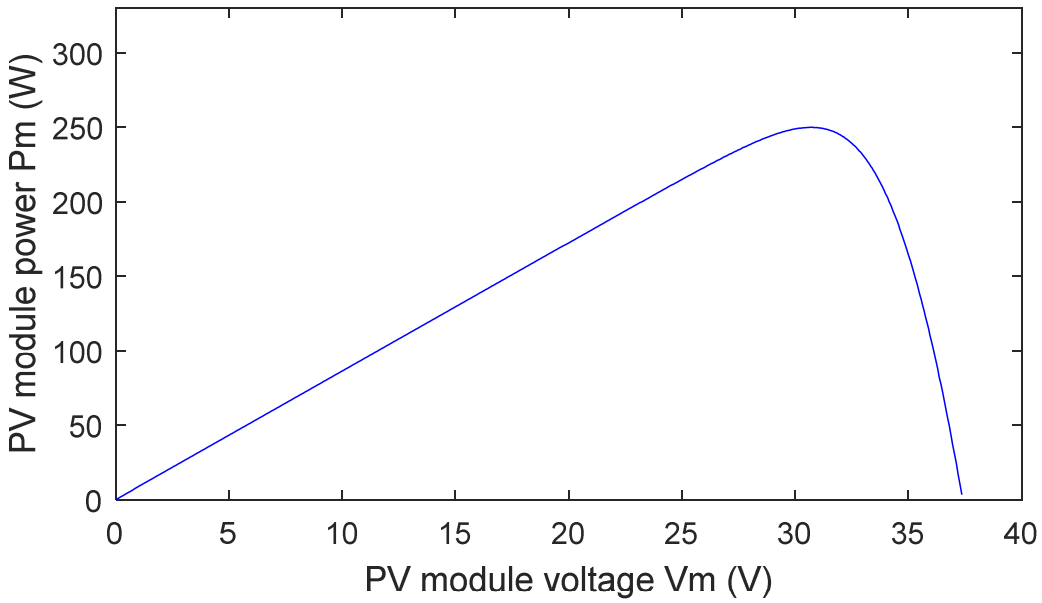

Figure A-18. The P-V curve of the PV module

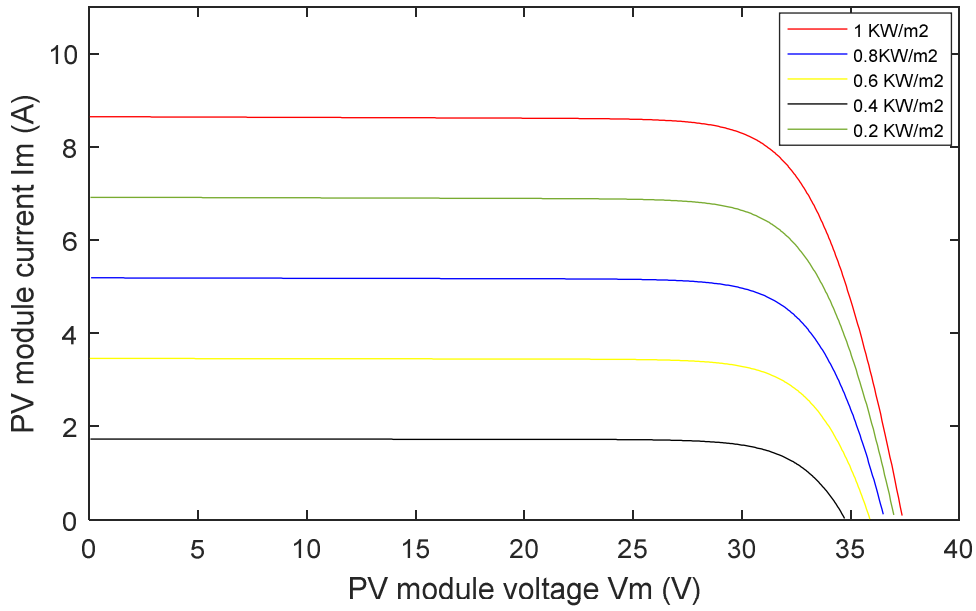

Figure A-19. I-V curve of the PV module at a constant temperature of 25°C and different irradiation

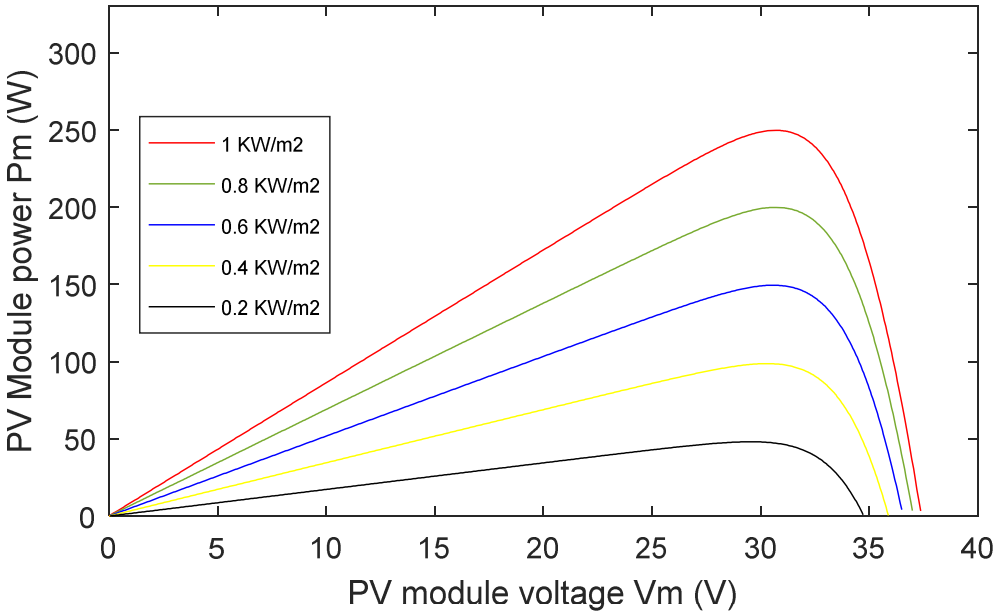

Figure A-20. The P-V curve of the PV module at a constant temperature of 25°C and different irradiation

Figure A-19 and A-20 show the I-V and P-V curve, respectively at a constant temperature of 25°C, but at different irradiation. As the sun begins to rise in the morning, the solar irradiation also begins to rise and as a result, the output voltage rises, the output current also rises

consequently, the output power rises. The two curves also show clearly that the short circuit current, Isc = 8.63A, and the actual capacity of the PV module, which is 250W, can only be obtained at an Irradiance of 1000W.

For a Photovoltaic module, the peak value of the operating power, usually referred to as its maximum power can be represented as:

$$P = I_{sc}.V_{oc}.ff \tag{8}$$

Where ff represents the fill factor, for a single- crystal silicon cell, the value of ff is 0.7 [4].

The temperature of the PV module has an effect on the voltage, and current generated by the module, the rise, and fall of the module temperature is a function of the operating temperature of the location, and this temperature of the location also has an effect on the module efficiency and can be related by equation 9 [5]

$$P_{mp} = V_{mp}.\mathrm{I}_{mp} = I_{sc}.V_{oc}.ff \tag{9}$$

The PV array Voc can also be expressed as shown below.

PV Voc = Rated Voc × {1 + [(Min. Temp. ºC - 25ºC) × Module Coefficient %/ºC]} × No of modules per Series String [6]

This capacity of the PV array for this PV system is 60kW and it is made of 250 W modules, modules are usually connected in series to increase the voltage and they can are also connected in parallel in order to increase the current [7]

The sizing of this hybrid system was carried out using the HOMER software simulator; the HOMER software simulator expresses the power output from the PV module/array using the expression in equation 10

$$P_{pv} = Y_{pv}.f_{pv}\left\{\frac{G_T}{G_{T,STC}}\right\}[1+\alpha_p(T_c - T_{c,STC}] \tag{10}$$

Where

Y_{PV} is the rated capacity of the PV array, which implies its output power under standard test conditions (kW)

f_{pv} is the PV derating factor (%),

G_T is the solar radiation incident on the PV array in the current time step (kW/m^2)

$G_{T,STC}$ is the incident radiation at Standard Test Conditions (1Km/m^2)

$\propto_P$ is the temperature coefficient of power (%/°C)

T_C is the PV cell temperature in the current time step (°C)

$T_{C,STC}$ is the PV cell temperature under standard test conditions (25°C)

Equation 10 can be modeled in MATLAB as shown in figure A-21

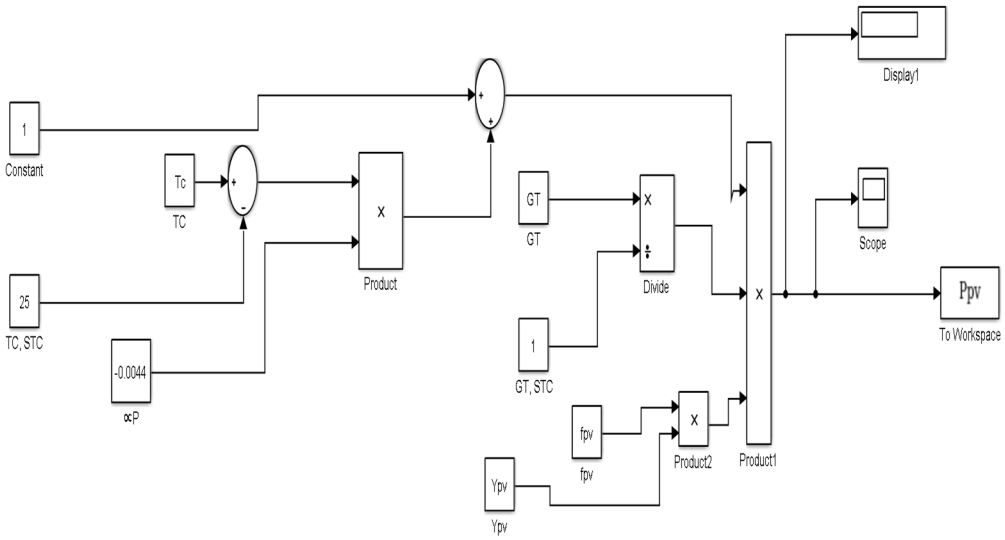

Figure A-21. MATLAB model of equation 10

The efficiency of the PV module can also be calculated using the HOMER software expression for efficiency as given in equation 11

$$\eta_{mp,STC} = Y_{pv} / (A_{pv}.G_{T,STC}) \quad (11)$$

Where:

$\eta_{mp,\,STC}$ represents is the efficiency of the PV module under standard test conditions [%]

Y_{PV} is the rated power output of the PV module under standard test conditions [kW]

A_{PV} is the surface area of the PV module [m2]

$G_{T,\,STC}$ is the radiation at standard test conditions [1 kW/m2]

From equation 11,

$$A_{PV}\ x\ \eta_{mp,STC} = \left(Y_{PV}\right) / \left(\ G_{T,\,STC}\right)$$

By substituting for (Ypv)/($G_{T,\,STC}$) in equation 10, the PV module efficiency is represented as

$$\eta_{mp} = \frac{P_{pv}}{(A_{pv}.f_{pv}.G_T)[1+\alpha_p(T_c - T_{c,STC})]} \quad (12)$$

The MATLAB model of equation 12 is represented as shown in figure A-22.

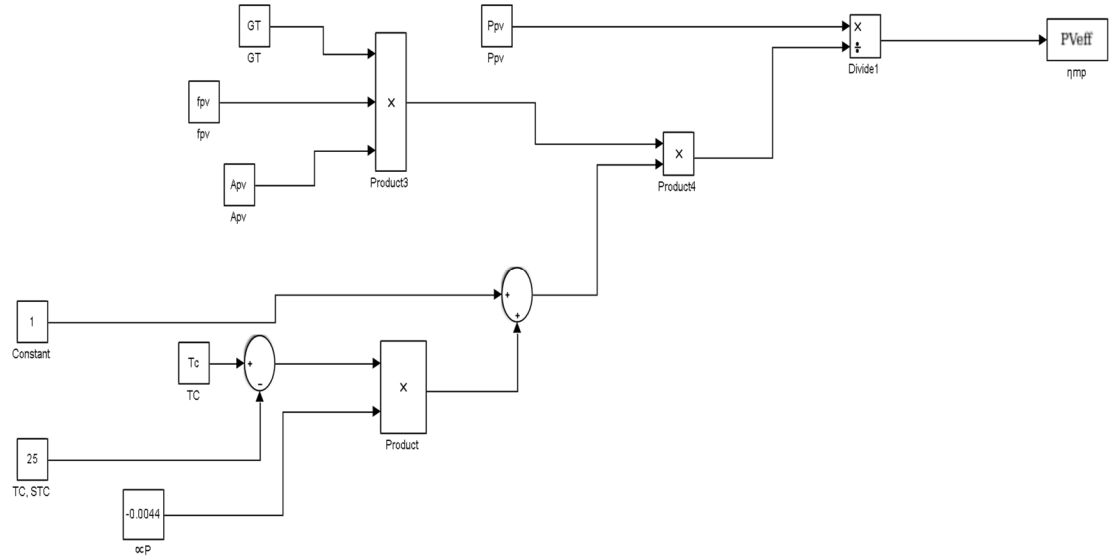

Figure A-22. MATLAB model of equation 13.

A.1.1 Maximum power point, MPPT charge controller

This a charge controller, which uses the principles of maximum power point tracking to extract maximum power from the system. This is because the PV system experiences a lot of loss in power, which may be in the form of heat energy, etc. and as a result, it is important to extract the maximum amount of power possible from the system. The basic functions of the MPPT charge controller are as shown in figure A-23

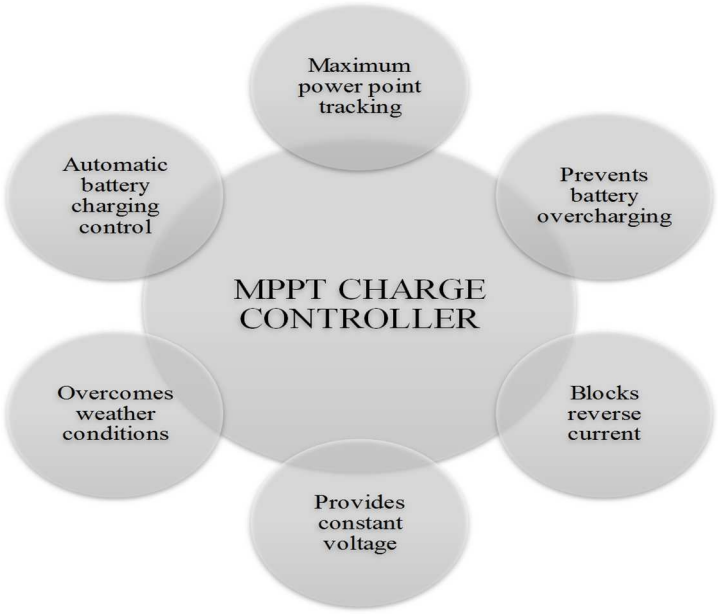

Figure A-23. Functions of the MPPT charge controller.

The maximum power point refers to the point on the PV power curve where maximum power is achieved at varying operating conditions. The relationship between the maximum power voltage, V_{mp} and the open circuit voltage, V_{oc} of the module is as given in equation (13)

$$V_{mp} \approx 0.8 * V_{oc} \quad (13)$$

Conversely, the relationship between the maximum power current, Imp and the short circuit current, Isc of the PV is given by equation (14) [8].

$$I_{mp} = 0.8 * I_{sc} \quad (14)$$

The importance of the MPPT charge controller is as shown in figure A-24.

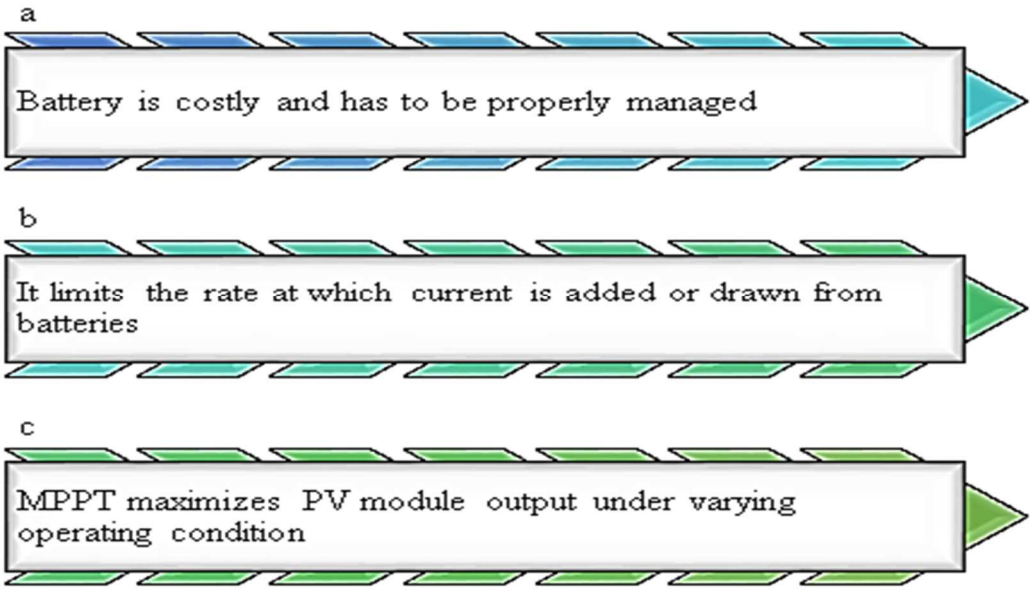

Figure A-24. Importance of MPPT charge controller

The maximum power point tracking device helps to increase the amount of energy conveyed to the system from the PV module, it ensures the output voltage from the panel is adjusted in order that the load is supplied with the maximum energy from the PV module. It comprises of three main components namely, control system, tracking component and the switch-mode dc-dc converter. The entire supply is managed by the switch-mode converter as it ensures that the energy acquired, and stored in the form of magnetic energy are given out at different potential levels. By ensuring that the MMPT switch-mode is set to serve either as a boost or buck converter, voltage converters are able to provide fixed input current or voltage that correspond to the system maximum power point, thereby matching the output resistance with the battery. In order to achieve, the mechanism above, a controller is required to monitor the Photovoltaic device to ensure it operates at its maximum power point, this is achieved via tracking of the MPPT [9].

The controller ensures the current and voltage from the PV module are measured continuously and compared with certain threshold values so as to implement either power feedback control or voltage controlled method.

The maximum power point of a PV module can be assessed using any of the several techniques of maximum power techniques as in [10] is as shown in figure A-25.

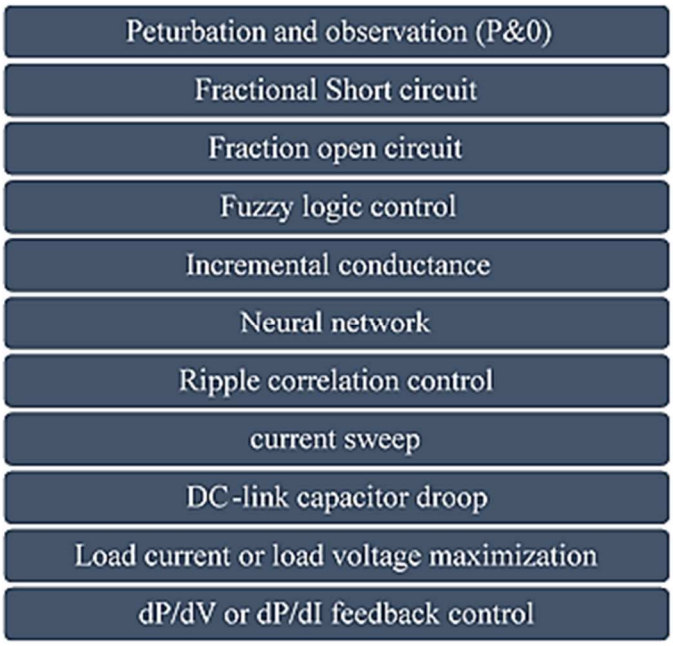

Figure A-25. PV module's maximum power point techniques

Among the numerous methods mentioned above, this research work adopted the perturbation and observation method also referred to as the hill climbing method.

A.1.2 Perturbation and observation (P&O) method.

The principle adopted by this method is to adjust the PV module operating voltage or current until maximum power is obtained. The tracker operates by decrementing or incrementing the PV module voltage and only voltage sensor is used to sense the PV voltage. The principle involves shifting the operating point of the solar module in the direction that power increase. A perturbation on the power converter's duty cycle means perturbing the DC link voltage between the converter and the PV module. The sign of the last power increase and that of the perturbation carried out last is very important as they help to determine the nature of the next perturbation. If a shift in the operating point results in an increase in power, the perturbation is maintained in that direction and if it results in a decrease in power, then the direction of perturbation changes in the opposite direction [11].

An algorithm for the perturbation and observe method is as shown in figure A-26.

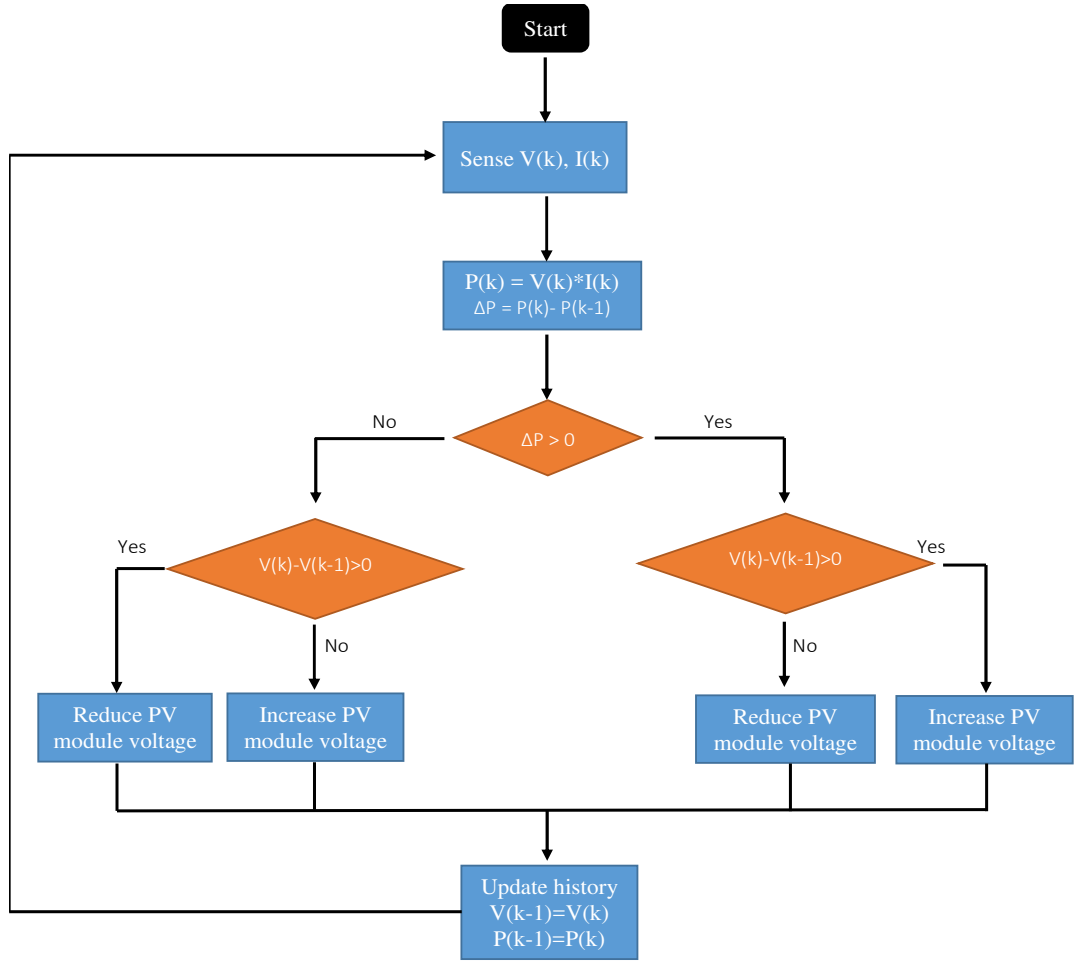

Figure A-26. Algorithm for Perturbation and observation method

A.2 Modelling of the battery

The battery is very important in this project and this is because the solar energy system requires the battery for energy storage. The basic use of the battery energy storage in the PV system as in [10], involves:

- Current and voltage stabilization
- System autonomy and energy storage
- Supply of surge current

Among the several types of batteries, the lead-acid batteries, which are typically used for solar energy systems, is selected for this design, and this is because, they are available in a variety

of sizes, they are low in cost and have good performance characteristics. Some of the basic parameters of the battery system include the followings:

Battery voltage: this is the battery terminal voltage under no load condition

Battery capacity: it refers to the battery's maximum charge storage capacity, and is usually expressed in Ah.

Battery depth of discharge (DoD): it accounts for the quantity of energy that has been removed from the battery compared to the total fully charged capacity.

Battery life cycles: this refers to the number of the complete charge-discharge cycle that a battery can carry out before its nominal capacity drops below 80% of its initial capacity.

Autonomy: this is a measure of the time; the battery can provide energy to a load when there is a power failure or energy input from the PV array.

Battery state of charge (SOC): this is defined in [12] as the ratio of the battery's present capacity to nominal capacity provided by its manufacturer. The nominal capacity of the battery refers to the maximum quantity of charge that can be stored inside the battery.

The disparity, which exists between the amount of power required by the load on the network and the power produced by the sources, determines if the battery discharges or charges. The state of charge of the battery for hourly time, t is expressed as

$$SOC(t) = SOC(t-1).(1-\delta_{bat}(t)) + \left(\frac{P_b(t)}{V_{bus}}\right).\eta_{bat}.\Delta t \tag{14}$$

Where the $\delta_{bat}(t)$, which represents the hourly self-discharge rate, takes the value of zero since it is negligible, the round trip efficiency of the battery is chosen to be 0.8 and 1 during the battery bank's process of charging and discharging. For the design of the battery bank, one particular constraint that was considered is that the state of charge of a battery is confined within the SOC_{min} and SOC_{max} such that

$$SOC_{min} \le SOC(t) \le SOC_{max} \tag{15}$$

In order for the battery bank to last long, the upper limit is considered as the maximum state of charge, SOC_{max}, and it assumes the value of the entire battery bank's nominal capacity, Cn. The relationship between the nominal capacity of each of the batteries C_{Nbat}, the amount of batteries connected in series, Nsbat, and the sum of the entire batteries is given by equation 16.

$$SOC_{\max} = C_n = \frac{Nbat}{Nbat,s}.C_B \tag{16}$$

The amount of batteries required for parallel connection helps in the determination of the battery bank capacity. The battery minimum state of charge when it is discharging is expressed as

$$SOC_{min} = (1 - DOD).SOC_{max} \quad (17)$$

Where DOD represents the maximum depth of charge [13] [14]

The relationship between the battery terminal voltage, open circuit and, the voltage drop across the battery internal resistance as in [15] is shown in equation 18

$$V_b = E_{oc} + I_b R_b \quad (18)$$

Where R_b is the battery internal resistance, E_{oc} is the open circuit voltage, I_b is the current of the battery while V_b is the terminal voltage of the battery. The relationship between the battery state of charge, SOC and the full charge voltage of the battery is expressed in equation 19 [15]

$$Eoc = VF + b\log(SOC) \quad (19)$$

Where the full charge rest voltage, is denoted by VF

A.3 Modelling of diesel generator

The diesel generator is made up a diesel engine and an alternator for electricity generation; the diesel generator is made up of a diesel engine, a synchronous generator, an excitation system and speed controller. The diesel engine and governor system exert control on the speed of the governor so as to supply mechanical power. The diesel engine comprises of the governor and an internal combustion (IC) engine. The diesel generator ensures the conversion of energy from a fuel such as diesel or bio-diesel into mechanical energy with the help of its internal combustion engine, after which, this mechanical energy is converted into electrical energy with the help of its electric machine operating as a generator. The governor is made up of actuator and speed controller, the maintenance of a constant speed during the period of operation of a diesel generator is maintained by the governor [15] [17]

The transfer function of the actuator, as well as that of the regulator as in [14], is as shown in equation 20 and 21 respectively

$$H_a = \frac{(1+T_{a1}s)}{s(1+T_{a2}s)+(1+T_{a3}s)} \quad (20)$$

$$H_r = \frac{\Upsilon_r(1+T_{ra}s)}{(1+T_{r1}s+T_{r2}s^2)} \quad (21)$$

Where, T_{a1}, $T_{a2,}$ and T_{a3} represent the time constants of the actuator, Υ_r represents the gain of the regulator while, the time constants of the regulator is represented by T_{r1}, $T_{r2,}$ and T_{r3}. Conversely, the speed regulation and diesel engine of the diesel generator can be described using differential equations as in [15] as equation (22) and equation (23).

$$\frac{dm_B}{dt} = \frac{1}{\tau_2}(K_2 P_c - \frac{K_2}{\omega_{ref} R}\Delta\omega - m_B) \tag{22}$$

$$\frac{dPc}{dt} = \frac{-K1}{\omega_{ref}}\Delta\omega \tag{23}$$

Where the rate of fuel consumption of the diesel engine is denoted m_B, ω_{ref} is the engine reference speed in rad/sec, R is the permanent speed drop of the diesel engine, K_1 is the summing loop amplification factor of the governor, the gain and dead time of the engine is represented by K_2 and Υ_2 respectively.

The dead time, Υ_2 can be represented as in [15] as equation (24).

$$\tau_2 = \frac{60 S_t}{2Nn} + \frac{60}{4N} \tag{24}$$

N refers to the speed in rev/min, n is the number of cylinders, S_t represents the number of stroke engine, in this case, S_t=4 and due to combustion, the generated mechanical power output can be expressed as equation (25)

$$P = \mathrm{E}_1 m_B \eta \tag{25}$$

η represents the efficiency and E_1 represents the proportionality constant.

A.4 Modelling of wind energy conversion system

With the help of the wind turbine, wind energy is converted into mechanical power, and hence, the mechanical power is transformed into electrical power. The value of the mechanical power can be computed using equation 26 [18]

$$P_m = 0.5\rho \mathrm{A} C_p(\lambda, \beta) V_{wind} \tag{26}$$

Where ρ represents the density of air and its value is within the range of 1.22-1.3Kg/ms, V_{wind} refers to the speed of the wind in m/s, A represents the swept area of the turbine blades (m^2). The coefficient of power is denoted by $C_p(\lambda,\beta)$, its influenced by two factors, the pitch angle of the blade, β and the speed slip ratio, mathematically, the tip speed ratio is defined as

$$\lambda = \Omega R / V_{wind} \tag{27}$$

R is the radius of the blade (m) and Ω refers to the angular speed (m/s)

The coefficient of power is defined as in [18] as

$$C_p(\lambda,\beta) = C_1\left(\frac{C_2}{\lambda_1} - C_3\beta - C_4\right)\exp\left(\frac{-C_5}{\lambda_1}\right) + C_6\lambda \tag{28}$$

Where $$\frac{1}{\lambda 1} = \left(\frac{1}{\lambda + 0.08\beta} - \frac{0.035}{\beta^3 + 1}\right) \tag{29}$$

The rotational torque can be expressed as $T_m = P_m / \Omega$ (30)

The optimal angular speed is represented by the relation

$$\Omega opt = \lambda_{opt} V_{wind} / R \tag{31}$$

In order to achieve the maximum mechanical power, the following relation is used

$$P_{m\_\max} = 0.5\rho A C_{p\max} V^3{}_{wind} \tag{32}$$

A.4.1 PMSG wind turbine

The PMSG driven wind turbine was chosen for this project as a result of certain advantages in [19] as follows:

- There is the absence of brush/slip ring.
- The mechanical stress is low
- The rotor does not experience any form of copper loss
- Reactive/active power controllability is higher

The sign of the torque input of the PMSG is what determines its mode of operation if its sign is negative, the PMSG operates as a generator and if its sign is positive, the PMSG operates as a motor [20].

The bulk of wind turbines has a gearbox, but as a result, of the high rate of failure associated with the gearbox, the direct driven wind turbine is now becoming the preferred choice due to its advantages over wind turbines, which contains a gearbox. The advantages of direct driven wind turbines include; its maintenance is lower, especially with offshore, reduced losses in the drive drain, reduced noise, besides, it has a simpler structure [21].

In the transformation of mechanical power to electrical power in the direct-drive wind energy system, the permanent magnet synchronous machines/ generator is very useful, in this work, the mathematical model in abc three-phase stationary reference frame, as well as the dq rotating reference frame, are considered.

A.4.2 Mathematical model of the Permanent magnet synchronous generator in the abc reference frame

The PMSG comprises of a stator referred to as the stationary armature and is linked to the grid and a rotor, the rotor is a permanent magnet. The voltages at the terminals of the PMS machine stator is represented as in [22] [23] as

$$V_{a-s} = R s l_{a-s} + \frac{d\psi_{a-s}}{dt} \quad (33)$$

$$V_{b-s} = R s l_{b-s} + \frac{d\psi_{b-s}}{dt} \quad (34)$$

$$V_{c-s} = R s l_{c-s} + \frac{d\psi_{c-s}}{dt} \quad (35)$$

Where $V_{a\text{-}s}$, $V_{b\text{-}s}$, $V_{c\text{-}s}$ represent the instantaneous a, b, and c stator voltages and the instantaneous stator currents, R_s represents the winding resistance of the stator per phase. Conversely, the instantaneous flux linkages that are induced in the system by the PMs and the three-phase AC currents are represented by $\psi_{a\text{-}s}$, $\psi_{b\text{-}s}$, $\psi_{c\text{-}s}$.

In the PMSG exist balanced phase currents, and these are represented as:

$$l_{a-s} = \mathrm{I_m} \cos(\omega_s t) \quad (36)$$

$$l_{b-s} = \mathrm{I_m} \cos(\omega_s t - 120) \quad (37)$$

$$l_{c-s} = \mathrm{I_m} \cos(\omega_s t + 120) \quad (38)$$

Where $\omega_s = 2\pi f$ represents the stator currents angular frequency while Im represents the sinusoidal varying current maximum value.

A.4.3 Mathematical model of the Permanent magnet synchronous generator in the dqo reference frame.

The equivalent circuit of the permanent magnet synchronous generator in the dqo reference frame is as shown in figure A-27

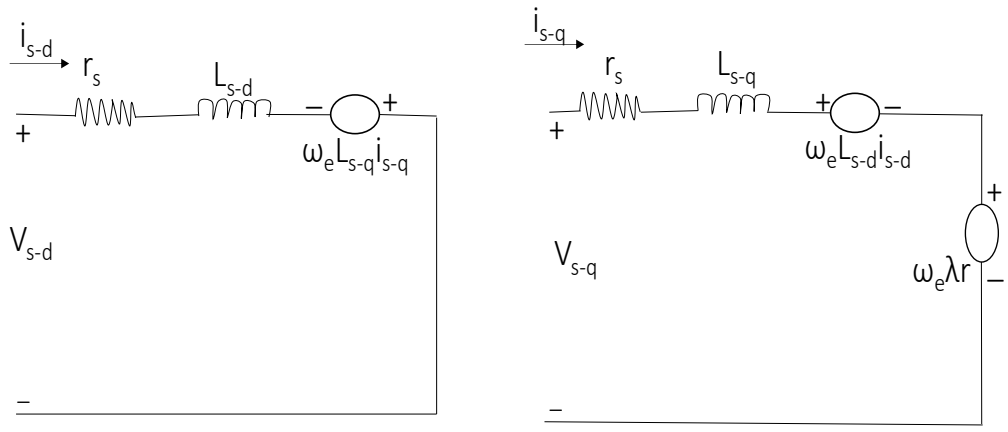

Figure A-27. PMSG equivalent circuit in the dqo reference frame

Based on the dqo synchronous rotating frame, the mathematical model of the permanent magnet synchronous generator as in [24] [25] is represented as

$$\frac{di_{s-d}}{dt} = \frac{1}{l_{s-d}}(-R_s l_{s-d} + \omega_e l_{s-q} i_{s-q} + V_{s-d}) \tag{39}$$

$$\frac{di_{s-q}}{dt} = \frac{1}{l_{s-q}}(-R_s l_{s-q} - \omega_e (l_{s-d} i_{s-d} + \lambda p) + V_{s-q}) \tag{40}$$

Where the inductances of the generators are represented by l_d and l_q, the stator resistance is represented by R_s, and the flux induced in the system is represented by λ, the speed of the rotor is represented by ω_e. The currents and voltages are represented by

i_{s-d}, i_{s-q} and V_{s-d}, V_{s-q} respectively.

The electrical torque is given as

$$T_e = 1.5\, p(\psi_f i_{s-q} + (l_{s-d} - l_{s-q}) i_{s-d} - i_{s-q}) \tag{41}$$

Since the q-axis and d-axis inductances are equal

$$(l_{s-d} - l_{s-q}) = 0$$

Hence, the electrical torque equation becomes

$$T_e = 1.5 p \psi_f i_{s-q} \tag{42}$$

A.5 Control of Permanent magnet synchronous generator

There are several ways of controlling the power converters of the PMSG driven wind turbine, the network-side or grid-side converter is usually controlled by adopting load angle control

techniques, while the generator-side or machine-side converter control is achieved by adopting vector control or load angle control techniques [21].

Conversely, it was reported in another research work [26], that the control of the amount of reactive power injected into the grid is done by the network-side or grid-side converter, according to the report, the DC voltage, which exists between the converters is also maintained by the network-side or grid-side converter. While the machine-side or generator-side converter controls the reactive power on the machine side and the maximum power generated at varying wind speed.

A.5.1 The methodology of the network-side or grid-side converter controller

The Primary function of the network-side or grid-side converter is to ensure that the DC link voltage is regulated, this is achieved by transporting active power to the grid or network. Besides, the controller is built in such a manner that facilitates the exchange of reactive between the network and the converter [21] [27].

A.5.1.1 Load angle control technique

In this control technique, the network or the grid serves as the receiving source, $V_{n/g}\angle 0$ while the network-side or grid-side converter serves as the sending source, $V_{VSC}\angle\delta$. Since the voltage in the network is known, it is chosen as the reference voltage; therefore, the phase angle δ is positive. These two sources are coupled by an inductor referred to as the network or grid reactance, $X_{n/g}$.

In order for the load angle control method to be implemented, the reference value of the network reactive power $Q_{n/g-rf}$ may perhaps be put at zero for the system to operate at unity power factor. Therefore, the V_{VSC} magnitude, and the phase angle, δ at the network-side or grid-side converter terminal can be achieved as in [21] as follows:

$$\delta = \frac{P_{n/g-rf} X_{n/g}}{V_{VSC} V_{n/g}} \tag{43}$$

$$V_{VSC} = V_{n/g} + \frac{Q_{n/g-rf} X_{n/g}}{V_{VSC}} \qquad Q_{n/g-rf} = 0 \tag{44}$$

The magnitude of the phase angle, δ and the voltage, V_{VSC} of the network-side or grid-side converter, can be computed from equations (43) and (44) as

$$\delta = f(P_{n/g-rf}, V_{n/g}) = sin^{-1}(\frac{P_{n/g-rf} X_{n/g}}{3V_{VSC} V_{n/g}}) \quad (45)$$

$$V_{VSC} = g(Q_{n/g-rf}, V_{n/g}, \delta) = V_{VSC}\cos\delta + \sqrt{(V_{n/g}\cos\delta)^2 + 4(Q_{n/g-rf}/3)X_{n/g}} \quad (46)$$

A.5.2 *The methodology of the generator-side or machine-side converter controller*

The wind turbine operation is done with the vector control or the load angle technique by the generator-side or machine-side converter.

A.5.2.1 Vector control technique

The implementation of this technique is done on the basis of the dynamic model of the synchronous generator, which is expressed in the dq frame, this dq frame refers to the rotor (field) magnetic axis alignment with the d axis.

The electrical torque of the generator is defined as the cross product of the stator current and the stator flux, this is represented by the equation (47)

$$T_{el} = \overline{\psi}_{ds}.\bar{i}_{qs} - \overline{\psi}_{qs}.\bar{i}_{ds} \quad (47)$$

From the stator flux equation

$$\overline{\psi}_{ds} = -\bar{i}_{ds}\bar{i}_{qs} + \bar{l}_{md}\bar{i}_{f} \quad (48)$$

In the vector control technique,

i_{dsrf} is adjusted to zero and i_{qsrf} is obtained from equation (47)

By setting adjusting i_{ds} to zero, equations (47) and (48) become

$$T_{el} = \overline{\psi}_{ds}.\bar{i}_{qs} \quad (49)$$

$$\overline{\psi}_{ds} = \bar{l}_{md}\bar{i}_{f} \quad (50)$$

Assuming $\bar{l}_{md}\bar{i}_{f} = \overline{\psi}_{fd}$ and we substitute for $\overline{\psi}_{ds}$ from equation (50) into equation (49)

$$T_{el} = \overline{\psi}_{fd}.\bar{i}_{qs} \quad (51)$$

From equation (51), for a given torgue reference, $\overline{T}_{sp}$

$$\bar{i}_{qs_{rf}} = \frac{\overline{T}_{sp}}{\psi_{fd}} \tag{52}$$

We have that the moment the reference currents, $i_{qs_{rf}}$ and $i_{ds_{rf}}$ are obtained by the controller, the corresponding magnitudes of the voltage is computed from equation (53) and (54) as equation (55) and (56)

$$\overline{V}_{ds} = -\bar{r}_s \bar{i}_{qs} + \overline{\omega}_s \overline{L}_{qs} \bar{i}_{ds} = -\bar{r}_s \bar{i}_{ds} + \overline{X}_{qs} \bar{i}_{qs} \tag{53}$$

$$\overline{V}_{qs} = -\bar{r}_s \bar{i}_{qs} - \overline{X}_{ds} \bar{i}_{ds} + \overline{E}_{fd} \tag{54}$$

$$\overline{V}_{ds} = -\bar{r}_s \bar{i}_{ds} + \overline{X}_{qs} \bar{i}_{qs} \tag{55}$$

$$\overline{V}_{qs} = -\bar{r}_s \bar{i}_{qs} - \overline{X}_{ds} \bar{i}_{ds} + \overline{E}_{fd} \tag{56}$$

The error, which exist between the actual and reference values of the current is regulated with a PI controller. $i_{ds_{rf}}$ is adjusted to zero when the generator operation is below the base speed, but when it operates above the based speed, $i_{ds_{rf}}$ is adjusted to negative in order to neutralize some part of the flux linkage [21].

A.5.2.2 Load angle control technique

In this technique, in order for the transfer of reactive and active power between the DC link and the generator to be determined, steady-state power flow equations are employed [25].

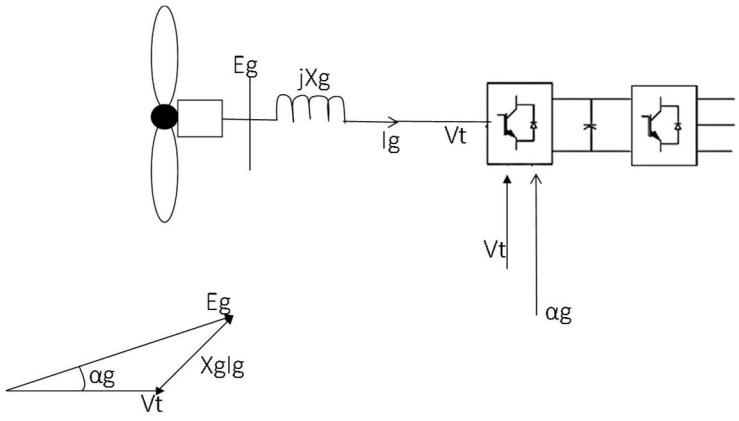

Figure A-28 PMSG driven load angle control technique.

From the figure A-28,

Under steady state condition, the reactive and active power flows in the system are expressed below

$$Q = \frac{E_g{}^2 - E_g V_t \cos \alpha_g}{X_g} \tag{57}$$

$$P = \frac{E_g V_t}{X_g} \sin \alpha_g \tag{58}$$

Where Xg is the generator synchronous reactance, Vt is the magnitude of the voltage at the terminals of the converter, Eg is the magnitude of the internal voltage of the generator while the phase difference between the Vt and Eg is represented by αg. It can be deduced from equations (57) and (58) that the transfer of reactive power depends majorly on the magnitude of the voltage, its transfer is usually from the where there is higher voltage magnitude to where there is lower voltage magnitude. On the other hand, the transfer of active power depends majorly on the system's phase angle. Through the process of adjusting the angle and magnitude of the voltage at the generator-side converter AC terminals, the generator operation and the transfer of power to DC link from the generator can be controlled. The phase angle is given by the expression:

$$\alpha_g = \frac{P_{g_{rf}} X_g}{E_g V_t} \tag{59}$$

Conversely, the voltage magnitude is given by

$$V_t = E_g - \frac{Q_{g_{rf}} X_g}{E_g} \tag{60}$$

$P_{g_{rf}}$ Represents the reference value of the amount of active power that should be passed from the generator to the DC link while the reactive power reference value is represented by $Q_{g_{rf}}$

A.5.3 DC link modelling

In order to determine the reference value of the active power, $P_{g_{rf}}$ required for transmission, let us consider the diagram of figure A-29

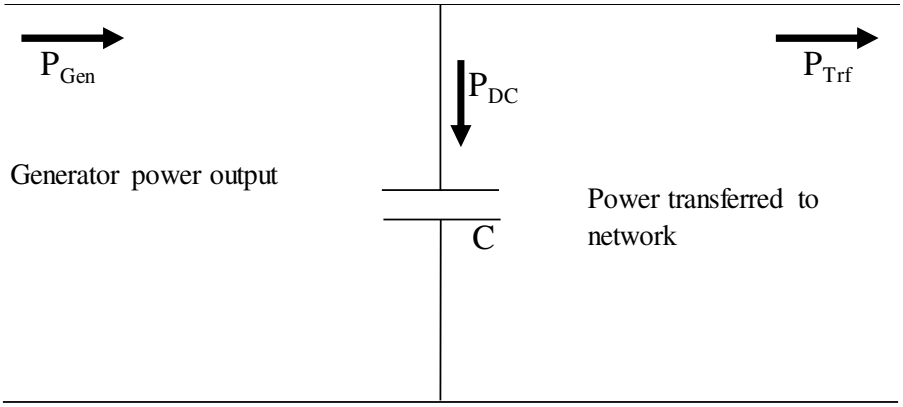

Figure A-29 DC link power flow analysis

The diagram shows the DC link power balance, and it is expressed as given below

$$P_{DC} = P_{Gen} - P_{Trf} \tag{61}$$

Where P_{Trf} refers to the transferred to the network or grid from the DC link, P_{Gen} is the generator power output transferred to the DC link, P_{DC} refers to the power, which passes via the DC link.

The active power that passes via the DC link capacitor is expressed as

$$P_{DC} = V_{DC} I_{DC}$$

$$= V_{DC} C \frac{V_{DC}}{dt} \tag{62}$$

V_{DC} is expressed as

$$P_{DC} = V_{DC} C \frac{dV_{DC}}{dt} = \frac{C}{2} x 2 x V_{DC} \frac{dV_{DC}}{dt}$$

$$= \frac{C}{2} \frac{dV_{DC}^{2}}{dt} \tag{63}$$

By adjusting equation (63) and applying integration on both sides, we have that

$$V_{DC}^{2} = \frac{2}{C} \int P_{DC} dt \tag{64}$$

Therefore, $V_{DC} = \sqrt{\frac{2}{C} \int P_{DC} dt}$ (65)

In order to express V_{DC} with respect to the power transferred to the network or grid and the power output of the generator, we have that

$$V_{DC} = \sqrt{\frac{2}{C}} \int (P_{Gen} - P_{Trf}) dt \tag{66}$$

The value of the V_{DC} is achieved using equation (66), by comparing the desired voltage of the DC link, V_{DCrf} with the actual voltage at the DC link, V_{DC} the reference value of the power, P_{Trf-rf} that has to be transferred to the network or grid can be computed.

Note: to implement this in the field physically, measurement via the Transducer is required in order to get the DC link actual voltage, V_{DC}.

A.6 References

[1] N. Pandiarajan and R. Muthu, "Mathematical modeling of photovoltaic module with Simulink Mathematical Modeling of Photovoltaic Module with Simulink," no. October, pp. 3–5, 2015.

[2] P. Sudeepika and G. G. Khan, "Analysis Of Mathematical Model Of PV Cell Module in Matlab / Simulink Environment," pp. 7823–7829, 2014.

[3] H. Tsai, C. Tu, and Y. Su, "Development of Generalized Photovoltaic Model Using MATLAB / SIMULINK," *Proc. World Congr. Eng. Comput. Sci. 2008 WCECS 2008, Oct. 22 - 24, 2008, San Fr. USA*, p. 6, 2008.

[4] E. Erdil, M. Ilkan, and F. Egelioglu, "An experimental study on energy generation with a photovoltaic (PV)-solar thermal hybrid system," *Energy*, vol. 33, no. 8, pp. 1241–1245, 2008.

[5] V. P. Sethi, K. Sumathy, S. Yuvarajan, and D. S. Pal, "Mathematical Model for Computing Maximum Power Output of a PV Solar Module and Experimental Validation," *Ashdin Publ. J. Fundam. Renew. Energy Appl.*, vol. 2, no. 5, p. pp 1-5, 2012.

[6] H. Mike, *Mike Holt's Illustrated Guide to Understanding the Nec Requirements for Solar Photovoltaic Systems*. Publisher: Mike Holt ISBN-13: 9781932685541, 2011.

[7] J. B. V Subrahmanyam, P. Alluvada, Bandana, K. Bhanupriya, and C. Shashidhar, "Perspectives Renewable Energy Systems : Development and Perspectives of a Hybrid Solar-Wind System," vol. 2, pp. 177–181, 2012.

[8] M. B. Eteiba, E. T. El Shenawy, J. H. Shazly, and A. Z. Hafez, "A Photovoltaic (Cell,

Module, Array) Simulation and Monitoring Model using MATLAB ® /GUI Interface," *Int. J. Comput. Appl.*, vol. 69, no. 6, pp. 975–8887, 2013.

[9] L. El Chaar, *Photovoltaic System Conversion*, Third Edit. Elsevier Inc., 2011.

[10] S. Sumathi, L. Ashok Kumar, and P. Surekha, *Solar PV and Wind Energy Conversion Systems*. 2015.

[11] U. Patel, M. D. Sahu, and D. Tirkey, "Maximum Power Point Tracking Using Perturb & Observe Algorithm and Compare With another Algorithm," *Int. J. Digit. Appl. Contemp. Res. Website www.ijdacr.com*, vol. 2, no. 2, 2013.

[12] W.-Y. Chang, "The State of Charge Estimating Methods for Battery: A Review," *ISRN Appl. Math.*, vol. 2013, no. 1, pp. 1–7, 2013.

[13] A. S. O. Ogunjuyigbe, T. R. Ayodele, and O. A. Akinola, "Optimal allocation and sizing of PV/Wind/Split-diesel/Battery hybrid energy system for minimizing life-cycle cost, carbon emission and dump energy of remote residential building," *Appl. Energy*, vol. 171, pp. 153–171, 2016.

[14] Z. Lu, G. Barakat, and A. Yassine, "Design and optimal sizing of hybrid PV/wind/diesel system with battery storage by using DIRECT search algorithm," in *Power Electronics and Motion Control Conference (EPE/PEMC), 2012 15th International*, 2012, p. DS3b.19-1-DS3b.19-7.

[15] Faten Hosney Fahmy, "PV/Diesel Hybrid System for Fuel Production from Waste Plastics Recycling," *Ijmer*, vol. 4, no. 12, pp. 68–79, 2014.

[16] D. O. Akinyele and R. K. Rayudu, "Community-based hybrid electricity supply system: A practical and comparative approach," *Appl. Energy*, vol. 171, pp. 608–628, 2016.

[17] A. Pachori, P. Suhane, and P. Scholar, "Design and modelling of standalone hybrid power system with MATLAB/Simulink," *Int. J. Sci. Res. Manag. Stud.*, vol. 1, no. 2, pp. 2349–3771.

[18] N. R. Babu and P. Arulmozhivarman, "Wind energy conversion systems - A technical review," *J. Eng. Sci. Technol.*, vol. 8, no. 4, pp. 493–507, 2013.

[19] H. S. Kim and D. D. Lu, "Wind Energy Conversion System from Electrical Perspective — A Survey," vol. 2010, no. November, pp. 119–131, 2010.

[20] S. Mishra, M. Gupta, A. Garg, R. Goel, and V. K. Mishra, "Modeling and Simulation of Solar Photo-Voltaic and PMSG Based Wind Hybrid System," in *lEEE Students' Conference on Electrical, Electronics and Computer Science*, 2014.

[21] O. Anaya-Lara, N. Jenkins, J. Ekanayake, P. Cartwright, and M. Hughes, *Wind energy*

generation : modelling and control, vol. 54, no. 2. 2009.

[22] N. Huang, "Simulation of Power Control of a Wind Turbine Permanent Magnet Synchronous Generator System," 2013.

[23] A. E. Fitzgerald, *Electric Machinery*, vol. 319, no. 4. McGraw Hill, 2003.

[24] F. M. Gonzalez-Longatt, P. Wall, and V. Terzija, "A simplified model for dynamic behavior of permanent magnet synchronous generator for direct drive wind turbines," in *2011 IEEE Trondheim PowerTech*, 2011, pp. 1–7.

[25] Kundur P, *Power System Stability and Control*, 1st edition. McGraw-Hill: New York, NY, USA., 1994.

[26] K. Nieradzinska, "Multi-Technology Offshore Wind Power Systems : Control and Dynamic Performance Assessment," 2017.

[27] Y. Errami, M. Ouassaid, and M. Maaroufi, "Optimal Power Control Strategy of Maximizing Wind Energy Tracking and Different Operating Conditions for Permanent Magnet Synchronous Generator Wind Farm," *Energy Procedia*, vol. 74, pp. 477–490, Aug. 2015.